

NASA CR-120943
AT-6133-R

F

ADVANCED TWO-STAGE COMPRESSOR
PROGRAM
DESIGN OF INLET STAGE

CASE FILE
COPY

by

Dr. C. A. Bryce
C. J. Paine
Dr. A. R. S. McCutcheon
Dr. R. K. Tu
G. L. Perrone

AIRESEARCH MANUFACTURING COMPANY OF ARIZONA

Prepared for

NATIONAL AERONAUTICS AND SPACE ADMINISTRATION

NASA Lewis Research Center
Contract NAS 3-15324

11/8

NOTICE

This report was prepared as an account of Government-sponsored work. Neither the United States nor the National Aeronautics and Space Administration (NASA), nor any person acting on behalf of NASA:

- A.) Makes any warranty or representation, expressed or implied, with respect to the accuracy, completeness, or usefulness of the information contained in this report, or that the use of any information, apparatus, method, or process disclosed in this report may not infringe privately-owned rights; or
- B.) Assumes any liabilities with respect to the use of, or for damages resulting from the use of, any information, apparatus, method or process disclosed in this report.

As used above, "person acting on behalf of NASA" includes any employee or contractor of NASA, or employee of such contractor, to the extent that such employee or contractor of NASA or employee of such contractor prepares, disseminates, or provides access to any information pursuant to his employment or contract with NASA, or his employment with such contractor.

Requests for copies of this report should be referred to:

National Aeronautics and Space Administration
Scientific and Technical Information Facility
P. O. Box 33
College Park, Maryland 20740

1. Report No. NASA CR-120943		2. Government Accession No.		3. Recipient's Catalog No.	
4. Title and Subtitle ADVANCED TWO-STAGE COMPRESSOR PROGRAM DESIGN OF INLET STAGE				5. Report Date August 1973	
				6. Performing Organization Code	
7. Author(s) Dr. C.A. Bryce, C.J. Paine, Dr. A.R.S. McCutcheon, Dr. R.K. Tu, G.L. Perrone				8. Performing Organization Report No. AT-6133-R	
				10. Work Unit No.	
9. Performing Organization Name and Address AiResearch Manufacturing Company of Arizona Phoenix, Arizona 85010				11. Contract or Grant No.	
				13. Type of Report and Period Covered Contractor Report	
12. Sponsoring Agency Name and Address National Aeronautics and Space Administration Washington, D.C. 20546				14. Sponsoring Agency Code	
15. Supplementary Notes Program Monitor, Robert Y. Wong, NASA-Lewis Research Center, Cleveland, Ohio					
16. Abstract This final report covers the aerodynamic design of an inlet stage for a two-stage, 10/1 pressure ratio, 2 lb/sec flow rate compressor. Initially a performance comparison was conducted for an axial, mixed flow and centrifugal second stage. A modified mixed flow configuration with tandem rotors and tandem stators was selected for the inlet stage. The term "conical flow compressor" was coined to describe a particular type of mixed flow compressor configuration which utilizes axial flow type blading and an increase in radius to increase the work input potential. Design details of the conical flow compressor are described.					
17. Key Words (Suggested by Author(s)) Compressor/Impeller Inlet Stage Two-Stage Compressor Program			18. Distribution Statement Unclassified-unlimited		
19. Security Classif. (of this report) Unclassified		20. Security Classif. (of this page) Unclassified		21. No. of Pages 300	
				22. Price* 3.00	

* For sale by the National Technical Information Service, Springfield, Virginia 22151

Page Intentionally Left Blank

FOREWORD

This is the final report covering work performed under Contract No. NAS 3-15324 during the period May 1, 1971 through April 30, 1972.

This contract was under the technical direction of Mr. R. Wong, Lewis Research Center, of the National Aeronautic and Space Administration.

Mr. K. W. Benn was program manager, Mr. G. R. Metty, the project engineer, and Mr. G. L. Perrone, principal investigator. Recognition is given to Mr. J. R. Erwin for frequent consultations and to Mr. P. Dodge for his assistance in developing one of the computer programs required to analyze this design.

Page Intentionally Left Blank

TABLE OF CONTENTS

	<u>Page</u>
ABSTRACT	i
FOREWORD	iii
SUMMARY	1
INTRODUCTION	3
COMPRESSOR SELECTION	5
Centrifugal-Centrifugal Compressor Configuration	5
Axial-Centrifugal Compressor Configuration	10
Mixed-Flow Centrifugal Configuration	19
COMPARISON OF CANDIDATE COMPRESSORS	35
Stage Compatibility	38
Boundary Layer Control	42
Size and Weight Considerations	44
Impeller Erosion Considerations	47
CONFIGURATION SELECTION	49
GENERAL DESIGN LOGIC	50
ROTOR AND STATOR GEOMETRY SELECTION	53
DETAILED AERODYNAMIC DESIGN	53
General	53
Rotor 1A Design	56
Rotor 1B Design	73
Tandem Stator Design	90
Boundary Layer Control	115
Inlet Flowpath Design	126
Transitional Duct Design	128
Drive Turbine Aerodynamic Design	131
Drive Turbine Aerodynamic Design Summary	131
Turbine Design Point	140
APPENDIX A - Deviation Angle Prediction for the Conical Flow Compressor	32 pages
APPENDIX B - Blade Section for Rotors and Stators	33 pages
APPENDIX C - Turbine Blade Sections	9 pages
APPENDIX D - Complete Radial Equilibrium Flow Solution all Blade Rows	61 pages
APPENDIX E - Mechanical Design Analysis of NASA 10/1 Advanced Compressor Rig	11 pages
APPENDIX F - References	1 page
APPENDIX G - Performance Parameter and Symbol Definition	4 pages

ADVANCED TWO-STAGE COMPRESSOR PROGRAM DESIGN OF INLET STAGE

SUMMARY

The objective of this program was to design an inlet stage for an advanced two-stage compressor for an overall pressure ratio of 10/1 and 2.0 pounds per second mass flow. As a part of this program, an optimization study was conducted for various inlet stages in combination with a centrifugal compressor second stage. Axial, mixed flow, and centrifugal compressors were examined as inlet stages with analyses made for the optimum pressure ratio split between stages and the optimum speed for each combination. A form of mixed flow compressor, with a tandem bladed rotor and a tandem bladed stator, was selected for detailed design on the basis of performance potential.

The flow path in the selected mixed flow compressor incorporates axial flow type blading and a substantial change in radius along streamlines across each blade row to increase the work input without exceeding the loading criteria established for axial flow blading. The change in radius renders conventional methods for finding flow deviation largely inaccurate. An improved method for computing flow deviation was developed which essentially coupled the axisymmetric, radial equilibrium flow solution to a finite difference, blade-to-blade solution thereby yielding a quasi three-dimensional model of the flow through each blade row (secondary flows excluded). A complete description of the design philosophy used to establish blade sections for each blade row is presented. Predicted performance for the conical compressor looks favorable and, if experimentally verified, this design concept could have a wide range of applications.

Page Intentionally Left Blank

INTRODUCTION

In order to achieve low specific fuel consumption (SFC) and high specific thrust, high compressor pressure ratios and high turbine inlet temperature are required, while at the same time maintaining high component efficiencies. These objectives become progressively more difficult to achieve as gas turbine engines are reduced in size or power output. In the small power range (500 horsepower or less), the relative size of the components make manufacturing tolerances and minimum clearances critical factors in attaining high efficiencies.

In small engines it is desirable to employ a relatively simple compressor with a minimum number of stages consistent with performance goals and weight considerations. In this class of engine, the Lewis Research Center is particularly interested in a two-stage compressor with an overall pressure ratio of 10/1 and 2.0 pounds per second mass flow rate. Thus a compressor program was initiated to study a two-stage compressor consisting of a second-stage centrifugal compressor which is preceded by an inlet stage operating at the same shaft speed. The inlet stage may be an axial, centrifugal, or a mixed flow design. The first objective of this program was to optimize these combinations of stages for various pressure ratio splits and rotative speeds. Consideration was also given to turbine speed limitations in an actual engine application. From this study, a two-stage compressor was selected on the basis of performance potential, stage compatibility, size, weight, volume, and resistance to foreign object damage. A second objective was to incorporate the first stage of the selected configuration into a research package for delivery to the Lewis Research Center for experimental evaluation. This research package was to be complete with drive turbine and research instrumentation. Funding limitations resulting mainly from the need to develop analytical methods for handling a novel impeller prevented the completion of all of these objectives.

This report will describe the work that was completed under contract with the Lewis Research Center. Included in this report are a description of the optimization study of the three candidate configurations, trade-offs made in making the final selections, the detailed aerodynamic design of the first stage of the selected compressor configuration, the detailed aerodynamic design of the cross-over duct between the two stages, and the detailed aerodynamic design of the drive turbine for the research package. The drive turbine was designed to have the capability of driving the combined two-stage configuration to a speed of 110-percent of design speed. Also included in this report are:

- (a) Blade shapes, coordinate, and stacking information for (1) the first stage of the selected compressor (Appendix A) and (2) the research package drive turbine (Appendix C)

- (b) A complete non-isentropic radial equilibrium flow solution for all blade rows (Appendix D)
- (c) Mechanical design analysis of first-stage compressor blade and disk (Appendix E)

COMPRESSOR SELECTION

The selection of the two-stage compressor configuration for 10/1 pressure ratio and 2 lb/sec flow rate is based on an optimization study of each candidate configuration for efficiency as a function of speed and pressure ratio split. The configurations examined analytically were (1) an axial stage followed by a centrifugal stage, (2) a mixed flow stage followed by a centrifugal stage, and (3) a centrifugal stage followed by a second centrifugal stage. The results of this study were then used with the criteria listed below to select the compressor configuration for this application.

- (a) Overall compressor efficiency
- (b) Aerodynamic compatibility of the two stages
- (c) Potential for boundary layer control
- (d) Stage size and weight considerations
- (e) Impeller erosion considerations

Centrifugal-Centrifugal Compressor Configuration

The prediction of performance of a centrifugal compressor is based on a correlation of polytropic efficiency against specific speed. The use of a specific speed correlation originates from pump practice where peak adiabatic efficiency has been experimentally found to be uniquely related to this parameter. Published derivations of specific speed correlations rely on dimensional analysis and certain intuitive arguments. A theoretical basis for the application of specific speed as a correlating parameter for compressor performance can be derived from the corresponding momentum equations in nondimensional form. The subject derivation indicates that dynamic similarity for solutions to the equations of motion depends on specific speed and certain dimensionless geometric parameters for the rotor. In the AiResearch derivation, the specific speed is based on a mean volume flow through the compressor. This formulation uses the square root of the product of the compressor inlet and outlet volumetric flow rates instead of the usual specific speed definition based on the inlet volumetric flow. AiResearch experience has shown that the mean effective definition of specific speed best describes conditions for dynamic similarity in a centrifugal compressor.

Polytropic efficiency is used to correlate centrifugal compressor performance since it represents the true aerodynamic efficiency exclusive of pressure ratio of preheat effects. An empirical correlation of experimental results from a variety of centrifugal compressor tests with inlet tip relative Mach numbers up to 1.3 has shown that polytropic efficiency is essentially independent of compressor pressure



ratio. Therefore, obtainable performance for centrifugal compressors can be represented by a single line on a plot of polytropic efficiency against specific speed as shown on figure 1. This correlation is restricted to compressors with throughflows (W_{corr}) of 7 pounds per second or greater, nominal clearances of 0.010 inch or less, and a Reynolds number (Re) of 3×10^6 or higher. Scaling these results to lower flow rates is a separate problem and will be discussed later in this report. This polytropic efficiency correlation is used in the design point computer program to compute state and overall efficiency for a given overall pressure ratio, rotative speed, and first-stage pressure ratio.

With several assumed values of first-stage pressure ratio at constant rotating speed and overall pressure ratio, the program will curve fit the resulting overall efficiencies and determine the optimum stage pressure ratios. Results from this program are presented on figure 2. This figure shows overall compressor efficiency for two centrifugal stages with an overall pressure ratio 10/1 as a function of first-stage pressure ratio and rotating speed. Peak stage efficiency is indicated for each speed in figure 2 corresponding to the optimum pressure ratio split between stages. A crossplot of the peak efficiency results against rotating speed is shown in figure 3. This plot is used to determine design conditions tabulated below for the optimum centrifugal-centrifugal configuration for this application.

Note that the first stage of a two-stage compressor does not require diffusion to as low a Mach number as the second stage and thus the diffusion losses are lower. Experience has indicated, however, that the turning and ducting losses associated with the interstage duct are sufficiently high to compensate for the reduced diffusion. Therefore in the above analysis, the efficiency correlations that are based primarily on single-stage performance with diffusers are also assumed to apply to stages with interstage ducts.

DESIGN CONDITIONS FOR THE OPTIMUM
CENTRIFUGAL-CENTRIFUGAL COMPRESSOR CONFIGURATION

	<u>First Stage</u>	<u>Second Stage</u>	<u>Overall</u>
Rotor speed, rpm	75,500	72,500	72,500
Pressure ratio	4.75/1	2.1/1	10/1
Specific speed, N_s	70	64	N/A
Adiabatic efficiency, η_{ad}	0.84	0.862	0.826

Previous AiResearch test experience with a two-stage centrifugal compressor at approximately 11/1 pressure ratio has demonstrated an adiabatic efficiency of 80.3 percent with a corrected

POLYTROPIC EFFICIENCY VS SPECIFIC SPEED

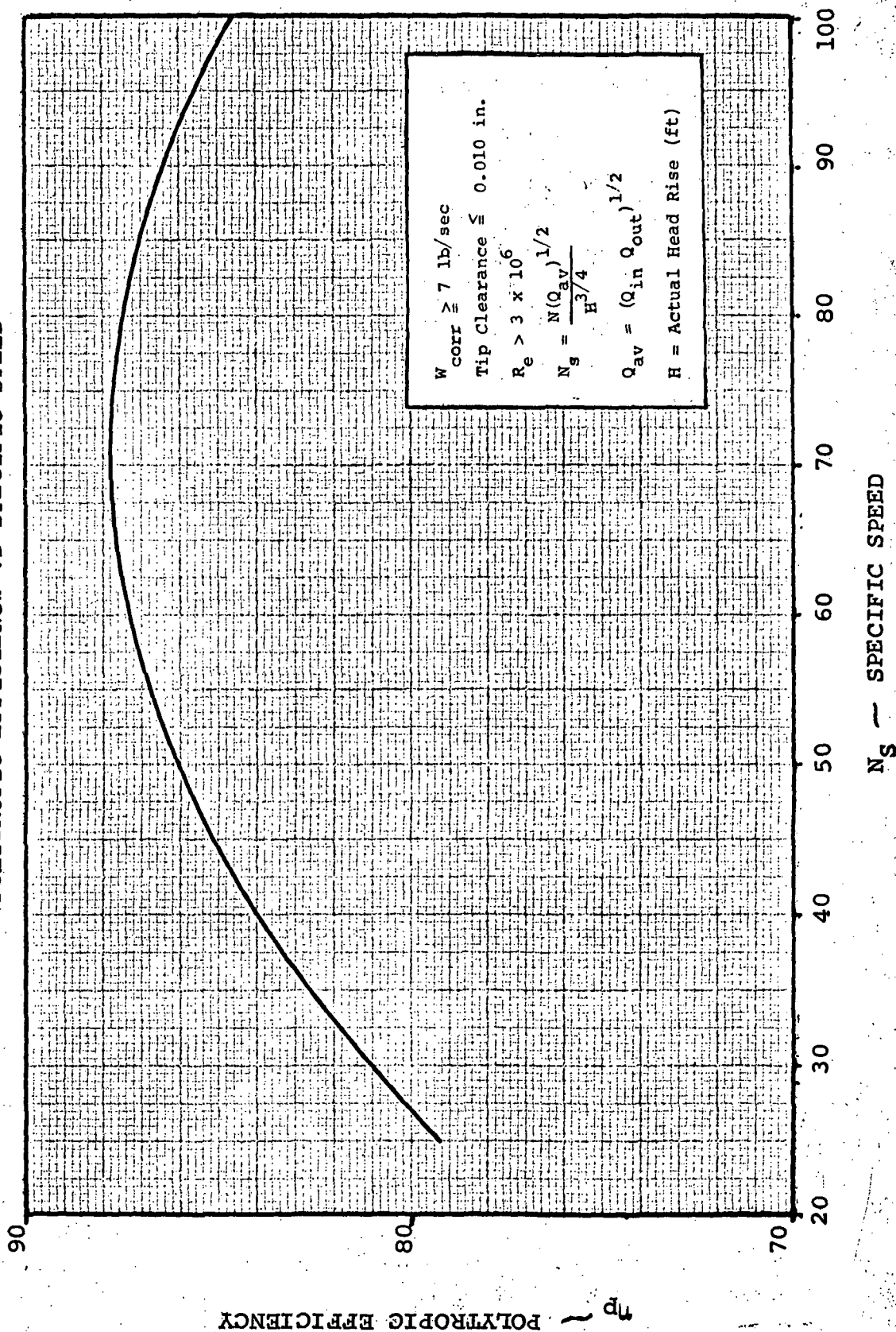


Figure 1. - Centrifugal Compressor Performance.

η_{ad} ~ OVERALL EFFICIENCY (SCALE AND MATCHING EFFECTS NOT INCLUDED)

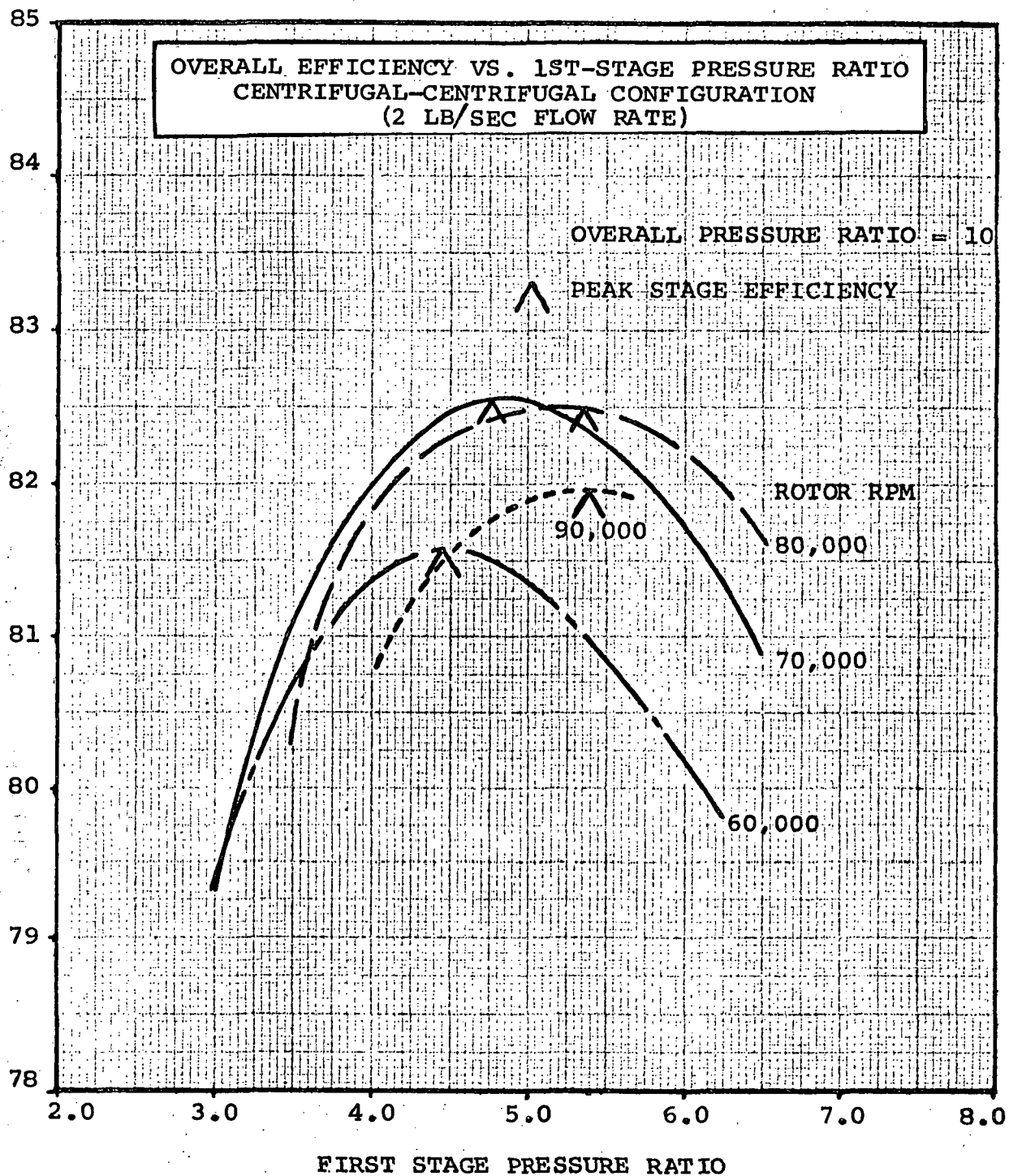


Figure 2.

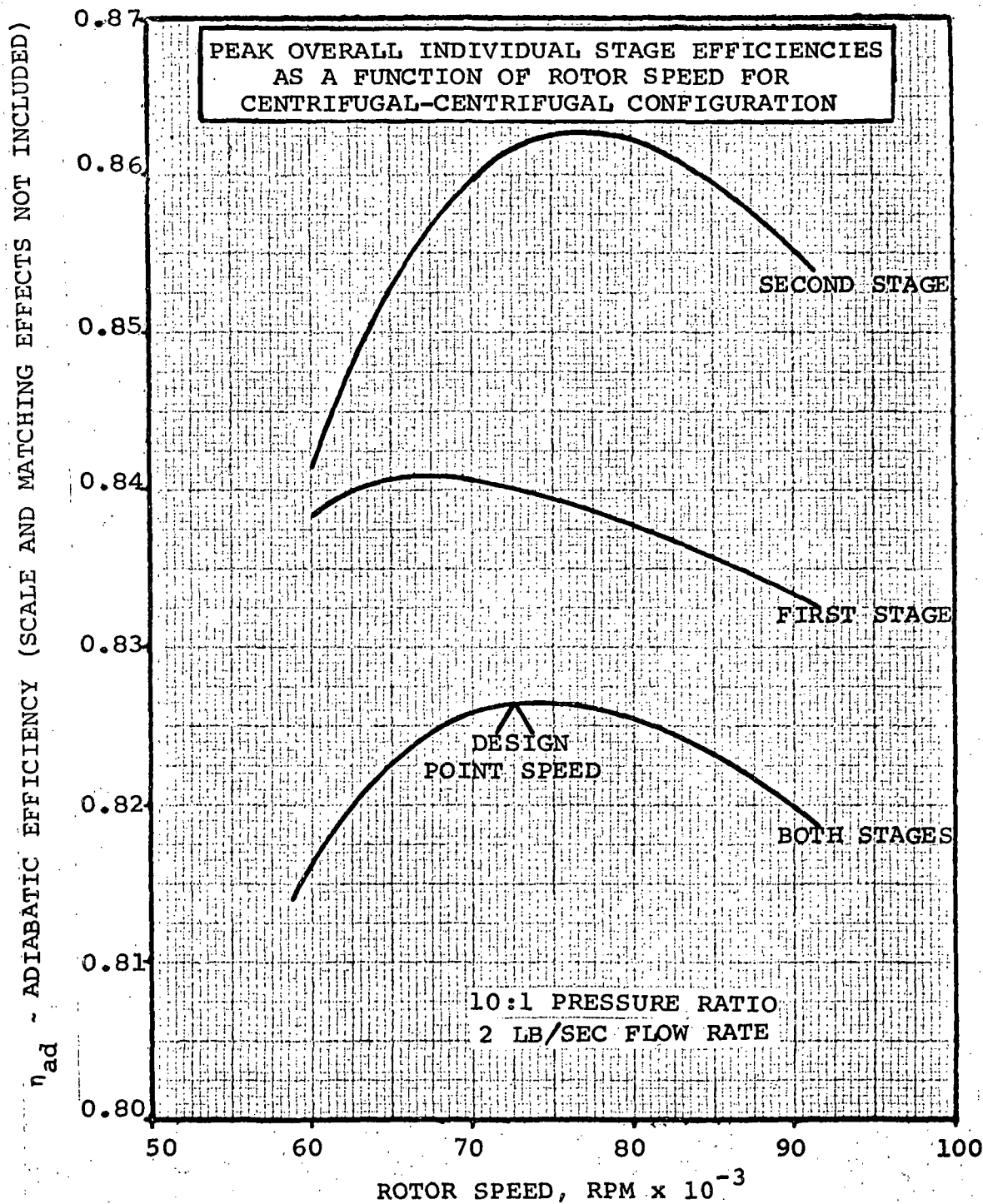


Figure 3.



flow to the first stage of 8.0 pounds per second. Predicted performance for this configuration from the polytropic efficiency correlation is 81.6 percent. The difference, 1.3 points, is attributed to the fact that in order to obtain the operating range required for a practical two-stage compressor, it is often necessary to match the two stages so that their individual peak efficiencies do not coincide at the design operating point. Thus, even though each stage may achieve the peak efficiency level indicated by the specific speed correlation, the overall compressor peak efficiency may be significantly lower than the value obtained by assuming both stages to be operating at their peaks simultaneously.

It seems logical to assume that the 10/1 compressor would require a similar matching to insure good range and, therefore, the overall optimum efficiency should be lowered about 1.3 points to account for this effect.

In addition to a stage matching correction, a scale must be applied to the predicted performance to account for the lower airflow of the present design. Predicted efficiency from the polytropic performance correlations is based on experimental data for centrifugal compressors with corrected flows of 7.0 pounds per second or higher. At the 2.0 pounds per second airflow of the present design, clearance problems and secondary flow effects are more severe than for a corresponding condition in the empirical correlation. Experience has shown that a decrement of 2.3 points in the overall adiabatic efficiency is necessary to account for scaling down to the 2.0 pounds per second airflow. Thus, the combined correction for the two-stage centrifugal combination is 3.6 points (staging loss plus flow rate scaling). This results in a predicted overall adiabatic efficiency for the centrifugal-centrifugal configuration of 79 percent.

A sketch showing a meridional view of the flowpath for the centrifugal-centrifugal configuration is presented as figure 4. In this design the Mach number at the entrance to the transition section between stages is 0.3. This is a reasonable level for efficient turning in the transition duct. Flow leaves the second-stage diffuser at an average Mach number of 0.2. This value was a requirement of the contract.

Axial-Centrifugal Compressor Configuration

Axial compressor performance prediction requires much more parametric definition than for centrifugal compressor performance. A computer program has been developed by AiResearch which predicts stage efficiency of an axial compressor for specified conditions of inlet corrected flow, rotational speed, and stage pressure ratio. The program solves for conditions along the pitch line with continuity being satisfied on a one-dimensional basis. The rotor and

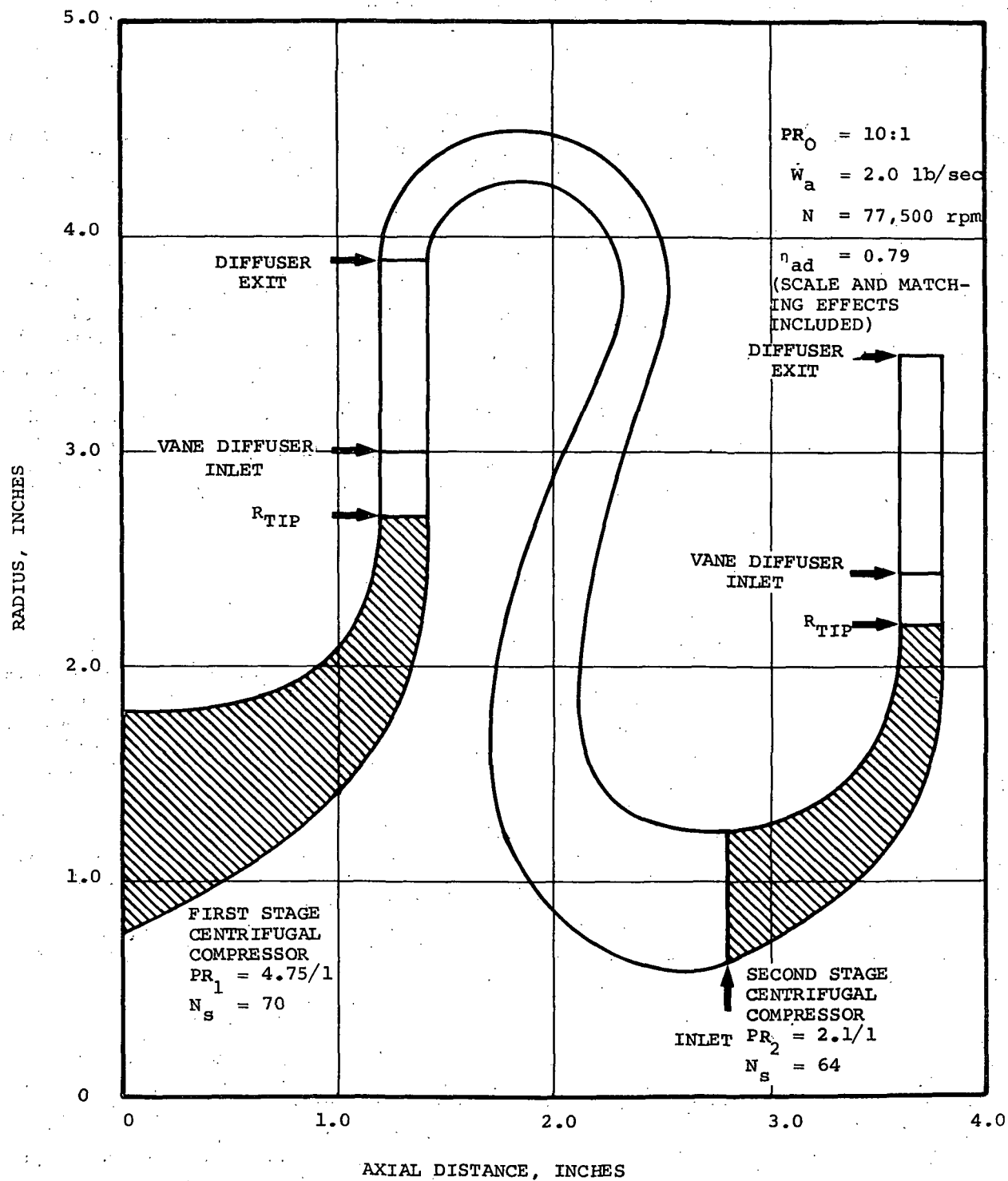


Figure 4. - Meridional View At Flow Path For Centrifugal-Centrifugal Configuration.



stator efficiencies are calculated from mean effective profile loss coefficients using pitch line flow conditions. Loss coefficients for both shock losses and profile losses are computed as briefly discussed in the following paragraph.

The shock loss in the blade tip regions is directly related to boundary layer separation along the blade which is governed by the static pressure rise across the shock. If the shock is strong enough to separate the boundary layer, the losses will be greater than that associated with a normal shock at the inlet relative Mach number. However, if the boundary layer does not separate, the shock losses can be lessened. A correlation of the limiting static pressure rise that the boundary layer can sustain before separating was derived from shock separation data for turbulent boundary layers on a flat plate as a function of Mach number (ref. 1).^{*} An average pitch line Mach number corresponding to:

$$M_{avg} = \frac{1.0 + M_{tip}}{2}$$

was used to calculate a normal shock loss for the entire blade. This value of loss was then multiplied by a ratio of total pressure rise across the blade to the limiting value for boundary layer separation to obtain shock-related losses. The blade element profile losses were based on a correlation of AiResearch experimental data (airflow of 20 to 30 lb/sec) in the form of loss coefficient versus D-factor as done in Reference 2.

The rotational speed is determined from the inlet conditions, the desired work input, and hub turning across the rotor. This speed is continuously corrected as the work input is varied to achieve the required overall pressure ratio. After the program results converge, the vector diagram for the rotor and stator are calculated and a preliminary size established for the compressor stage.

The results from this computer program are plotted (figure 5) in nondimensional form for an assumed absolute inlet Mach number of 0.6 and an air angle of ten degrees at the rotor hub exit station. Several different hub exit air angles were investigated ($\beta_{H2} = 0; 10^\circ, \text{ and } 20^\circ$) with the results showing the same general trend with hub radius ratio and pressure ratio. The selected air angle at the rotor hub exit ($\beta_{H2} = 10^\circ$) was found to be a good representation of several existing axial compressor stages. Measured performance of these axial stages compare quite favorably with that calculated by the program. It should be noted that these axial stages are larger and have design corrected flows much higher than the present design. Initial design calculations were made without any scaling.

^{*}Refer to Appendix F for list of references.

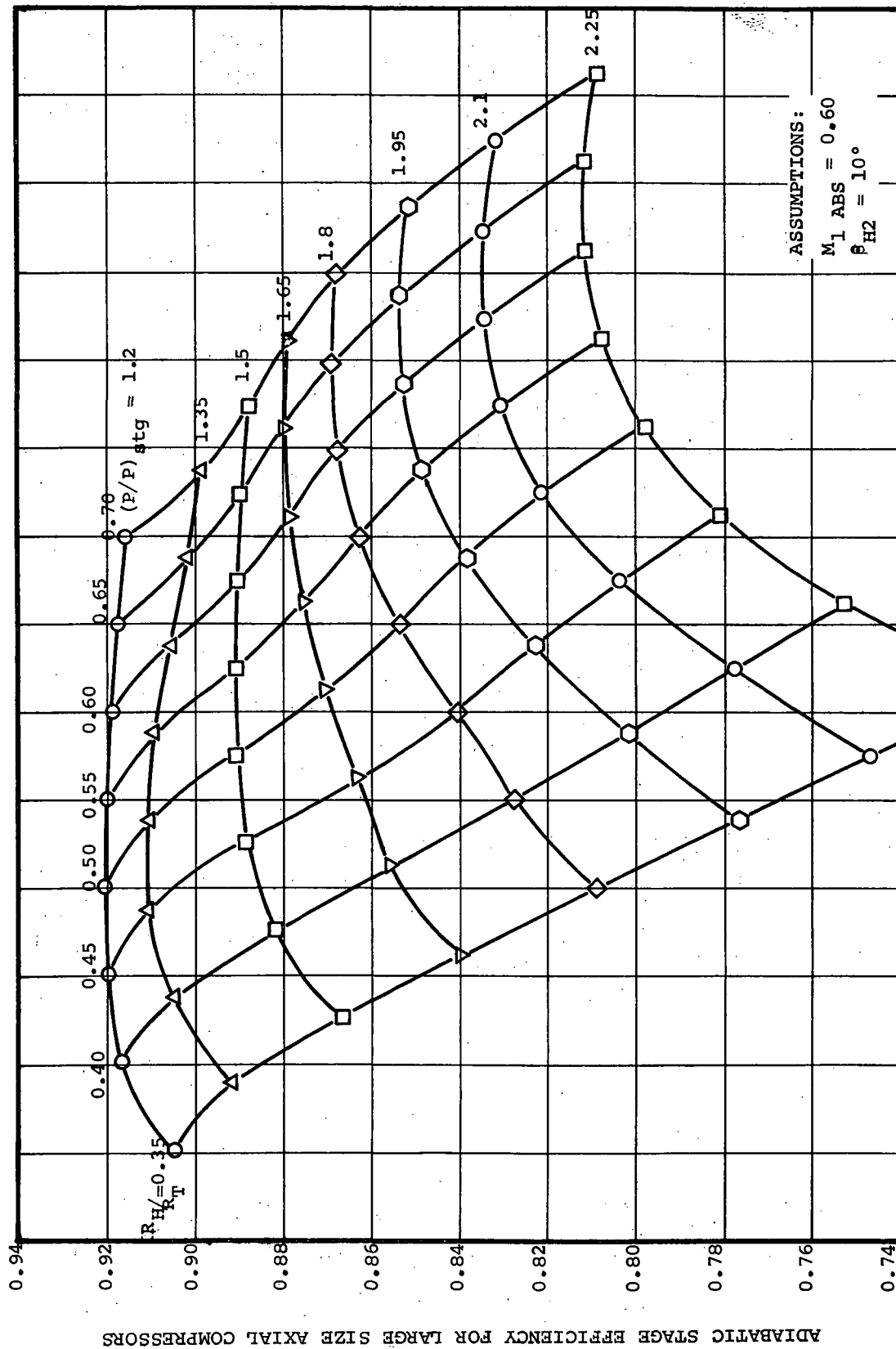


Figure 5. - Axial Compressor Stage Performance As A Function Of Hub/Tip Ratio.

ADIABATIC STAGE EFFICIENCY η_s STAGE (NO SCALE OR MATCHING EFFECTS INCLUDED)

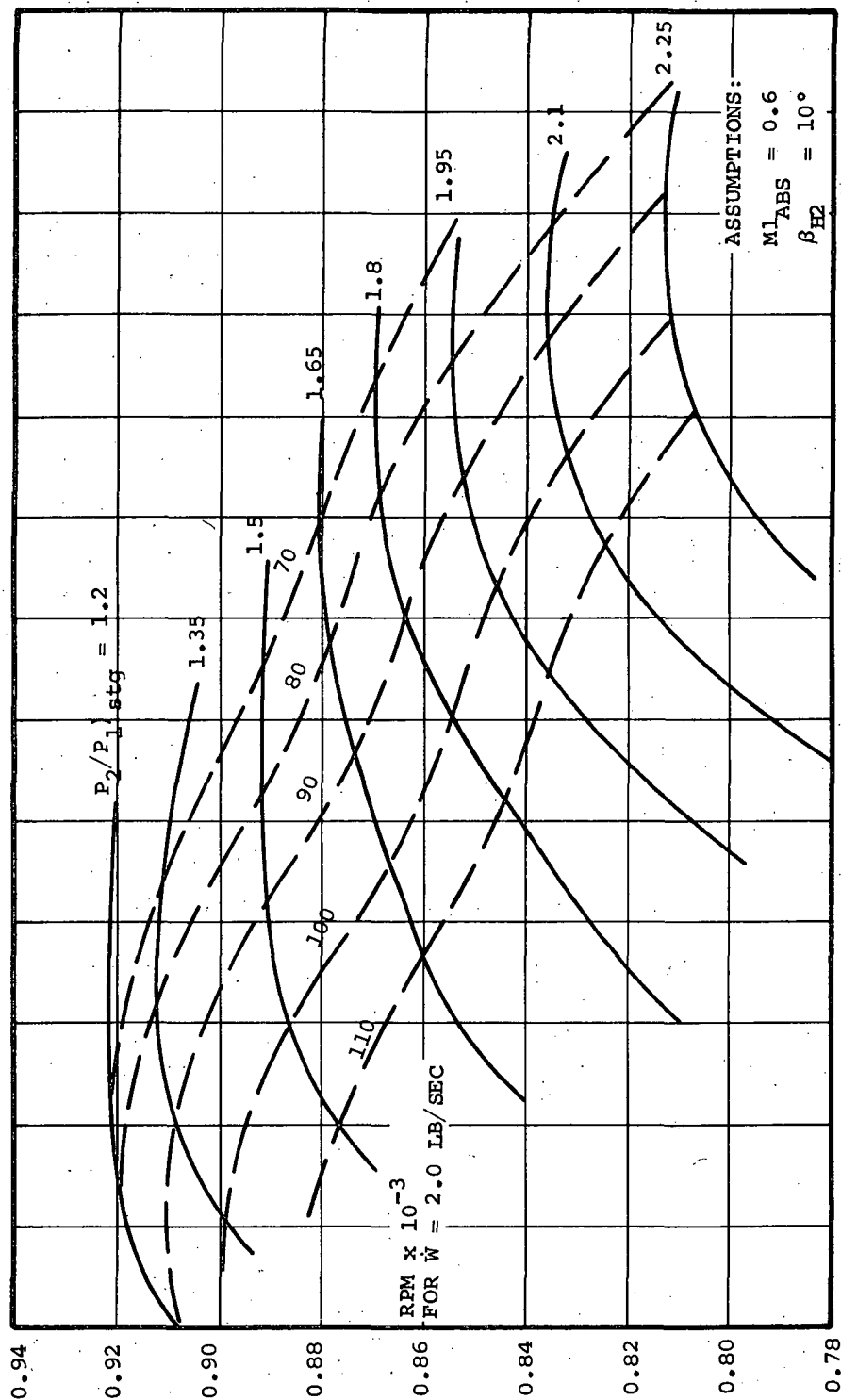


Figure 6. - Axial Stage Performance As a Function Of Rotor Speed For 2 lb/sec Flow.

effects on performance included. A discussion of overall scaling effects is undertaken in the latter portion of this section. The nondimensional results in figure 5 are converted to dimensional results in figure 5 are converted to dimensional results by specifying the stage weight flow and inlet conditions. Axial-stage performance at constant values of rotative speed for 2 lb/sec flow rate is presented in figure 6.

Overall compressor performance for an axial first-stage followed by a centrifugal compressor second stage is obtained from the design point matching program. In this program, the axial-stage performance is input as a function of first-stage pressure ratio at constant wheel speed. The centrifugal stage performance is obtained from the specific speed correlation described previously. The program computes overall performance for a 10/1 pressure ratio stage as a function of input first-stage pressure ratio values and curve fits the results to define the optimum pressure ratio split between stages. No matching penalty has been included.

A summary of the predicted overall performance for the axial-centrifugal compressor configuration is presented in figure 7. Overall compressor efficiency is shown as a function of pressure ratio across the axial stage for several values of rotor speed. Peak overall compressor efficiency for each speed is indicated by the arrows in this figure. Note that overall efficiency increases with rotor speed. The increase is directly attributable to the centrifugal stage operating at a more favorable specific speed condition at higher rotor speeds. The optimum wheel speed for peak overall compressor efficiency is above 100,000 rpm. Turbine stress considerations for this size engine have shown the wheel speed should be limited to approximately 90,000 rpm. Therefore, no attempt was made to define an optimum efficiency above 100,000 rpm in the axial-centrifugal combination. Design point wheel speed was set at 90,000 rpm for this configuration. Design conditions for this configuration are summarized in the following tabulation:

DESIGN CONDITIONS
AXIAL-CENTRIFUGAL COMPRESSOR

	<u>First-Stage</u>	<u>Second-Stage</u>	<u>Overall</u>
Compressor Type	Axial	Centrifugal	-
Rotor Speed, rpm	90,000	90,000	90,000
Tip Relative Mach Number	1.4	1.192	-
Pressure Ratio	1.73/1	5.78/1	10/1
Specific Speed	235	54.2	N/A
η_{ad} (no scale or matching effects included)	0.866	0.821	0.813

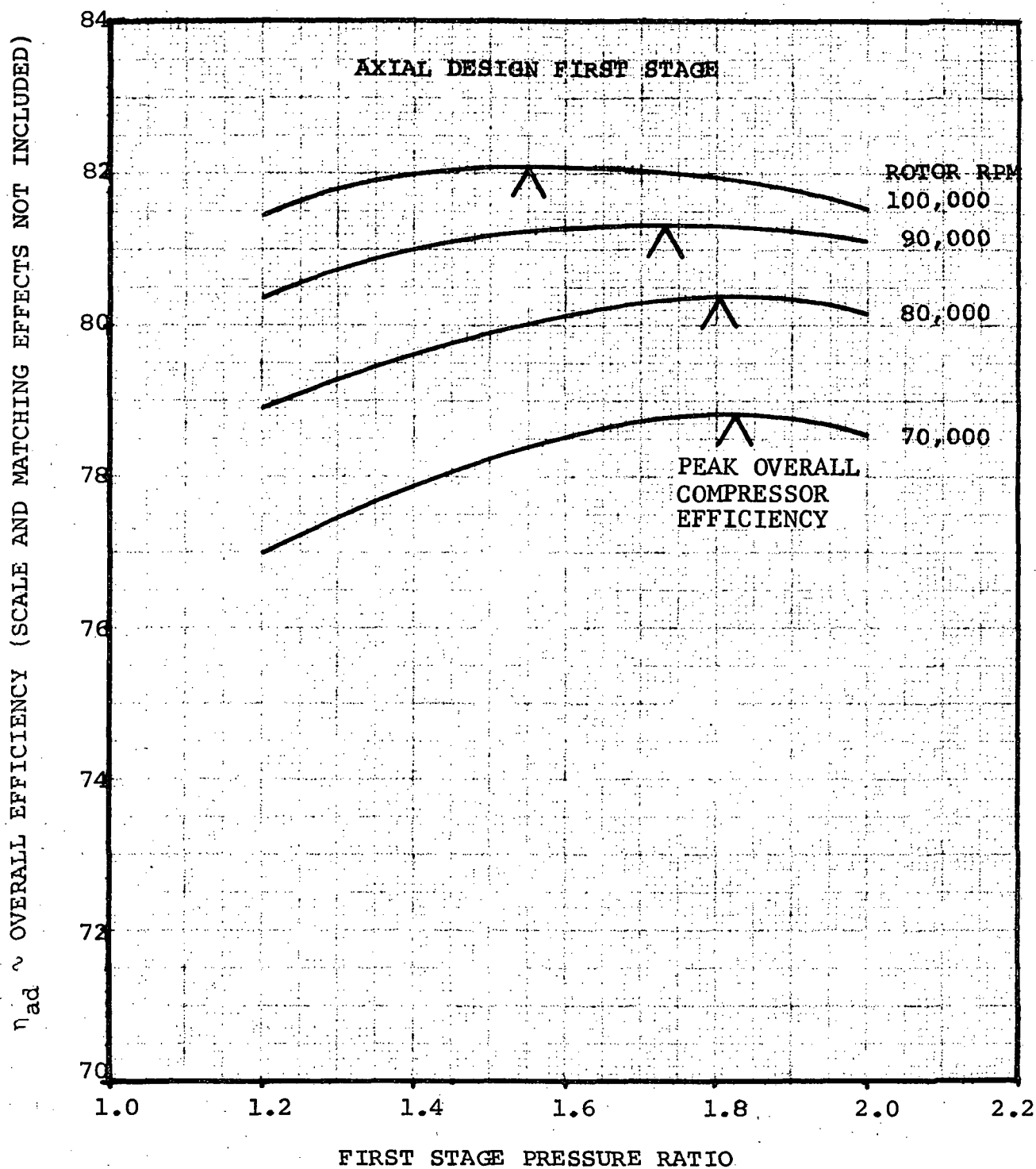


Figure 7. - Overall Efficiency vs 1st Stage Pressure Ratio
Axial-Centrifugal Configuration, 2 lb/sec Flow
Rate, 10/1 Overall Pressure Ratio.

Again, it should be noted that scaling and stage matching effects have not been included in the efficiencies stated above. Little data is available to estimate the effects of scaling axial flow compressors to low airflows. Therefore, in scaling the axial-centrifugal configuration, the incremental effect of size on overall efficiency was assumed to be the same as that estimated for the centrifugal-centrifugal configuration. Application of a total correction of 3.6 points to the axial-centrifugal configuration indicates that this configuration should have an overall adiabatic efficiency of 77.7 percent at design conditions (turbine speed limit). This assumes that the axial stage scales identically with a centrifugal stage. In the axial-centrifugal stage combination, the centrifugal stage does about five times as much work as the axial first-stages. Therefore a scaling effect error for the axial stage would have a minimum effect on the overall efficiency.

A meridional view of the flow path through the axial-centrifugal compressor combination is presented as figure 8. Mach number in the transition section between stages is approximately 0.43. Diffuser exit conditions for the second-stage centrifugal compressor correspond to an average Mach number of 0.2 as required.

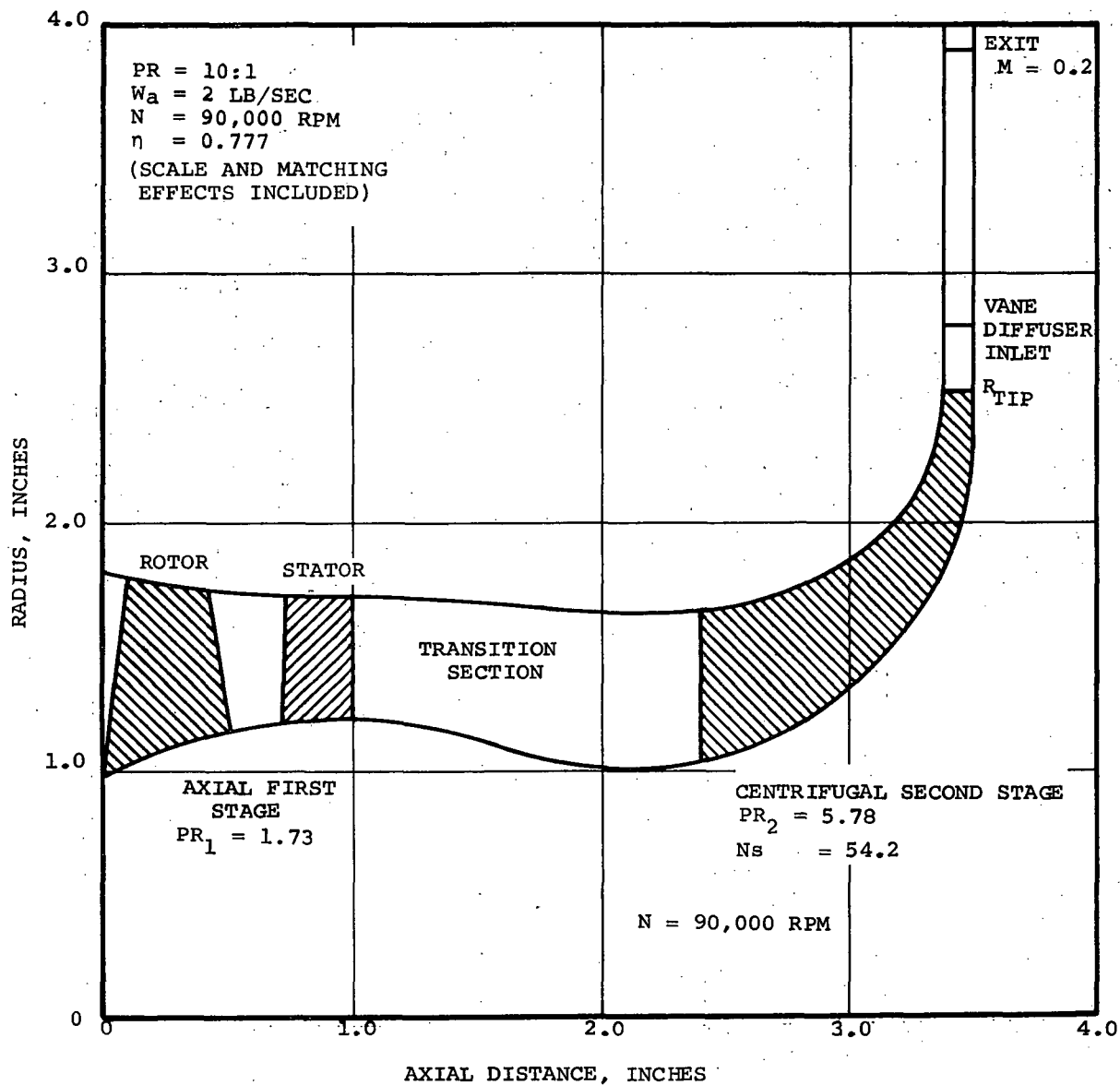


Figure 8. - Meridional View of Flow Path For Axial-Centrifugal Configuration.

MIXED-FLOW CENTRIFUGAL CONFIGURATION

The design technique employed for a conventional mixed-flow compressor is identical to that currently used for centrifugal compressor design. Based on this fact, the specific speed efficiency correlation for centrifugal compressors is also used to predict the efficiency level for the mixed-flow configuration. This, of course, yields the same result as the two-stage centrifugal configuration analysis, except that the mixed-flow configuration has a longer axial length.

In an attempt to improve the efficiency potential of a mixed-flow type of compressor, a new mixed-flow compressor concept was proposed. This concept which embodies a combination of axial design techniques with a mixed-flow type of flowpath was given the name conical-flow compressor to distinguish it from the conventional mixed-flow compressor.

Fundamentally, the conical-flow compressor combines axial flow compressor blade shapes with a large radius change (analogous to that occurring across a mixed-flow or centrifugal compressor rotor). Axial compressor design criteria are used to select blade loadings and loss estimates. Centrifugal compressor design criteria are used in selecting the design relative velocity ratios across the rotor. The capability for improved performance arises from the use of a large change in radius, which gives increased static pressure rise, with blade loadings designed to axial compressor loading criteria. If blade aspect ratios are kept similar to those acceptable to axial compressor design criteria, it is felt that secondary flow losses, which comprise a large portion of conventional mixed-flow losses, will be minimized. Frictional losses due to large blade surface areas will also be reduced. Additional advantages may be achieved by use of a tandem blading in the conical flow rotor and/or stator.

There is no data available for this type of compressor on which to base a performance prediction. Therefore, the approach used in making performance calculations on the conical-flow compressor was to assume that the pressure rise occurring due to radius change did not directly influence boundary layer growth. This approach has been used in the calculation of boundary layer growth in centrifugal impellers at AiResearch. Reasonable agreement has been achieved between losses based on loss correlations and boundary layer calculations up to the point of separation. Good agreement has also been obtained between the predicted point of boundary layer separation and experimental indication of boundary layer separation using lamp black traces on the surface of impellers. This assumption permits use of criteria established for axial flow blading to calculate blade losses for conical-flow compressor.

Various conical flow configurations were examined analytically. The performance prediction computations involved an iteration process where a meridional shape was assumed to specify a radius change across the blade row. From the desired pressure ratio and assumed loss coefficients, inlet and outlet velocity diagrams were calculated at several radial positions. These velocity diagrams were used to compute D-factors and shock losses (similar to procedure used for axial stages described earlier) which were converted into loss coefficients from a loss correlation for axial flow blading (Reference 2) for the computation of new velocity diagrams. Once there were no further changes in the loss coefficients between successive calculations, a satisfactory flow solution was assumed.

After a satisfactory flow solution was obtained, the hub, mean, and tip vector diagrams were examined at the blade inlet and exit stations. The variation in velocities from hub-to-tip, the air angle changes across the blade, and the relative velocity ratio across the rotor tip sections were critically examined for consistency with axial flow design practice. Where a single rotor was used, the relative velocity ratio for the tip section was limited to approximately 0.6. With two rotor blade rows, this limit was increased to the neighborhood of 0.65 for each row to provide additional stall margin and a small degree of conservatism to the design. Where undesired values were evident from the vector triangles, a change in meridional contours (i.e., flow width, wall shape, and/or wall curvature) was necessary and a new flow solution obtained.

A summary of the configurations examined by the method just described is shown on table I. These are listed in chronological order to illustrate the direction in which the study progressed. In the first two cases investigated, a single rotor and single stator were employed in a conical flow configuration with a 45-degree meanline slope at the stator exit. Based on previous computations made for the axial-centrifugal arrangement, a design pressure ratio of 2.5 at wheel speeds of 65,000 and 80,000 rpm was examined.

At the lower speed, the flow solution indicated that too much turning was needed to reach the design pressure ratio (the rotor hub exit flow was overturned to discharge the flow in the direction of rotor rotation). The operating characteristics in an engine would be undesirable with this velocity diagram because, as weight flow is reduced, the hub work decreases. Thus, engine acceleration characteristics might be undesirable. Furthermore, the compressor would be more sensitive to inlet distortion. A high rotor speed would avoid this situation by meeting the work requirements with less turning in the blades. At 80,000 rpm, the required flow turning was satisfactory but the diffusion factors across the blades were greater than the normal range for moderate loss coefficients. Thus, the profile losses for a single rotor would be too high to efficiently produce a pressure ratio of 2.5. Consequently, a conical flow rotor with two

TABLE I.

CONICAL FLOW FIRST STAGE

TWO STAGE, 10/1 PRESSURE RATIO PERFORMANCE SUMMARY

N	(PR) ₁	(η_{ad}) ₁ [*]	(η_{ad}) ₂ [*]	(η_{ad}) ₀ [*]	DESCRIPTION
<u>SINGLE BLADES</u>					
65,000	2.5	Too Much Turning Required			Single Rotor/ Single Stator
80,000	2.5	"D" Factors Off Curve			Single Rotor/ Single Stator
<u>TANDEM ROTORS</u>					
65,000	2.5	0.9	0.802	0.8151	Tandem Rotor/ +Single Stator
70,000	2.0	0.9431	0.7975	0.8192	Tandem Rotor/ +Single Stator
70,000	2.5	0.9150	0.8123	0.8289	Tandem Rotor/ +Single Stator
70,000	3.0	0.8758	0.8248	0.8233	Tandem Rotor/ +Single Stator
<u>TANDEM ROTORS AND STATORS</u>					
70,000	2.5	0.9308	0.8123	0.8370	Tandem Rotor/ Tandem Stator
70,000	2.96	0.8983	0.8241	0.8345	Tandem Rotor/ Tandem Stator
<u>REALIGNED ROTORS (TANDEM STAGES)</u>					
70,000	2.5	0.9395	0.8123	0.8406	Tandem Rotors/ Tandem Stators
70,000	3.06	0.9067	0.8265	0.8413	Tandem Rotors/ Tandem Stators

*Efficiency level valid for compressors with corrected flows of 8 lb/sec or more.

blade rows in tandem was investigated in order to lower diffusion factors and, thus the rotor losses.

The initial tandem rotor configuration investigated was with a design pressure ratio of 2.5 and a design speed of 65,000 rpm. The flow solution for the tandem rotor configuration for these conditions indicated that the flow overturning problem of the single rotor was eliminated as a result of a larger radius change across the rotor with this tandem configuration. Computed stage efficiency for this tandem rotor-single stator configuration was 90.0 percent. (It should be noted that these efficiency values have not been depreciated for size effects. A discussion of size effects on performance will be presented later.) When this configuration was matched to a second-stage centrifugal compressor, the estimated overall efficiency for both stages was 81.5 percent at 10/1 pressure ratio. A meridional view of this tandem rotor-single stator configuration is presented in figure 9.

Another tandem rotor-single stator conical flow compressor was examined at a pressure ratio of 2.5 but with a wheel speed of 70,000 rpm. The effects of wheel speed on component and overall efficiencies are shown on table II.

A clear performance advantage for the higher wheel speed is evident since the rotor and stator efficiencies are higher due to reduced blade loadings. It is quite possible that further increases in rotational speed would show some performance improvement based on the analytical model used here, which define losses in terms of a normal shock loss at the inlet relative Mach number and a blade profile loss. Experience has shown that, above an inlet relative Mach number of approximately 1.3, the shock strength is often sufficient to cause boundary layer separation on the suction surface of the rotor. When this happens, the losses increase rapidly and the loss model used here is no longer applicable. The inlet relative Mach number for the rotor tip section at 70,000 rpm is 1.29. Therefore, design wheel speed for the remaining mixed-flow configurations analyzed here was specified at 70,000 rpm in an attempt to avoid shock-separation problems at design conditions.

The effect of first-stage pressure ratios of 2.0, 2.5, and 3.0 on component and overall efficiency at 70,000 rpm was investigated and is shown on table III. These results are for one tandem rotor-single stator conical flow configuration in combination with a second-stage centrifugal compressor. These results show first-stage efficiency decreases with increasing stage pressure ratio as might be expected. At the same time, the centrifugal stage performance increases with first-stage pressure ratio reflecting more favorable specific speed values. The combined effect on the overall efficiency at 10:1 pressure ratio produces an optimum first-stage pressure ratio for the tandem rotor-single stator conical flow configuration of approximately 2.5 to 2.6.

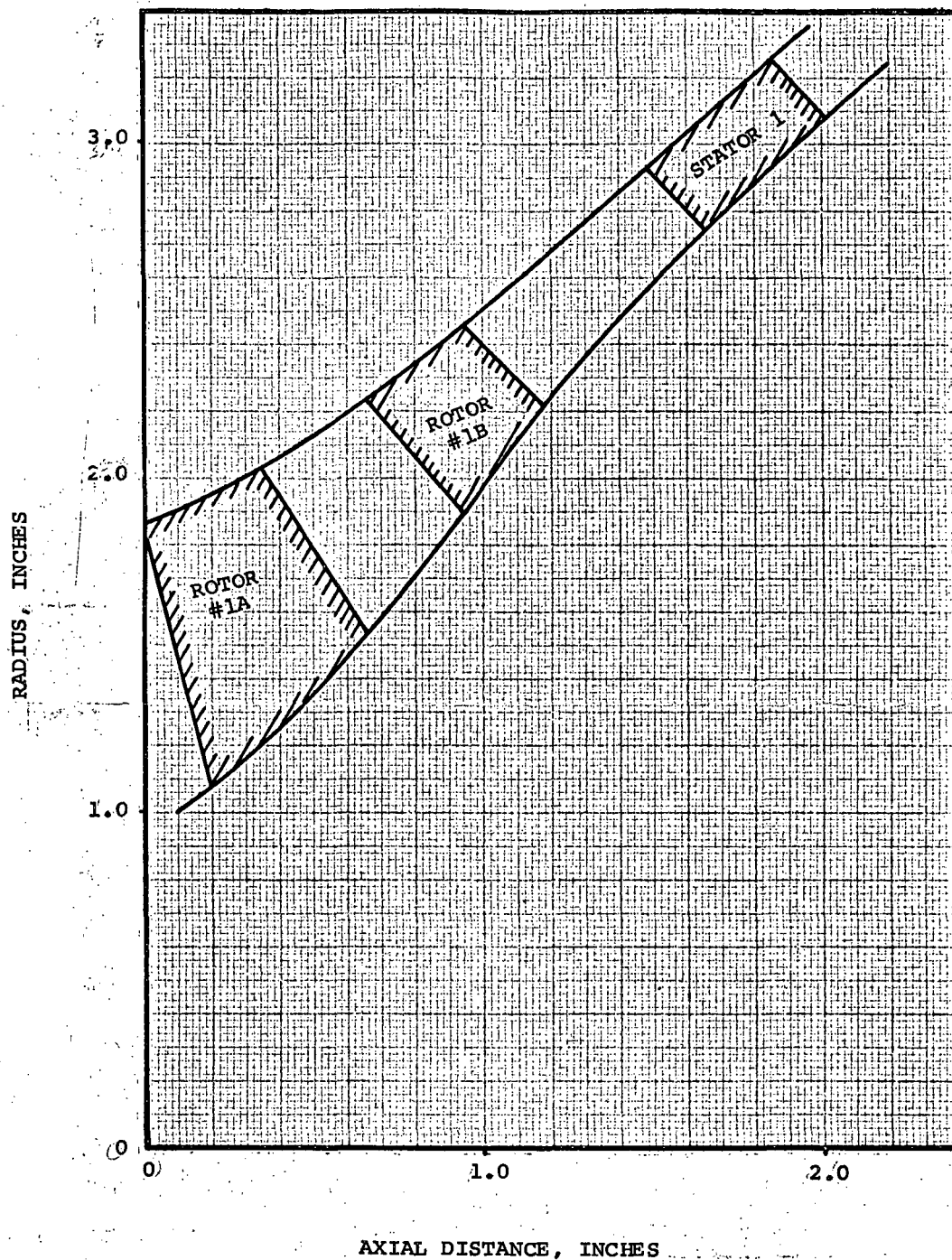


Figure 9. - Meridional View - Conical Flow Stage - Tandem Rotor and Single Stator.

TABLE II.
EFFECT OF WHEEL SPEED ON PERFORMANCE
OF CONICAL-CENTRIFUGAL COMPRESSOR

Wheel speed	65,000 rpm	70,000 rpm
Conical flow stage		
(a) Pressure ratio	2.5	2.5
(b) Rotor efficiency, η_{ad}^*	0.959	0.963
(c) Stage efficiency, η_{ad}^*	0.90	0.915
Centrifugal stage		
(a) Pressure ratio	4.0	4.0
(b) Specific speed	41.3	44.9
(c) Stage efficiency, η_{ad}^*	0.802	0.822
Combined stages		
(a) Pressure ratio	10.0	10.0
(b) Overall efficiency, η_{ad}^*	0.815	0.829

*Efficiency level valid for compressors with corrected flow of 8 lb/sec or larger.

TABLE III.

FIRST STAGE PRESSURE RATIO COMPARISON
TANDEM ROTOR, SINGLE STATOR

1.	Wheel speed, rpm	70,000	70,000	70,000
2.	Conical flow stage			
	(a) Pressure ratio	2.0	2.5	3.0
	(b) Rotor efficiency, η_{ad}^*	0.969	0.963	0.946
	(c) Stage efficiency, η_{ad}^*	0.943	0.916	0.876
3.	Centrifugal stage			
	(a) Pressure ratio	5.0	4.0	3.33
	(b) Specific speed, N_s	42.4	44.9	47.6
	(c) Stage efficiency, η_{ad}^*	0.798	0.812	0.825
4.	Combined stages			
	(a) Pressure ratio	10.0	10.0	10.0
	(b) Overall efficiency *	0.819	0.829	0.823

*Efficiency level valid for compressors with equivalent flows of 8 lb/sec or more.

At this point in the investigation, it became evident that the blade loadings for the single-stator configurations were quite large and that there could be an overall performance improvement associated with tandem stators. A conical flow compressor configuration was then laid out which included a tandem rotor and a tandem stator. The effect of tandem stators on the first-stage component efficiencies is listed as follows:

COMPARISON OF TANDEM AND SINGLE STAGE STATOR

Number of stators	Single	Two
Wheel speed, rpm	70,000	70,000
Conical flow stage:		
(a) Pressure ratio	3.0:1	2.96:1
(b) Rotor efficiency, η_{ad}^*	0.946	0.944
(c) Stage efficiency, η_{ad}^*	0.876	0.898

*Efficiency levels valid for compressors with equivalent flows of 8 lb/sec or more.

The comparison indicates that the tandem stator configuration is 2.2 points better in stage efficiency than the single stator design at a stage pressure ratio of 3/1. This difference is equivalent to a gain of 1.2 points of overall efficiency for the combined two-stage performance as shown on table III. A similar comparison can be made for a 2.5:1 pressure ratio first stage by referring to the results on table III. This indicates the first-stage performance for tandem stators is 1.6 points higher than a single stator with the overall two-stage efficiency gain of approximately 0.8 point. The relative comparison of component efficiencies between the different first-stage pressure ratio cases appears reasonable considering the fact that stator loadings are much higher for the 3/1 pressure ratio stage. Therefore, there is more to be gained by the use of a tandem stator configuration for the higher first-stage pressure ratio design.

Preliminary stress calculations made for the initial rotor blade configuration, shown in figure 10 by dashed line, indicated that orientation of the blade approximately normal to the flow direction could cause blade stress problems because of the overhung blade configuration. As a result, a blade stacking arrangement where the blade edges are placed more nearly in a radial direction, as shown by the solid line in figure 10 was examined for efficiency and stress. This arrangement was found to be satisfactory from a stress standpoint and also produces a backward swept blade configuration

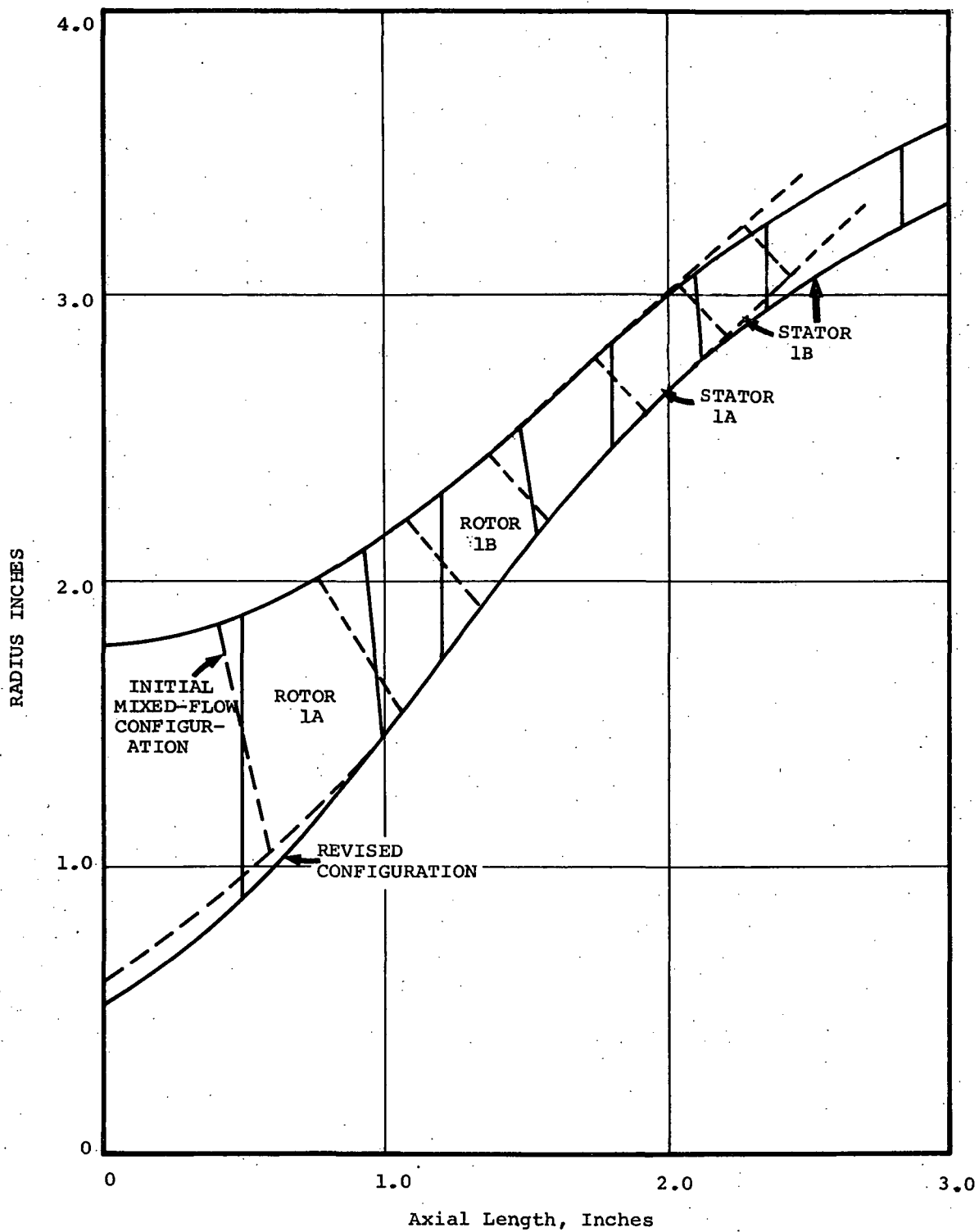


Figure 10. - Meridional View of Conical - Flow Stage.

with respect to the streamline flow path over the blades. Investigators of swept blades for axial compressors have indicated favorable effects of transonic compressors (References 3 to 7). The advantages of swept wings on high-speed aircraft are well understood at this time. The aerodynamic performance of a swept wing has been related to the component of relative velocity normal to the leading edge. Using this loss model, lower losses would be predicted for the backswept blade configuration. In the preliminary design calculations for the revised stacking arrangement, no attempt was made to include any benefit of leading edge sweep on the predicted performance results.

Performance for the different blade stackings is shown on table IV. This comparison indicates a slight performance advantage for the revised stacking arrangement despite the fact that blade sweep effects were not taken into consideration. Investigation of the detailed flow calculations indicated the revised stacking arrangement had a higher radius change between rotor inlet and exit stations than for the initial design. This, in effect, reduced the loadings for each rotor blade with a greater portion of the static pressure ratio generated by centrifugal forces.

The effects of first-stage pressure ratio on overall stage efficiency for tandem-rotor/single-stator configurations as previously discussed show that optimum first-stage pressure ratio was approximately 2.5:1. With the tandem-rotor/tandem-stator configurations the optimum first-stage pressure ratio shifts toward a value in the neighborhood of 3/1 (Table V). However, the difference in overall performance between the 2.5/1 and 3/1 cases is essentially insignificant in light of the approximate nature of the design calculations performed here. The true optimum condition appears to be within this range of design pressure ratios for the first stage. Therefore the 3/1 design was selected as the best configuration for a mixed-flow first stage based on the premise that the higher pressure ratio value would permit a better demonstration of the performance potential of the tandem-rotor/tandem-stator configuration.

A design overall efficiency of 84.1 percent was predicted for the selected conical flow compressor configuration. To be consistent with the performance estimates of the other candidate compressors, an efficiency decrement of 3.6 points was assumed for scaling and matching effects resulting in an adjusted efficiency of 0.805.

A meridional view of the two stage 10/1 pressure ratio conical-centrifugal compressor configuration is presented in figure 11. This shows the tandem-rotor/tandem-stator conical flow first-stage followed by a transition duct leading to the centrifugal compressor second stage. Average Mach number for the transition section is approximately 0.32 and the design Mach number for the second-stage diffuser exit is 0.2. Total stage length is approximately four

TABLE IV.

CONICAL-CENTRIFUGAL COMPRESSOR WITH
INITIAL AND REVISED ROTOR BLADE STACKING
(SEE Figure 10)

1.	Blade stacking	Initial	Revised
2.	Wheel speed, rpm	70,000	70,000
3.	Conical flow stage		
	(a) Pressure ratio	2.96	3.06
	(b) Rotor efficiency, η_{ad}^*	0.944	0.955
	(c) Overall efficiency, η_{ad}^*	0.898	0.907
4.	Centrifugal stage		
	(a) Pressure ratio	3.38	3.27
	(b) Specific speed, N_s	47.5	48.1
	(c) Stage efficiency, η_{ad}^*	0.824	0.827
5.	Overall compressor		
	(a) Pressure ratio	10.0	10.0
	(b) Overall efficiency, η_{ad}^*	0.834	0.841

*Efficiency level valid for compressors with equivalent flows of 8 lb/sec or more.

TABLE V.
DESIGN PARAMETERS AND PERFORMANCE RESULTS
TANDEM CONICAL FLOW COMPRESSOR

	<u>Tip</u>	<u>Mean</u>	<u>Hub</u>
ROTOR 1A (20 BLADES, AR = 1.028)			
SOLIDITY	1.25	1.5	2.33
TOTAL PRESSURE RATIO	1.82	1.78	1.75
EFFICIENCY, η_{ad} *	0.874	0.971	0.987
DIFFUSION FACTOR	0.443	0.418	0.399
ROTOR 1B (40 BLADES, AR = 0.84)			
SOLIDITY	1.57	1.68	1.79
TOTAL PRESSURE RATIO	3.27	3.19	3.32
EFFICIENCY, η_{ad} *	0.883	0.977	0.988
DIFFUSION FACTOR	0.441	0.362	0.333
STATOR 1A (53 BLADES, AR = 0.584)			
SOLIDITY	1.73	1.75	1.76
TOTAL PRESSURE RATIO	3.1	3.1	3.1
EFFICIENCY, η_{ad} *	0.837	0.948	0.922
DIFFUSION FACTOR	0.535	0.502	0.525
STATOR 2A (53 BLADES, AR = 0.495)			
SOLIDITY	1.5	1.57	1.69
TOTAL PRESSURE RATIO	3.06	3.07	3.04
EFFICIENCY, η_{ad} *	0.827	0.939	0.905
DIFFUSION FACTOR	0.523	0.483	0.502

*Efficiency level valid for compressors with corrected flows of 8 lb/sec or more.

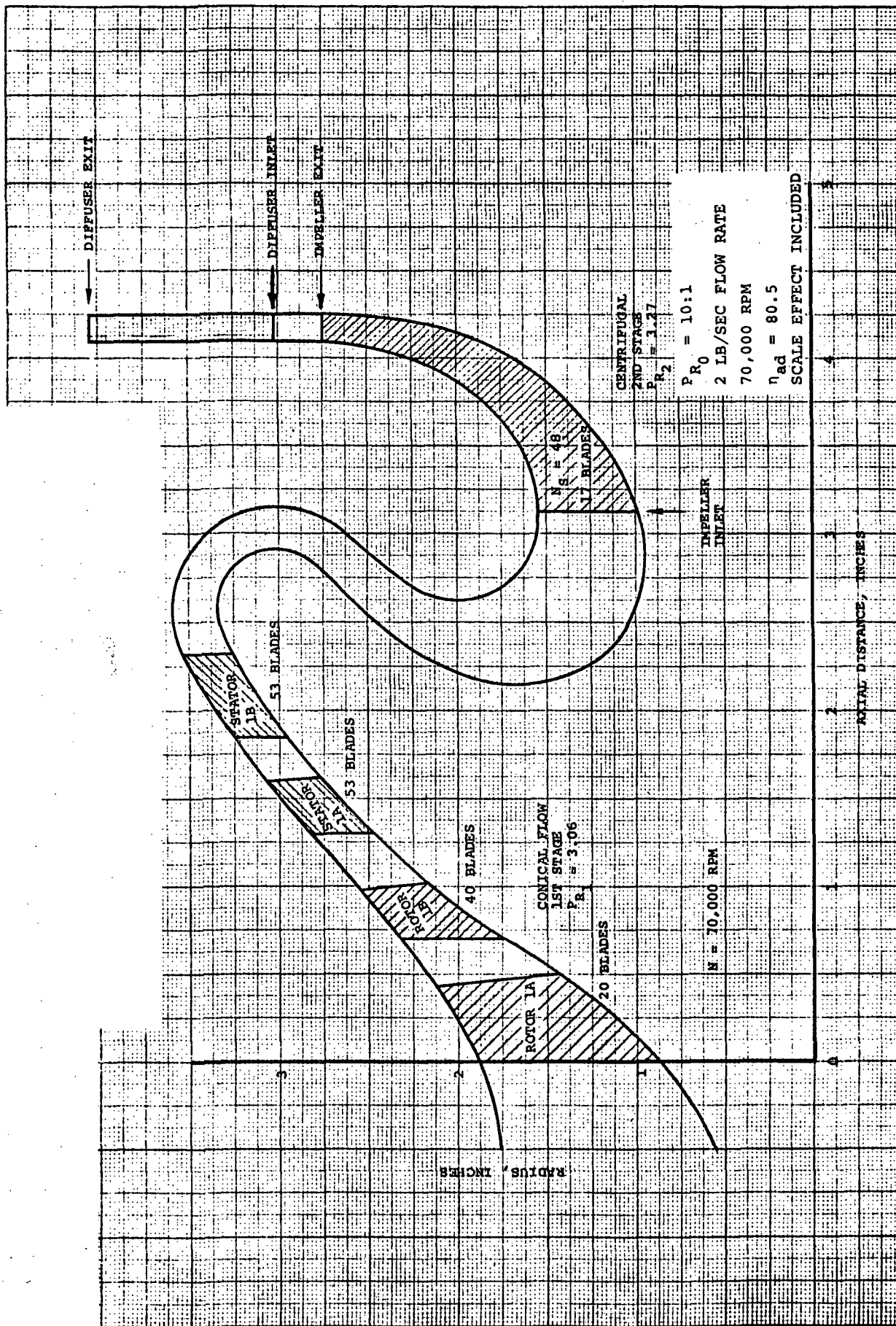


Figure 11. - Meridional View of Flow Path For The Mixed-Centrifugal Compressor Configuration.

inches with the maximum diameter of the mixed flow first stage being less than seven inches. Preliminary design vector triangles for the tandem-rotor/tandem-stator configuration are presented in figures 12 and 13. Additional design parameters and performance information along the tip, mean, and hub streamlines are presented on table V.

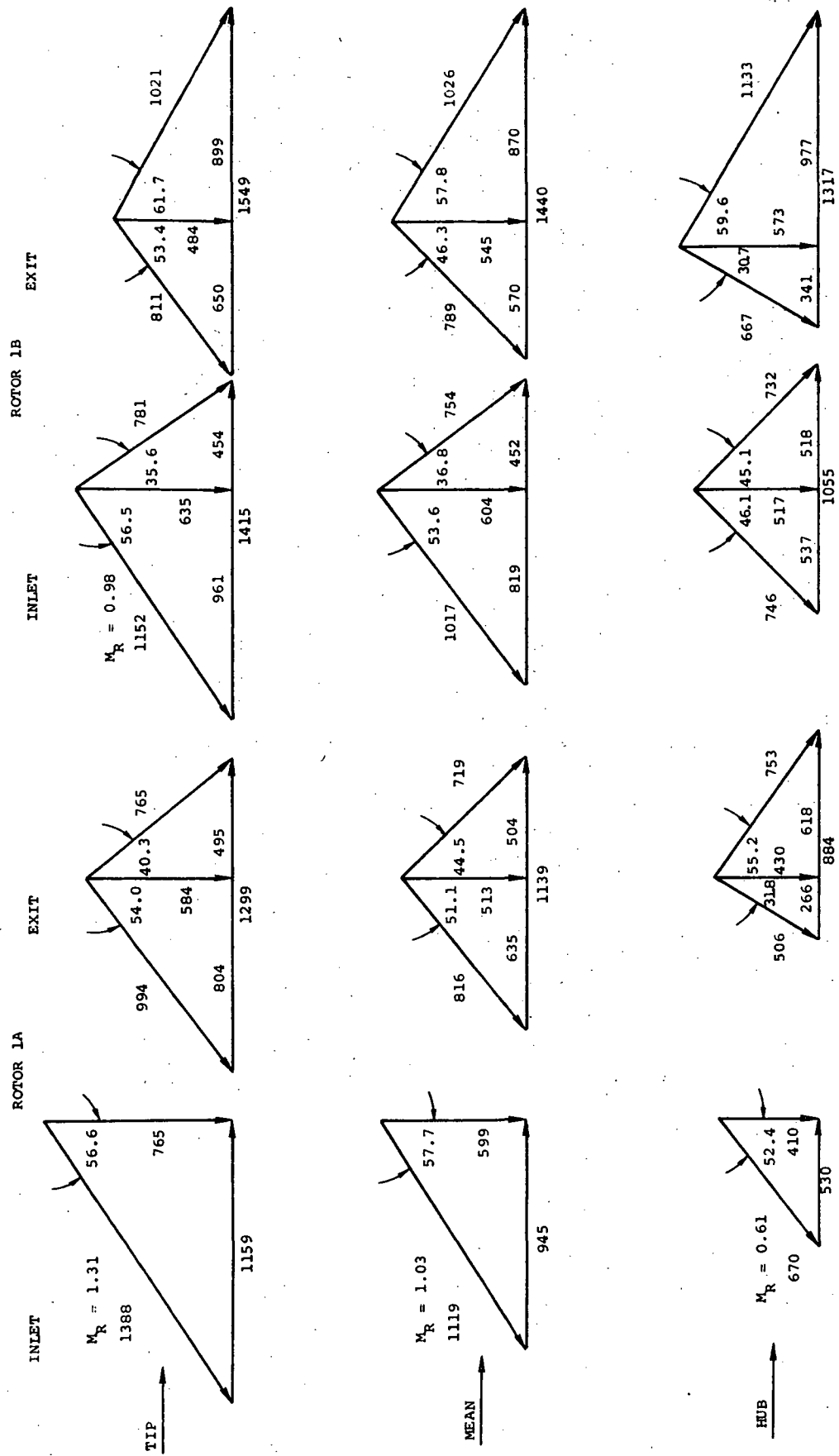


Figure 12. - Conical Flow Tandem Rotor Preliminary Design Vector Triangles.

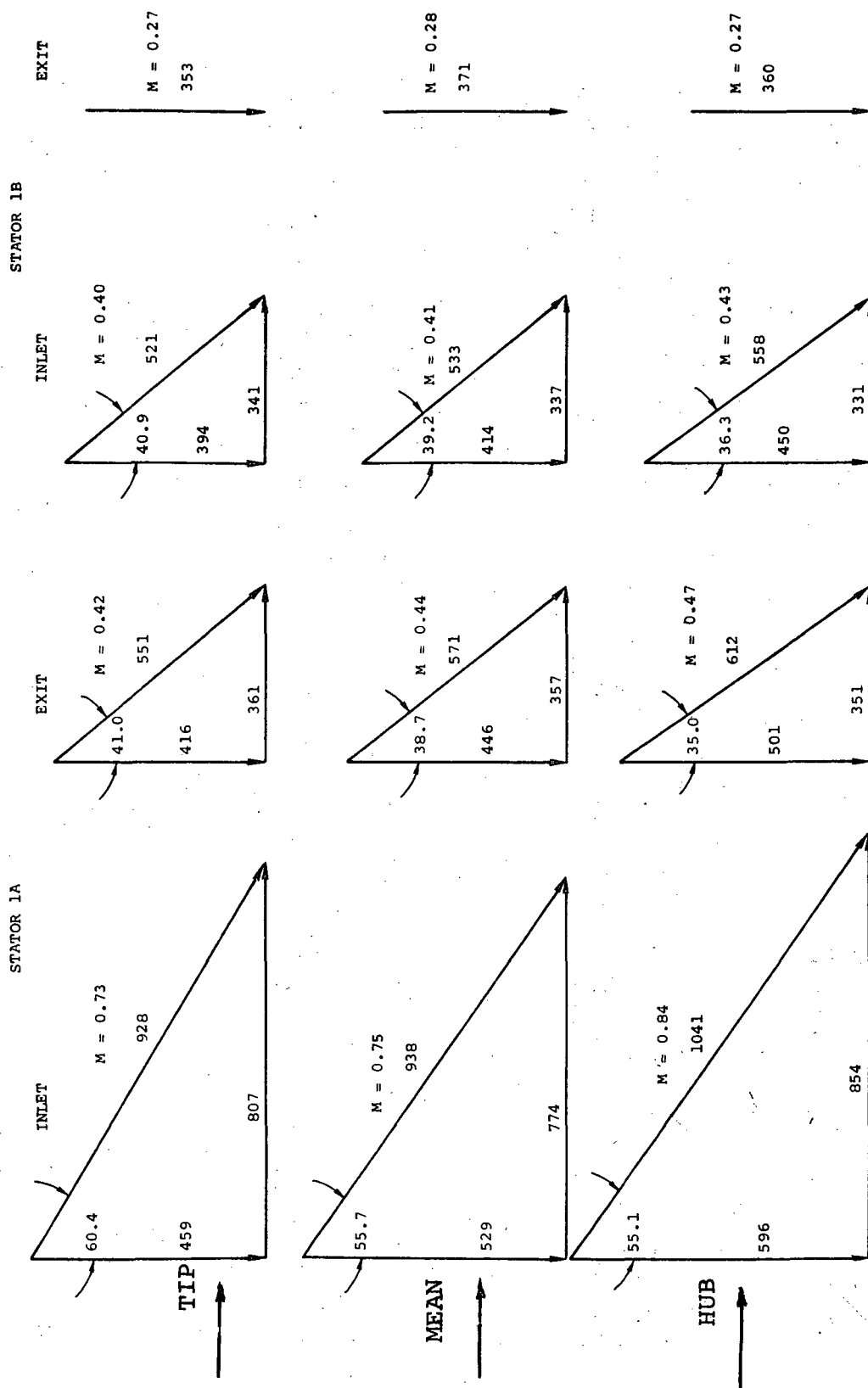


Figure 13. - Conical Flow, Tandem Stator Preliminary Design Vector Triangles.

COMPARISON OF CANDIDATE COMPRESSORS

In order to facilitate a comparison of the different candidate configurations, selected speeds, work splits, stage characteristics, and overall efficiency are tabulated on table VI.

The predicted overall efficiency of 0.790 for the centrifugal-centrifugal configuration is the most reliable because of recent AiResearch experience with a similar 11/1 pressure ratio compressor with eight pounds-per-second weight flow. The dominating factor in the overall efficiency is the rotating speed which was set at 72,500 rpm in order to place both stages as close to their optimum specific speed as possible.

The predicted overall efficiency of 0.777 for the axial-centrifugal configuration is less reliable than the centrifugal-centrifugal configuration due to a lack of scaling effect data on axial compressors. As discussed, this performance adjustment, of 3.6 efficiency points, used for the centrifugal-centrifugal configuration was also applied to this configuration. The predominating factor in the low overall efficiency of the axial-centrifugal compressor is the low specific speed of the second stage. It was indicated that operation at a higher rotative speed would improve the second-stage specific speed and, therefore, the overall compressor efficiency. Increasing the rotative speed was ruled out because the calculated turbine blade stress in an engine application would be excessive above 90,000 rpm.

The predicted efficiency for the conical-centrifugal configuration is the least reliable because of the complete lack of experimental data on the conical flow type compressor. However, the concept is believed to have an excellent chance for success because, based on axial flow design criteria, the design is conservative. The tip inlet relative Mach number was limited to 1.3 and the diffusion factor at the tip was limited to 0.44 for the rotors and 0.54 for the stator.

The overall efficiency for the conical-centrifugal configuration adjusted for scaling effects and matching is 1.5 points higher than the centrifugal-centrifugal configuration and 2.8 points higher than the axial-centrifugal configuration. The higher performance shown for the conical-centrifugal configuration is primarily a result of the high efficiency predicted for the conical flow first stage. This stage operates at a pressure ratio of 3.06/1 with a calculated adiabatic efficiency of 90.7 percent.

If this concept is successful, a less conservative first-stage design could give greatly improved second-stage specific speed and,

TABLE VI.
PREDICTED OVERALL PERFORMANCE COMPARISON

	<u>Cent-Cent</u>	<u>Axial-Cent</u>	<u>Conical-Cent</u>
1. Wheel speed, rpm	72,500	90,000	70,000
2. First stage	centrifugal	axial	conical
(a) Pressure ratio	4.75/1	1.73/1	3.06/1
(b) Specific speed	70	235	95
(c) Adiabatic efficiency*	0.84	0.866	0.907
3. Second stage	centrifugal	centrifugal	centrifugal
(a) Pressure ratio	2.11/1	5.78/1	3.27/1
(b) Specific speed	64	54	48
(c) Adiabatic efficiency*	0.862	0.821	0.827
4. Overall compressor			
(a) Pressure ratio	10/1	10/1	10/1
(b) Adiabatic efficiency*	0.826	0.813	0.841
(c) Scaled performance, η_{ad}	0.790	0.777	0.805

*Efficiency level valid for compressors with corrected flows of 8 lb/sec or larger.

therefore, greater gains in overall compressor efficiency than predicted herein. It is believed that the relative level of efficiency computed for large compressors is valid for the scaled compressors. Thus, only the magnitude of the difference between the centrifugal-centrifugal compressor and the other two configurations is subject to question. The use of a constant correction factor maintains the relative levels of efficiency and gives an indication of the levels of efficiency expected. A check was made to see how much error would be required in the conical flow stage efficiency prediction to make the overall conical-centrifugal performance equivalent to the two-stage centrifugal combination. The required value was 3.2 efficiency points. This means that the conical-compressor loss factors would have to be more than 30 percent in error, which is unlikely.

Before making a final selection of candidate compressors, several additional considerations were explored. These are discussed in the following sections.

STAGE COMPATIBILITY

Aerodynamic compatibility between the two stages is concerned with:

- (a) Design of the interstage duct for an efficient transition between stages
- (b) The off-design operation with regard to inlet guide vane requirements
- (c) The influence of compressor configuration on engine mechanical problems

With a two-stage centrifugal compressor combination, the transition duct makes a 180-degree turn followed by a 90-degree turn. While this would seem to be a rather tortuous flow path, AiResearch experience with similar transition sections has demonstrated very good performance with proper design. Recommended design practice in this case is to accelerate the flow through each turn; this practice results in very little distortion at the inlet to the second stage. By setting the Mach number at the diffuser exit from the first stage reasonably lower than the impeller inlet Mach number of the second stage, the necessary acceleration can be designed into the turns. The final meridional shape is analytically evaluated using the radial equilibrium flow program to ensure a favorable velocity distribution downstream of the transition duct.

The transition section for the conical-centrifugal stage combination is quite similar to that shown for the centrifugal stages but may require somewhat less overall turning, since the flow has an axial component at the impeller exit. This should make the design and performance of the transition duct for the conical-centrifugal stages more favorable than the corresponding centrifugal stage combination design. Again, the flow accelerates through each bend in the transition duct, and the velocity distribution to the second-stage is evaluated analytically. The first-stage exit and second-stage inlet Mach numbers can be adjusted to accomplish the desired acceleration. Therefore, the design and performance of the transition section for the conical-centrifugal stage combination would seem to present few, if any, problems based on AiResearch experience with staged centrifugal compressors.

A cursory look at the transition section between an axial stage followed by a centrifugal stage would seem to indicate few reasons for concern to the designer. The interstage flow requires little turning and the duct lengths are quite short. For high pressure

ratio, low hub/tip ratio designs, the absolute Mach number at the rotor hub discharge can be on the order of 1.0. This value must then be diffused to approximately $M = 0.45$ which requires a large amount of diffusion. This situation requires special design consideration to prevent deteriorated flow conditions at the centrifugal stage inlet.

Careful attention to design details can minimize or eliminate many pitfalls in the transition region design. As a first step, the axial stage should be designed to deliver as low a discharge Mach number as feasible while still maintaining high stage efficiency. Secondly, the inlet hub and tip diameters of the centrifugal stage are matched closely to the corresponding diameters on the axial stage to minimize any necessary turning of the flow. Then, potential flow and boundary layer analyses are made on the design meridional shape to assure that there are no flow separation problems and that the velocity distribution to the centrifugal stage inlet meets design requirements.

In summary, transition section design and performance for the conical-centrifugal stages and the combined centrifugal stages are normally quite satisfactory with sufficient attention to current design techniques. Transition section design for an axial-centrifugal stage combination requires careful attention be given to the rate of diffusion between stages. Here, again, a reasonable design with good performance characteristics is obtainable with astute design practice. In this light, the transition section design and performance do not seem to favor any one of the different two-stage configurations.

Stage compatibility with respect to off-design operation of two centrifugal stages in series is normally not a problem. AiResearch experience has shown that two centrifugal stages in series will match quite satisfactorily over a wide range of operating conditions without requiring guide vanes. An example of two-stage centrifugal compressor operating characteristics and performance is presented as figure 14. This stage combination has good design and off-design operation as is readily apparent from the experimental data shown on this figure.

The off-design operation of an axial first stage followed by a centrifugal second stage results in certain matching problems that normally require inlet guide vanes for the axial stage. At design speed, where the stages are usually matched, the range of the combined stages is often greater than demonstrated by the axial stage alone. This seems to be due to the centrifugal stage actually stabilizing flow through the axial stage when the first stage is supposedly in surge. However, low speed and start-up operation of the combined stages results in a mismatch between the stages. The axial stage wants to pass more flow than the centrifugal stage will accept,

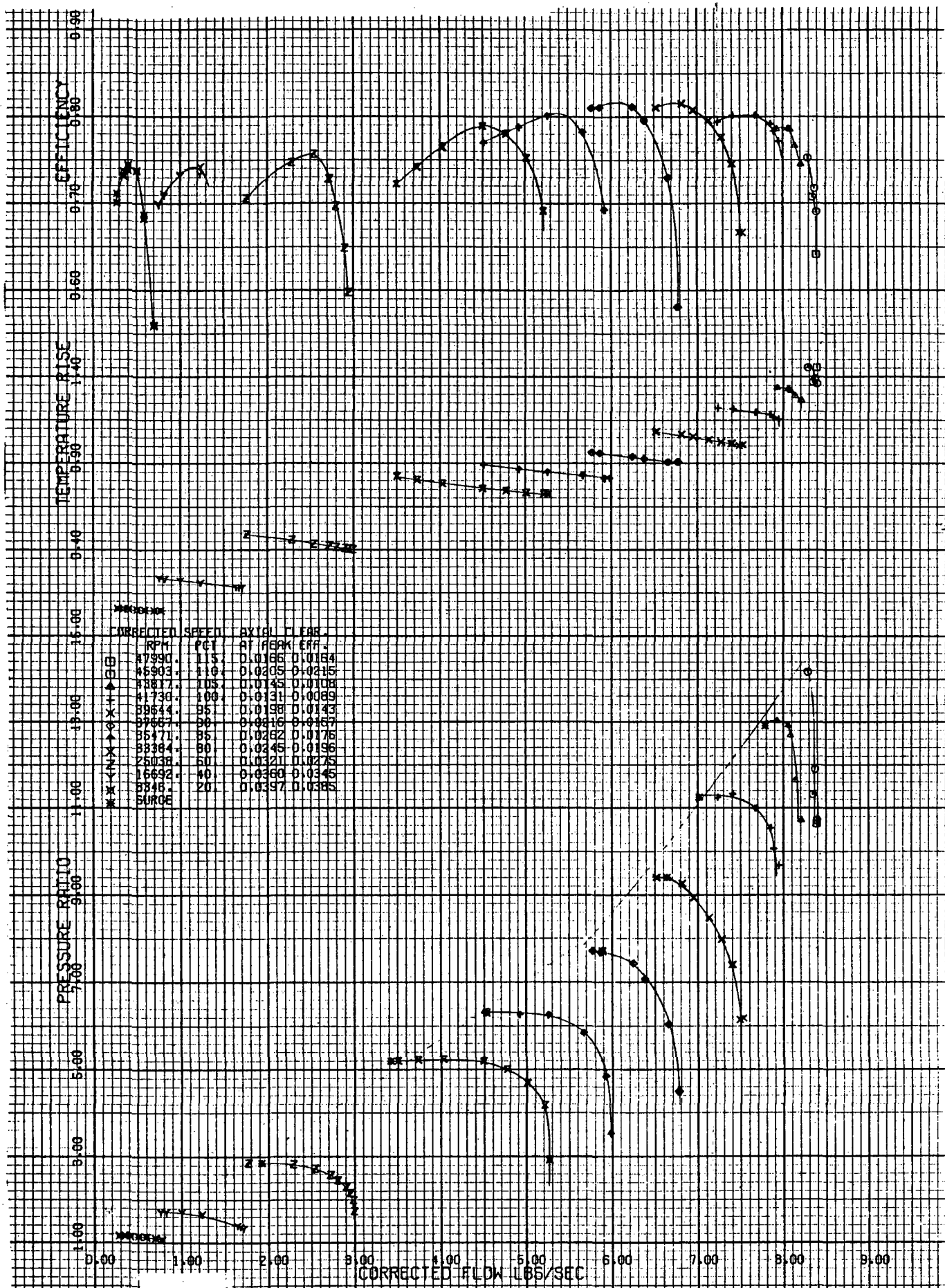


Figure 14. - Example Two-Stage Centrifugal Compressor Map.

tending to choke the back stage and stall the first stage. Therefore, inlet guide vanes are needed to limit the flow through the axial stage during low speed and/or start-up operation. This complicates somewhat the construction and operation of an axial-centrifugal stage combination and may result in this combination being unacceptable for certain applications.

In the conical-centrifugal stage combination, the off-design operating characteristics are expected to fall somewhere between the axial-centrifugal and centrifugal-centrifugal conditions. Low speed and start-up operation may be a problem since the tandem rotors and stators of the conical compressor are basically axial blade shapes. However, there is a significant radius change across each rotor section of the conical compressor which yields some static pressure rise during low speed operation. This would help the second stage to pass more flow and it is quite possible that the conical-centrifugal stage combination could start without variable inlet guide vanes. If this is the case, then off-design operation of the conical-centrifugal combination would be as good as two centrifugal stages in series and much better than an axial-centrifugal combination.

From a mechanical standpoint, a design goal of the program is to have a resonant-free operational speed range and a sufficient margin between the operating speed range and the criticals to ensure reasonable bearing life. The axial-centrifugal stage combination followed by a drive turbine can possibly be designed to meet this goal, despite its much wider operating speed range. Design speed for the axial-centrifugal combination is limited at 90,000 rpm so that it is desirable to set the first bending mode of the shaft critical above $\sim 120,000$. For this compressor to work, it must be straddled between the two bearings and the bearing span minimized to increase the first bending mode critical to help meet the design goal.

Overhanging the inlet impeller of the centrifugal-centrifugal compressor results in an unacceptable condition and, thus, straddle mounting the compressor stages is required. The only problem with the straddle-mounted bearing arrangement in the vertical shaft orientation specified by NASA is that it is difficult to get oil to and from the outboard bearing. It is obvious that the conical-centrifugal compressor exhibits a similar mechanical characteristic to the centrifugal-centrifugal stage. However, straddle-mounting the compressor stages is an acceptable solution and the final design of the conical-centrifugal stage is calculated to operate below the critical resonant frequency for bending.

Boundary Layer Control

The application of boundary layer control techniques to axial compressors has received considerable attention during recent years. Research has been conducted in the areas of:

- (a) Casing treatments over rotor tips
- (b) Slotted and tandem blading
- (c) Boundary layer suction along the blade surface
- (d) Wall suction

The effect of boundary layer control techniques on overall compressor performance is of primary interest in this program. A portion of the above research was conducted for the purpose of extending the stall margin and reducing noise. However, in most cases, the effect on compressor performance has been measured and presented as part of the test results. Therefore, it appears that there is sufficient data available, both in-house and in the literature, to select a reasonably effective boundary layer control technique for an axial stage should this type compressor be selected for the final configuration.

While there is considerable information available concerning boundary layer control with axial compressors, there is almost nothing available concerning this subject in centrifugal compressors.

The conical flow compressor is sufficiently different from conventional compressor design to warrant a somewhat closer examination of the boundary layer techniques. Obviously, this examination will have to draw extensively on related experience in axial compressors with consideration given to the larger radius change associated with the conical design.

In a recently completed program for NASA (Contract No. NAS3-14306), two forms of boundary layer control are built into the centrifugal compressor configuration. First, the centrifugal impeller is made up of separate inducer and impeller sections in tandem. As such, the configuration can be adjusted to discharge the inducer flow from the inducer pressure surface to energize the suction surface boundary layer on the downstream impeller. The second boundary layer control mechanism incorporated in this design is wall suction on the impeller shroud at two meridional locations and suction on both walls in the diffuser between stages of a cascade diffuser. These can be employed singly or in any desired combination. Both

concepts of boundary layer control look quite feasible for application to centrifugal compressor stages. However, experimental evaluation of the effectiveness of these techniques has not been established at this time.

In recent years, boundary layer removal from the junction of the convex stator surfaces and the convex inner wall of compressor and turbine casings has been found to be economically feasible (Reference 13 and unpublished American and British industrial data). Withdrawal of one percent or less of the flow through narrow slots has been found to improve performance.

The rotor and stator of the conical-flow first-stage compressor have been examined to determine the most logical location for boundary layer control slots. The junctions of the convex blade surfaces and the disks (or platforms) of rotors 1A and 1B are logical candidates for boundary layer removal, but these zones experience a relief due to the presence of the blade, the wall slope, and rotational effects. For a given level of diffusion, the rotor blade-disk junctions appear to be less critical than stator-casing intersections.

Spanwise boundary layer flow along the conical-flow rotor blades will be proportionately stronger than along axial blades due to the sweep of the blades adding to the normal outward forces on axial-blade boundary layers. If this outward flow is sufficient to interfere with proper performance of the outboard region of tandem rotor 1B, fences attached to rotor 1A blades near mid-span should be considered. Such fences would discharge the excess boundary layer near mid-passage. Energy addition to this wake-fluid would be rapid from the surrounding free-stream. The flow into the tip-section of rotor 1B should remain strong, since shock losses will be low due to the use of only moderate Mach numbers relative to the blades. Tip clearances can be held to low values through the use of soft, abradable inserts in the shroud, so tip clearance flows could be kept small.

The stator blades will not experience relief due to rotation, but will inhibit spanwise flow of low energy fluid if swept. To prevent separation and the generation of excessive quantities of low energy fluid, small narrow slots at the critical convex-blade/convex-wall chord length, located toward the rear, and sized to remove about 0.5 percent of the flow at design speed.

SIZE AND WEIGHT CONSIDERATIONS

In a volume and/or weight limited system, the axial-centrifugal stage combination would seem to offer a potential advantage over the other stage combinations under consideration. Obviously this is a result of the small stage diameter and relative stage length associated with the axial inlet stage.

An overall summary of the pertinent stage dimensions and a relative stage weight comparison is presented on Table VII. This tabulation includes the maximum diameter and length of each stage and both stages together for the three compressor combinations considered herein. Diameters for the centrifugal stages have been adjusted to account for the design as it would appear in an actual engine configuration. In an engine, the diffuser for the centrifugal stage would normally be divided between two stages. The initial diffuser would be oriented radially and diffuse to an intermediate Mach number ($M \sim 0.35$). Then the flow is turned to an axial orientation where further diffusion takes place. It was felt that a more valid size comparison could be made by comparing each configuration as it would appear in an actual engine installation. Also included on table VII is a relative weight comparison for the combined compressor stages above (not a complete engine), where the weights are normalized to the weight of the two centrifugal stages in series. These weights are estimated from existing hardware where applicable with considerable scaling involved. Because of the approximate nature of the weight estimates it was felt that this information could best be presented on a relative basis. Additional size and weight of inlet guide vanes, actuator and control, normally required for off-design operation and starting of an axial-centrifugal combination, have not been included in this comparison.

The size comparisons show the axial-centrifugal stage combination will fit in a smaller diameter and have a shorter stage length than the other combinations. As a result, the axial-centrifugal stage combination also weighs less than the other designs. On a relative weight basis, the axial-centrifugal stage combination weighs about 18 percent less than the two-stage centrifugal combination. These weights are representative of the impellers, stators, housings, bearings, shaft, and transition section for both compressor stages. The effect of the compressor configuration on the remaining engine component weights has been neglected.

The conical-centrifugal can be fit into a smaller diameter than the two-stage centrifugal combination because of the width of the transition section on the latter configuration. Stage length for the conical-centrifugal stages is greater than for the other two cases. However, the stage weight for the conical-centrifugal

TABLE VII.

ENGINE SIZE AND WEIGHT COMPARISON

1. <u>First Stage</u>	<u>Axial</u>	<u>Centrifugal</u>	<u>Conical</u>
Max Diameter, in.	3.7	9.0	6.94
Stage Length, in.	2.4	2.8	2.7
2. <u>Second Stage</u>	<u>Centrifugal</u>	<u>Centrifugal</u>	<u>Centrifugal</u>
Max Diameter, in.	7.0	6.4	7.2
Stage Length, in.	1.1	1.0	1.2
3. <u>Both Stages</u>	(1) <u>Axial-Centrifugal</u>	(2) <u>Centrifugal-Centrifugal</u>	(3) <u>Conical-Centrifugal</u>
Max Diameter, in.	7.0	9.0	7.2
Combined Length, in.	3.5	3.8	4.2
4. <u>Relative Weights</u>			
Two Stages	(4) 0.82	1.0	0.91

NOTE:

(1) Reference flowpath (see Figure 8)

(2) Reference flowpath (see Figure 4)

(3) Reference flowpath (see Figure 11)

(4) Does not include inlet guide vanes nor actuator/control

combination. Thus it appears that the conical-centrifugal combination would compare quite favorably with two centrifugal stages in series for a volume and/or weight limited system. But the axial-centrifugal stage combination still offers the most size and weight advantages of the combinations investigated.

IMPELLER EROSION CONSIDERATIONS

Foreign object damage (FOD) and performance degradation effects due to large amounts of sand, dust, and other foreign substances are significant factors that must be considered in the design of engines for aircraft installations. Various engine test programs and a USAF study (NASA Technical Report No. 54, Factors That Affect Operational Reliability of Turbojet Engines) conclude that centrifugal-type compressors afford inherently better protection from FOD and minimal performance degradation when compared with axial-type compressors.

A comparison of power decay due to erosion is tabulated below for several engines that utilize axial compressors as compared to AiResearch T76 and TPE331 engines that employ centrifugal compressors:

Engine	Operating Period	Power Decay Percent	Remarks	Source
T76 (Centrifugal)	1600 hr	1.35	Data from OV-10A operation Viet Nam (eight engines)	Third Quarterly Progress Report, AiResearch Document PE-8088-R2
TPE331 (Centrifugal)	1000 hr	5	Turbo-Porter STOL rough field operation	"Turboprop Operation in STOL Aircraft" SAE Paper 680228
T64 (Axial)	400 landings	14	CH53 Patuxent River tests	"Problems and Solutions for Sand Environment Operation" ASME Paper 68GT37
T63 (Axial)	10 hr	5	T-63-A-5A Qualification Test (0.0015 gm/cu ft)	"T63 Sand and Dust Tolerance....." SAE Paper 670334
	50 hr	10	LOH Test Data - Ft. Benning, Ga.	

This illustrates dramatically the severe effect erosion can have on axial compressor performance.

Blade configurations of the tandem rotors for the conical flow compressor are similar to an axial rotor configuration. However, the inlet flow intersects the leading edge of the conical flow blades at a relatively steep angle producing a swept effect across the blade rows. Sweeping the leading edge of an erosion specimen 45 degrees or more has been shown to dramatically reduce the rate of erosion. Apparently the effect of sweep is to convert the direct impact of the hard particles to glancing blows. The acceleration of the glancing particles, and the normal force developed due to the collision is greatly reduced. For a given foreign particle concentration, the number of impacts per unit leading-edge-length is reduced. In the case of transonic Mach numbers, the shock wave preceding the swept leading edge produces a static pressure gradient which helps divert the particles, causing some to miss the airfoil and to increase the "glancing" angle. All of these factors tend to reduce the amount of erosion caused by hail, rain, sand, and dust.

Conventional transonic and supersonic compressors require very small radius, essentially sharp, leading edge to minimize the strength and the extent of the detached bow waves and the aerodynamic losses associated with strong shock waves. Sharp edges are subject to rapid erosion damage. The use of swept blades reduces the Mach number normal to the leading edge to subsonic values. Subsonic-type airfoils having larger leading edge radii can be employed without suffering excessive losses. One method of explaining this behavior is to consider that the weak three-dimensional shock which precedes the blade leading edge generates a pressure gradient which "forewarns" the air particles that a blade is approaching and causes them to divert automatically. Thus, larger leading edge radii and thicker leading edge regions to support the impact zone against local fracture are available. Therefore, it is quite possible that the conical flow compressor may show considerable resistance to erosion and low FOD.

CONFIGURATION SELECTION

The axial-centrifugal stage combination appears to offer the least potential advantages for this application. Examination of the two-stage performance results showed this combination is the least efficient of those considered. The low efficiency is directly attributable to the second-stage centrifugal compressor which operates at a low design specific speed. There could also be stage compatibility problems associated with the axial-centrifugal stage combination. First, diffusion is required between the stage, in the transition duct, and at off-design operation, a definite need for variable inlet guide vanes in front of the axial stage for start-up and low speed operation is indicated. Engine size and weight considerations would favor the axial-centrifugal combination in a volume and/or weight limited system. However, for the application considered, the axial-centrifugal compressor is least favorable based on performance potential, susceptibility to foreign object damage, and potential stage compatibility problems.

The centrifugal-centrifugal stage combination clearly showed higher design performance than the axial-centrifugal stage combination but somewhat less performance potential than the conical-centrifugal stage combination. In the stage compatibility comparison, the centrifugal-centrifugal stage combination and conical-centrifugal stage combination were essentially identical. In a volume limited system where compressor diameter is a concern, the conical-centrifugal stage combination may also have a slight weight advantage over the centrifugal-centrifugal stage combination. From an erosion and foreign object damage standpoint, the conical compressor is probably better than a typical axial but inferior to a centrifugal.

With all criteria considered, the conical-centrifugal was selected to meet the objective of this contract primarily because of its improved performance potential. Therefore, the mixed flow or conical flow compressor was subjected to the detailed design analysis discussed in the subsequent sections of this report.

GENERAL DESIGN LOGIC

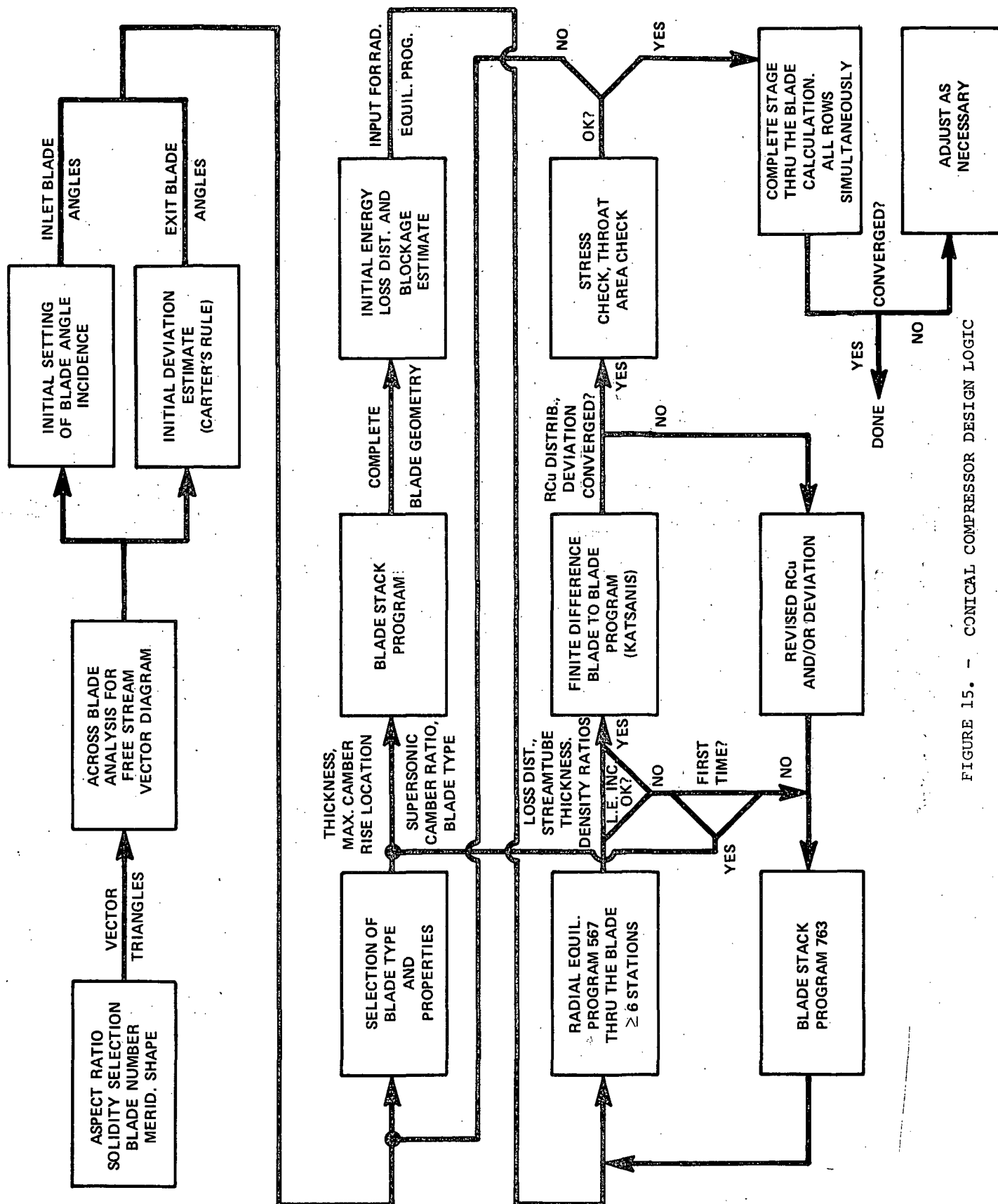
The logic used in the calculation of blade shapes for the conical compressor is diagrammatically presented in Figure 15. The various calculation procedures encompassed by the logic are discussed in the following paragraphs. Details of the various program input requirements and selection of blade element airfoil sections will be given in ensuing sections.

The air inlet and exit vector triangles were calculated in the optimization study using the non-isentropic, radial equilibrium program. This calculation has been referred to as the across-the-blade solution, where calculations were made just outside of the leading and trailing edges of each blade (and vane) row. The detailed blade shape design uses the same program with calculations made inside of each blade row. This is referred to as the through-the-blade calculation. Each rotor blade was designed separately, i.e., the aerodynamic calculations were made with only one rotor blade in the flow field. This was done for expediency. However, the stator vanes were analyzed aerodynamically in tandem. When all blade shapes were finalized, a through-the-blade solution was made with all blades in place. This was done to evaluate the aerodynamic interaction between blade rows.

A second aerodynamic calculation program, referred to as a blade-to-blade calculation (also Katsanis), was used for the two-fold purpose of calculating inviscid flow deviation at the blade exit, where applicable, and the rate of change in angular momentum along each axisymmetric stream surface through a blade. Both results are used (except as noted) in the through-the-blade calculation. Details of this calculation procedure are contained in Appendix D.

Both the through-the-blade analysis and the blade-to-blade analysis require a definition of the blade geometry. This information is obtained from a blade stacking program. The function of this calculation procedure is to take the specified aerodynamic blade element along each stream surface of a given blade and generate stacked blade properties for both aerodynamic programs. Details of this calculation procedure are contained in Appendix B.

From the across-the-blade calculation, initial setting of each blade element leading edge is made, based on incidence angle criteria. The blade element deviation angle is estimated from Carter's rule. A specification of the aerodynamic blade element shape can then be made for input to the blade stacking program. A through-the-blade calculation is now made with initial assumptions of the loss, aerodynamic blockage, and energy distributions.



The thermodynamic properties along each axisymmetric stream surface from the through-the-blade calculation are used to calculate a stream-surface height distribution from inlet to exit of the blade row. This distribution of stream-surface height, along with the definition of blade suction and pressure surfaces bounding the stream surface, are input to the blade-to-blade calculation. The inviscid deviation calculated by the blade-to-blade program added to an estimated viscous deviation (see Appendix A) is now compared to the across-the-blade vector triangle (for each streamline). The blade element camber is then changed by the amount of the difference. Also, the energy addition distribution is adjusted, where applicable, according to this calculation.

A revised blade shape is then calculated with the blade stacking program. The through-the-blade analysis is then rerun with the new blade shape and energy distribution. This iterative loop is continued until the through-the-blade vector triangles agree reasonable well with the across-the-blade solution. The blade is then checked for choke flow margin and a stress analysis performed.

The final individual rotor blade designs and the tandem stator design were then analyzed in a full through-the-blade calculation. In this way, blade interactions attributable to streamline slope and curvatures effects were established. Ideally, blade designs should then be adjusted if significant difference exist between the inlet and exit vector diagrams from the individual designs compared to the complete solution.

ROTOR AND STATOR GEOMETRY SELECTION

The performance of each rotor blade row and stator vane row is strongly dependent upon the selection of aspect ratio and solidity. The blade element aspect ratio, defined as

$$AR = \text{mean blade height/mean chord}$$

requires rotor blade and stator vane chords to be quite small if the aspect ratio is to be within the limit of current experience. For rotors and stators, a lower limit for aspect ratio is 1.25. A minimum chord length value acceptable to stress and manufacturing criteria is approximately 0.5 inch. For rotors, chord length may be adjusted upwards for stress reasons, depending upon the aspect ratio selected.

As the flow path height is contracted through each blade row to maintain acceptable meridional velocity ratios and D-factors, the aspect ratio is no longer under control of the designer. Hence, the aspect ratio of rotor 1B and stators 1A and 1B was considerably less than desired. For this reason, blade element losses used in the analysis tend to be optimistic and must be verified by an experimental test program.

Rotor 1A tip solidity was selected to be consistent with current AiResearch design experience for transonic rotor blading. Rotor 1B required twice the number of blades 1A to account for radius increase and a decreased chord length. Stator solidities were selected to give acceptable blade loadings while being maintained within current design experience.

Selection of the type of airfoil section to be used along each axisymmetric stream surface of a given blade was determined by the inlet relative Mach number. These section types were subject to modification if the resultant blade loading was not satisfactory. In rotors 1A and 1B, a combination of multiple circular arc (MCA) and double circular arc (DCA) sections were used. Double circular arcs were used throughout both stator vane designs. A general MCA section with pertinent parameters required for definition is shown in Figure 17. Upper and lower surfaces and meanline are made up of arcs which have tangency at the point of maximum thickness. The DCA section is a specific form of the MCA section in which the maximum camber rise and maximum thickness occur at 50 percent of the chord length and the camber is distributed uniformly along the entire meanline. Parameters required for specification of a section are total camber (ϕ), maximum thickness, location of maximum thickness, amount of front (or supersonic) camber, and leading edge meanline direction.

DETAILED AERODYNAMIC DESIGN

The section will cover in detail the aerodynamic design of the inlet stage of the conical-centrifugal compressor, the interstage duct between the conical flow inlet stage and the centrifugal second stage, and the drive turbine for the proposed research package.

General

As seen in the discussion of the design logic, three computer programs were required to design each blade. To carry out a through-the-blade, non-isentropic radial equilibrium calculation, an initial estimate of the blade geometry was required for stacking the blade. For this design, six streamlines were used in each blade design analysis.

Experience at AiResearch and elsewhere (Reference 14) indicates that for supersonic relative Mach numbers, the leading edge suction surface should be made parallel with the inlet relative air angle (0° incidence). As the Mach number decreases below 1.0, the suction surface incidence (i) was decreased to -2.0 degrees. At the blade trailing edge, deviation (δ) was initially estimated using Carter's rule. The total amount of blade element camber along the streamline can then be calculated from

$$\Phi = (\beta_1' - \beta_2') - i + \delta$$

Ensuing iterations used the value calculated by the blade-to-blade plus a viscous correction, where applicable.

With the airfoil shape, position of each surface (r, Z) and stack axis specified, a blade shape can be calculated. For all blades in this design, the blade leading and trailing edges were held fixed in the meridional view with sections stacked on their respective center of mass in the circumferential direction only (Appendix B). This calculation provided input of blade geometry for the through-the-blade analysis and blade-to-blade analysis.

Additional information needed in the through-the-blade calculation are the rate of change in the angular momentum, distribution of the loss, and distribution of the aerodynamic blockage along each streamline. For blade rows operating with supersonic relative inlet Mach numbers, the angular momentum change was approximated for all iterations by a sinusoidal function of axial length given by:

$$\frac{r V_u - r_1 V_{u1}}{r_2 V_{u2} - r_1 V_{u1}} = \sin^A \left[\frac{\pi}{2} \left(\frac{Z - Z_1}{Z_2 - Z_1} \right) \right]$$

The value of A was varied from 2.0 to 1.50 based on previous design experience. The initial estimate of angular momentum distribution for streamlines with subsonic inlet relative Mach numbers was linear. In subsequent iterations, the distribution resulting from the blade-to-blade solution was used. The loss and aerodynamic blockage were distributed linearly with axial distance for all blade rows. The loss values were held constant on the basis that the final through-the-blade calculation would give the same diffusion factors as the across-the-blade solution.

Rotor 1A Design

The final rotor 1A design parameters are as follows:

Corrected flow, lb/sec	2.0
Tip diffusion factor	0.443
Tip relative velocity ratio	0.7068
Inlet hub/tip ratio	0.45
Tip relative Mach number	1.26
Aspect ratio	1.028
Tip solidity	1.34
Number of blades	20

Figure 16 shows a meridional view of the final blade shape. Radial equilibrium calculation station lines are shown along with straight line approximations of the six streamlines on which each airfoil section was specified for stacking the blade. Details of the final airfoil sections specified along each of the conical stream surfaces are contained in table VIII. Figure 17 provides a schematic representation of symbols used to describe the airfoil section.

Selection of the airfoil sections used along each axisymmetric stream surface of rotor 1A was initially based on the inlet relative Mach number shown in figure 18. The multiple circular arc (MCA) type was used for all streamlines except the hub. Here an MCA meanline with an arbitrary thickness distribution was used to adjust the loading as discussed at the end of this design section (figure 19).

A comparison of the resulting and design minimum loss incidence angles are presented in figure 20. The two angles are not the same due to changes which occurred in the meridional velocity distribution at the rotor leading edge during the design iteration. The difference from design intent was deemed acceptable on the basis of the lower relative Mach number at which the maximum difference occurred, i.e., the low loss incidence range is somewhat wider for that Mach number level. Also shown are the incidence angles based on the complete through-the-blade solution.

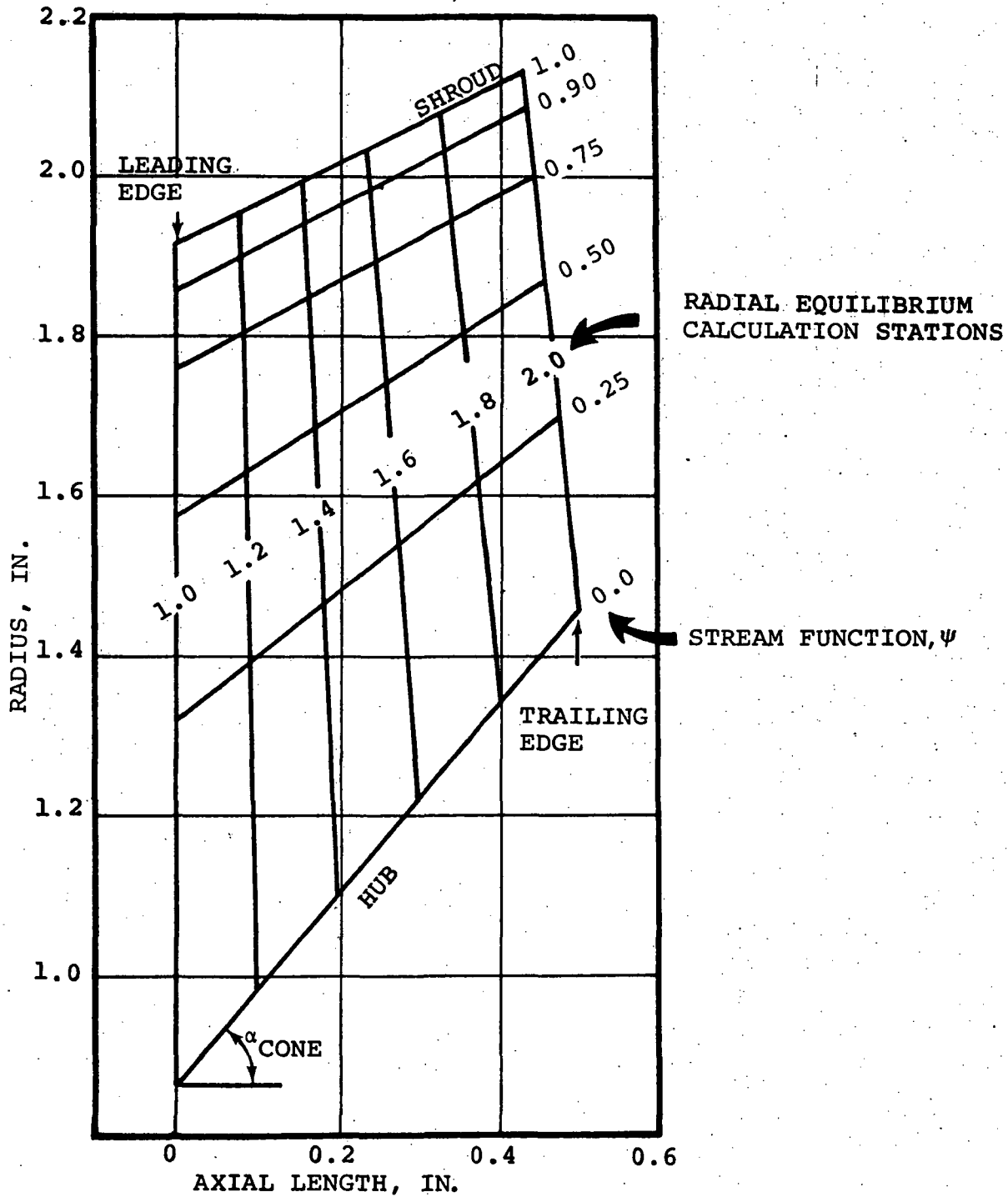


Figure 16.- Meridional Flow Path for Conical Flow Compressor, Rotor 1A.

TABLE VIII.

BLADE SETTING FOR ROTOR 1A

ψ	M_{REL}	$\beta_1(Air)$	$\beta_1(Blade)$	i	$\beta_{1SS}-\beta_{1MC}$	t_{LE}
Shroud	1.256	59.95	57.72	2.22	2.65	0.007
0.9	1.214	59.80	56.93	2.87	3.07	0.0075
0.75	1.153	59.21	55.83	3.38	3.70	0.0081
0.5	1.035	58.13	54.57	3.56	4.72	0.0095
0.25	0.865	58.10	53.77	4.33	5.84	0.0116
Hub	0.585	54.82	49.79	5.03	8.08	0.0178

ψ	$\beta_2(Air)$	$\beta_2(Blade)$	δ	t_{TE}	t_{max}/C_T
Shroud	55.78	50.54	5.24	0.0081	0.0395
0.9	55.44	50.15	5.29	0.0082	0.0423
0.75	53.97	49.11	4.86	0.0086	0.0470
0.5	50.66	44.89	5.77	0.0098	0.0550
0.25	44.31	35.25	9.06	0.0110	0.0630
Hub	28.95	14.76	14.19	0.0140	0.0850

ψ	C_T	Φ_T	a/C_T	Φ_{SS}/Φ_T	δ
Shroud	0.852	7.18	0.73	0.15	1.342
0.9	0.854	6.78	0.68	0.24	1.383
0.75	0.847	6.72	0.61	0.37	1.438
0.5	0.839	9.68	0.53	0.48	1.562
0.25	0.860	18.52	0.50	0.50	1.841
Hub	0.825	35.03	0.45	0.55	2.265

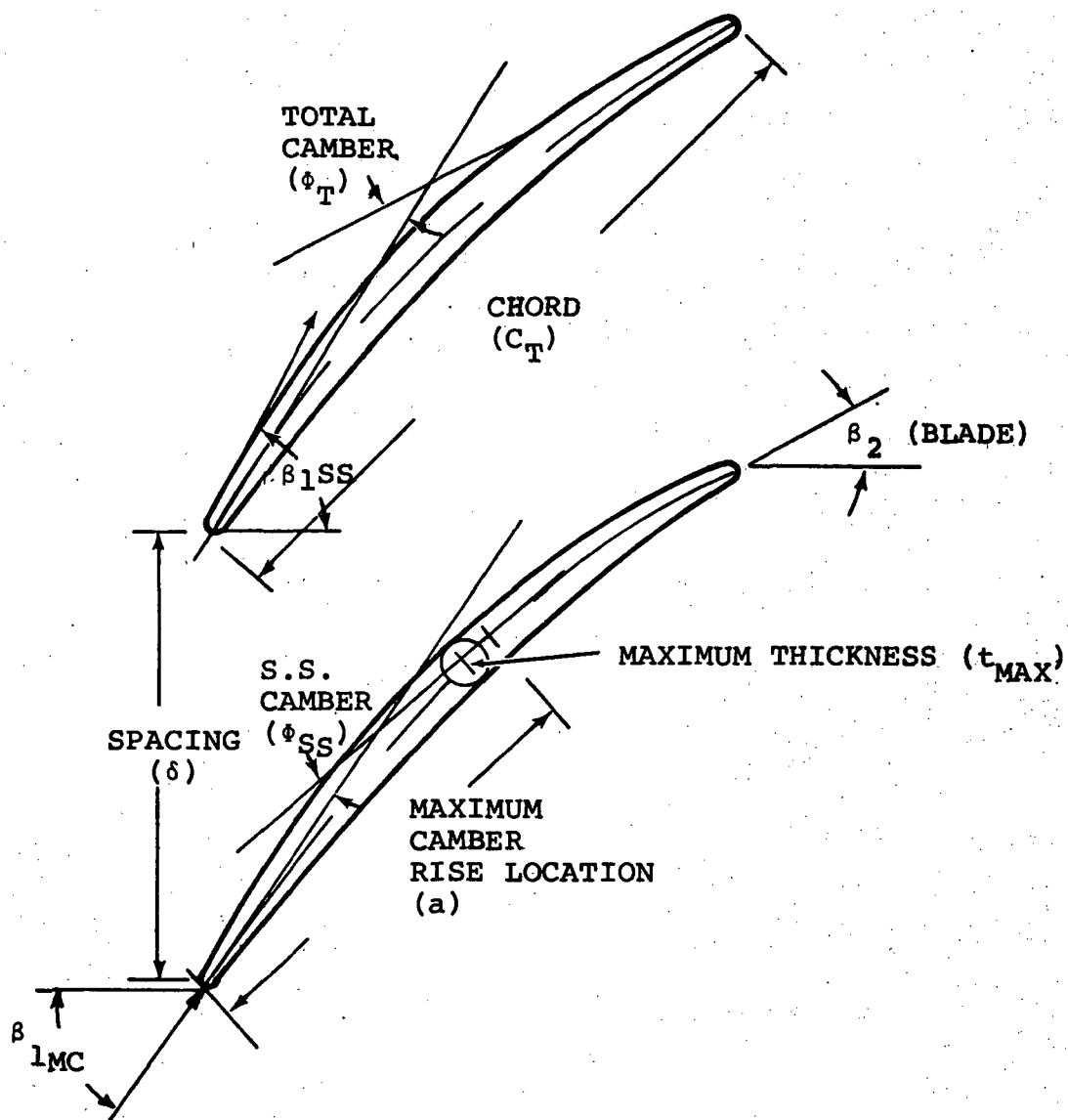


Figure 17. - Multiple-circular-arc airfoil description.

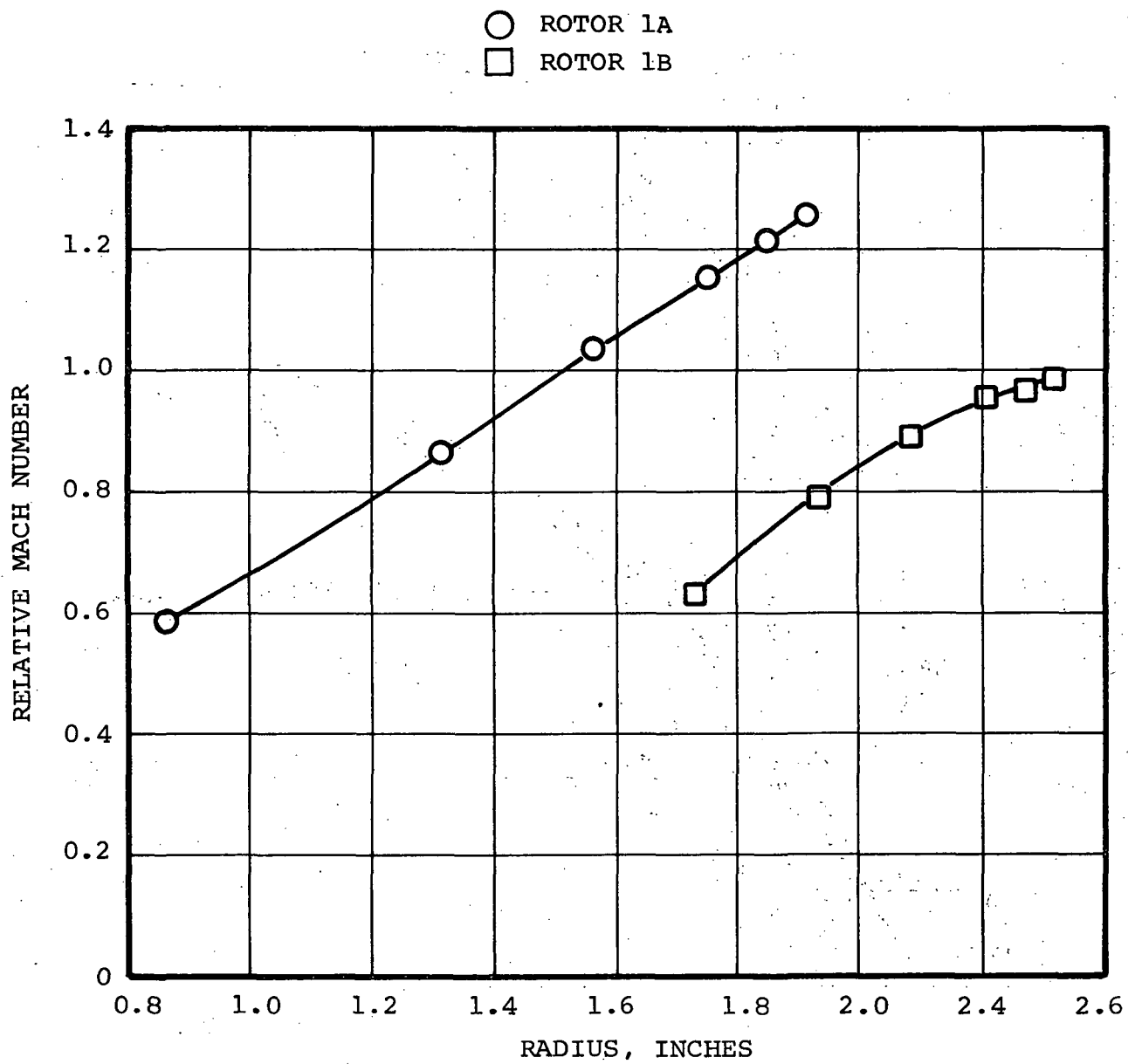


Figure 18. Inlet Relative Mach Number For Rotors 1A and 1B.

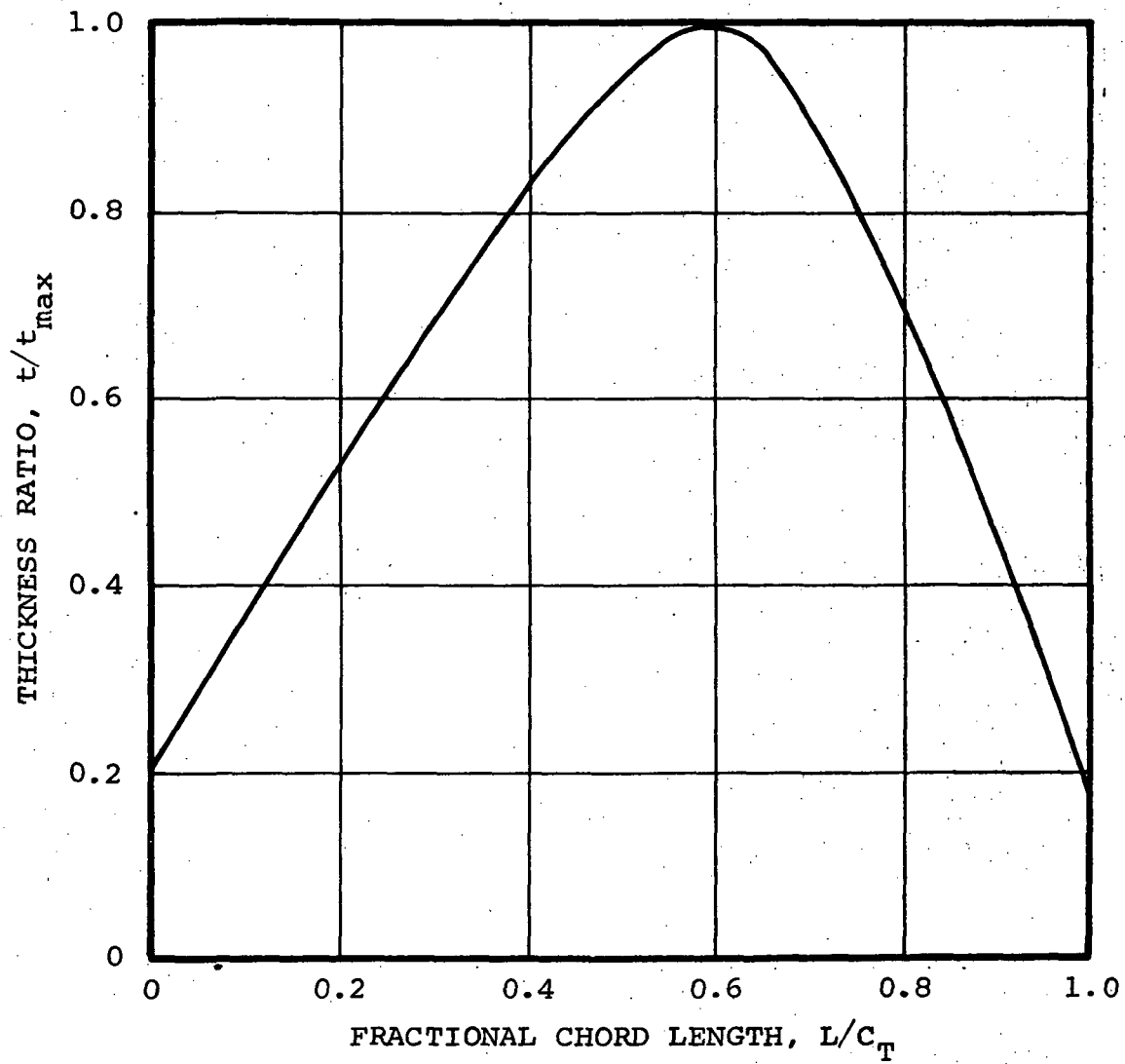


Figure 19. Final Thickness Distribution For Rotor 1A Hub Section.

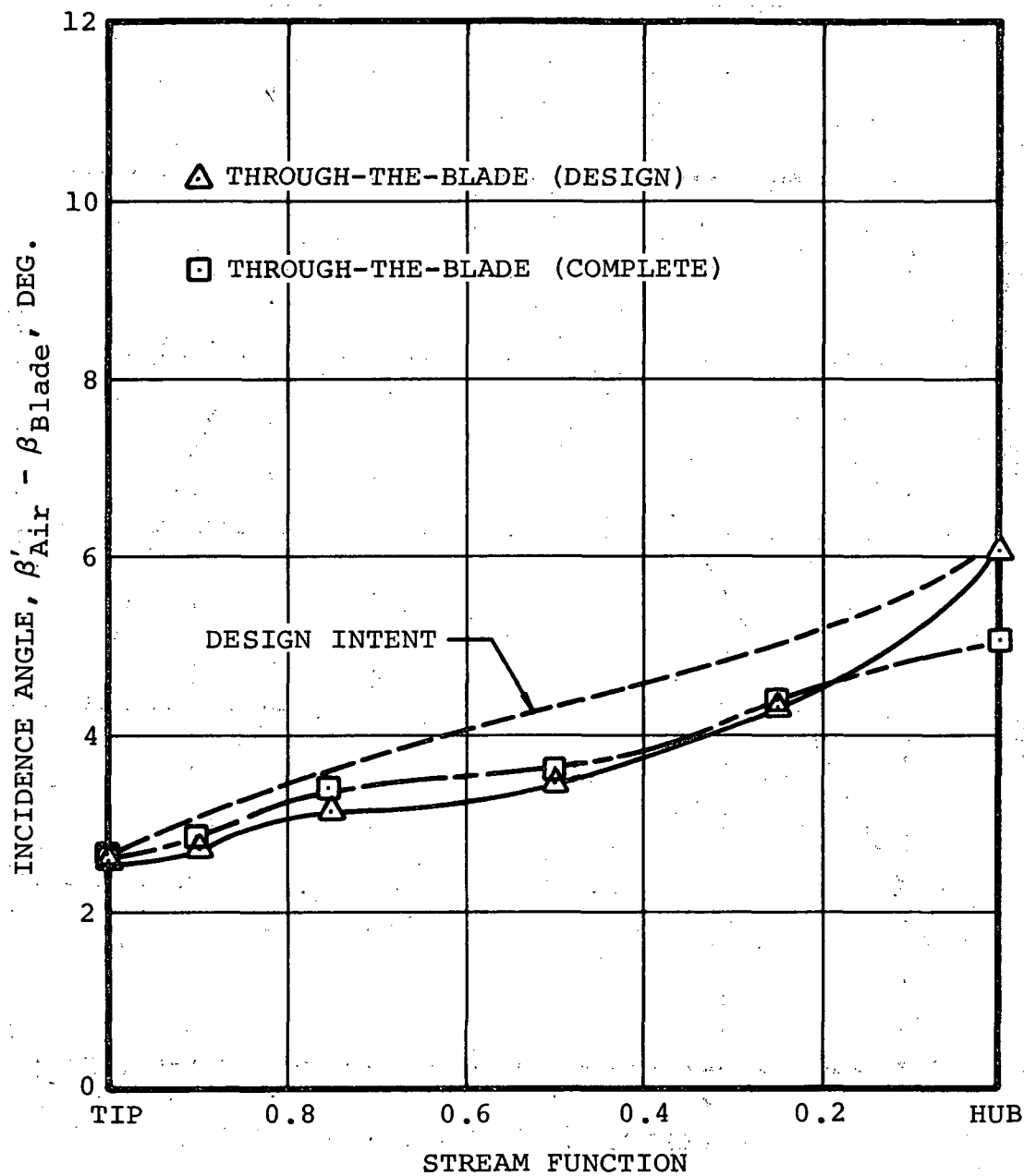


Figure 20.- Design Incidence Angles for Rotor 1A.

Final design deviation angle is shown in figure 21. These values were calculated to satisfy the angular momentum addition criteria from the across-the-blade analysis. As seen from the comparison of inlet and exit relative air angle distributions (figure 21), a difference exists between the across-the-blade analysis exit angle and those from the final through-the-blade design. The difference arises from introducing the blade into the flow field solution. Also included is the deviation calculated from the complete through-the-blade flow solution. The difference was insignificant implying virtually no blade interaction based on the analytical model.

The aerodynamic and blade blockage distributions used in the through-the-blade analysis along shroud, 50-percent flow and hub streamlines are shown in figures 22 and 23. Aerodynamic blockage along each streamline was distributed linearly with meridional distance, while the radial distribution (at each station calculation line) was held constant.

The distribution of angular momentum normalized to a reference velocity for the through-the-blade analysis is shown for all streamlines in figures 24 and 25. The hub and 25-percent streamline distributions were taken from the blade-to-blade Katsanis solution while the remaining streamlines used the sinusoidal distribution discussed previously on Page 54 because of their supersonic velocities.

A comparison of calculated diffusion factors at the rotor blade trailing edge for the preliminary across-the-blade solution and the design through-the-blade solution are shown in figure 26. Agreement is good except at the hub streamline. This difference was not accounted for due to the approximate nature of the estimated loss.

Only one blade loading is presented for Rotor 1A. This loading corresponds to the hub streamline and is shown on figure 27. The blade surface velocities were obtained from the blade-to-blade program. The resultant loading for the hub section streamline, while considered satisfactory for design purposes, has some undesirable features that could not be corrected in the time available for this design. One problem area associated with this loading is that the mean velocity initially accelerates and then diffuses quite rapidly toward the blade exit. It would be desirable to minimize the velocity peak. However, an adjustment of this condition may have an adverse influence on the total flow field, requiring considerable redesign to achieve the desired overall design intent.

The final step in the aerodynamic design of Rotor 1A involved a throat area check for each streamline to insure that the rotor will pass the design flow. This calculation is approximate in that mean flow properties and a constant height are employed to calculate flow

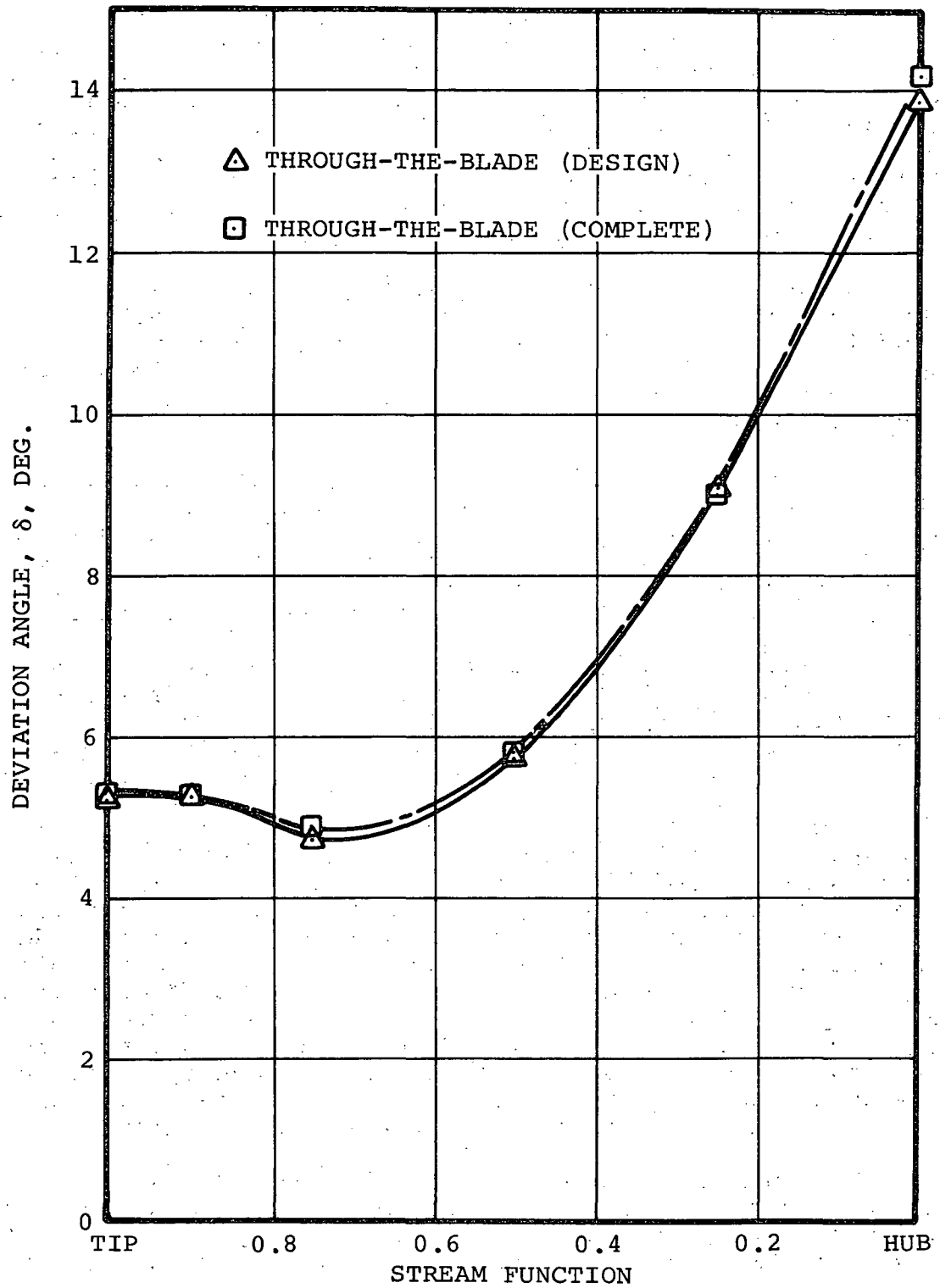


Figure 21.- Deviation Angle Agreement for Rotor 1A.

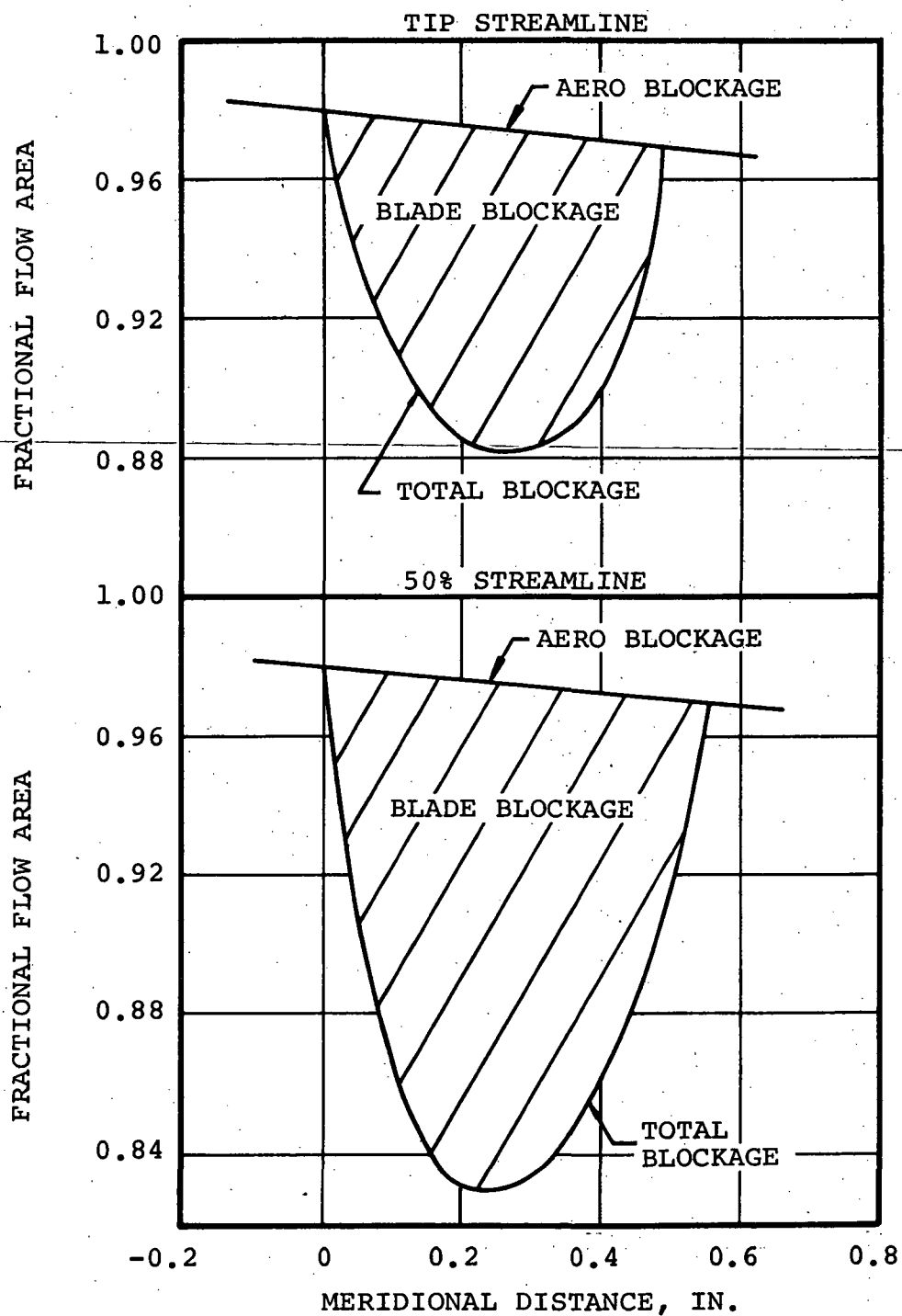


Figure 22.- Blockage Distribution for Rotor 1A
Tip and 50% Streamline.

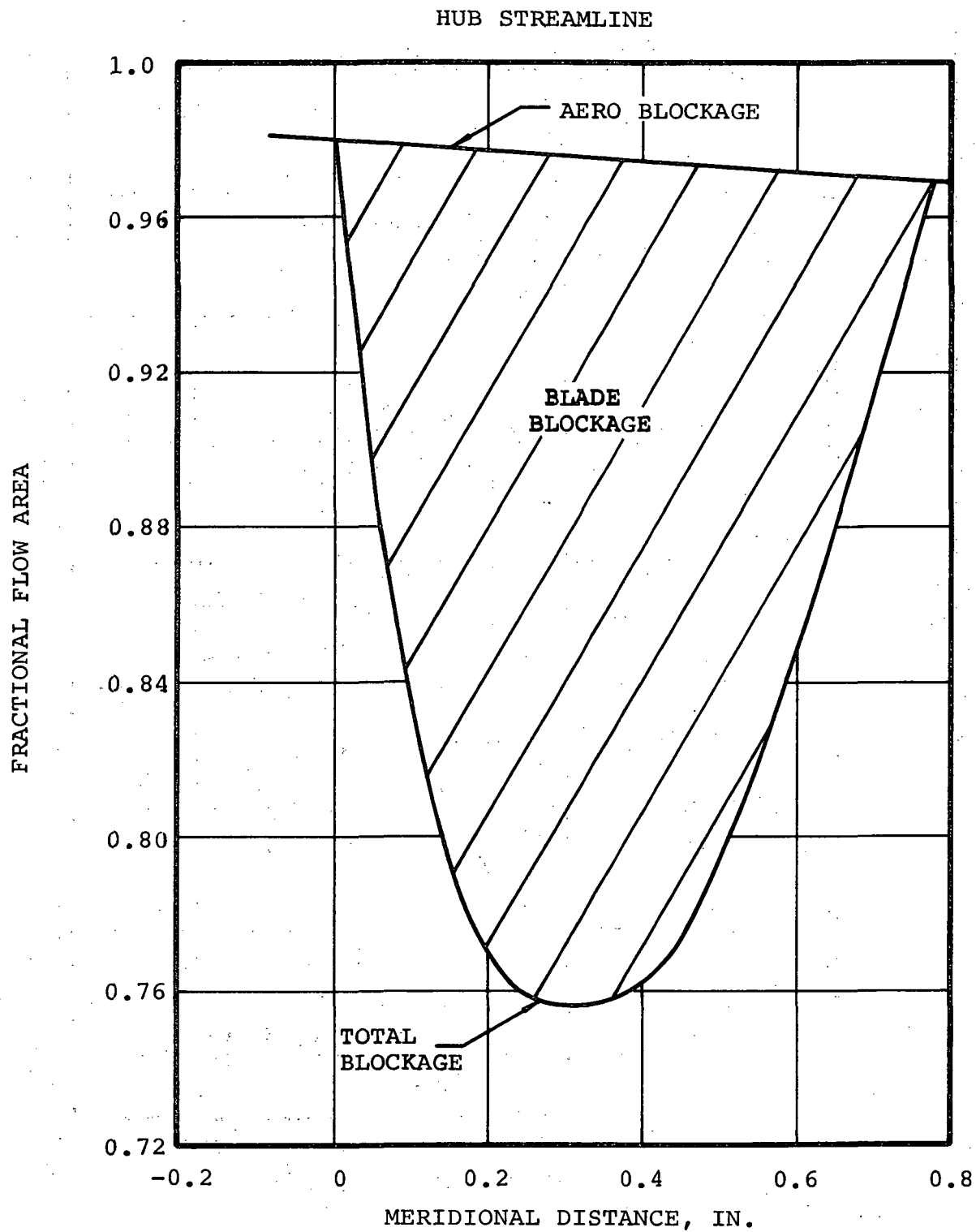


Figure 23.- Blockage Distribution for Rotor 1A Hub Streamline.

WHERE $U_t \text{ REF} = 610 \text{ FT/SEC}$

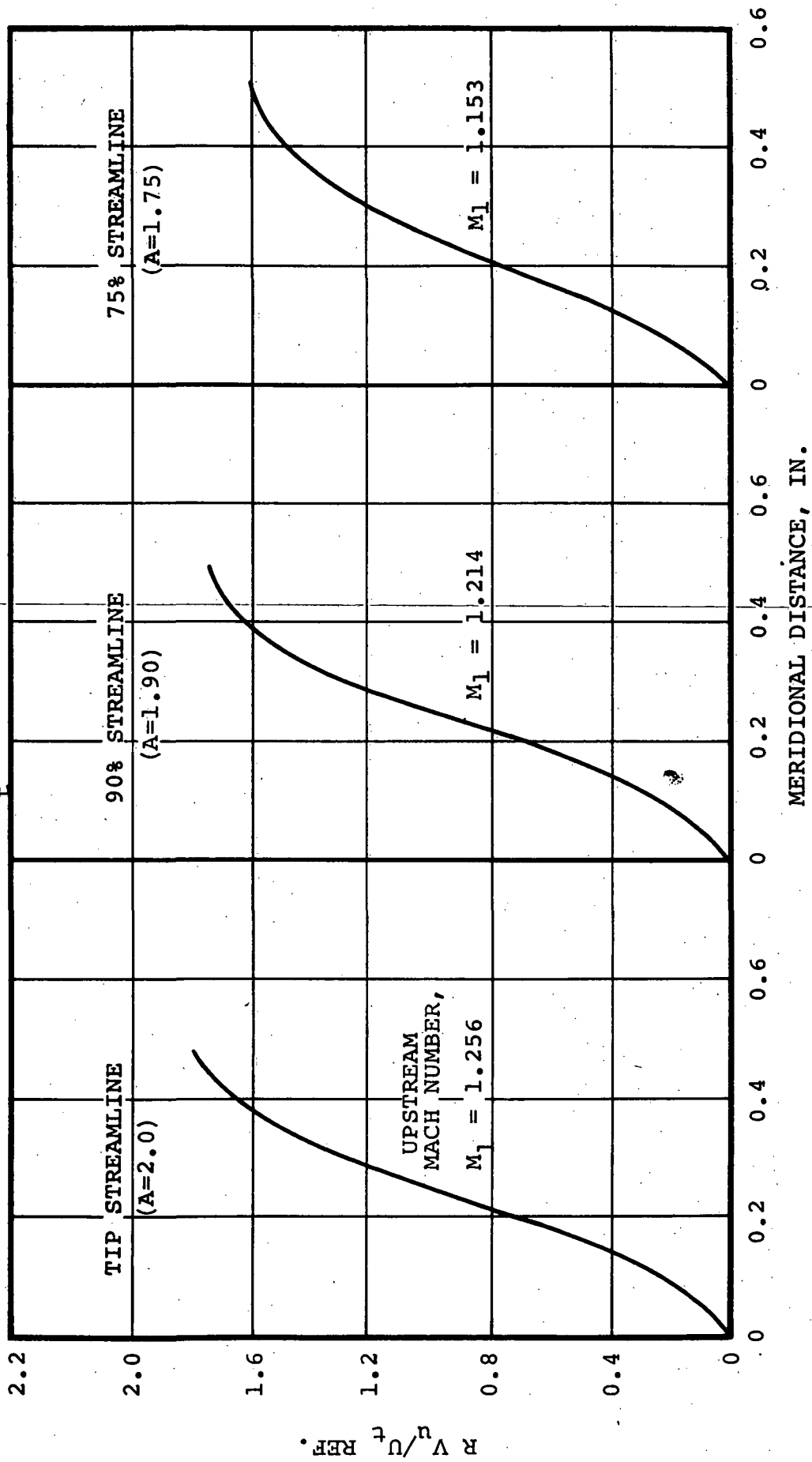


Figure 24.- Streamline Energy Distribution for Rotor 1A.

WHERE $U_{t\text{REF}} = 610 \text{ FT/SEC}$

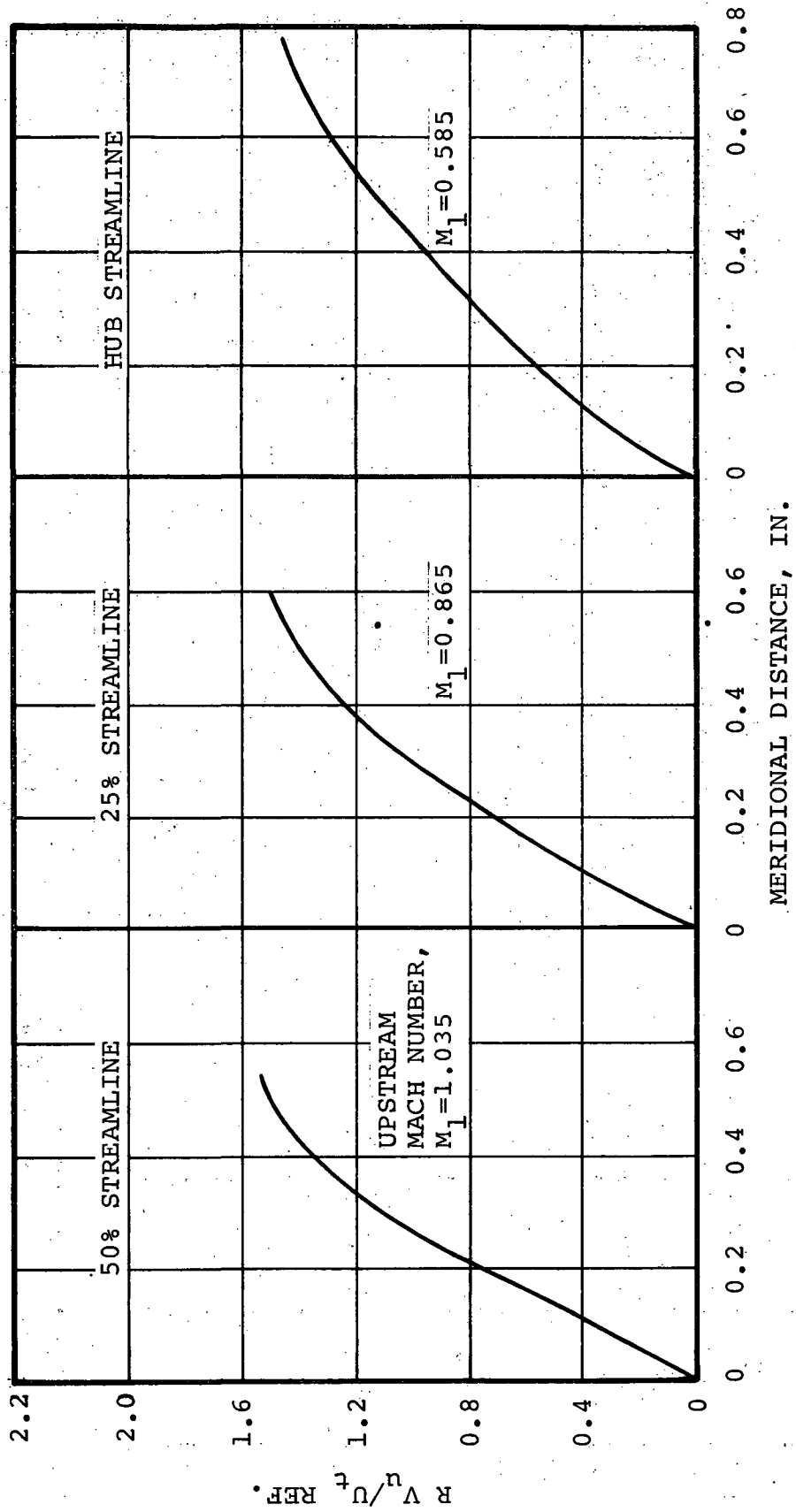


Figure 25.- Streamline Energy Distribution for Rotor 1A.

$$D = 1.0 - \frac{v_2'}{v_1'} + \frac{r_2 v_{u2} - r_1 v_{u1}}{2\bar{r} \sigma v_1'}$$

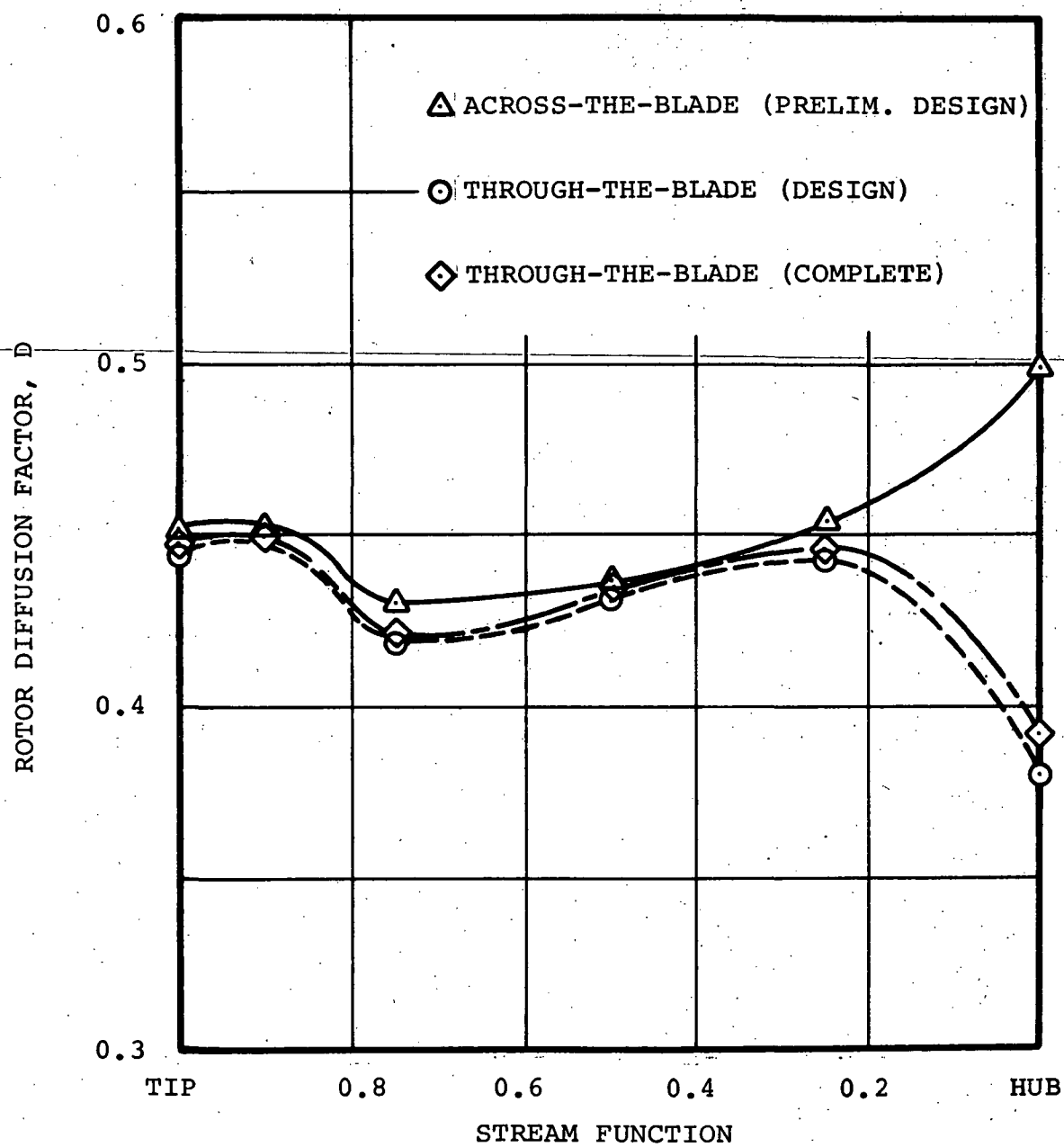


Figure 26.- Diffusion Factors for Rotor 1A.

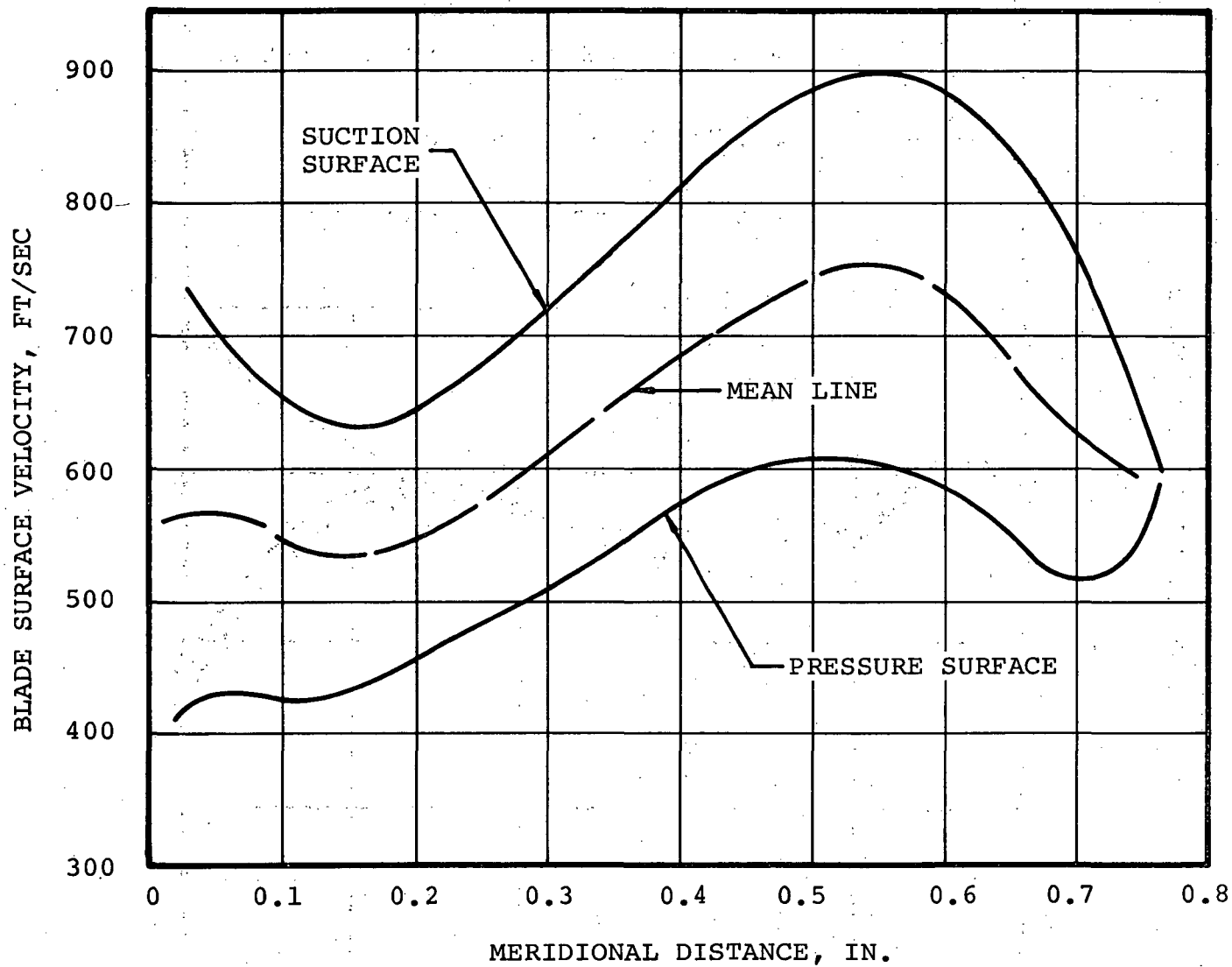


Figure 27.- Final Blade Loading for Rotor 1A Hub Streamline.

areas at a particular meridional streamline location. The passage width is obtained geometrically. Obviously, this does not account for secondary flows and/or warped stream surface thicknesses that are known to exist in the real case. In essence, the throat area check made here uses one-dimensional flow properties with area change to calculate the minimum passage area along a particular streamline.

Results of the throat area check for all the streamlines in Rotor 1A are presented on figure 28. These are shown as the flow area divided by the critical area for choked flow versus meridional distance along each streamline. Note that the first four streamlines indicate a choke margin of 2 percent or greater and that the throat location moves from the middle of the blade to near the leading edge going from the blade tip to the 50-percent streamline.

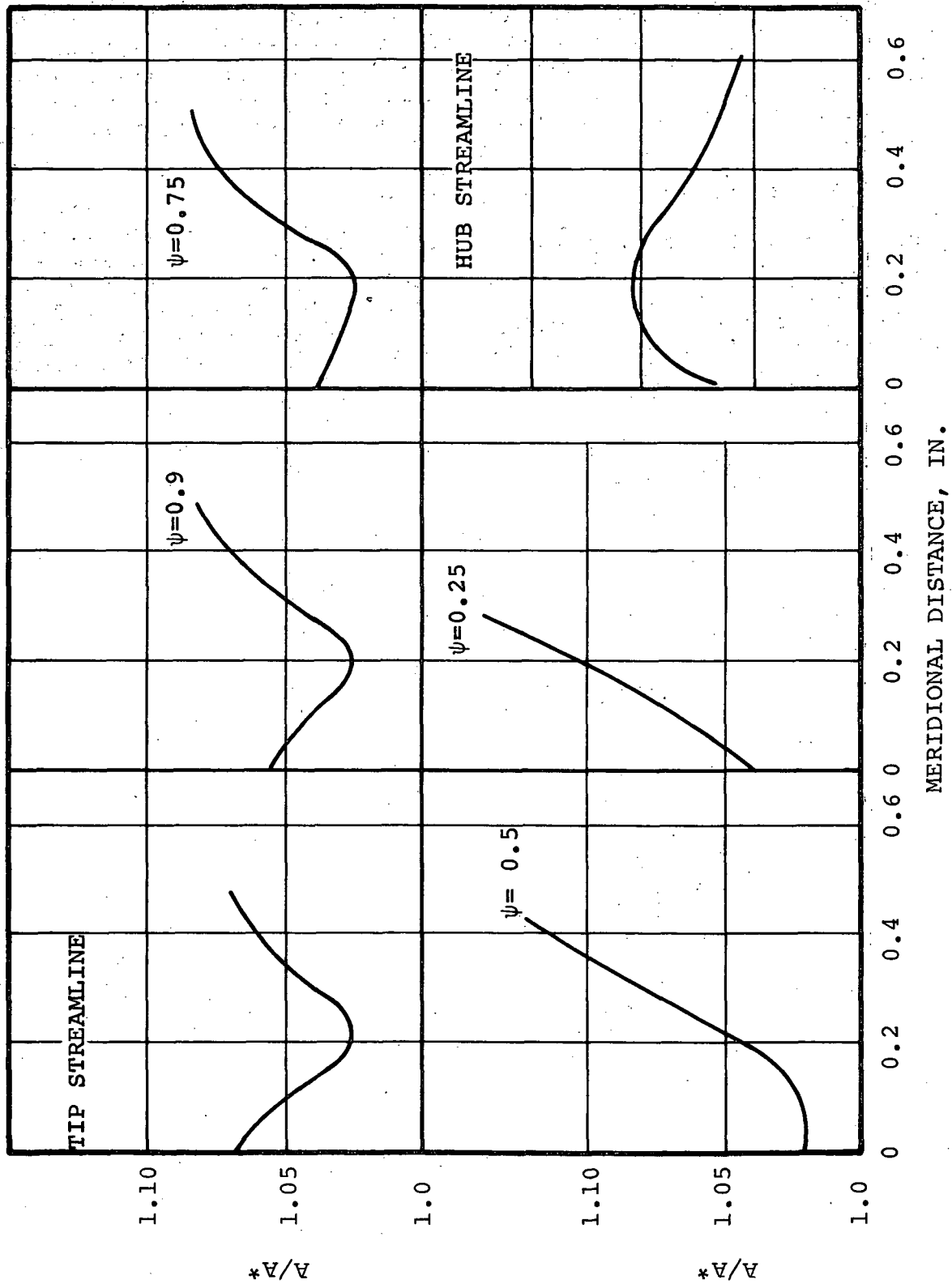


Figure 28.- Throat Area Check for Rotor 1A.

ROTOR 1B DESIGN

The final rotor 1B design parameters are as follows:

Corrected flow, lb/sec	1.225
Tip diffusion factor	0.493
Tip relative velocity ratio	0.655
Inlet hub/tip ratio	0.746
Tip relative Mach number	0.981
Aspect ratio	0.84
<hr/>	
Tip solidity	1.57
Number of blades	40

The final meridional shape is shown in figure 29. Also included are the through-the-blade calculation stations and final streamline positions. Details of the final airfoil sections specified along each of these axisymmetric stream surfaces are contained in table IX.

The rotor 1B inlet relative Mach number distribution is shown in figure 18. For this range of Mach numbers, the double circular arc meanline was selected for initial through-the-blade analysis. This selection was subsequently changed to the more general multiple circular arc to adjust blade loadings and to shift flow streamlines. The flow streamline shift was required to match, as closely as possible, the across-the-blade inlet and exit vector diagrams.

A comparison of design intent incidence angle and the resulting through-the-blade values are shown in figure 30. The two values do not agree perfectly, again due to the change (from the across-the-blade calculation) through-the-blade solution. However, the differences were judged acceptable based on the calculated loadings from the blade-to-blade program and the wider loss versus incidence characteristic associated with the lower Mach number level.

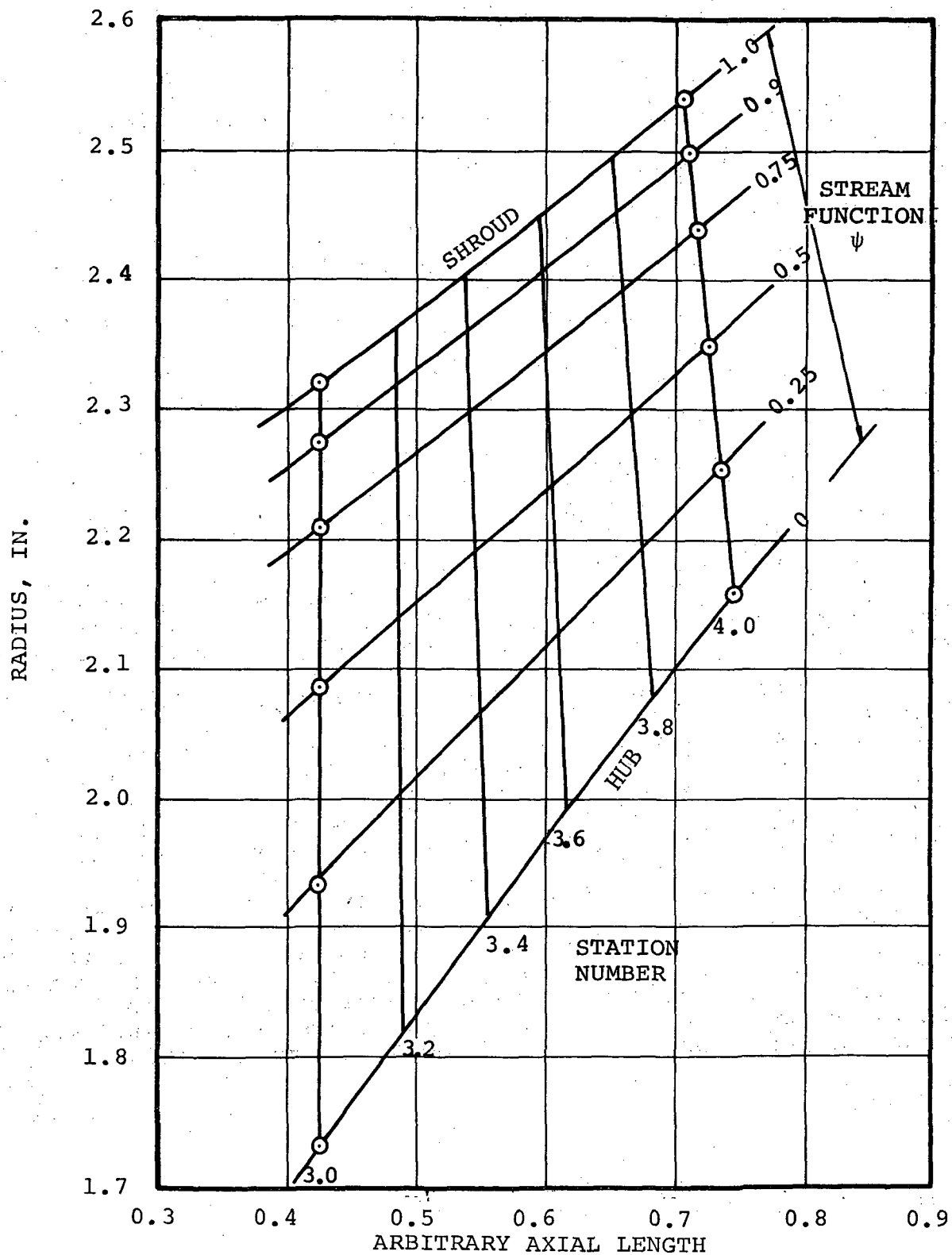


Figure 29.- Meridional Flow Path of Rotor 1B.

TABLE IX.

BLADE SETTING FOR ROTOR 1B

ψ	$M1_{REL}$	$\beta 1 (Air)$	$\beta 1 (Blade)$	i	$\beta 1_{SS} - \beta 1_{MC}$	t_{LE}
Shroud	0.981	55.02	53.04	1.98	3.08	0.0060
0.9	0.965	54.54	52.06	2.48	2.00	0.0064
0.75	0.955	54.38	51.00	3.38	2.60	0.0070
0.5	0.888	52.67	49.64	3.03	3.83	0.0080
0.25	0.784	50.89	47.00	3.89	5.34	0.0090
Hub	0.624	47.85	43.92	4.12	4.17	0.0116

ψ	$\beta 2 (Air)$	$\beta 2 (Blade)$	δ	t_{TE}	t_{max}/C_T
Shroud	57.23	49.89	7.34	0.0066	0.035
0.9	53.81	48.74	5.07	0.0075	0.0392
0.75	50.12	46.58	3.54	0.0086	0.0462
0.5	45.41	40.09	5.32	0.011	0.0586
0.25	37.74	30.65	7.09	0.0132	0.07
Hub	27.61	15.78	11.83	0.0144	0.0866

ψ	C_T	ϕ_T	a/C_T	ϕ_{SS}/ϕ_T	δ
Shroud	0.572	3.15	0.583	0.25	1.487
0.9	0.568	3.32	0.570	0.345	1.49
0.75	0.566	4.42	0.554	0.427	1.532
0.5	0.560	9.55	0.483	0.625	1.59
0.25	0.5625	16.35	0.466	0.74	1.707
Hub	0.6027	28.14	0.465	0.81	1.973

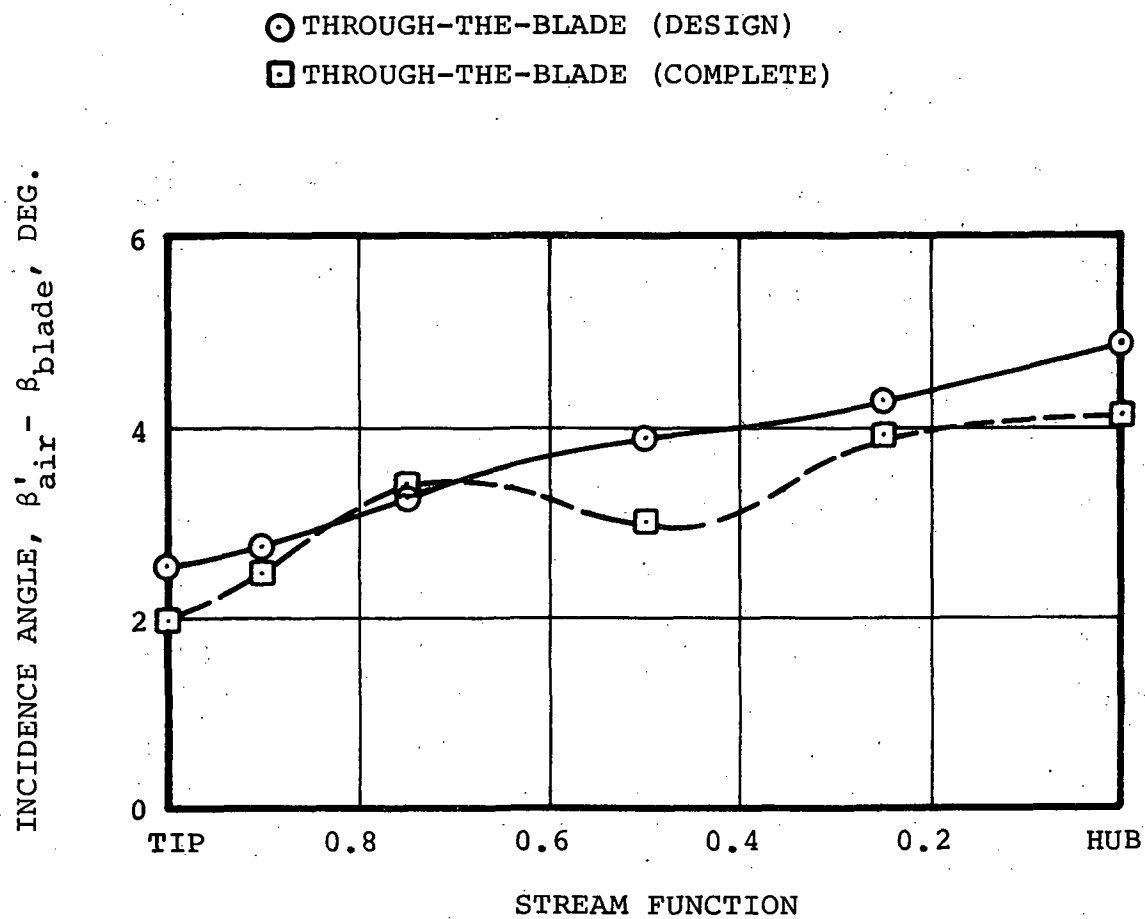


Figure 30.- Design Incidence for Rotor 1B.

The final design deviation angles are shown in figure 31. These values were calculated to give the correct angular momentum change across the second rotor blade. As seen from figure 32, the exit relative air angles from the across-the-blade solution do not agree with those from the final through-the-blade design. The trends are identical to those of the rotor 1A design. Also included are the complete through-the-blade values. Agreement is very good which assures the correct energy condition.

Final aerodynamic and blade blockage distributions are shown for the shroud, 50-percent flow, and hub streamlines in figures 33 and 34. The aerodynamic blockage was distributed linearly with streamline meridional distance and held constant across each calculation station line.

For rotor 1B, since all inlet relative velocities were subsonic, distribution of angular momentum from the blade-to-blade program was used for all streamlines. The final design distributions for the shroud, 50-percent flow, and hub streamlines are shown in figures 35, 36, and 37.

A comparison of across-the-blade diffusion factor distribution at rotor 1B exit to the final design solutions is shown in figure 38. Small differences exist across the entire blade. However, these differences were not felt to be significant enough to change the original loss values.

⊙ THROUGH-THE-BLADE (COMPLETE)

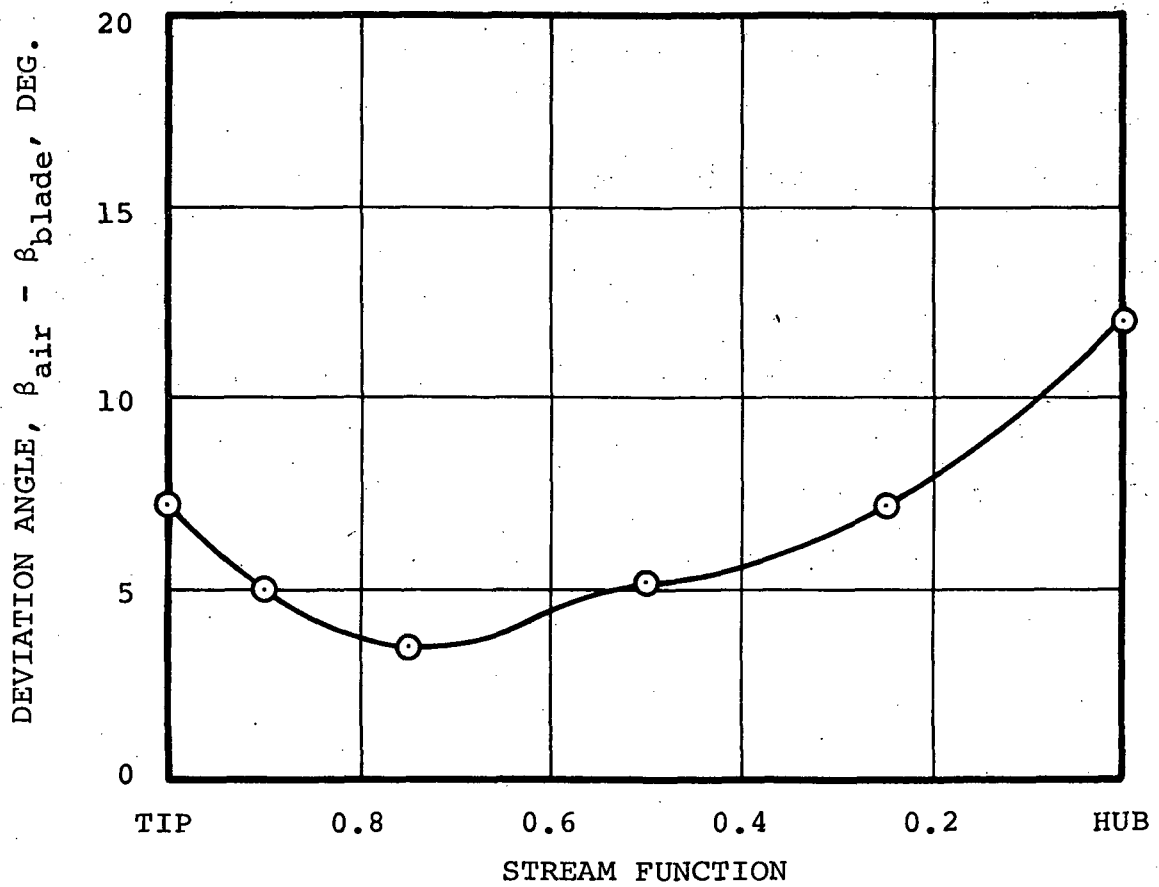


Figure 31.- Rotor 1B Final Design Deviation Angle.

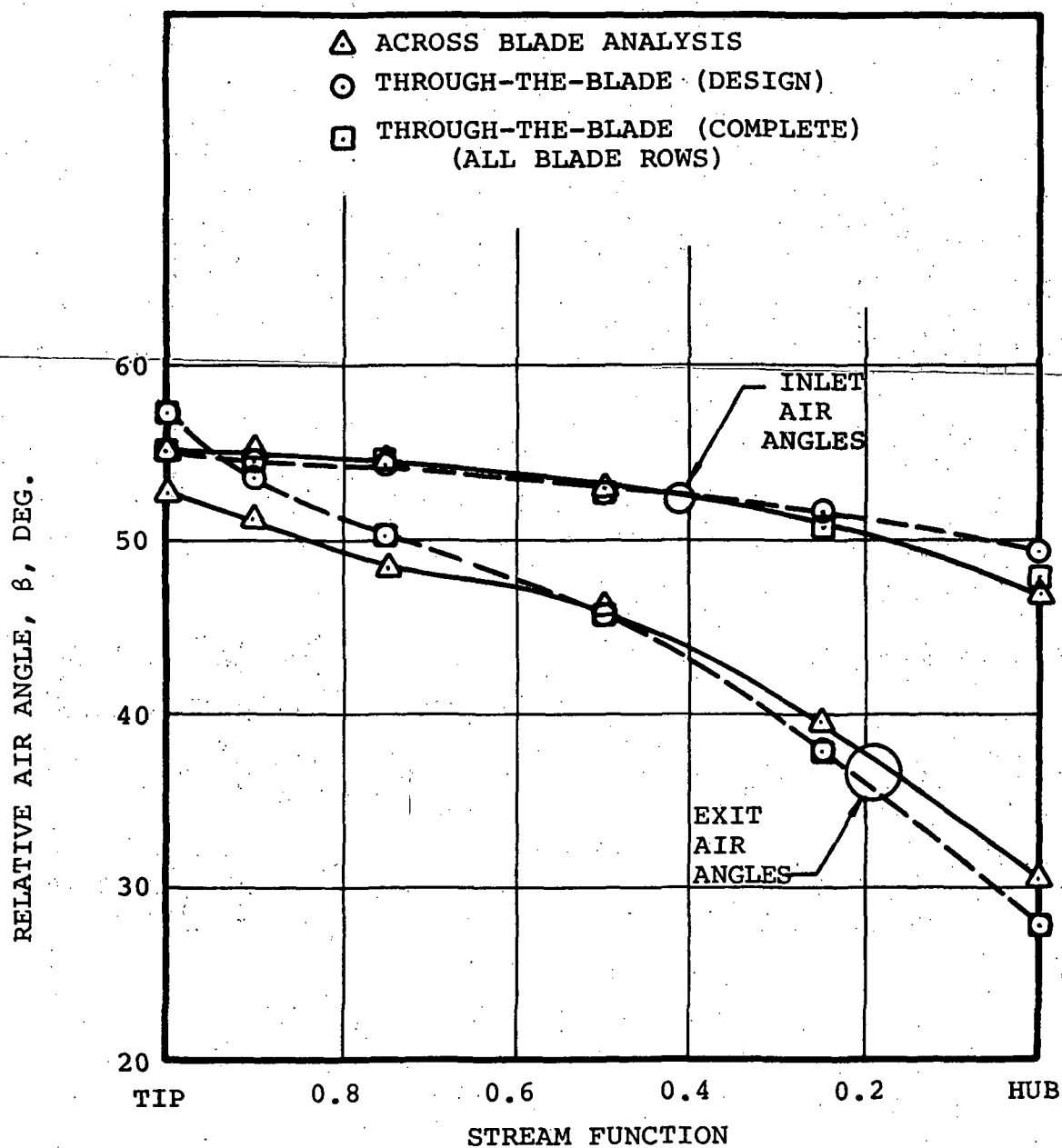


Figure 32.- Comparison of Rotor 1B Relative Air Angles.

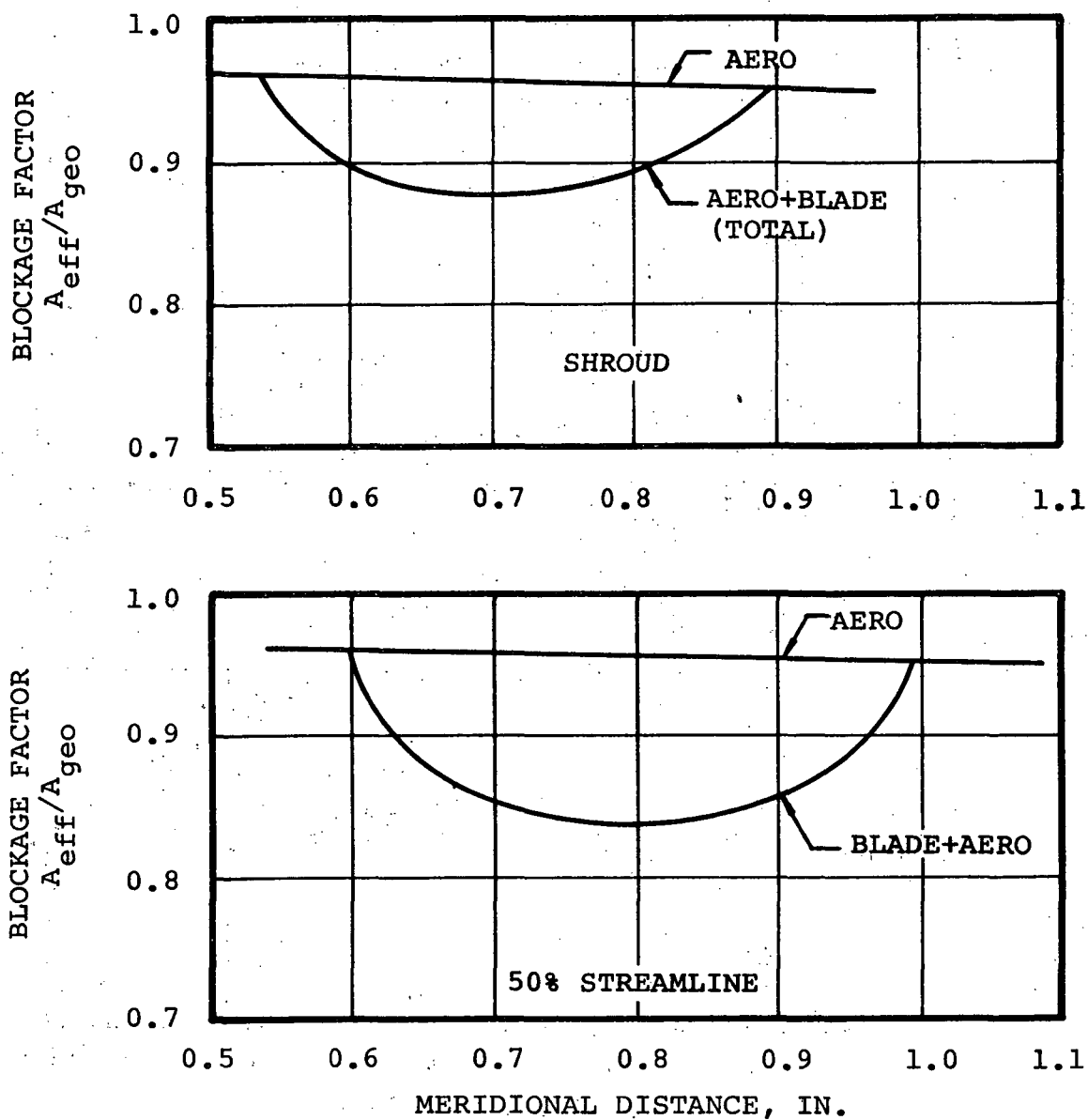


Figure 33.- Rotor 1B Blade Blockage Distribution.

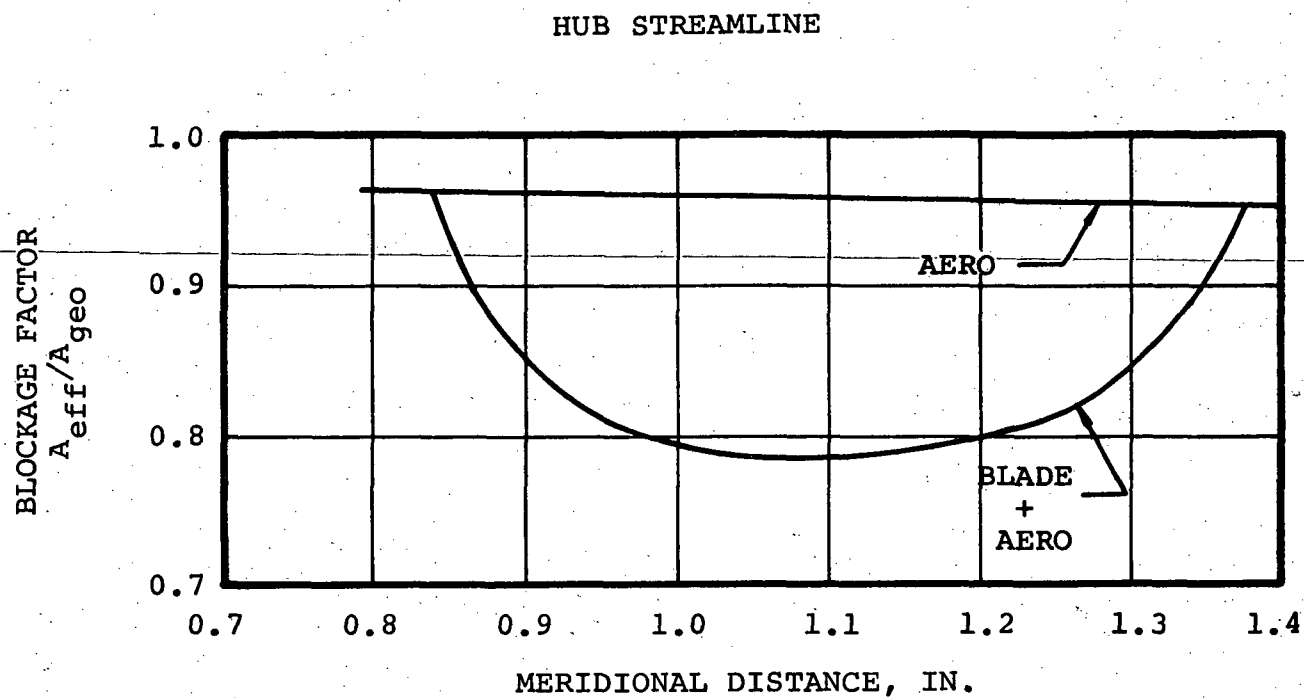


Figure 34.- Rotor 1B Blade Blockage Distribution.

WHERE $U_t \text{ REF} = 610 \text{ FT/SEC.}$

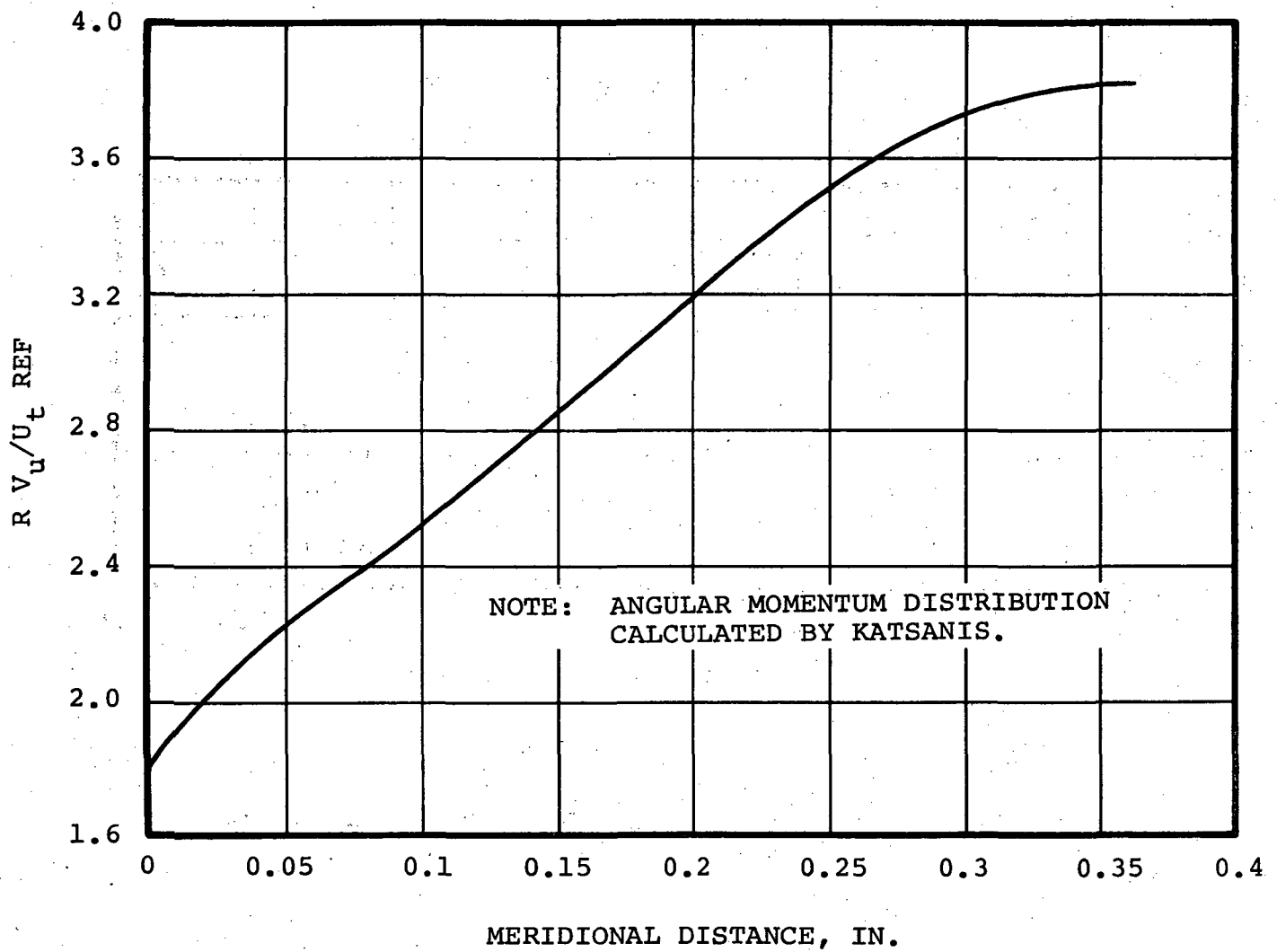


Figure 35.- Rotor 1B Tip Streamline Energy Distribution.

WHERE $U_t \text{ REF} = 610 \text{ FT/SEC}$

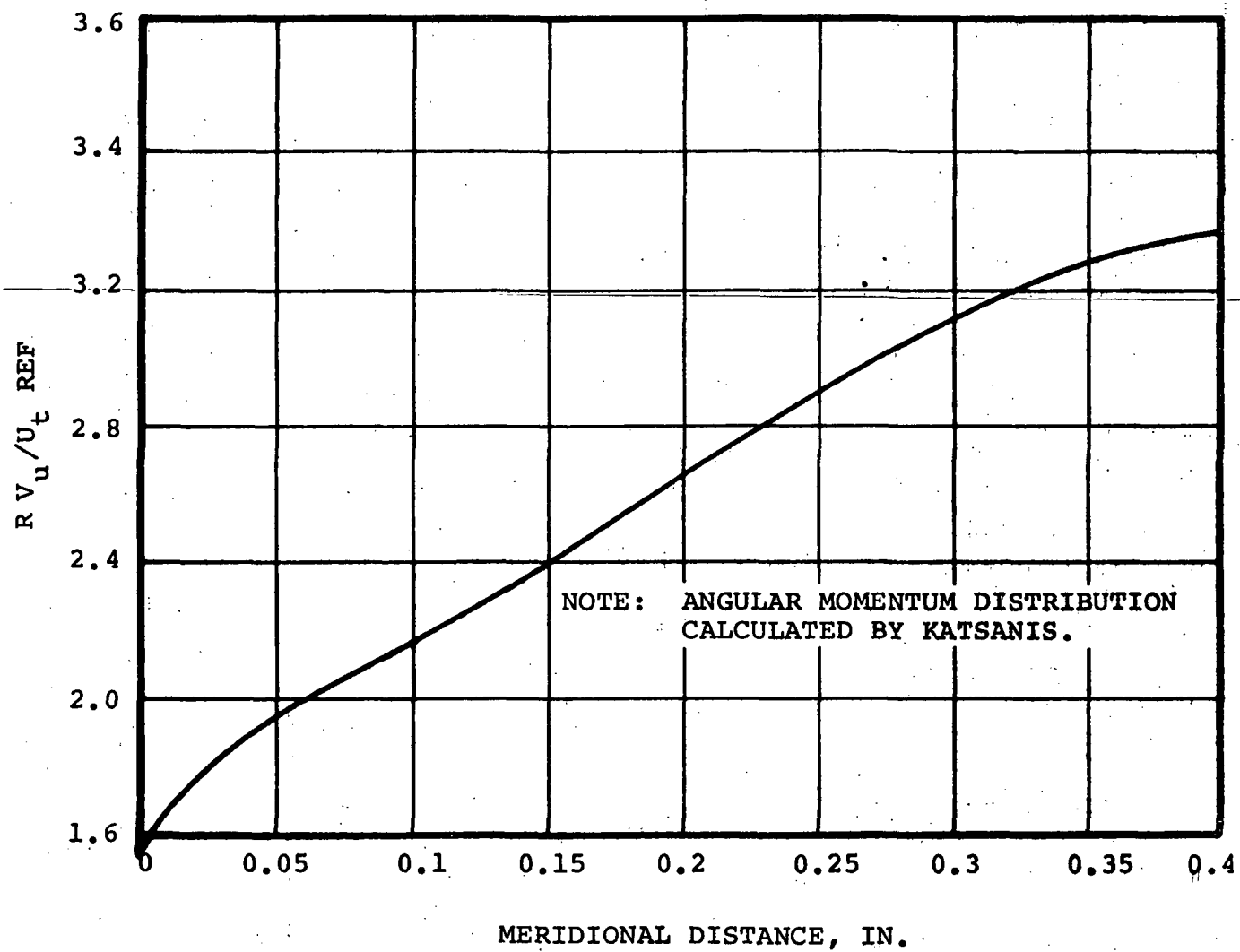


Figure 36.- Rotor 1B Fifty-Percent Streamline Energy Distribution.

WHERE $U_{t \text{ REF}} = 610 \text{ FT/SEC}$

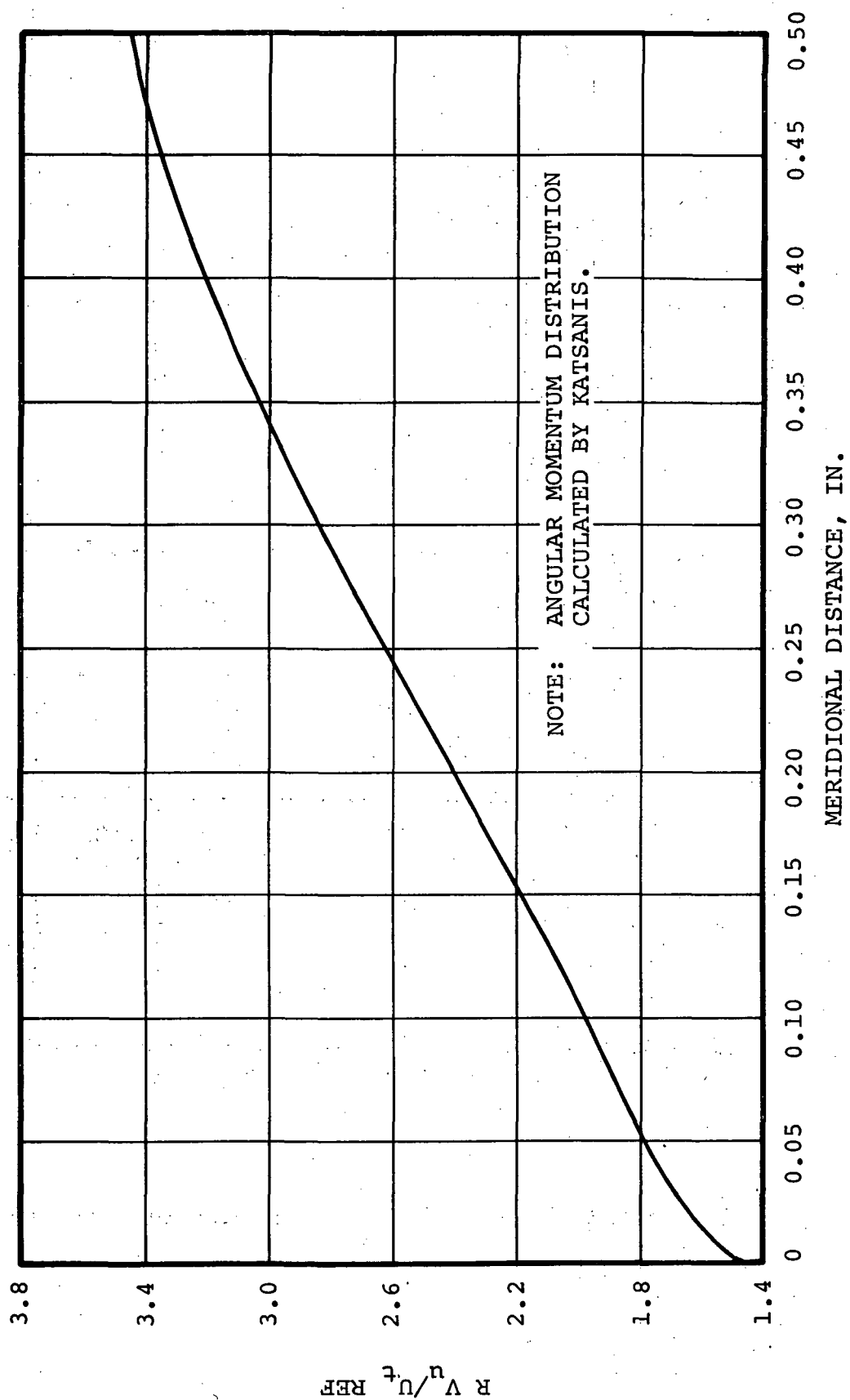


Figure 37.- Rotor 1B Hub Streamline Energy Distribution.

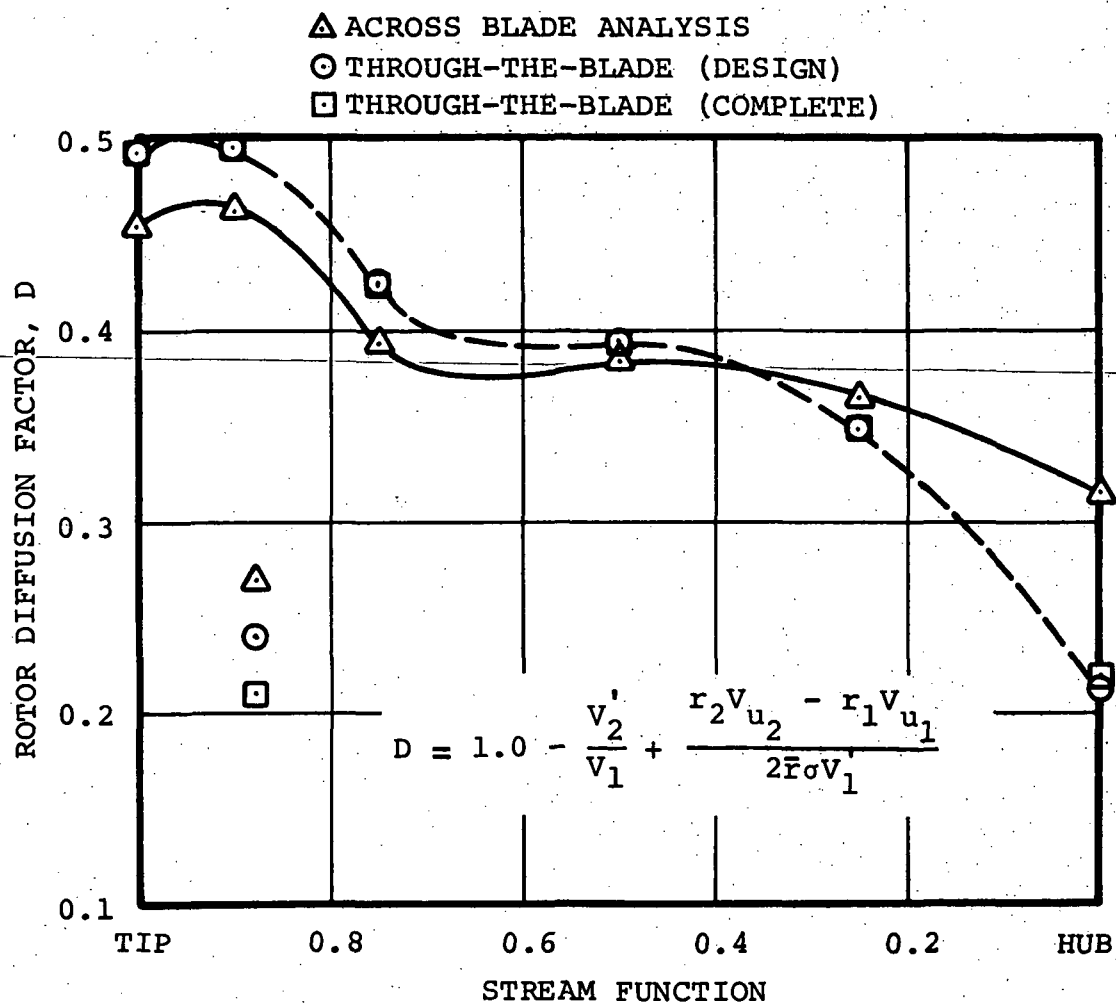


Figure 38. - Comparison of Rotor 1B Exit Diffusion Factor Distribution.

The final loadings from the blade-to-blade program for the shroud, 50-percent flow, and hub streamlines are shown in figures 39, 40, and 41. All distributions are uniform in their deceleration rate.

Throat area checks were made for each of the streamlines to preclude the possibility of rotor 1B choking at the design condition. The minimum area ratio occurred for streamlines 1 through 4 at 1.04 of the minimum value. Streamlines 5 and 6 were had considerably more margin.

A final comparison is the distribution of inlet and exit relative air angles (Figure 32) as calculated by the initial across-the-blade analysis and by the two through-the-blade analysis. This result is similar to that observed in the rotor 1A design.

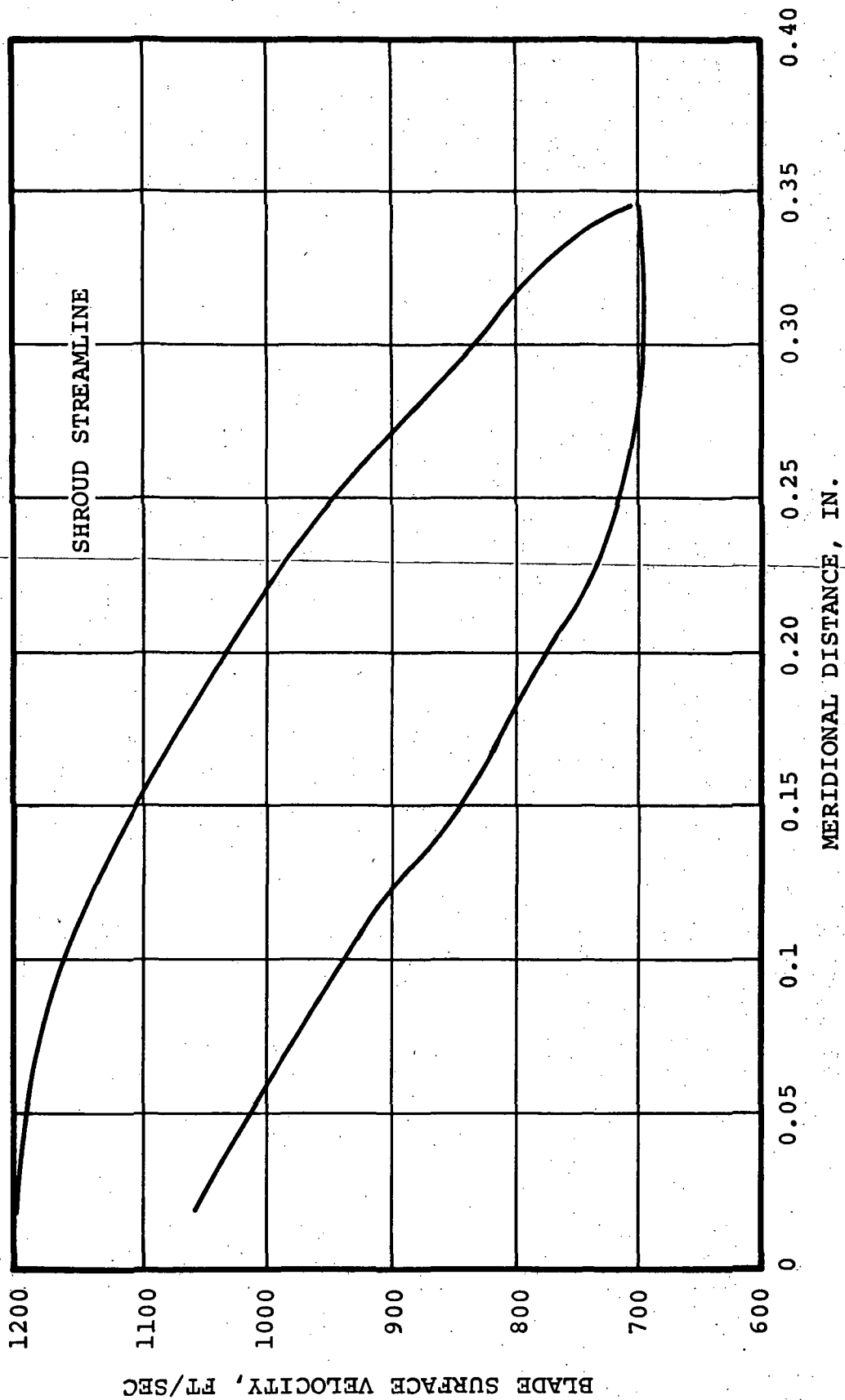


Figure 39. - Rotor 1B Final Blade Loading From The Blade-To-Blade Program Analysis.

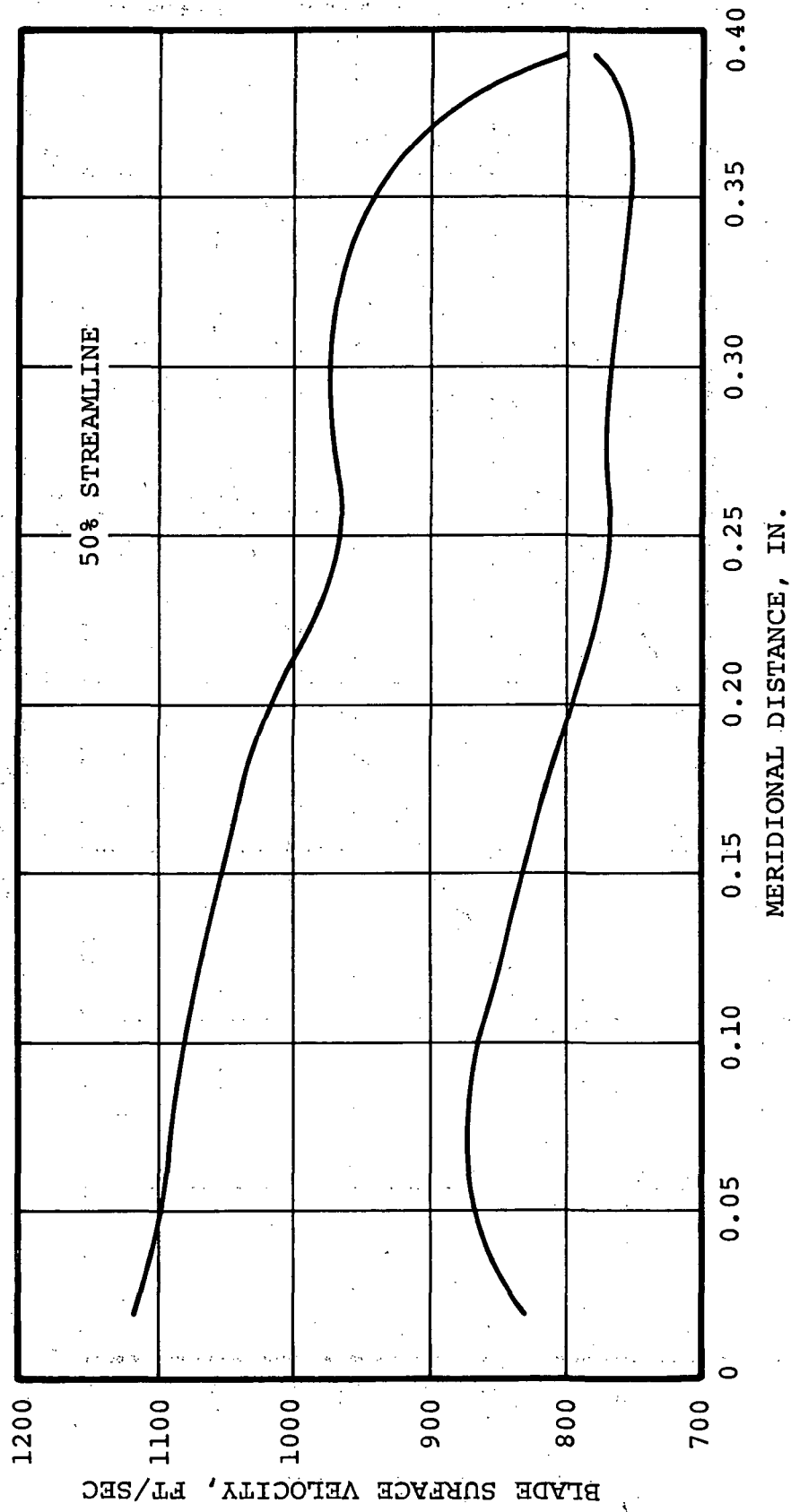


Figure 40. - Rotor 1B Final Blade Loading From The Blade-To-Blade Program Analysis.

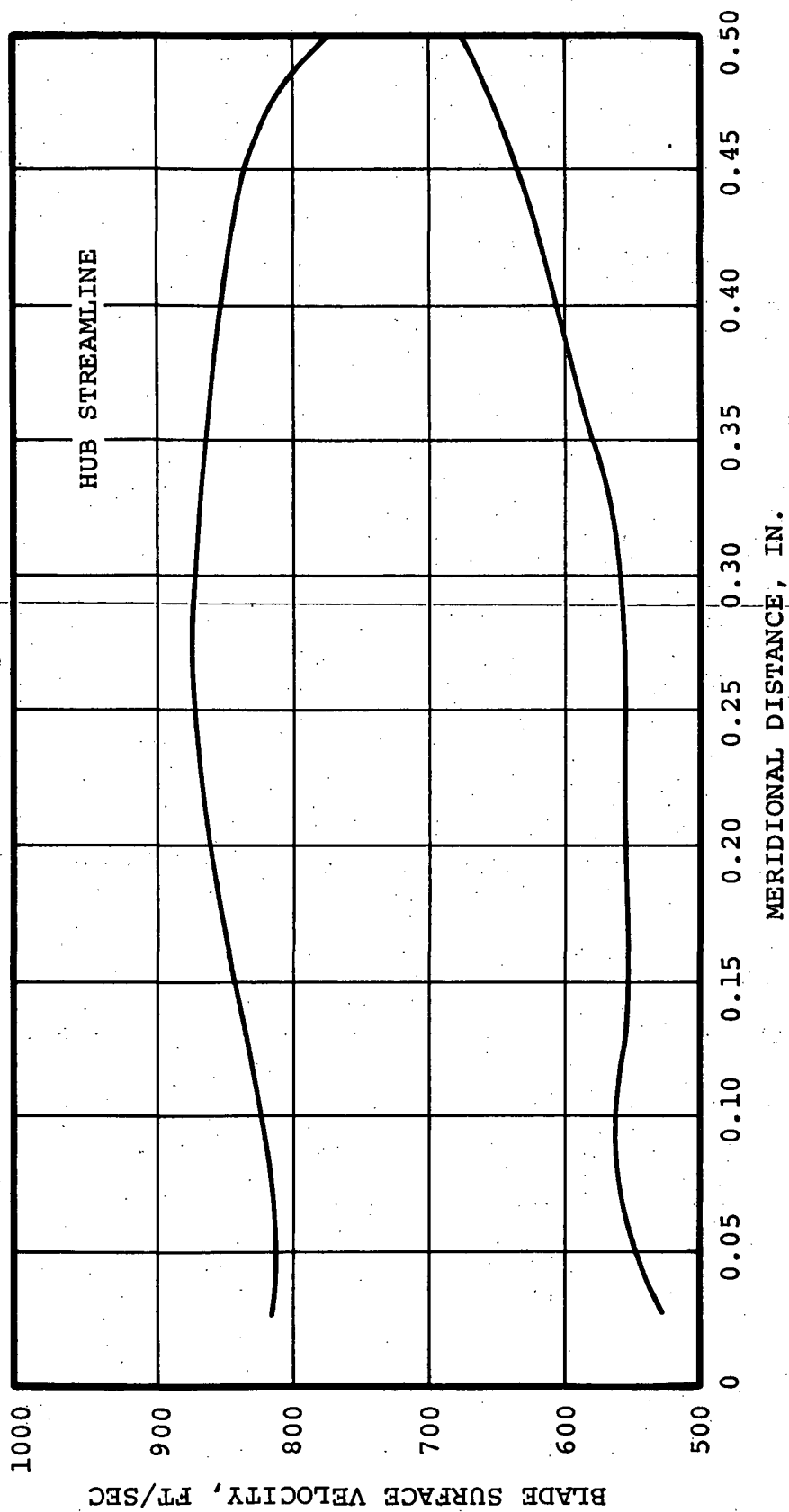


Figure 41. - Rotor 1B Final Blade Loading From
The Blade-To-Blade Program Analysis.

TANDEM STATOR DESIGN

The final design parameters for stators 1A and 1B are as follows:

	<u>Stator 1A</u>	<u>Stator 1B</u>
Hub inlet Mach number	0.845	0.423
Hub solidity	1.891	1.63
Number of vanes	53	53
Aspect ratio	0.604	0.494

The meridional shape and calculation station locations are shown in figure 41a for the first row and figure 41b for the second row. Appendix B presents plots of the stacked blades and the section coordinators.

The distribution of inlet Mach number for both stators is shown in figure 42. For these levels of Mach number, double circular arc airfoils were used throughout both stator vane designs.

The design incidence angle for both stators, based on current stator technology (Reference 10), was -2.0 degrees to the suction surface. A comparison of the design intent to the final values is shown in figure 43 for both stators. Deviations from the design intent vary approximately ± 2 degrees for stator 1A and from $+0.8$ degrees to -2.0 degrees for stator 1B. Time limitations prevented better matching with the design intent. However, the blade-to-blade analysis did not indicate excessive leading edge loadings.

The final stator deviation angles are as shown in figure 44. These values were required to achieve the correct amount of diffusion in each vane row. Air angles for the across-the-blade and through-the-blade analysis at the inlet and exit of each stator vane row are compared in figures 45 and 46. Good agreement (within 1 degree) was achieved at the inlet to each row whereas discrepancies up to 3.0 degrees occurred at the exit of each vane row.

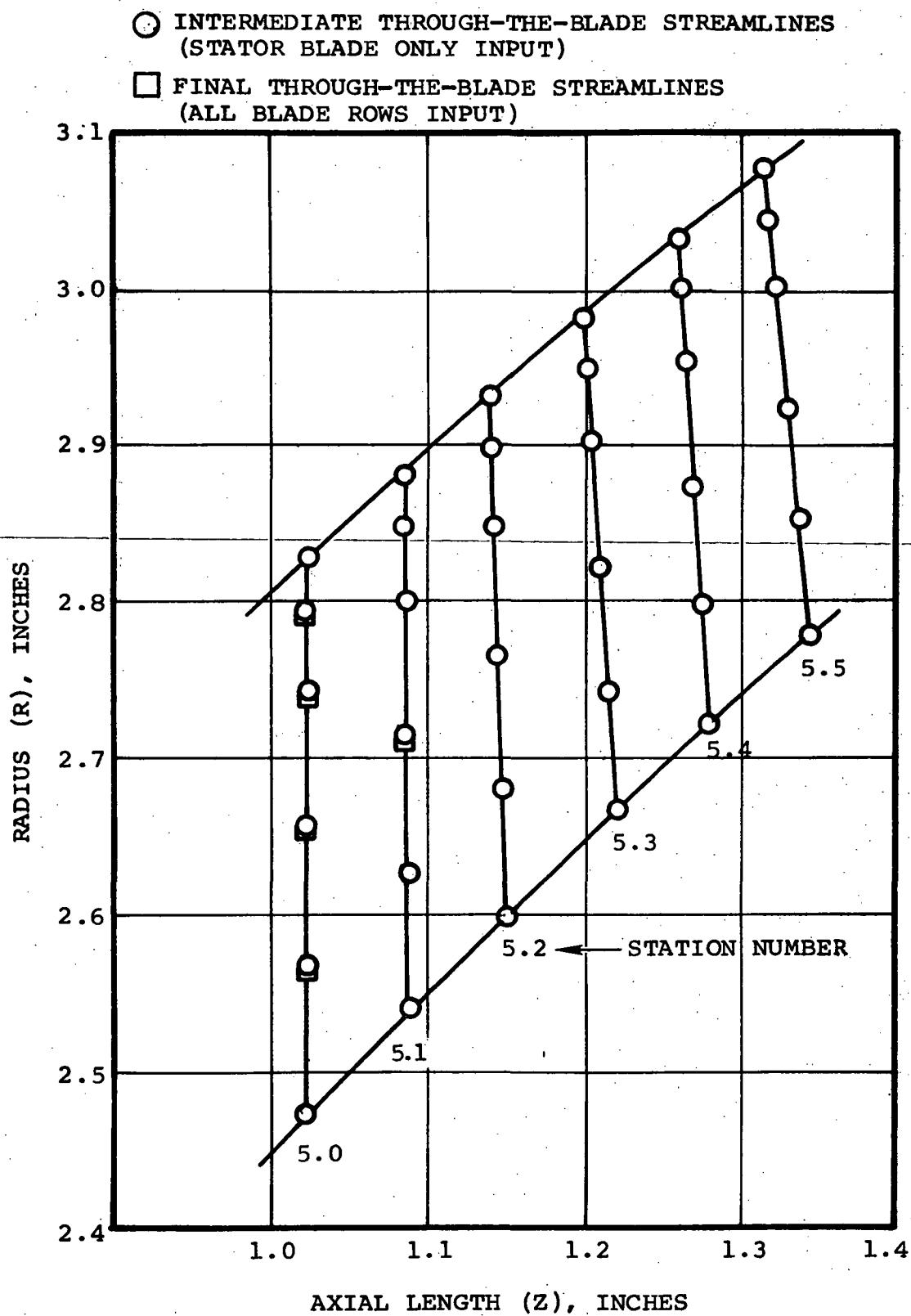


Figure 41a. - Meridional Shape for Stator 1A.

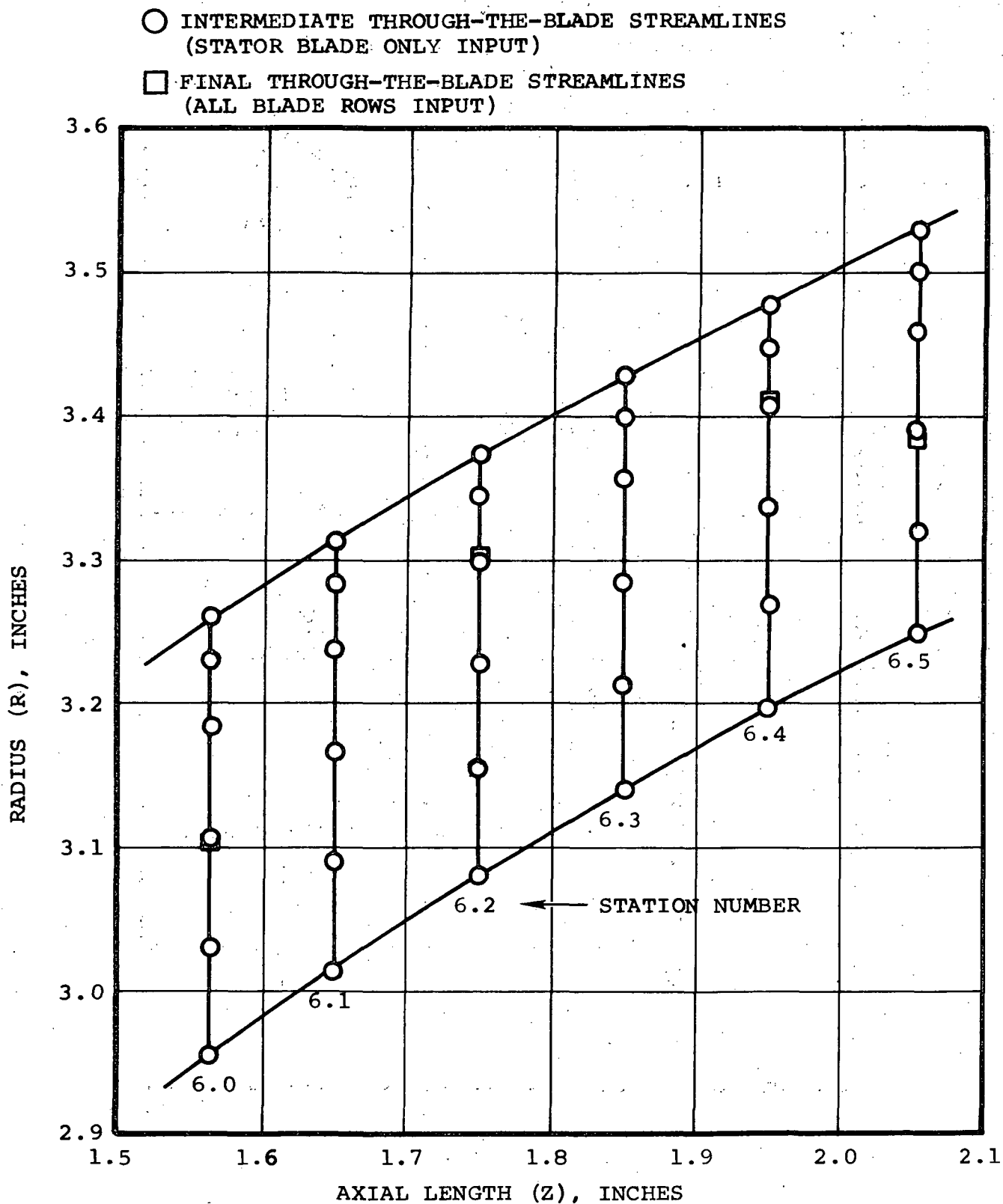


Figure 41b. - Meridional Shape for Stator 1B.

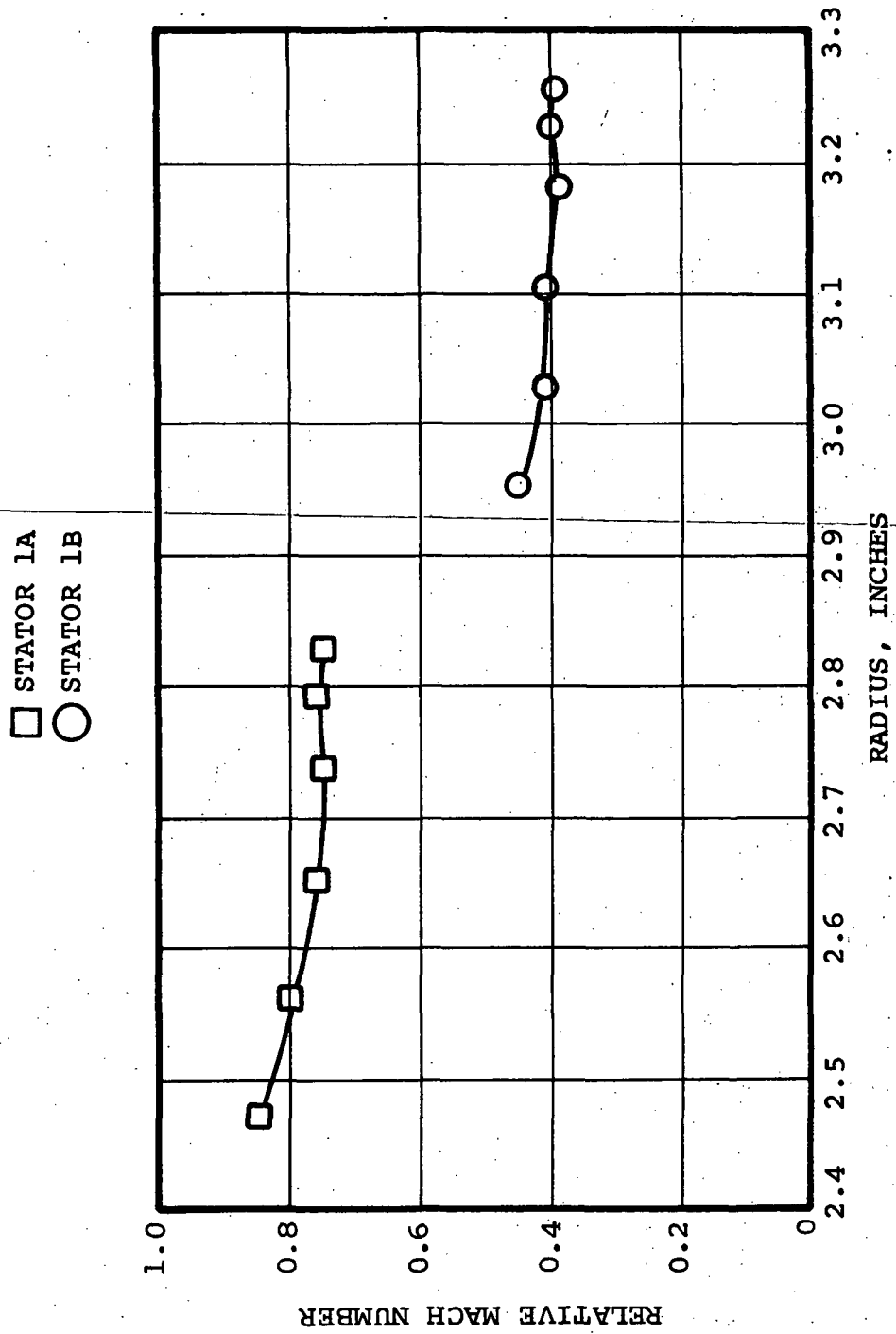


Figure 42. Inlet Mach Number For Stators 1A and 1B.

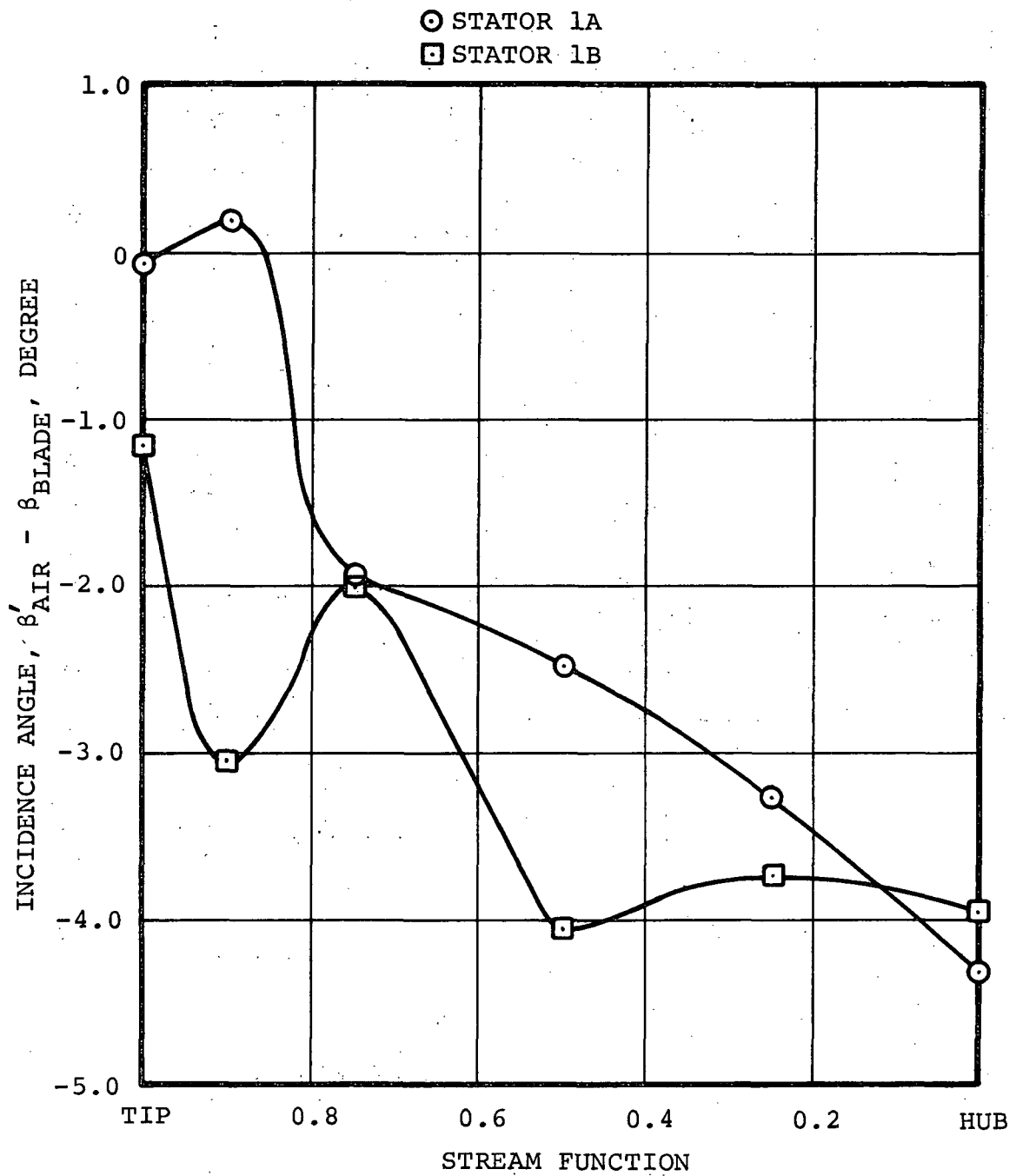


Figure 43. - Design Incidence Angles For Both Stators.

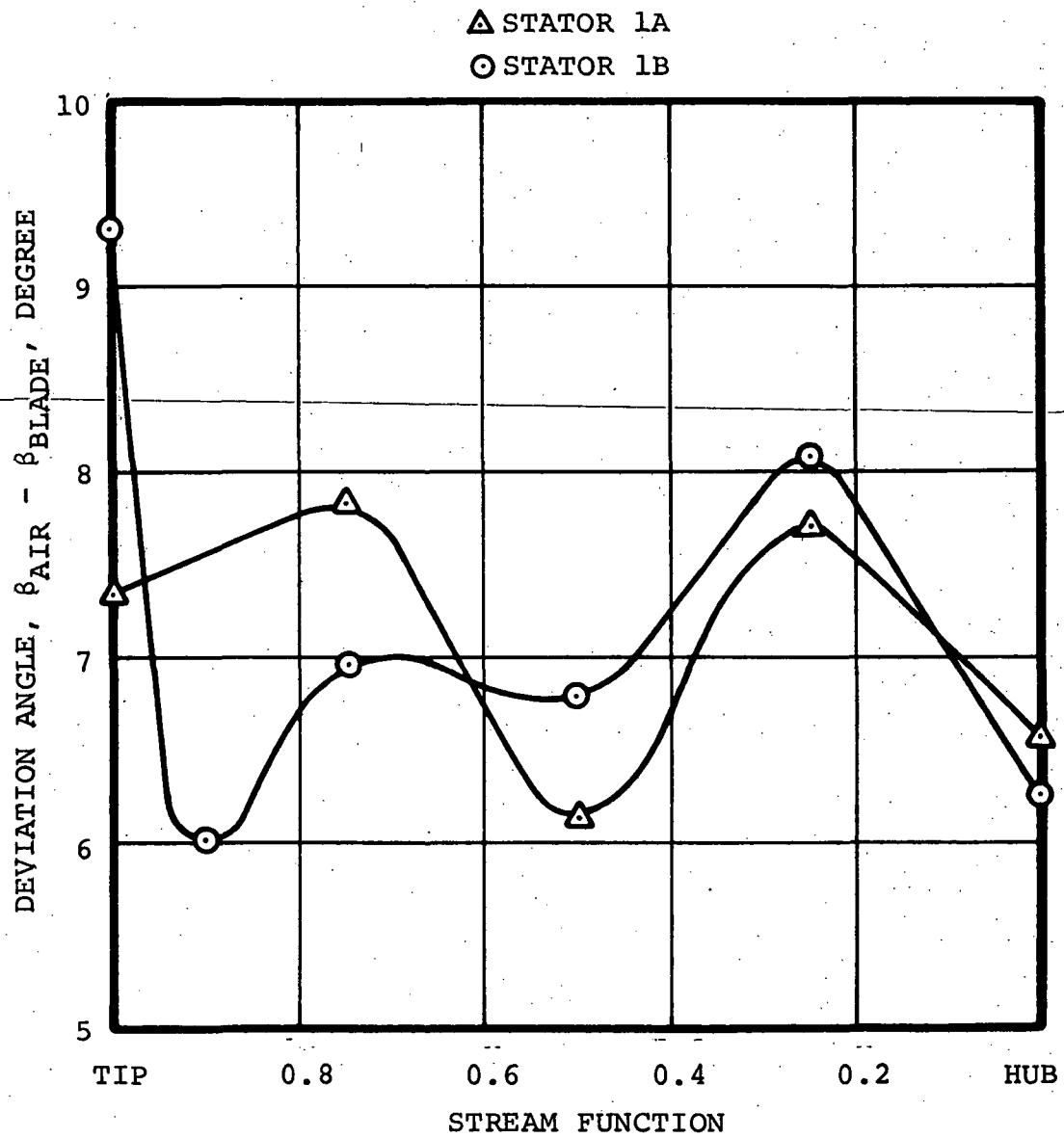


Figure 44. - Design Deviation Angles For Both Stators.

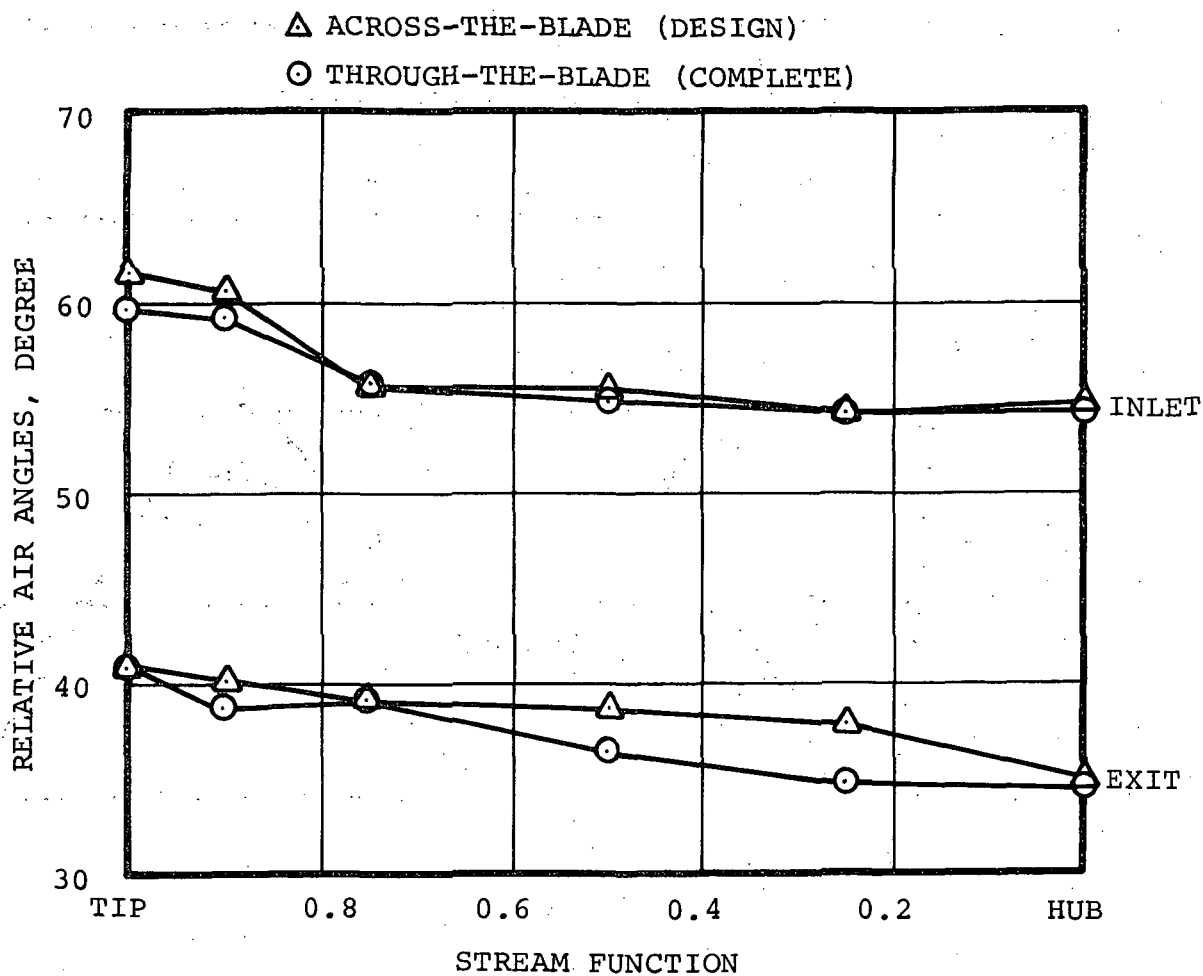


Figure 45. - Comparison of Stator 1A Relative Air Angles Between Initial and Final Design Solutions.

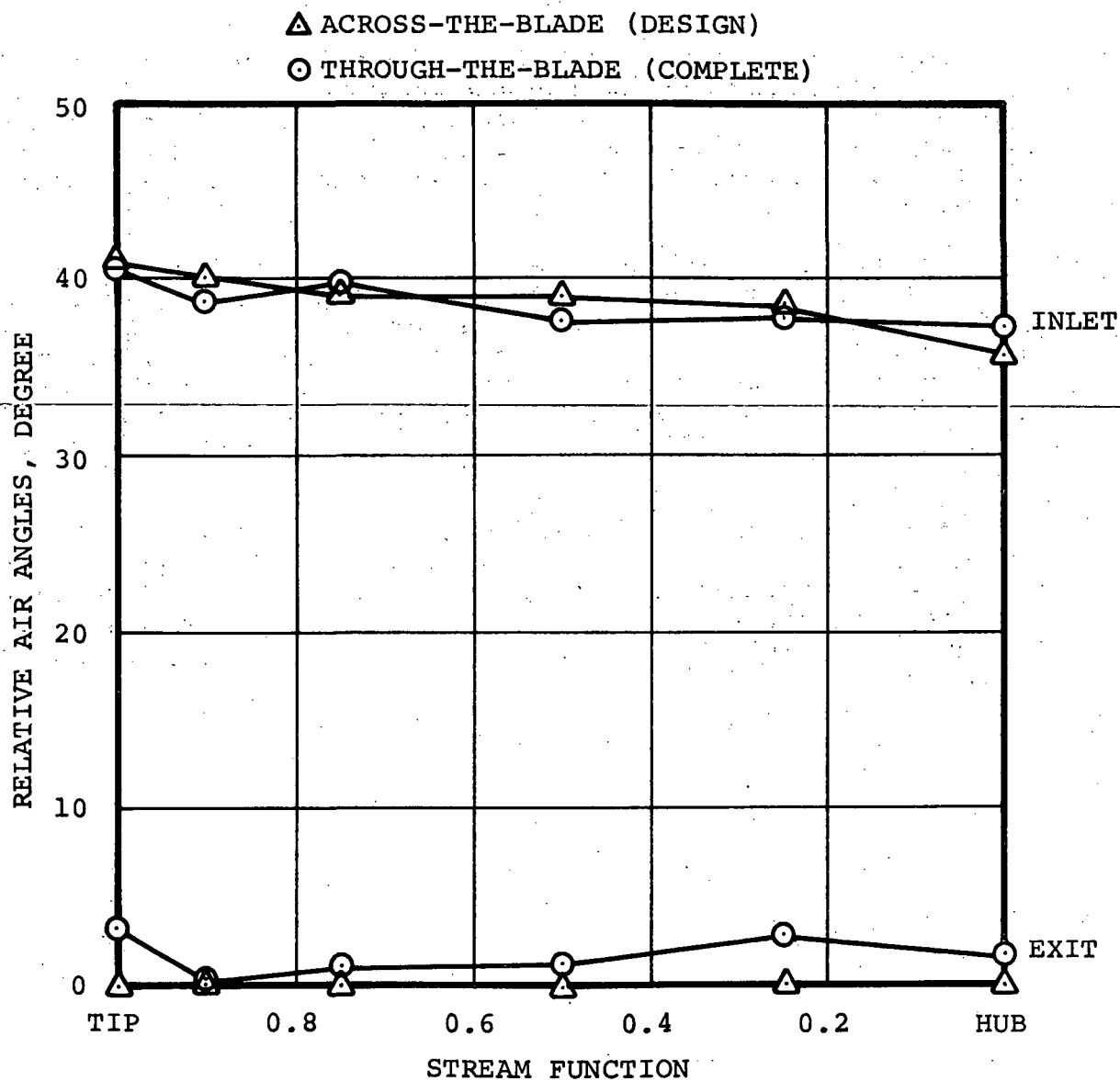


Figure 46. - Comparison of Stator 1B Relative Air Angles Between Initial and Final Design Solutions.

Distribution of the aerodynamic and blade blockage for the tip, 50-percent flow, and hub streamline for each stator vane are contained in figures 47 through 52. Aerodynamic blockage was again distributed as in the tandem rotor design.

The rate of angular momentum decreases through each of the stators as shown in figures 53 through 56. These values were obtained from the blade-to-blade calculation. Complete deswirl of the air was not achieved by the second stator. However, the amount of remaining angular momentum was not considered detrimental to the performance of a second stage.

Stator diffusion factors are compared in figures 57 and 58. Final 1A values for the design and complete through-the-blade analysis are somewhat lower than the across-the-blade analysis. For 1B, however, the design and complete through-the-blade analysis are not consistent due to streamline shifts caused by the rotor/stator blade interaction. Where the difference is largest, toward the hub in stator 1B, the diffusion factor is less which is advantageous from a loss consideration.

Final stator loadings along the tip, 50-percent flow, and hub streamlines for stators 1A and 1B are shown in Figures 59 through 64. The tip streamline loadings for both stators display the highest loading near the leading edge due to the more positive incidence angles. However, loadings are smooth and should provide acceptable performance.

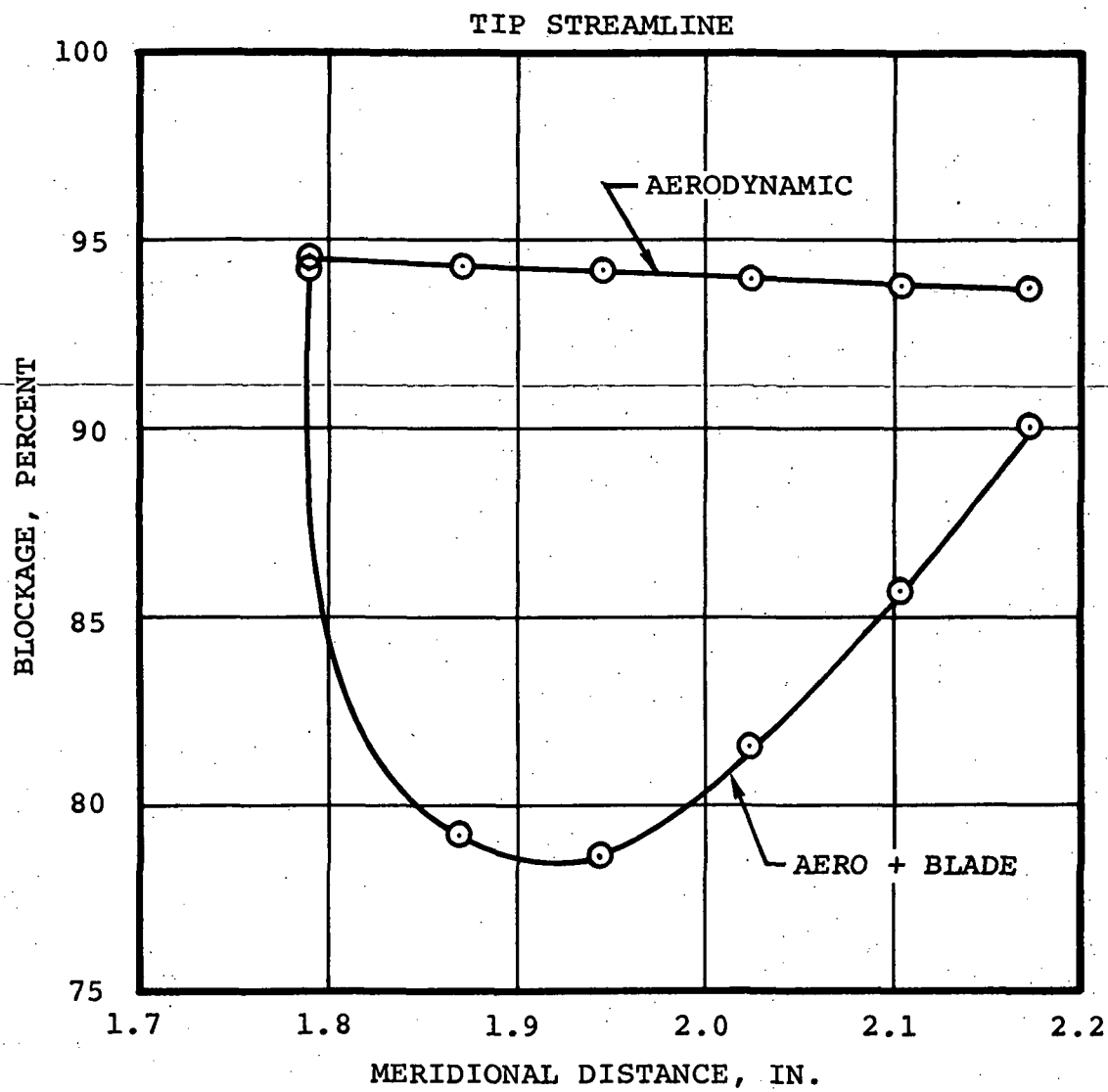


Figure 4. - Stator 1A Blockage Distribution.

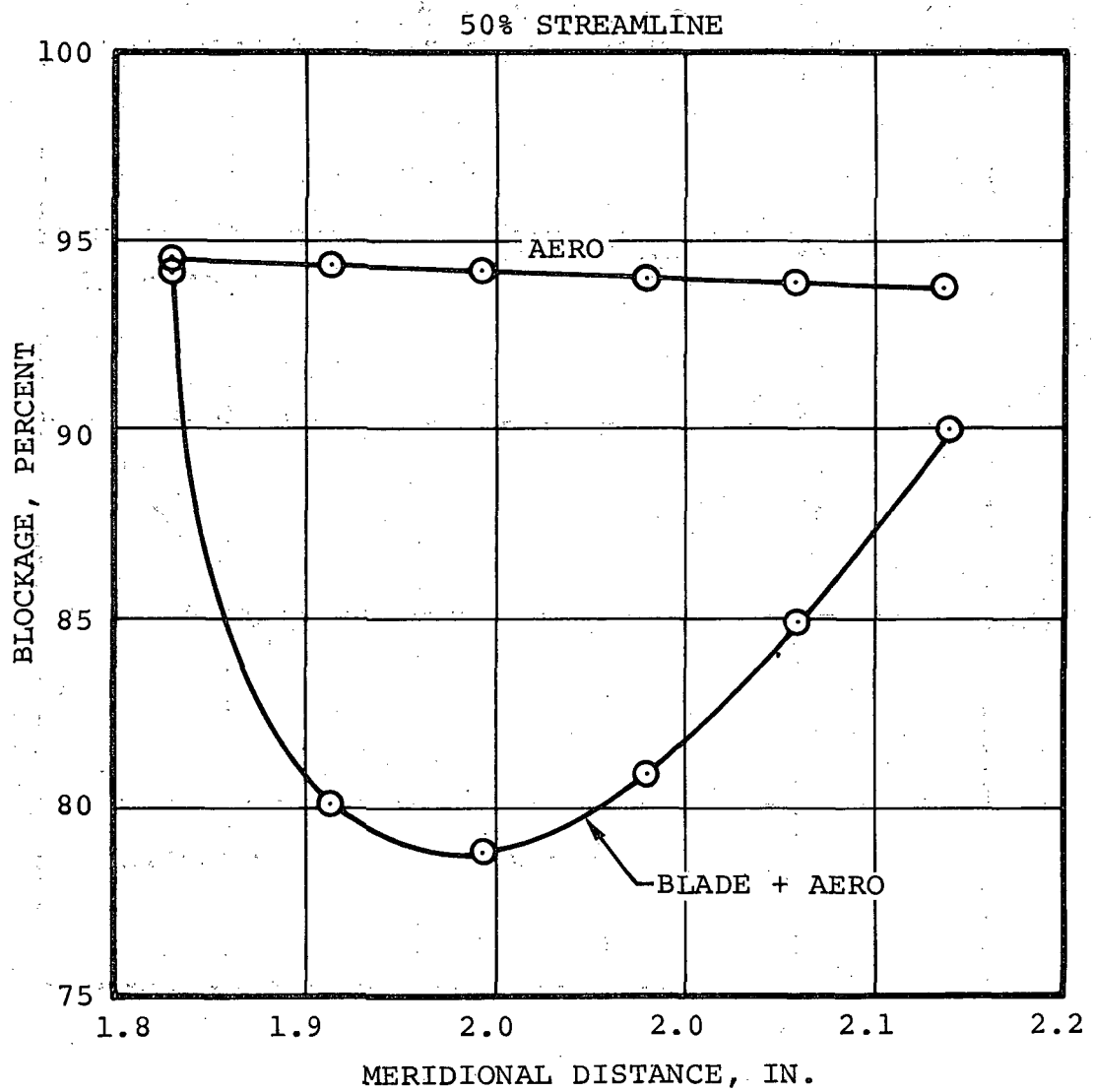


Figure 48. - Stator 1A Blockage Distribution.

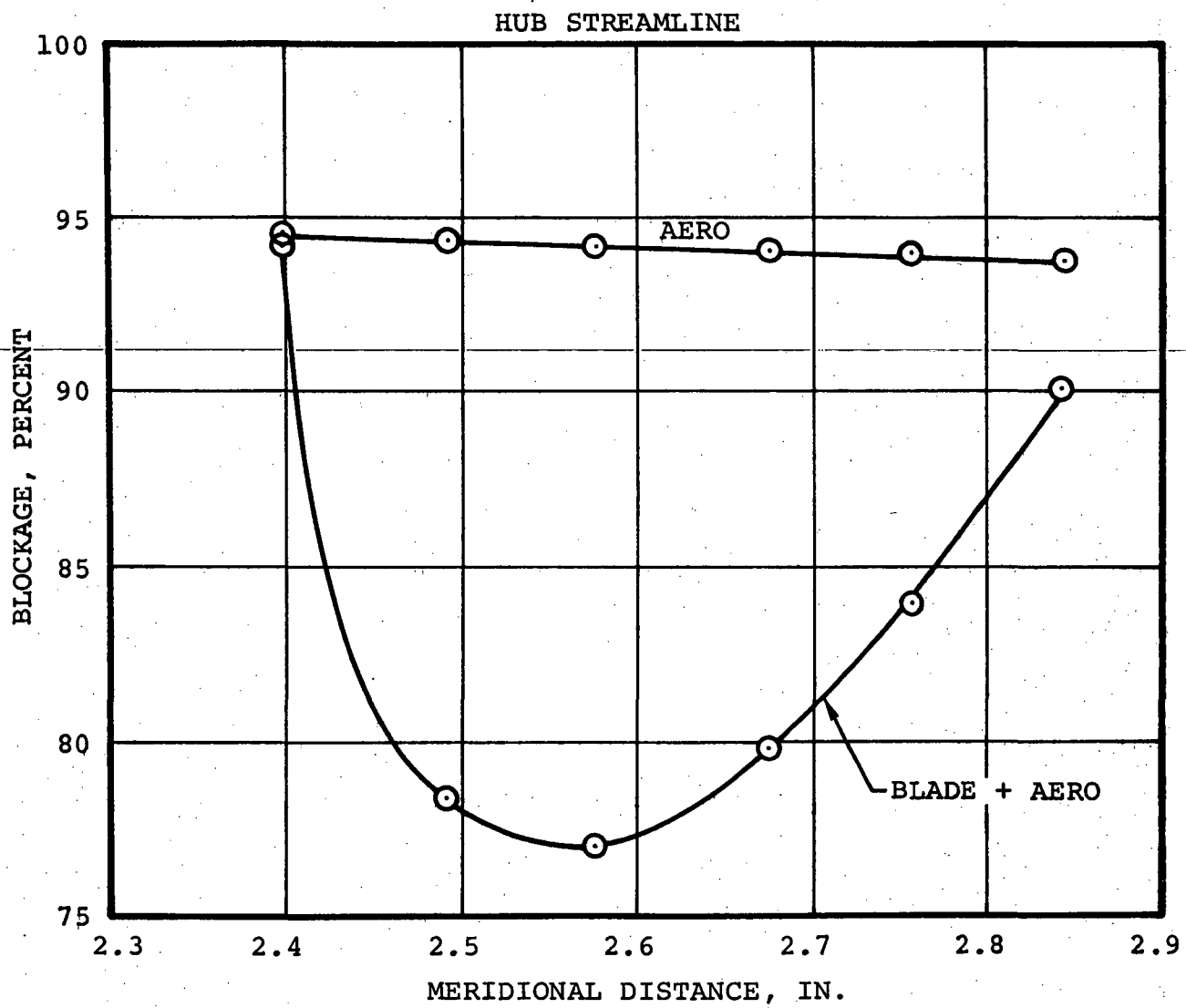


Figure 49. - Stator 1A Blockage Distribution.

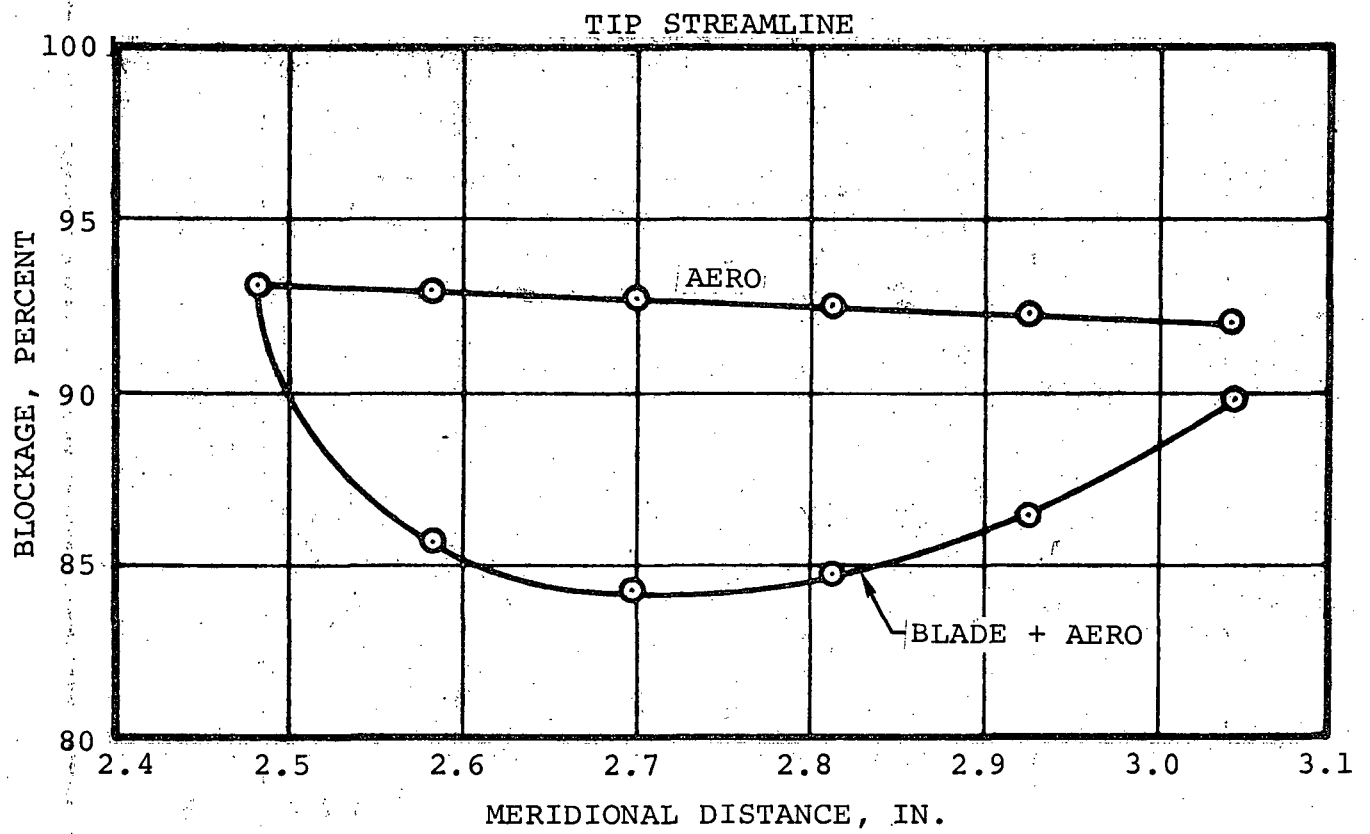


Figure 50. - Stator 1B Blockage Distribution.

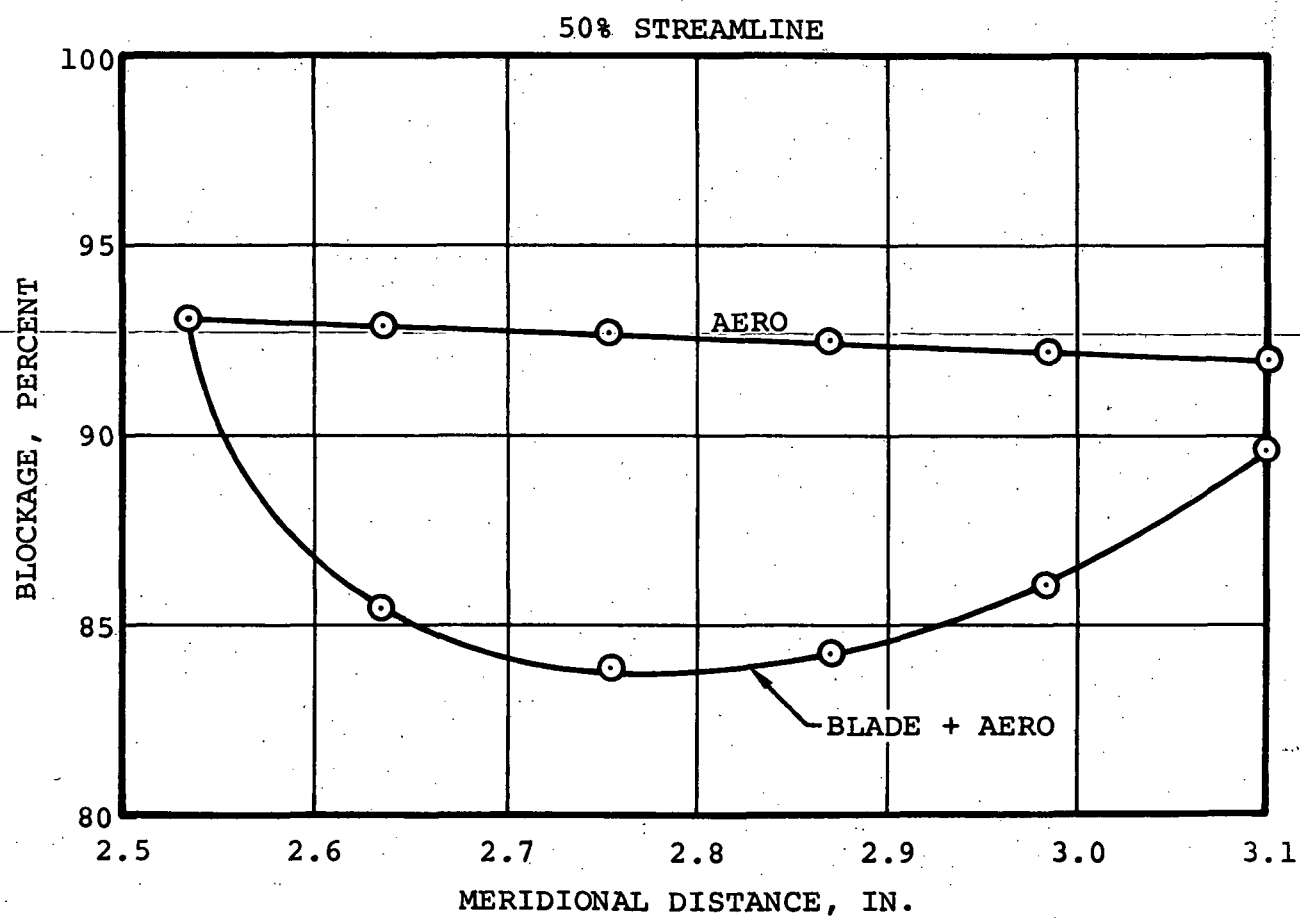


Figure 51. - Stator 1B Blockage Distribution.

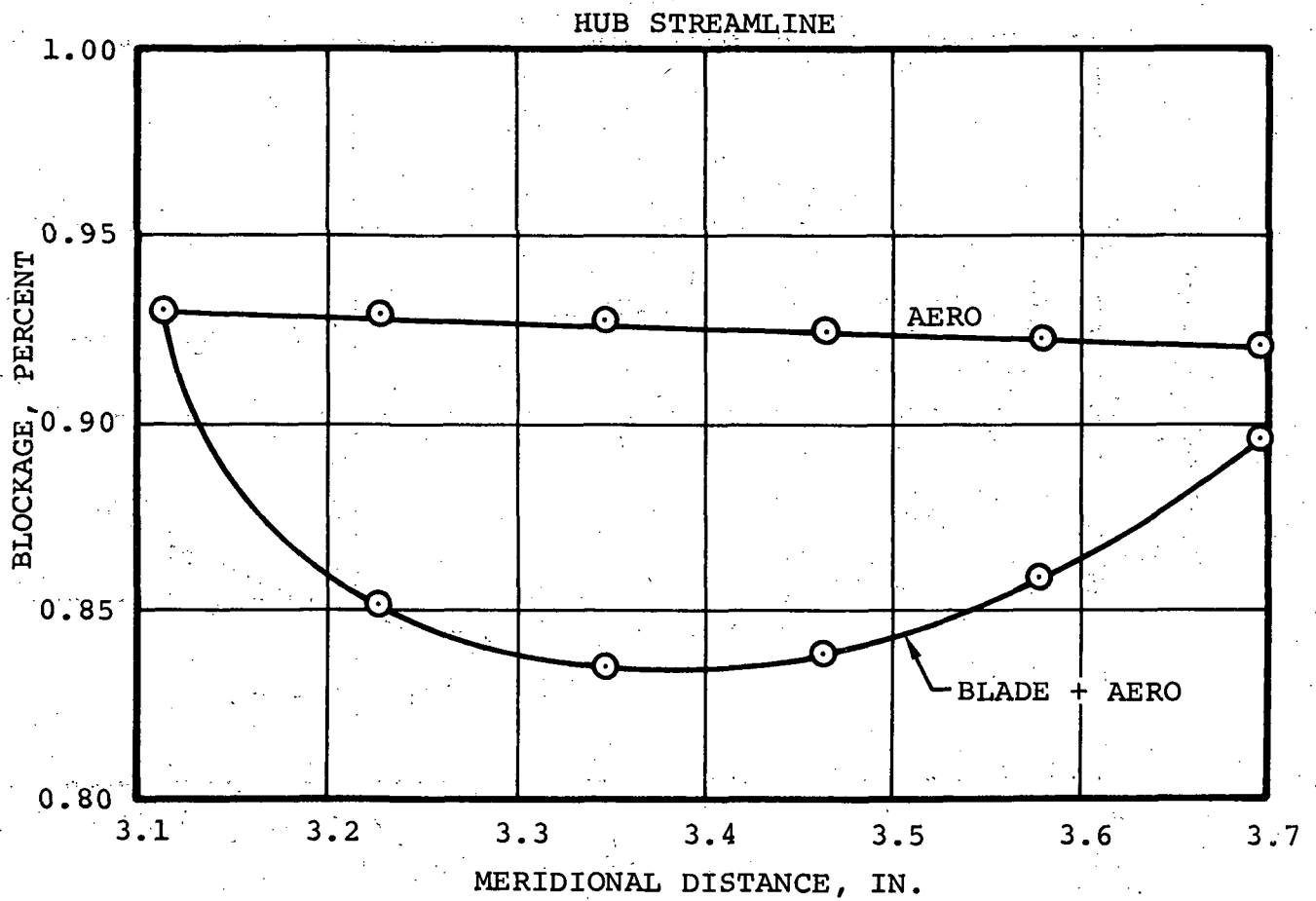


Figure 52. - Stator 1B Blockage Distribution.

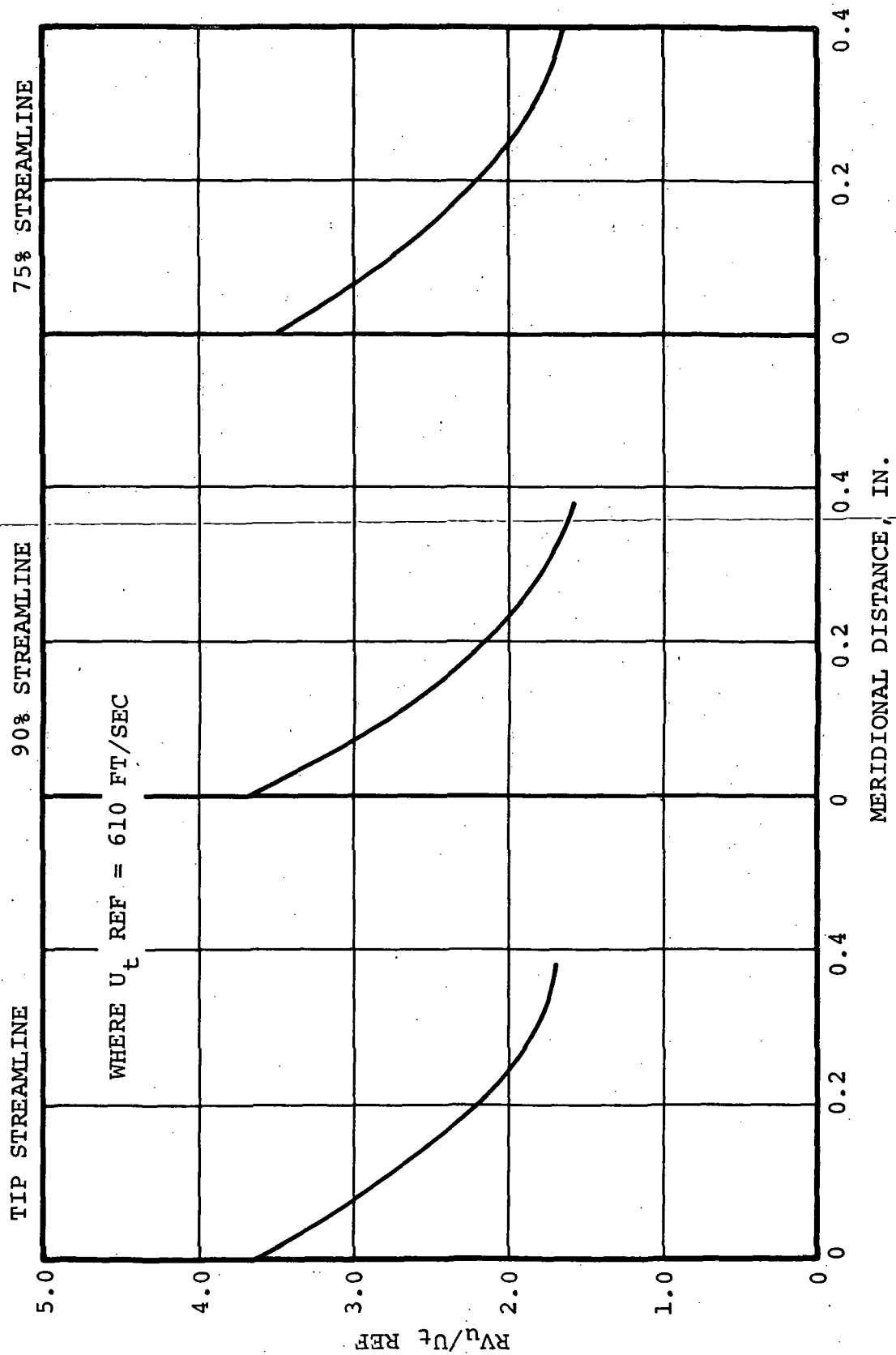


Figure 53. - Stator 1A Streamline Energy Distribution.

WHERE $U_t \text{ REF} = 610 \text{ FT/SEC}$

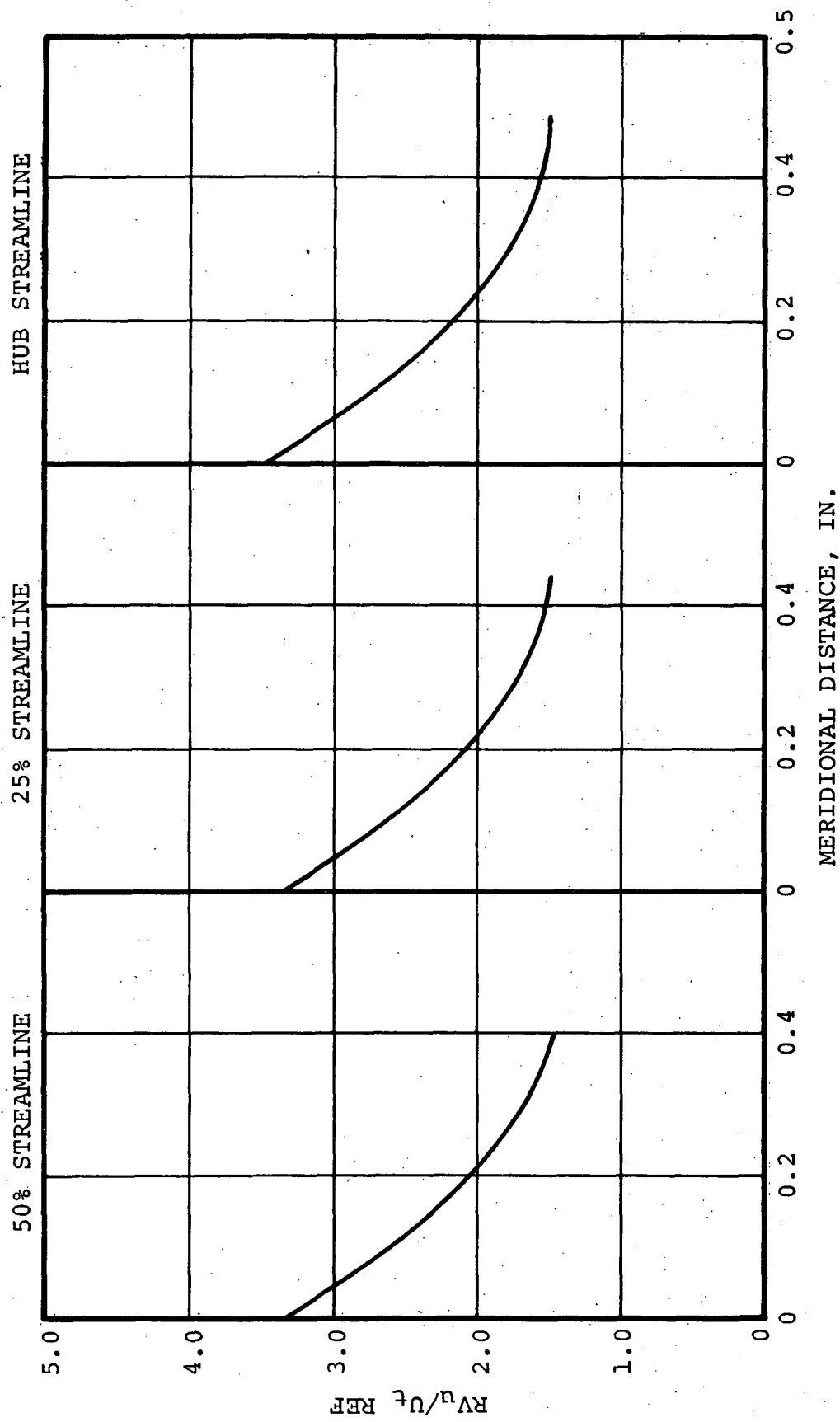


Figure 54. - Stator 1A Streamline Energy Distribution.

WHERE $U_t \text{ REF} = 610 \text{ FT/SEC}$

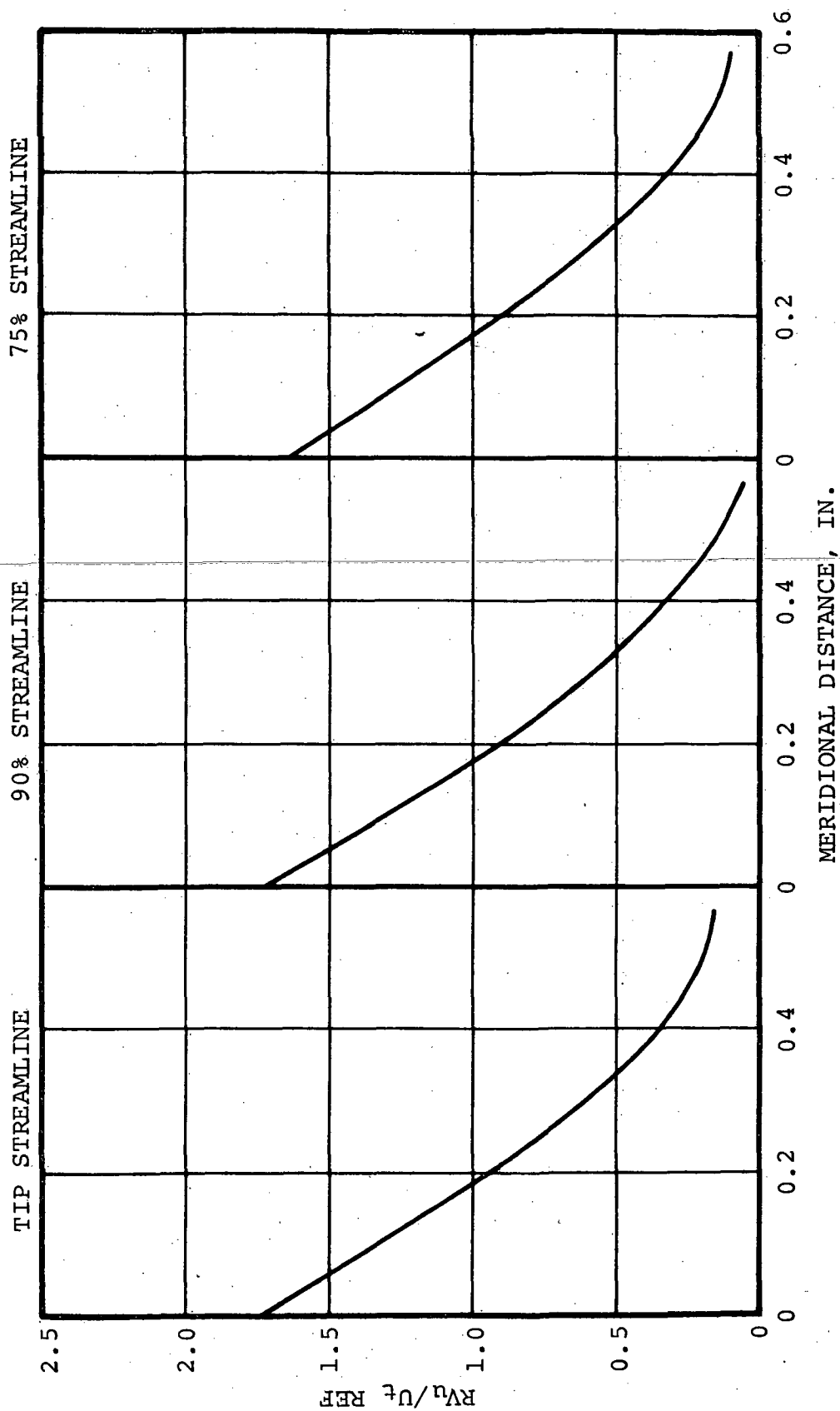


Figure 55. - Stator 1B Streamline Energy Distribution.

WHERE $U_t \text{ REF} = 610 \text{ FT/SEC}$

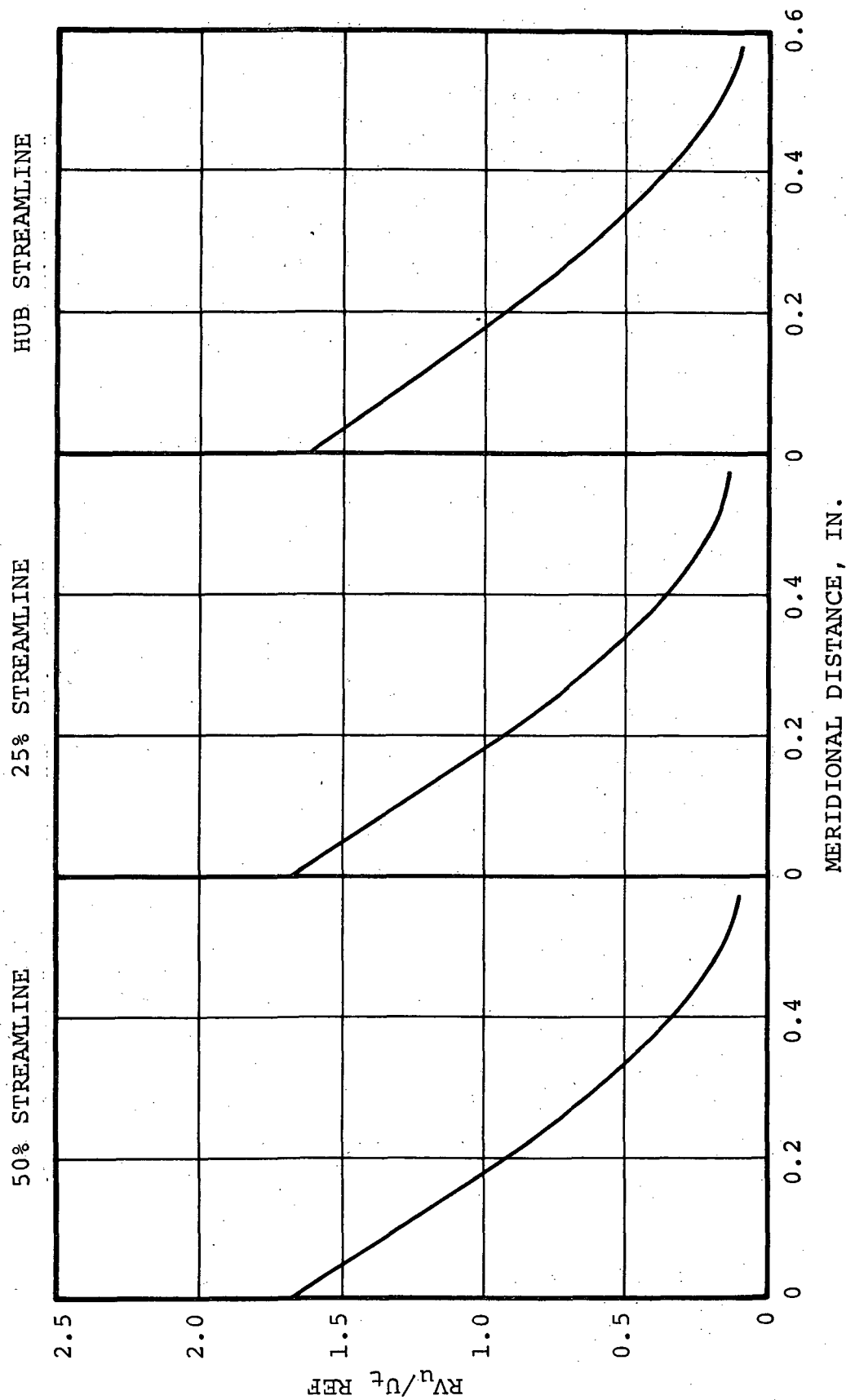


Figure 56. - Stator 1B Streamline Energy Distribution.

$$D = 1.0 - \frac{v_2}{v_1} + \frac{r_2 v_{u2} - r_1 v_{u1}}{2 \bar{r} \sigma v_1}$$

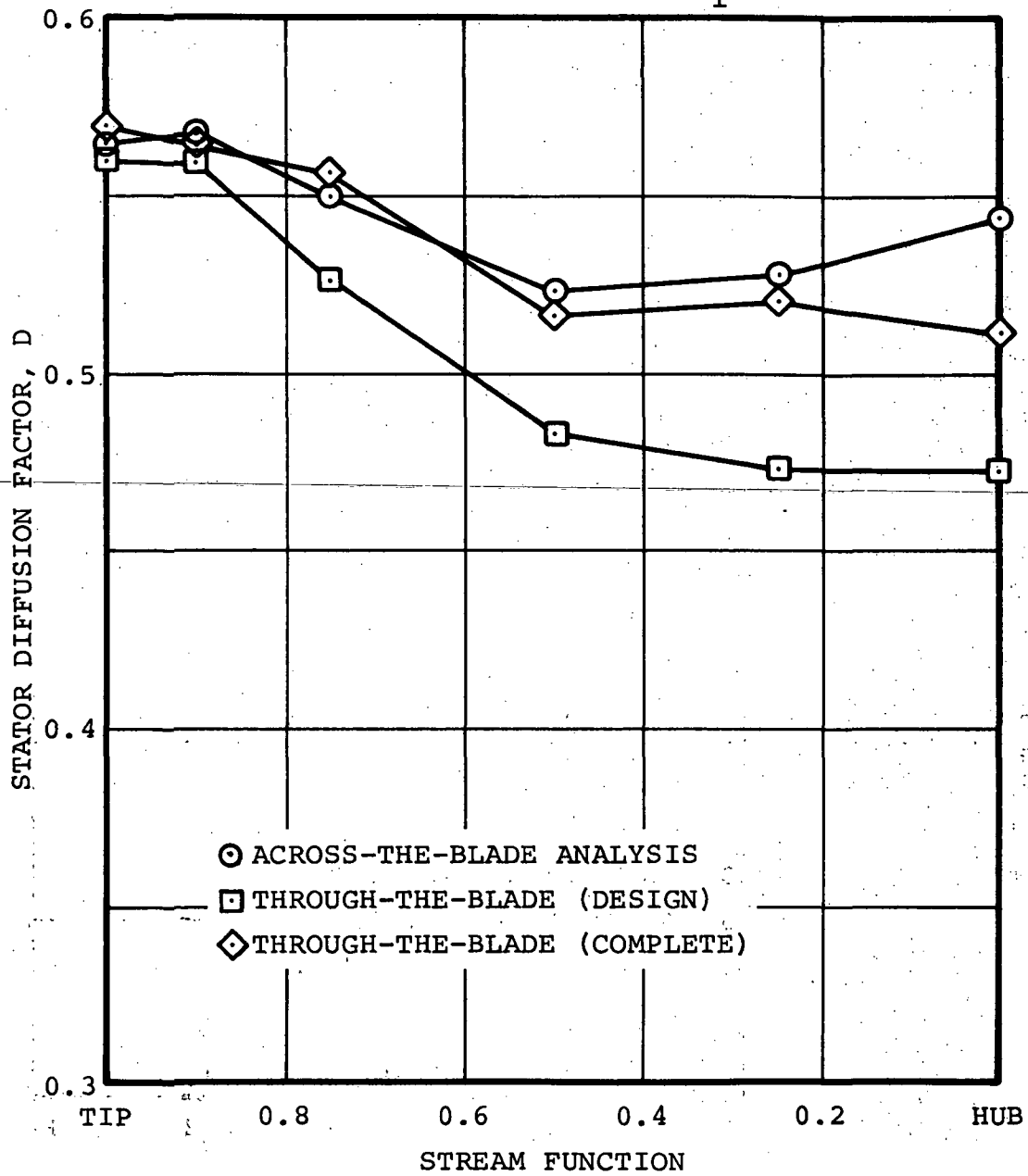


Figure 57. - Stator 1A Diffusion Factor Distribution.

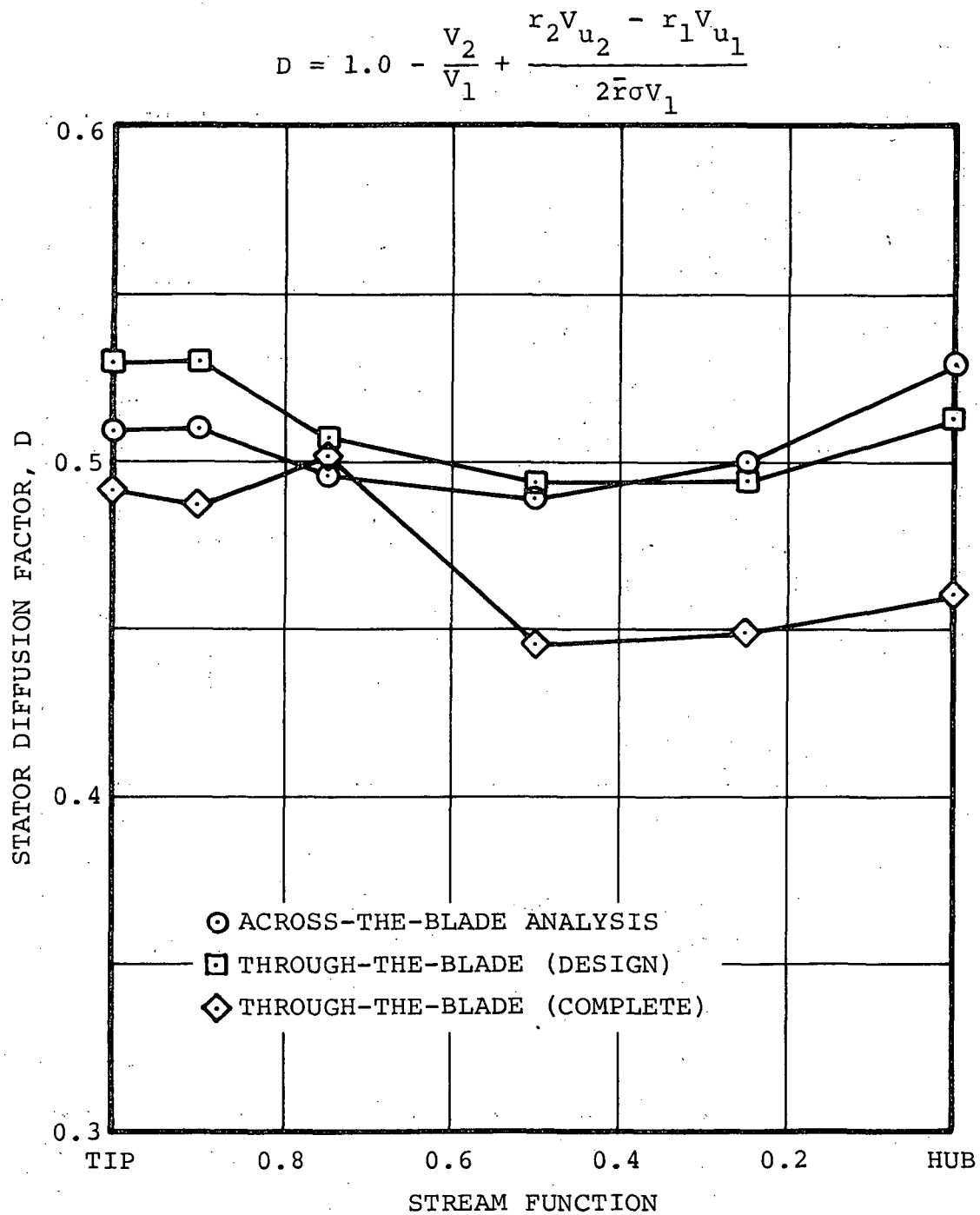


Figure 58. - Stator 1B Diffusion Factor Distribution.

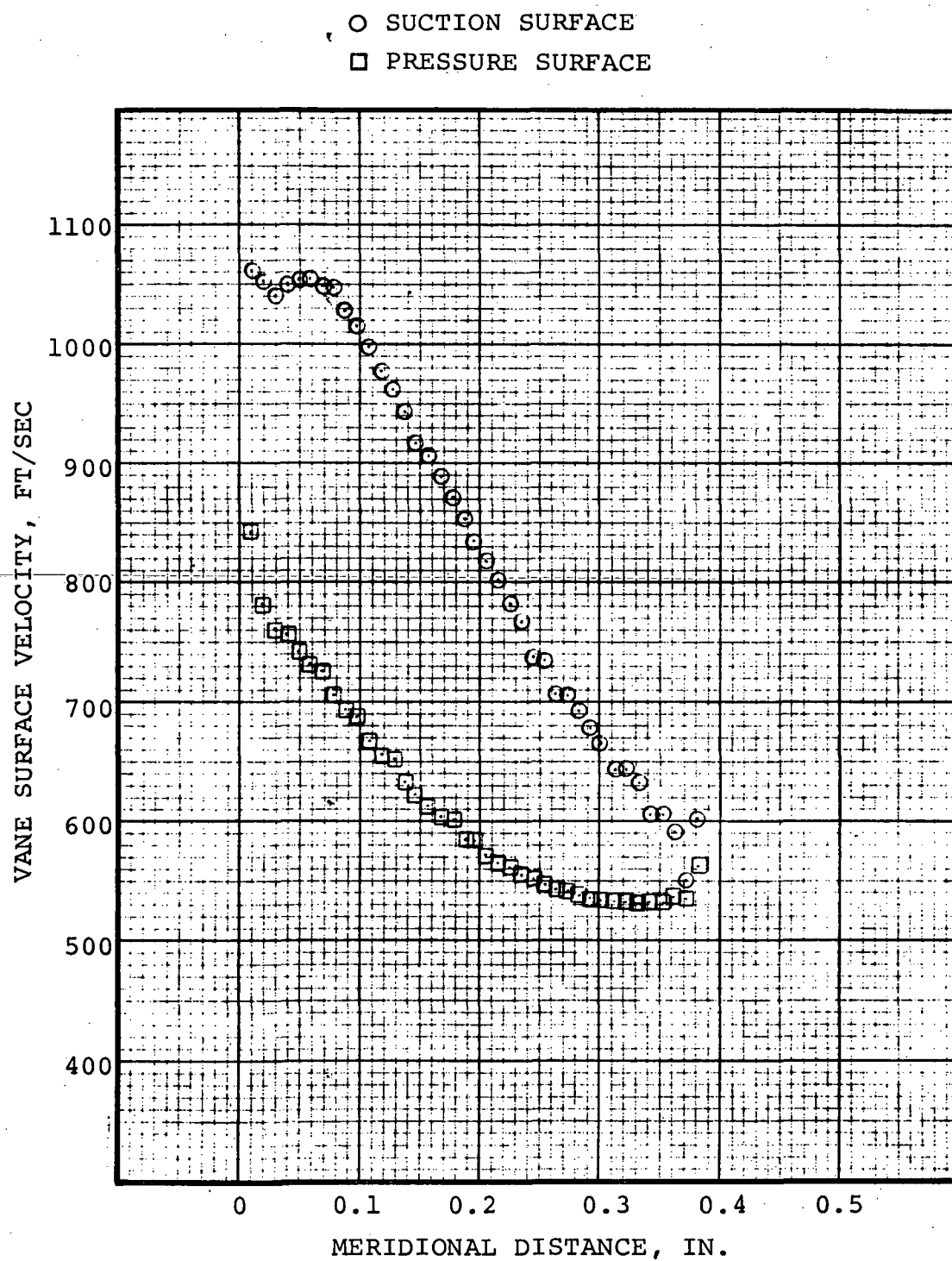


Figure 59. - Stator 1A Loading - Tip Streamline.

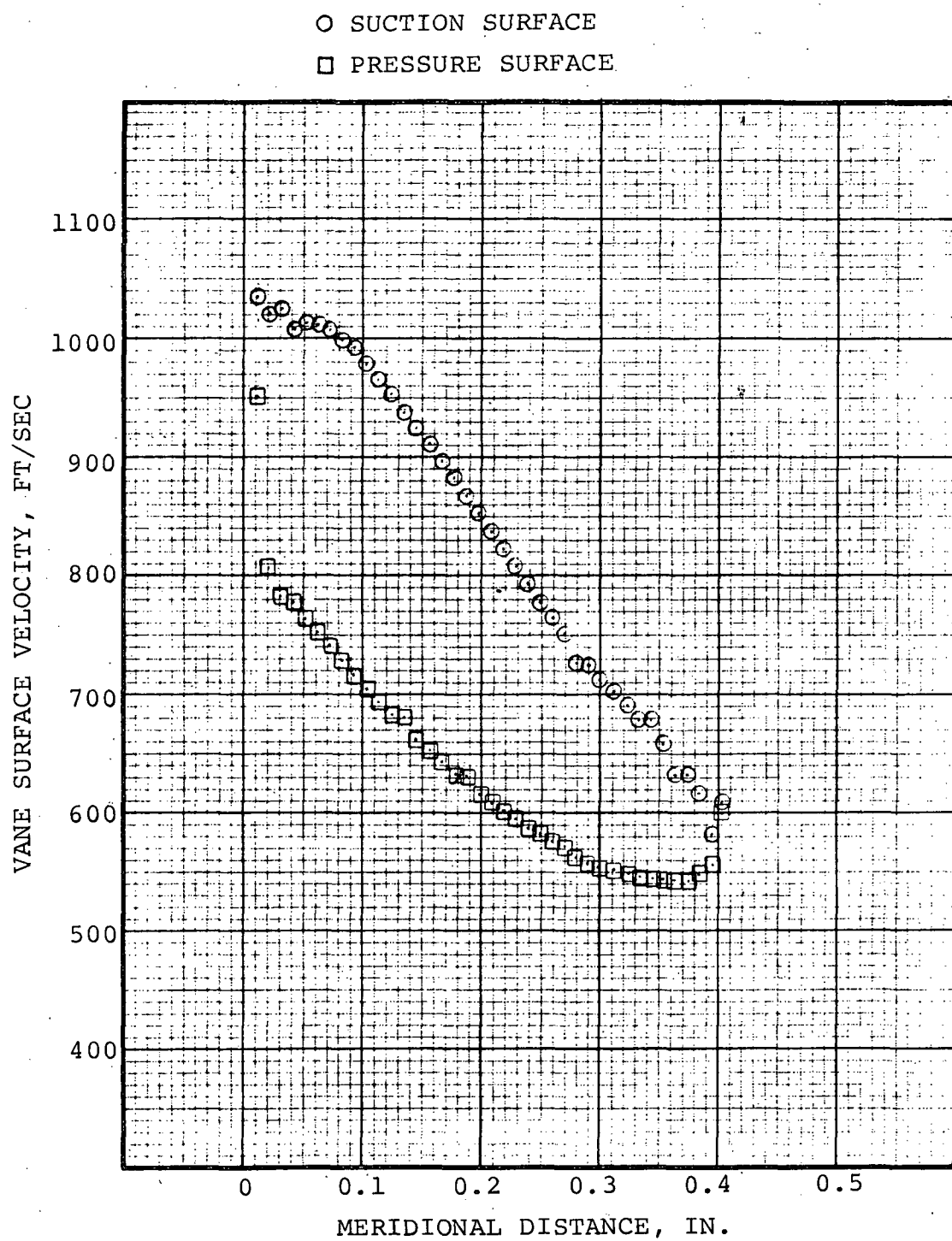


Figure 60. - Stator 1A Loading - Mean (50%) Streamline.

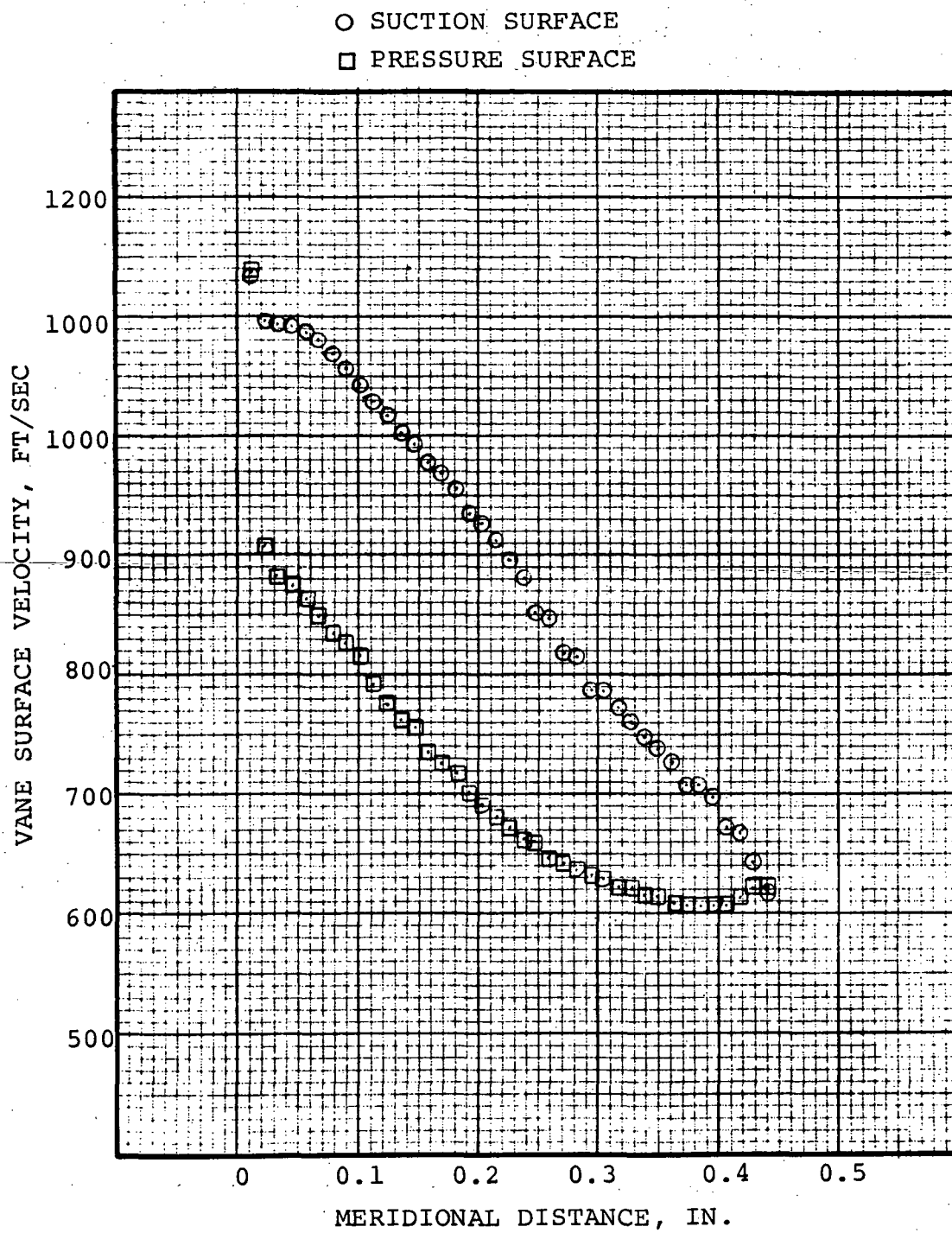


Figure 61. - Stator 1A Loading - Hub Streamline.

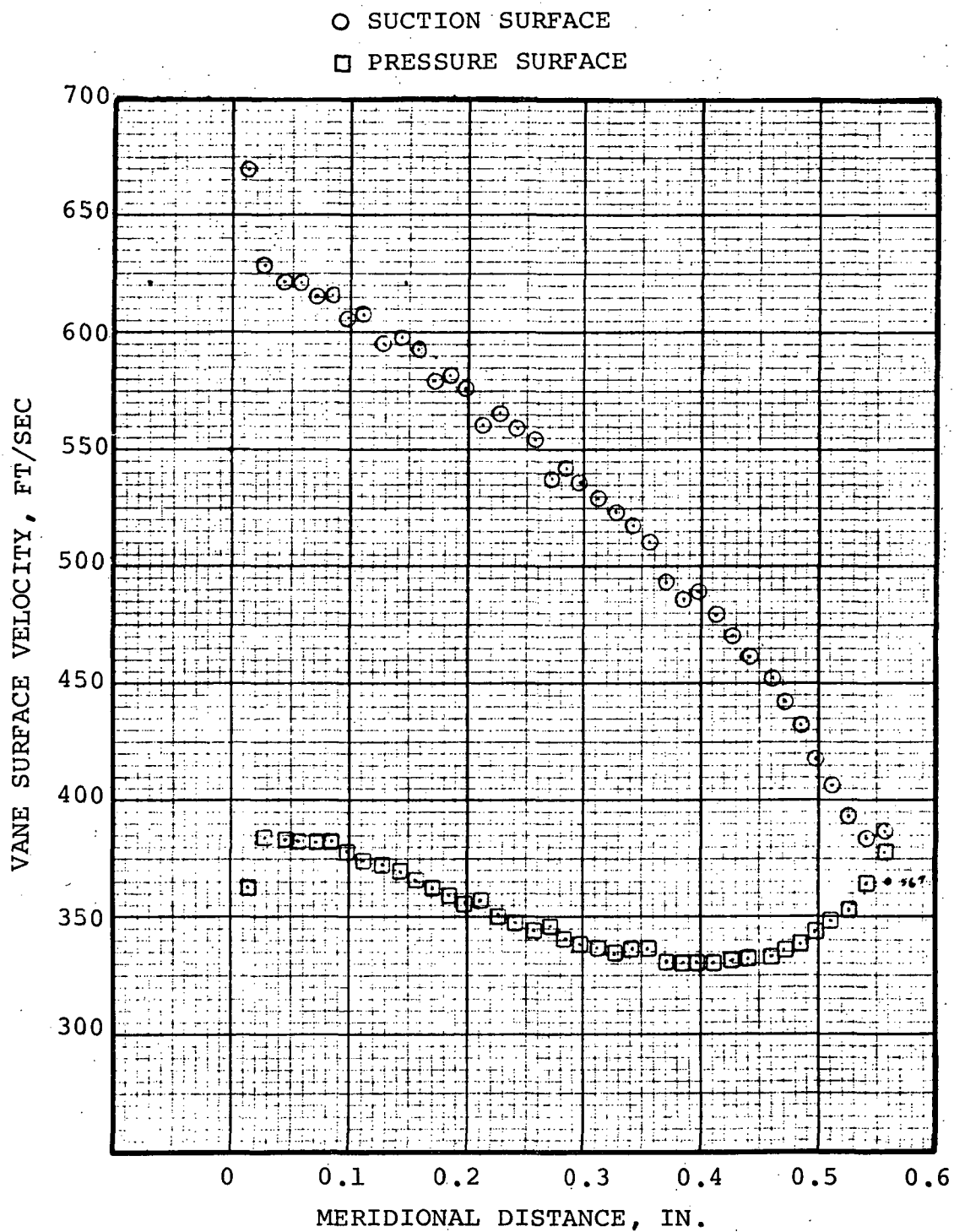


Figure 62. - Stator 1B Loading - Tip Streamline.

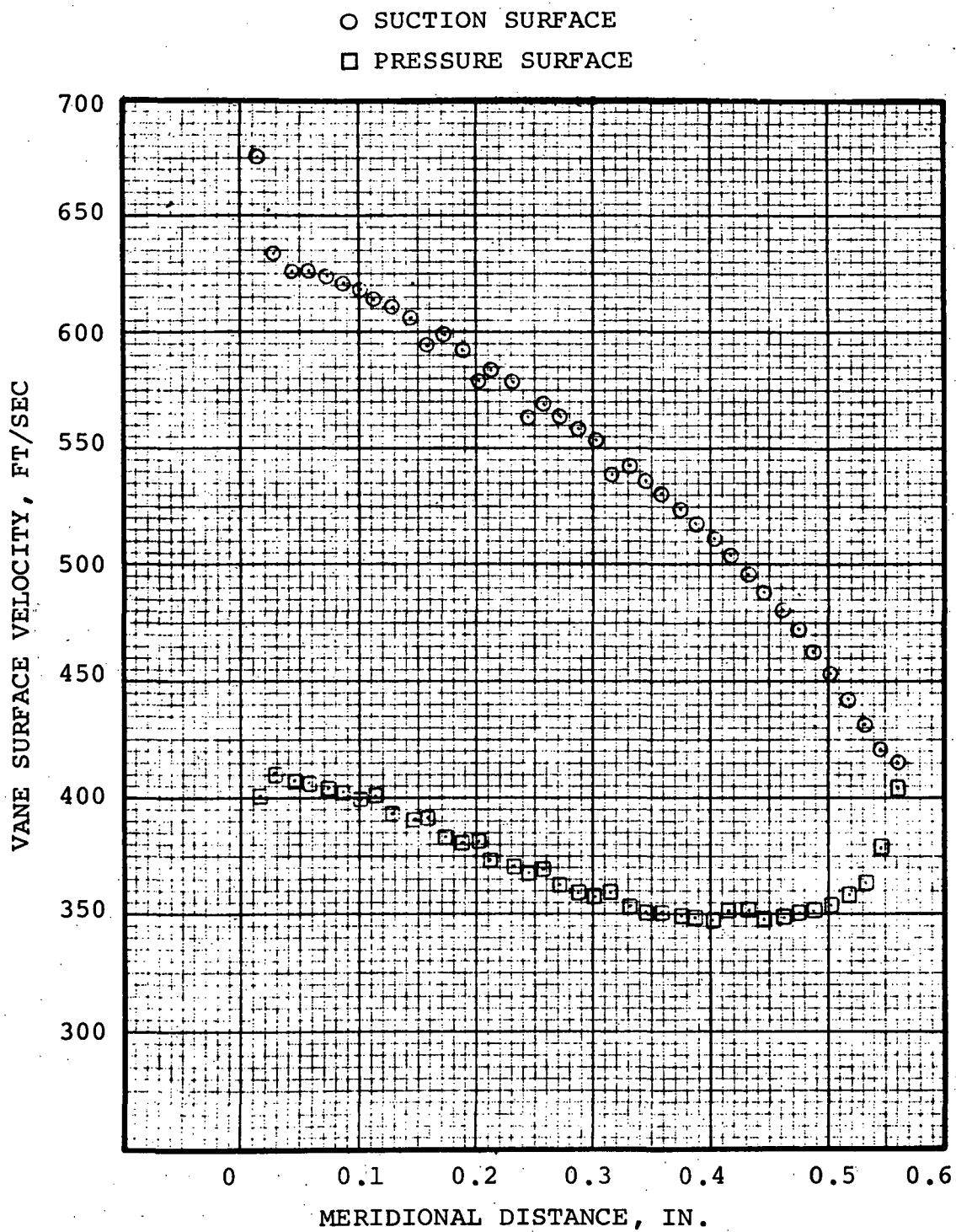


Figure 63. - Stator 1B Loading - Mean (50%) Streamline.

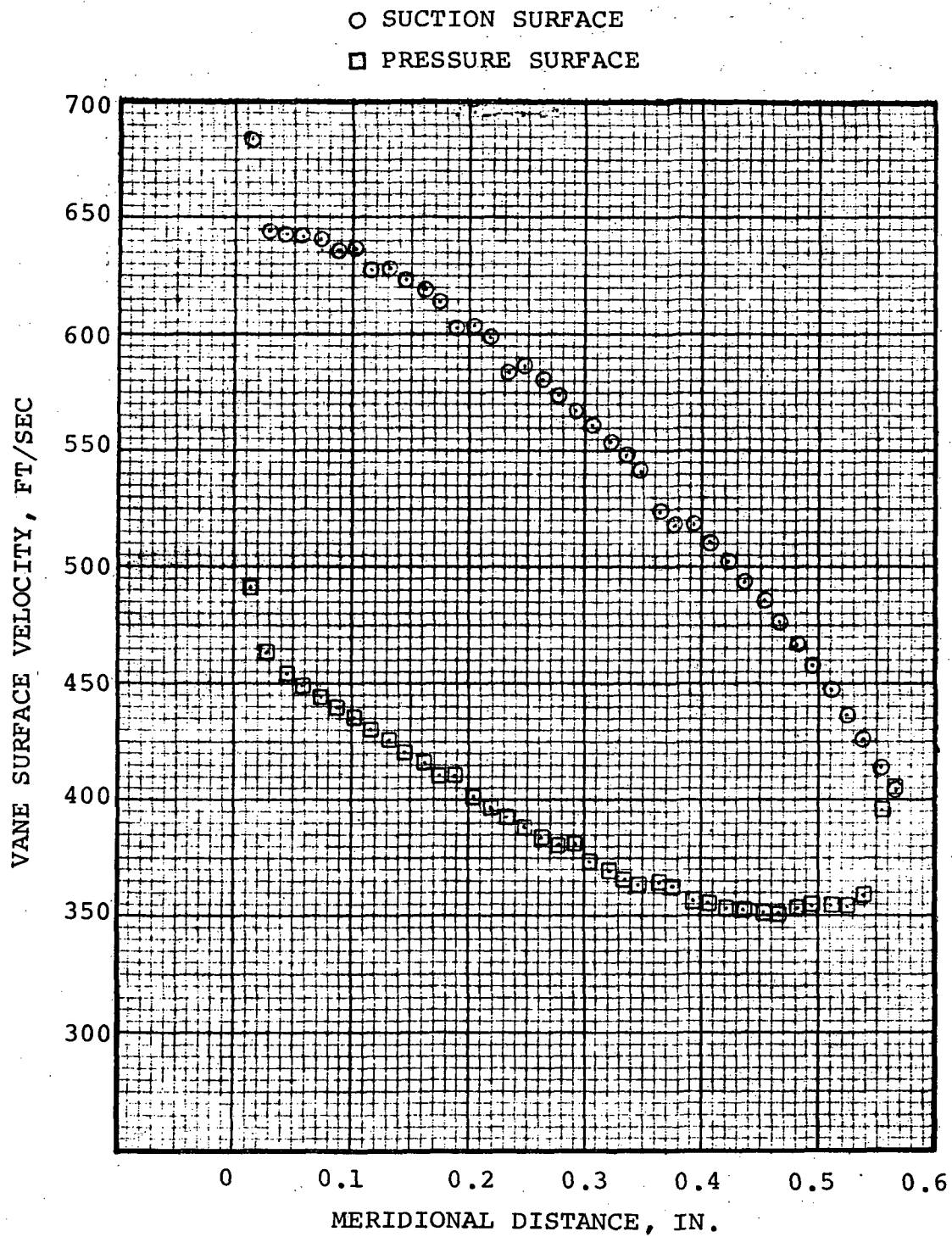


Figure 64. - Stator 1B Loading - Hub Streamline.

Boundary Layer Control

The purpose of any boundary layer control device is to prohibit flow separation from the confining walls. As a result of the inherent diffusion for the compression process, the boundary layers within a compressor are subject to adverse pressure gradients and, therefore, grow rapidly. Judicious design can minimize, but not eliminate, this growth. One of the objects for using tandem rotors and stators is to start each blade row with a new boundary layer. This permits the mixing and re-energization of low energy fluid at several points within the stage. Another attractive technique for removing boundary layers internal to the compressor stage is to bleed off fluid through the shroud or hub walls. Since these boundary layers grow continuously through the stage, a significant benefit should be possible. Location of bleed parts should be such that boundary layer removal is accomplished prior to probable separation regions. The new boundary layer created by the removal of low energy fluid is then better able to withstand adverse pressure gradient conditions, thereby inhibiting flow separation.

Analysis of the impeller boundary layers was accomplished as part of the finite difference blade-to-blade program. The subroutine for computing boundary layer properties is based on the method of Von Doenhoff and Tetervin (Ref. 11) as modified by Garner (Ref. 12). This program uses the free-stream velocities along flow surfaces, as predicted by the potential flow solution, to calculate boundary layer properties along streamlines. Flow separation is said to occur at the location where the shape factor (H) is equal to 2.2

In examining the blade row boundary layers, the hub and tip streamlines are of primary interest since flow separation on the blade surface in these locations may influence conditions circumferentially across the end walls. The blade surface boundary layers of interest have been plotted as curves (figures 65 through 71) with momentum thickness as a function of surface length. Results for Rotor 1A are shown on figure 65. Only the hub streamline was analyzed here. The potential flow field for the tip section is not adequately defined from the standpoint of the actual shock structure interval to the blade row to permit a valid solution of boundary layer conditions. The hub region of the first rotor does not indicate any regions of incipient separation. In general, the flow conditions exiting the first rotor should be sufficiently stable such that an external bleed system is not necessary prior to the second rotor.

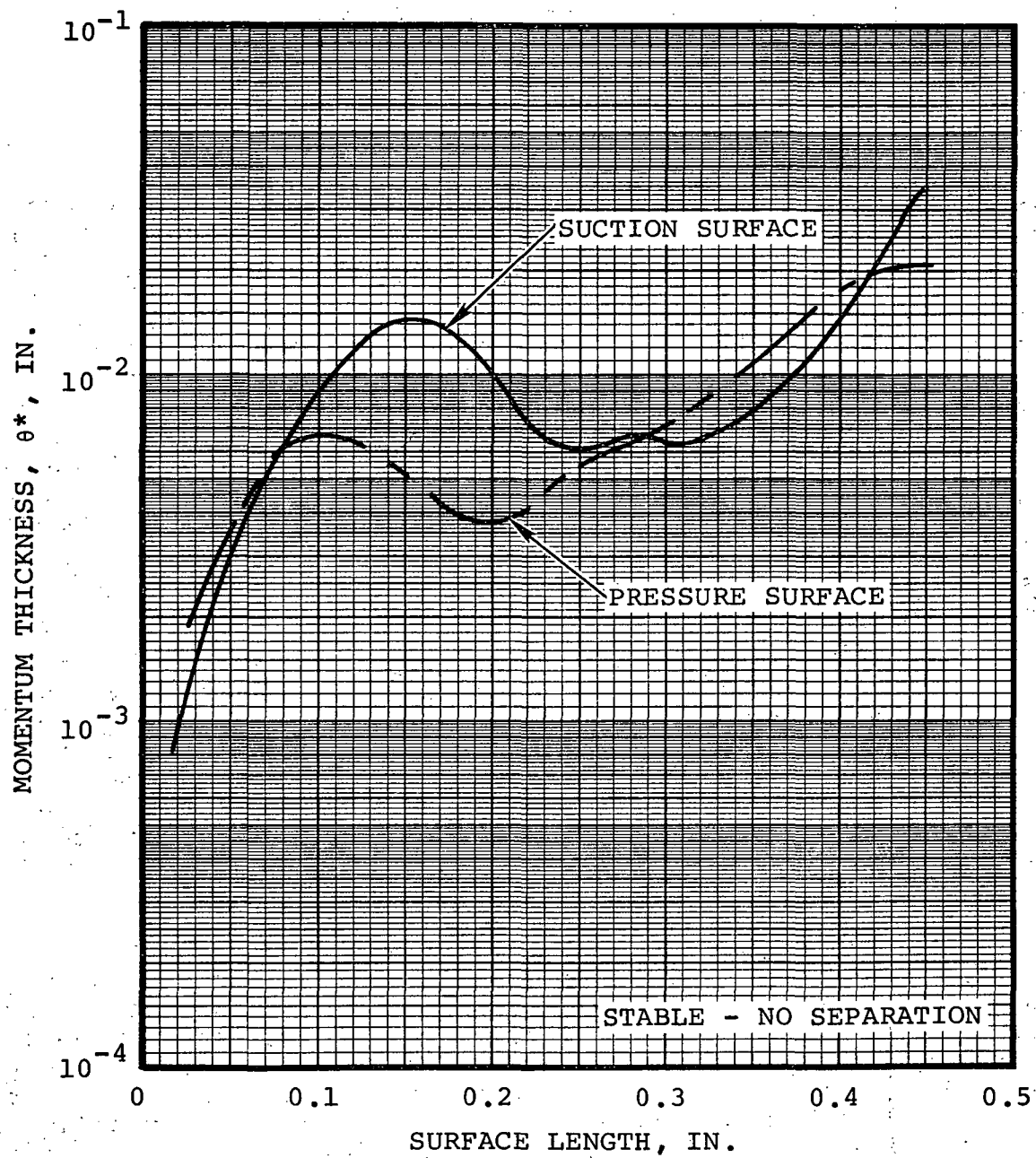


Figure 65. - Rotor 1A Blade Surface Boundary Layers - Hub Streamline.

Blade surface boundary layers for Rotor 1B are shown on figures 66 and 67 for the tip and hub streamlines, respectively. Note that a possible separation condition is predicted along the blade suction surface for the tip streamline. This potential separation zone occurs near the trailing edge of the blade in a region which should have little influence on the overall rotor performance. However, this might affect flow conditions entering the first stator row so that it may be desirable to install a series of bleed ports in the shroud wall between the second rotor row and first stator row. The consideration here being that a separated zone or a region of low energy fluid could possibly propagate a stall condition within the stators, thereby seriously penalizing the pressure recovery in this region. Thus, provision will be made for the installation of bleed ports on the shroud wall between the second rotor and first stator rows to permit experimental evaluation of this potential problem area.

Blade surface boundary layers on Stator 1A are shown on figures 68 and 69 for the tip and hub streamlines, respectively. Both streamlines indicate the possibility of separation on the suction surface of the blade. This is not an unusual circumstance and is experienced quite often with high turning stator rows in axial compressors. In fact, previous experience has shown good performance can be obtained with stator sections which are marginally stable with some portion of the blade exhibiting potential flow separation. A stator system was designed and tested where the calculations indicated an even greater separated condition than indicated here. Stage performance was not degraded for these stators, indicating either: (1) the separated area may have been localized to a small region on the blade followed by re-attached flow, or (2) the calculation may be in error such that separation is predicted prematurely. The instrumentation employed in these tests was insufficient to evaluate the existence or extent of flow separation in the stator system.

Since both the hub and tip sections for the first stator indicate a possibility of separated flow, it seems advisable to include bleed ports on both walls between the tandem stator rows. These should be set up to be operated either separately, or simultaneously with the rotor bleed. The recommended bleed port locations for the first-stage conical compressor are shown on figure 70.

Boundary layer conditions for the hub and tip streamlines on Stator 1B are presented on figures 71 and 72, respectively, computed for meanline loading. These results show a small region of possible flow separation along the suction surface for both cases. The effect of a small separated region in this part of the blade should be minimal and, therefore, does not require a bleed system for boundary layer stabilization.

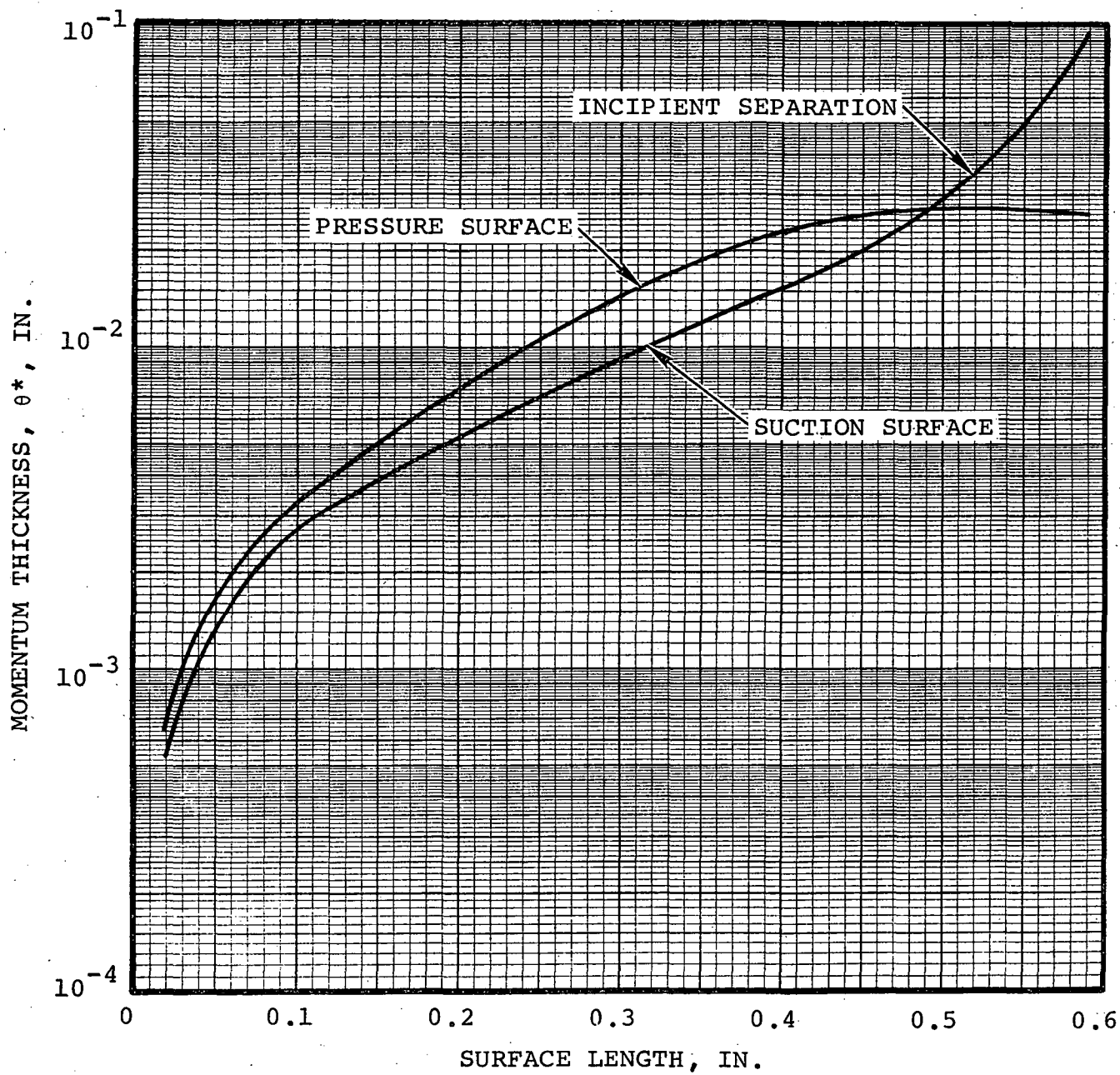


Figure 66. - Rotor 1B Blade Surface Boundary Layers - Tip Section Streamline.

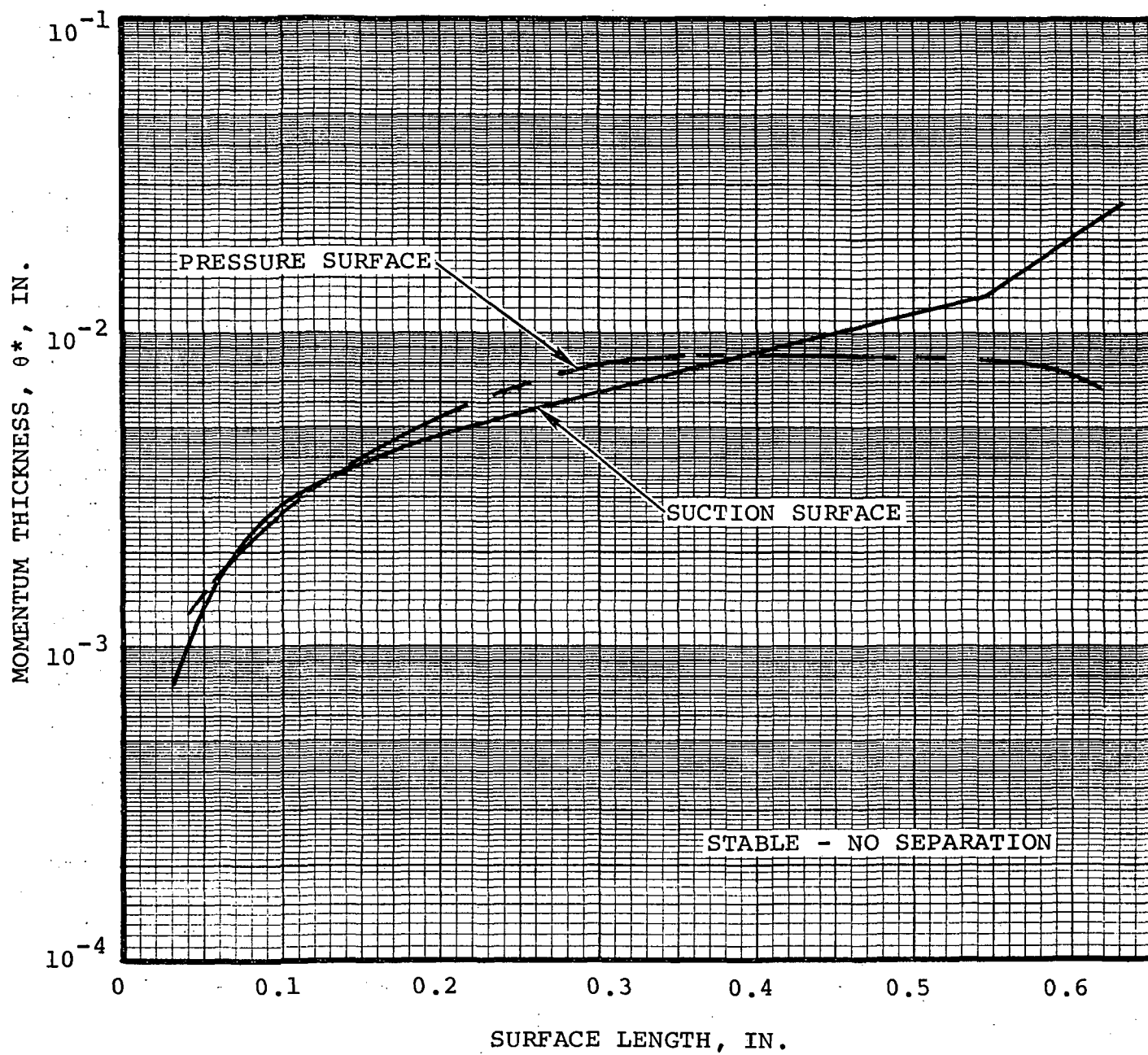


Figure 67. - Rotor 1B Blade Surface Boundary Layers - Hub Streamline.

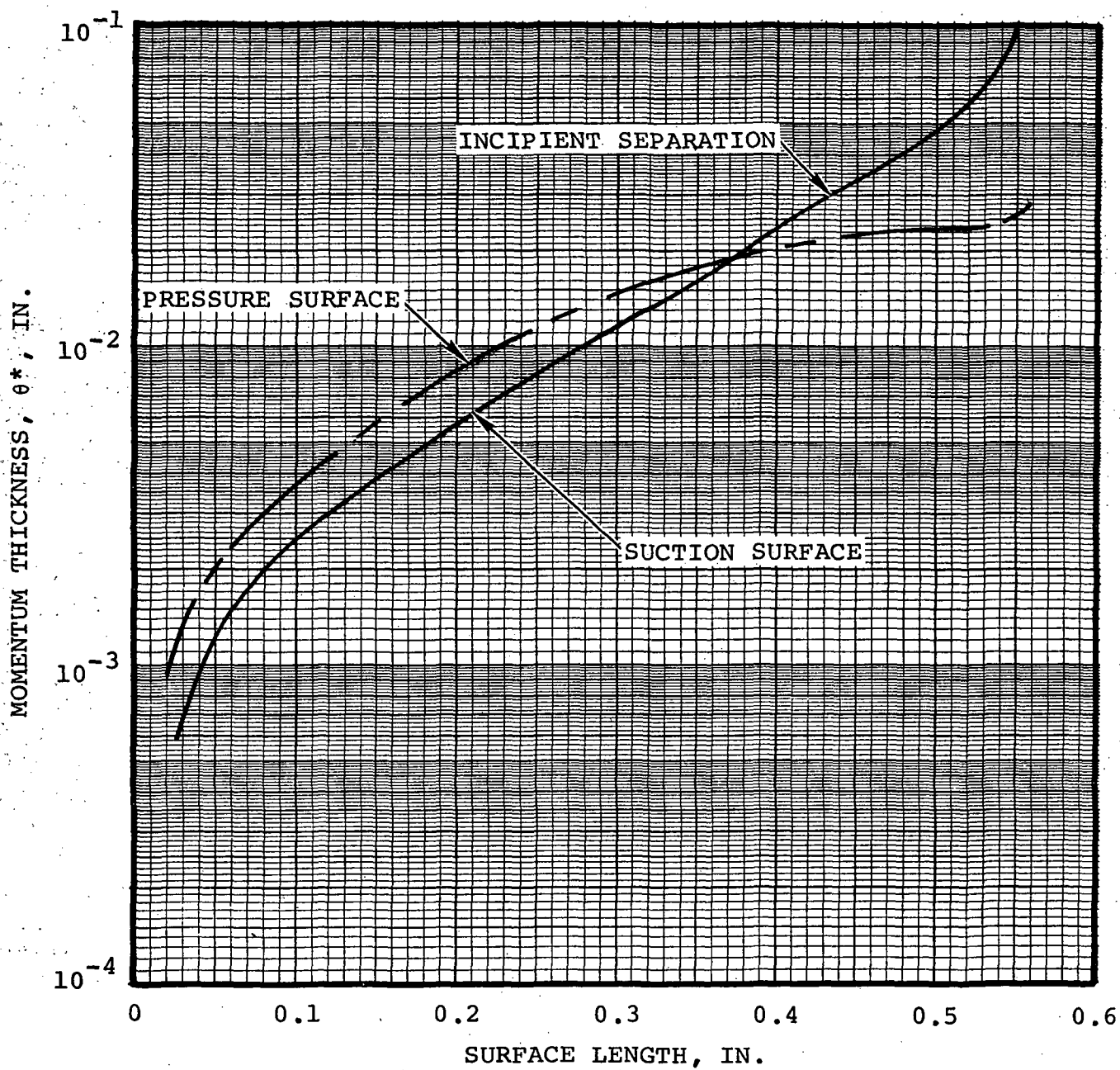


Figure 68. - Stator 1A Blade Surface Boundary Layers - Tip Streamline.

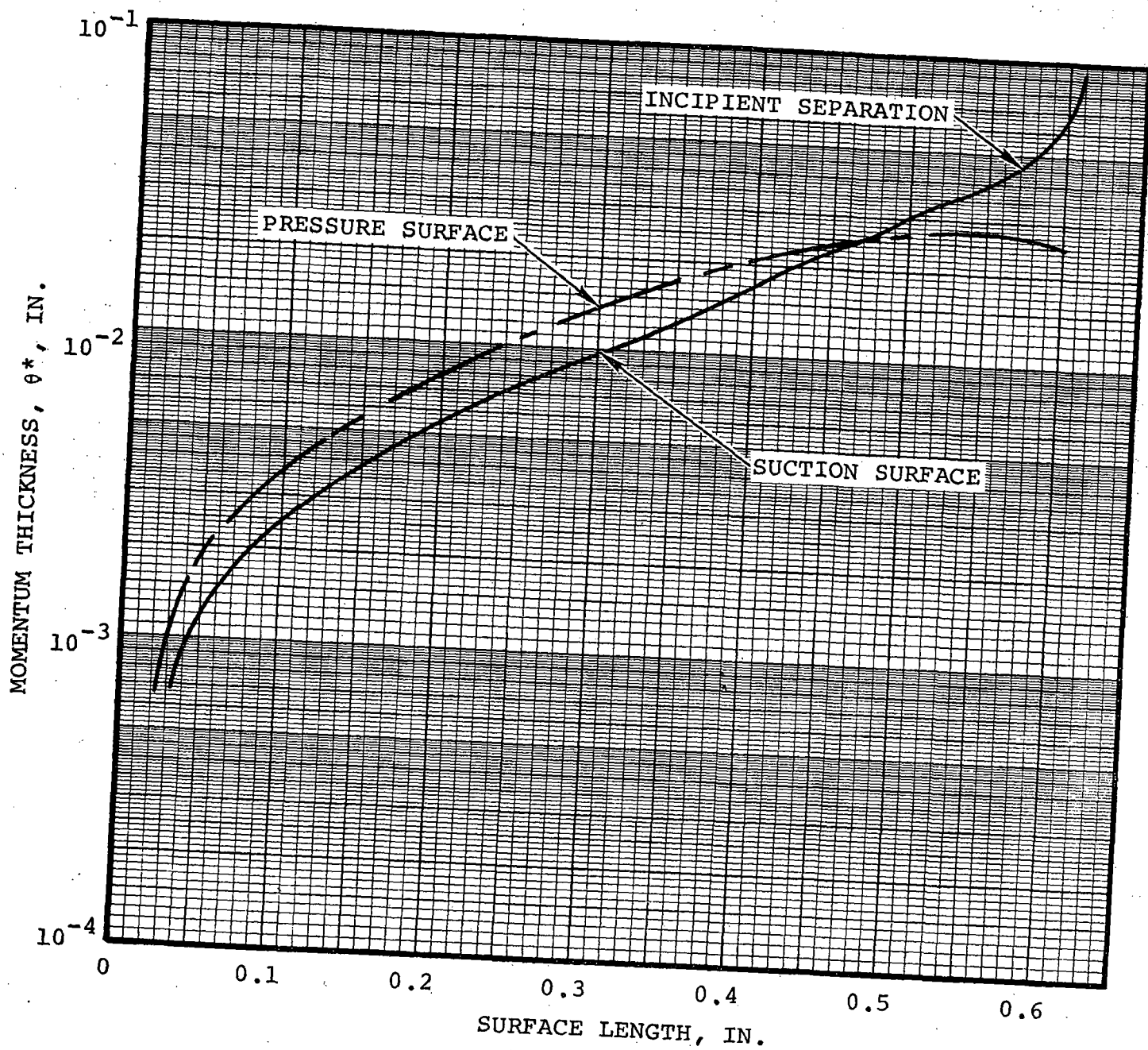


Figure 69.-- Stator 1A Blade Surface Boundary Layers - Hub Streamline.

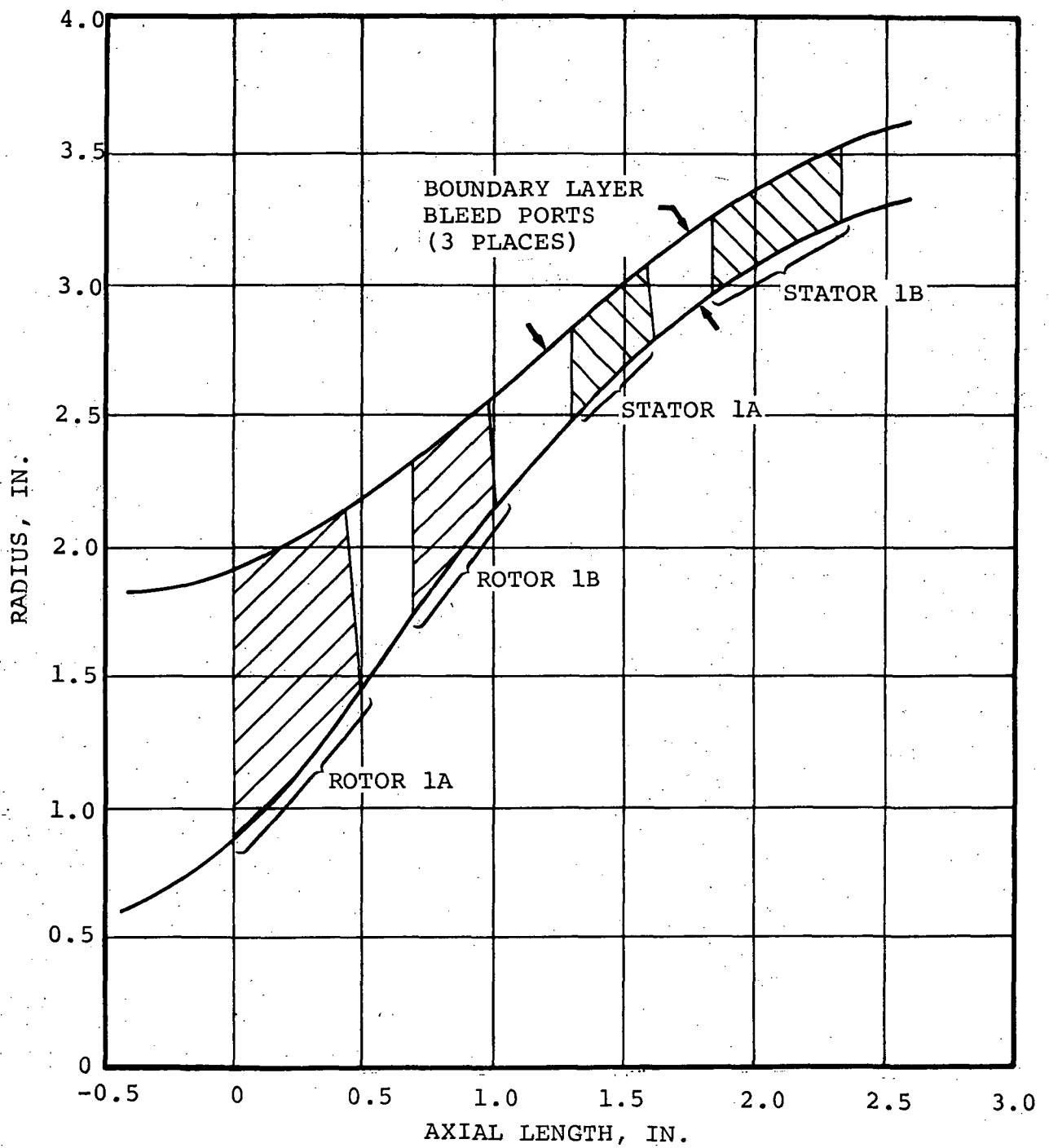


Figure 70. - Recommended Location of Boundary Layer Bleed Ports In Conical Compressor.

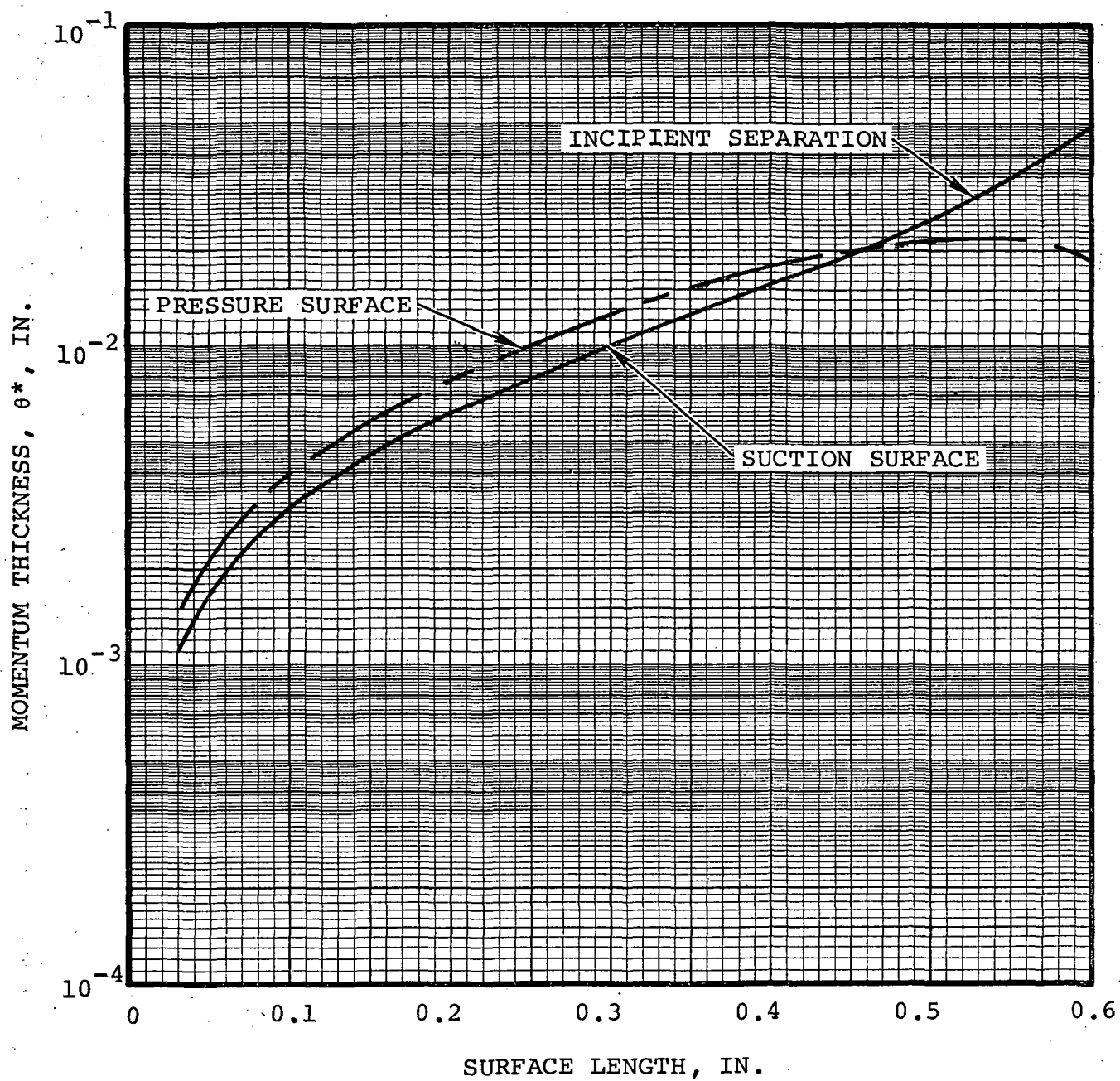


Figure 71. - Stator 1B Blade Surface Boundary Layers - Hub Streamline.

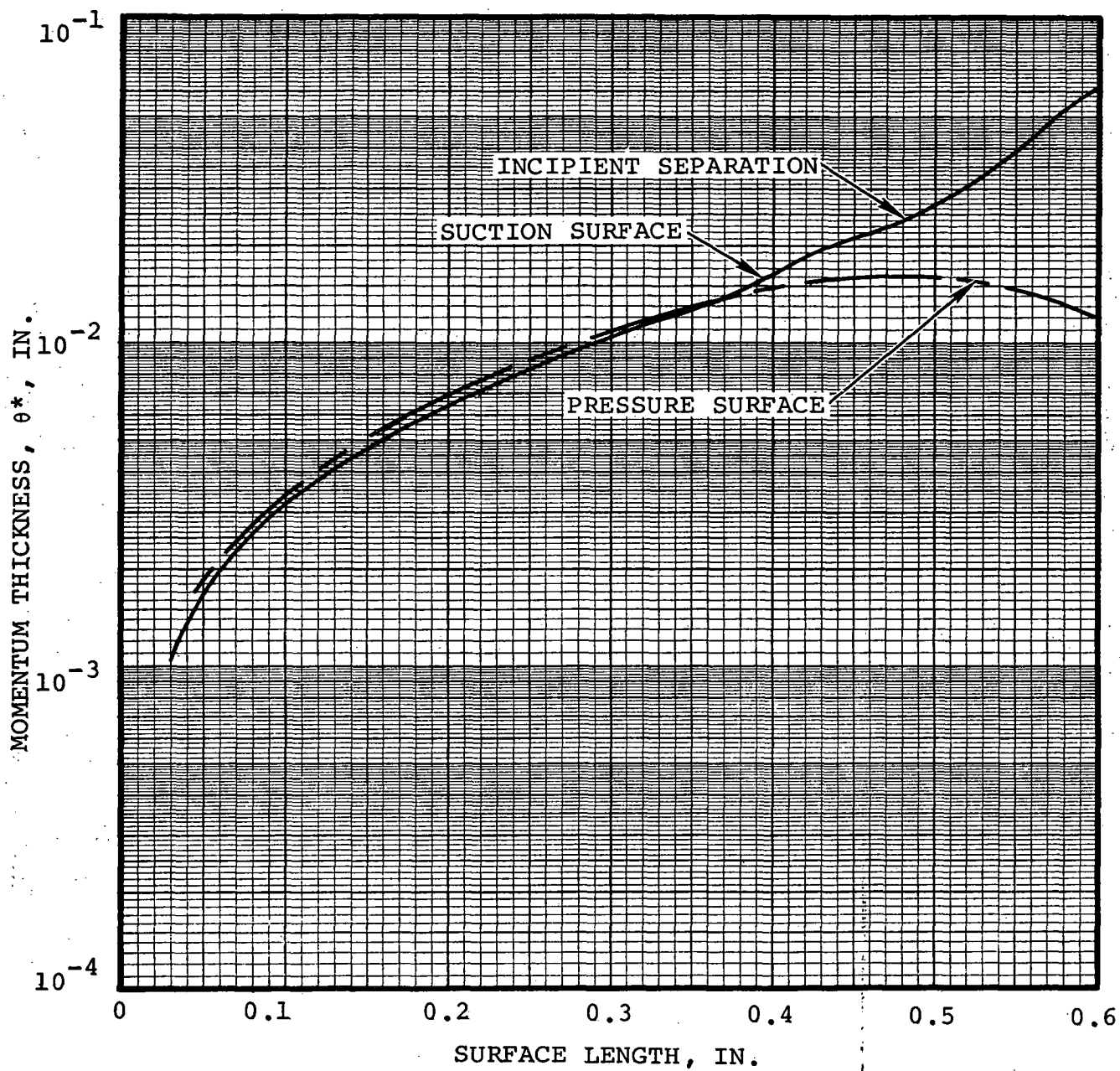


Figure 72. - Stator 1B Blade Surface Boundary Layers - Tip Streamline.

The design of the transition duct is such that the initial passage is converged slightly prior to any diffusion. This should tend to stabilize the flow prior to the turning section in the transition duct.

The boundary layer bleed ports will consist of a series of 40 holes, equally spaced circumferentially around the wall at each specified location. The diameters of the bleed ports should be $3/32$ nd of an inch, which will take a bleed flow ratio of two percent of the main flow. For the boundary layer bleed system to show a favorable performance trade-off, it will be necessary to operate the bleed systems at less than the design flow ratio (less than 2.0 percent). Optimum operating conditions will have to be determined experimentally since there are too many unknowns to permit this problem to be solved analytically.

Inlet Flowpath Design

Analysis of flow conditions in the inlet duct employed an axisymmetric flow program to solve for the potential velocity field. A boundary layer program was used to examine wall effects. Basically it is desirable to have the flow continuously accelerate throughout the entrance region to avoid excessive boundary layer buildup with the possibility of flow separation. The analytical programs were employed to examine various duct shapes on an essentially trial and error basis to arrive finally at an acceptable entrance configuration.

The selected inlet duct configuration is shown on figure 73. Also included on this figure are several streamlines in the flow field and the velocity distribution presented as lines of constant velocity. The upstream portion of their duct has several support struts which pass through the flow field. The blockage of the struts has been included in the potential flow calculations. This is evidenced by the hump in the velocity profile across the strut. The fact that the struts have been placed in a relatively low velocity region tends to minimize their effects on the downstream flow field. The resulting velocity distribution in the entrance duct looks quite satisfactory from the standpoint of potential core flow calculations. Examinations of the boundary layers along both walls also indicated a reasonable rate of boundary layer build-up with distance. A check of the resulting displacement thickness calculations as affecting blockage indicated the aerodynamic blockages assumed in the potential flow calculations were quite satisfactory. This final comparison then completed the analytical examination of the inlet duct configuration.

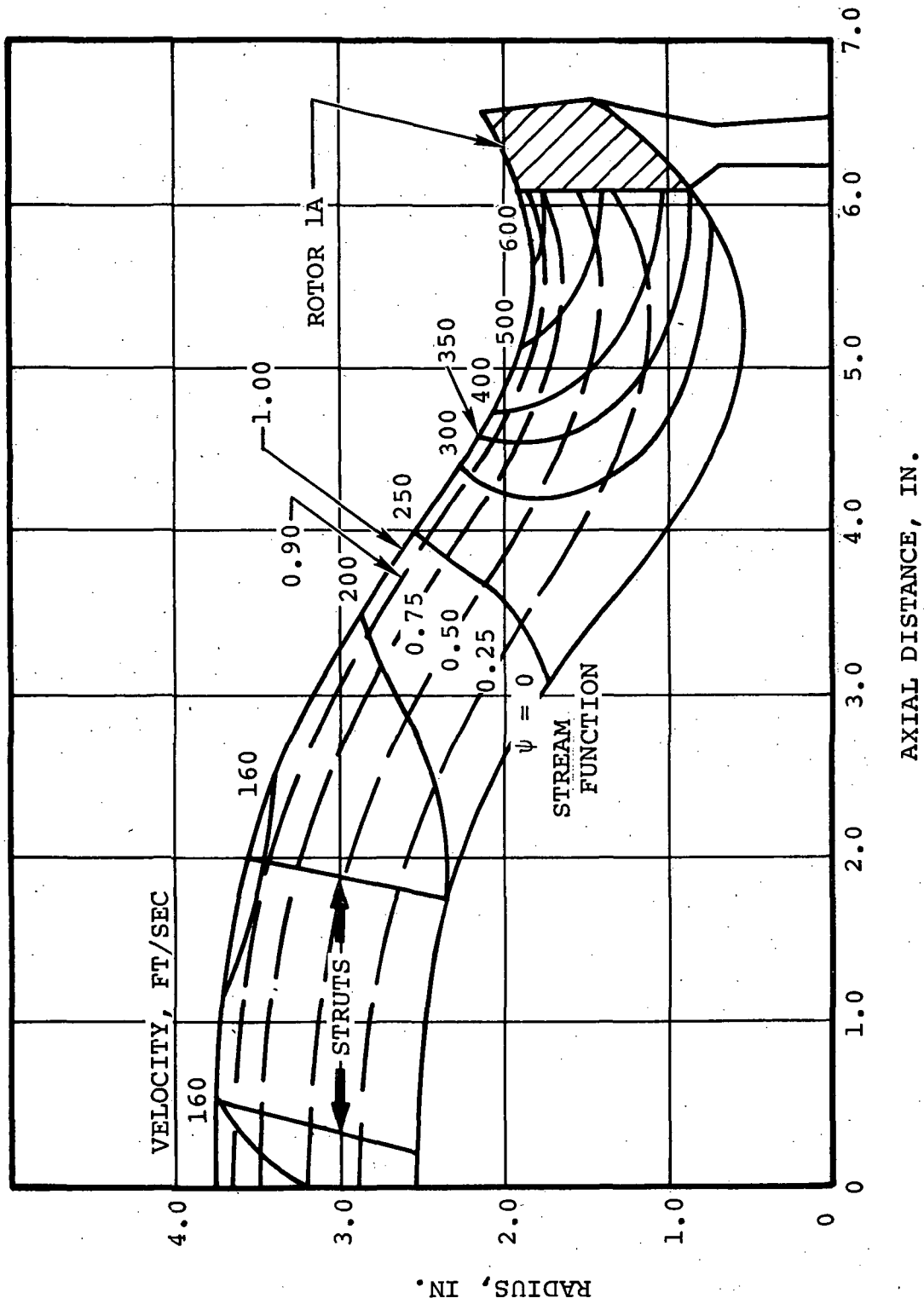


Figure 73. - Inlet Duct for Conical Flow Compressor -
Velocity Distribution.

Transition Duct Design

A cross-section of the final flowpath from the second row stator exit down to the inducer leading edge of the second stage compressor is shown in figure 74. The resultant surface velocities (for the design point) are presented in figure 75.

This design involved a trade-off between the area ratio distribution along the meanline and local wall curvatures to achieve hub and shroud wall velocity distributions which minimized the possibility of boundary layer separation. The final design was made within geometric constraints of radius and axial distance fixed by the mechanical considerations, and the aerodynamic constraint of a second-stage inlet shroud to meanline velocity ratio consistent with current radial compressor design technology requirements. (The second-stage inducer geometry was obtained from a preliminary design discussed earlier in this report.)

A calculation of the boundary layer conditions was conducted for each of the final hub and shroud wall velocity distributions. In each case, depending upon the assumed initial conditions of the boundary layer, a region exists where the shape factor value, H , indicates probable separation. These regions are shown on the meridional flow-path view (figure 74). Due to the positive wall curvature in each of these regions, the centrifugal body force will act opposite to the adverse pressure gradient tending to hold the fluid to the wall and the separated zone is expected to be small with rapid reattachment.

Considerable effort was expended in obtaining this situation since some separation is inevitable because of the severity of the curvature required to satisfy the envelope restrictions. The design is considered conservative in that the boundary layer blockage was not included in the flow-field solution. The inclusion of this blockage would decrease the effective area and increase the velocity level, the increase being greatest where the diffusion is greatest. This type solution requires an iterative process between the boundary layer program and the radial equilibrium program. A time limitation prevented this more detailed analysis.

The final configuration is representative of crossover ducts currently in use on production engines at AiResearch.

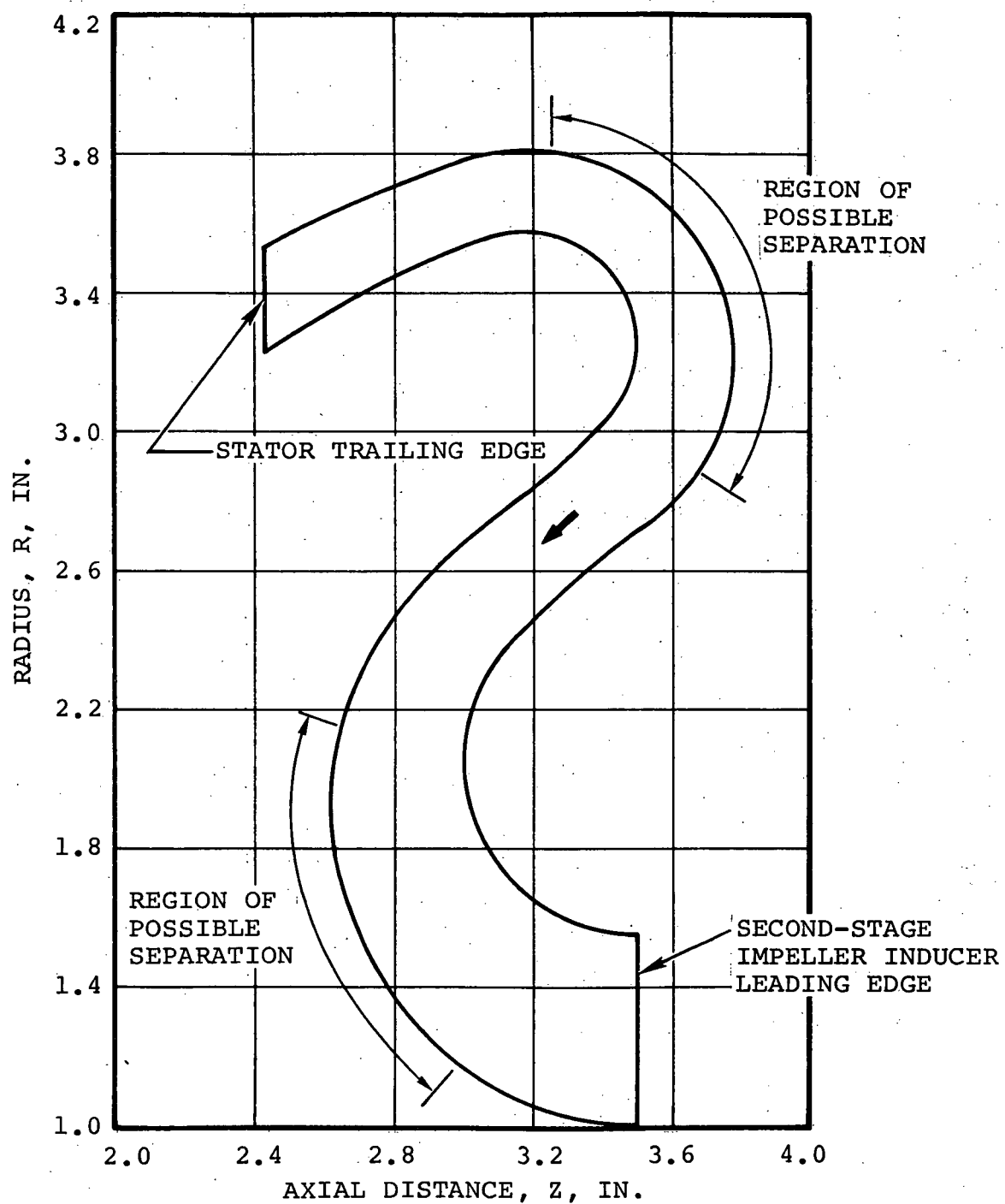


Figure 74. - Transition Duct Size and Shape.

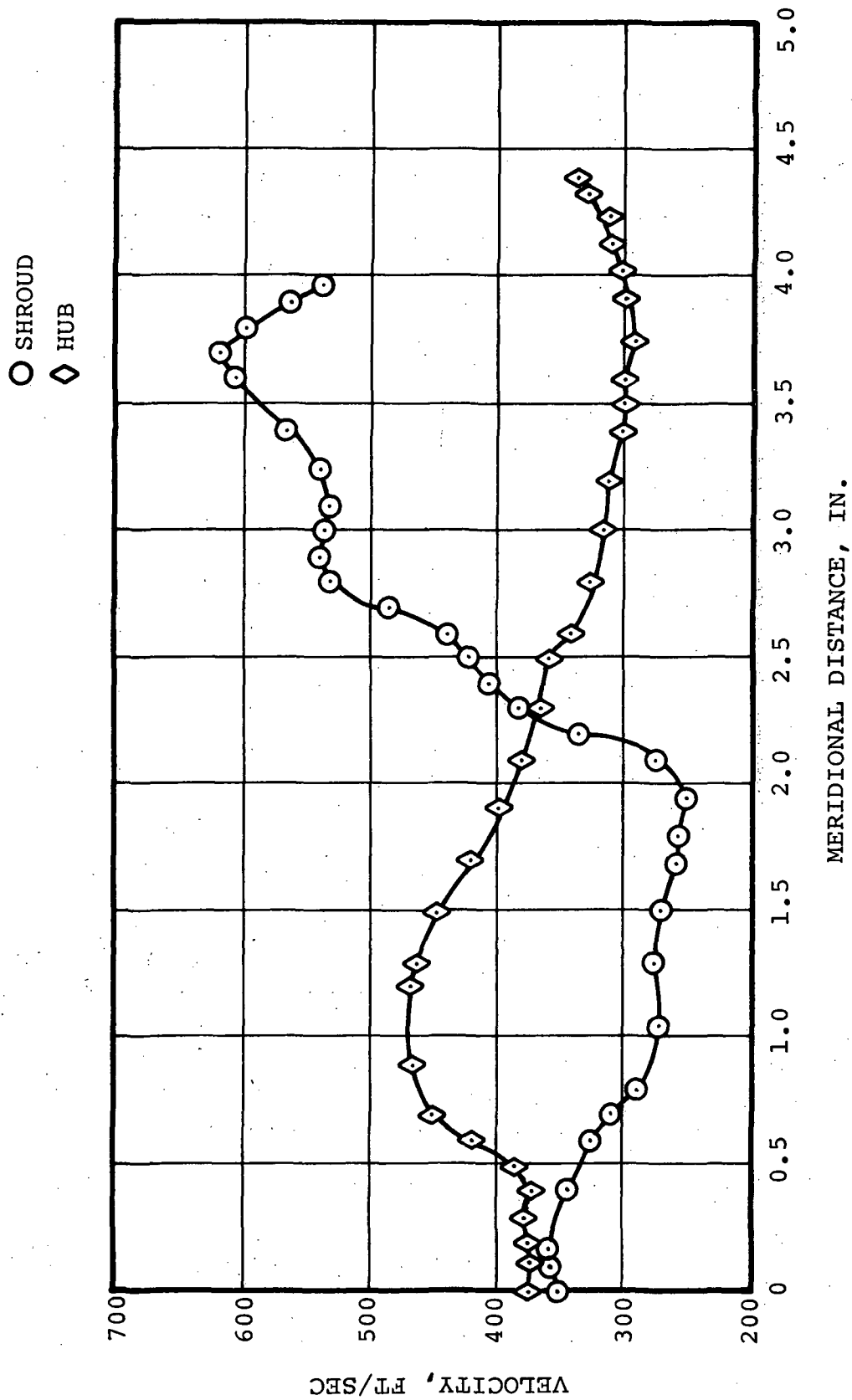


Figure 75. - Transition Duct Velocity Distribution.

Drive Turbine Aerodynamic Design

An existing radial inflow turbine design has been selected to drive the 10/1 compressor research rig. This selection is based on consideration of power capability, mechanical integrity, and contractually stipulated turbine inlet conditions. Of the two candidate drive turbines considered (radial and axial), the radial inflow design selected to drive the rig is superior in available power and mechanical integrity. It can also produce maximum power at lower turbine inlet temperature and integrates well with the research rig. An aerodynamic design summary follows. The blading geometry is defined in Appendix A.

Drive Turbine Aerodynamic Design Summary

The drive turbine for the NASA 10/1 compressor is required to produce sufficient power to test the two-stage compressor to 110 percent of design speed. The compressor design point used to size the turbine is as follows:

$$P_r = 10.0$$

$$W\sqrt{\theta}/\delta = 2.0 \text{ lb/sec}$$

$$\eta_{ad} = 0.805$$

$$N/\sqrt{\theta} = 70,000 \text{ rpm}$$

Achievement of this design goal requires an input horsepower of 411 and an overspeed power requirement of 547 horsepower based on the cubic power law. These horsepower requirements will be provided by the following available energy source:

Maximum flow: 7 lb/sec

Maximum T_{in} : 1000°R

Maximum P_{in} : 350 psia

Maximum P_{out} : 4 psia

From this energy source and the required overspeed of 77,000 rpm, an examination of existing turbines was made to determine which, if any, could produce the required 547 horsepower at 77,000 rpm and not exceed the available energy source. As a result of the examination, a radial inflow turbine design was selected for use in the research rig. The design point of the turbine is:

Speed, rpm:	81,800
$W\sqrt{\theta}/\delta$, lb/sec:	0.474
P_r , T-T:	4.167
η , T-T:	89.7
$\Delta H/\theta$, Btu/lb:	37.6

The performance of the selected turbine was tested in an actual size cold air rig. The test results are given in figures 76 through 82. Using the turbine performance test data, a computer model that would predict turbine performance at any desired operating point was created. Figure 78 shows the comparison between the measured performance and predicted performance based on the computer model. The agreement shown in figure 78 and like agreement at other test speeds indicates that the computer model could reliably predict performance at any operating condition. Using the computer model, a maximum power curve for the radial turbine was generated for a range of compressor speeds and inlet temperatures. Figure 82 presents a carpet plot of this information and clearly shows that the required objective of 547 horsepower and 110-percent compressor speed can be obtained without exceeding the facility limitations.

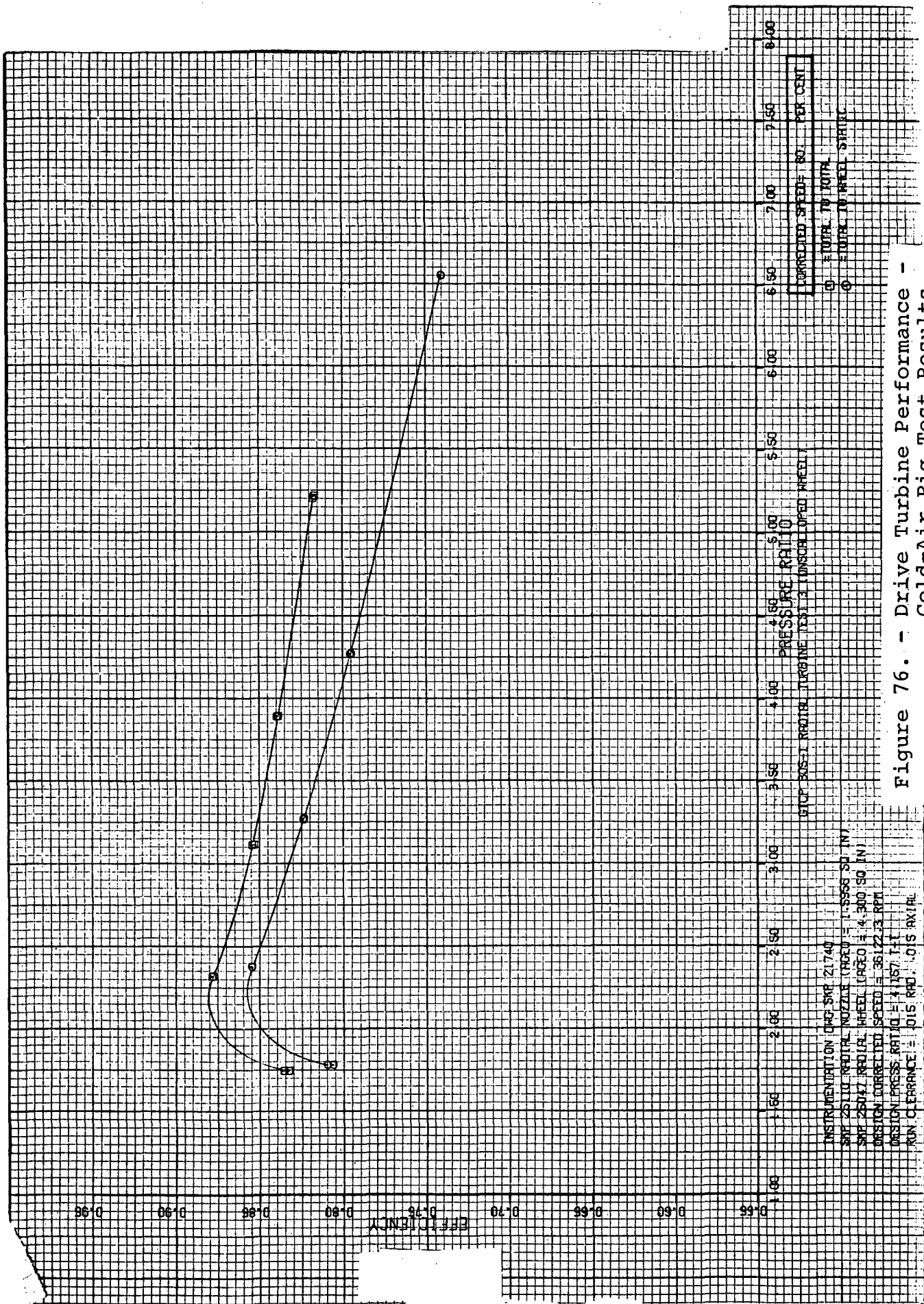
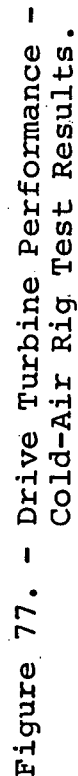


Figure 76. - Drive Turbine Performance - Cold-Air Rig Test Results.



PREDICTED PERFORMANCE

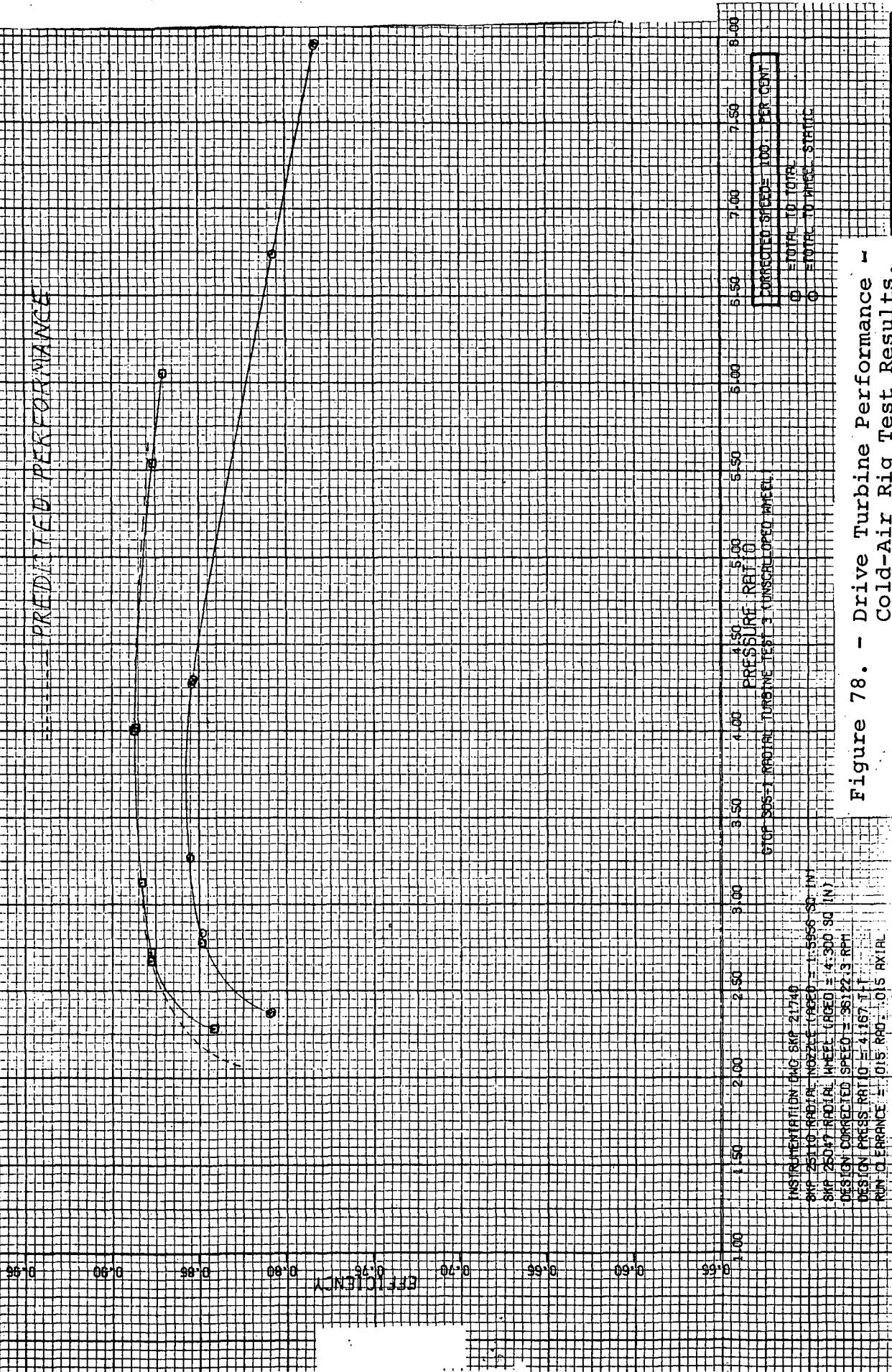
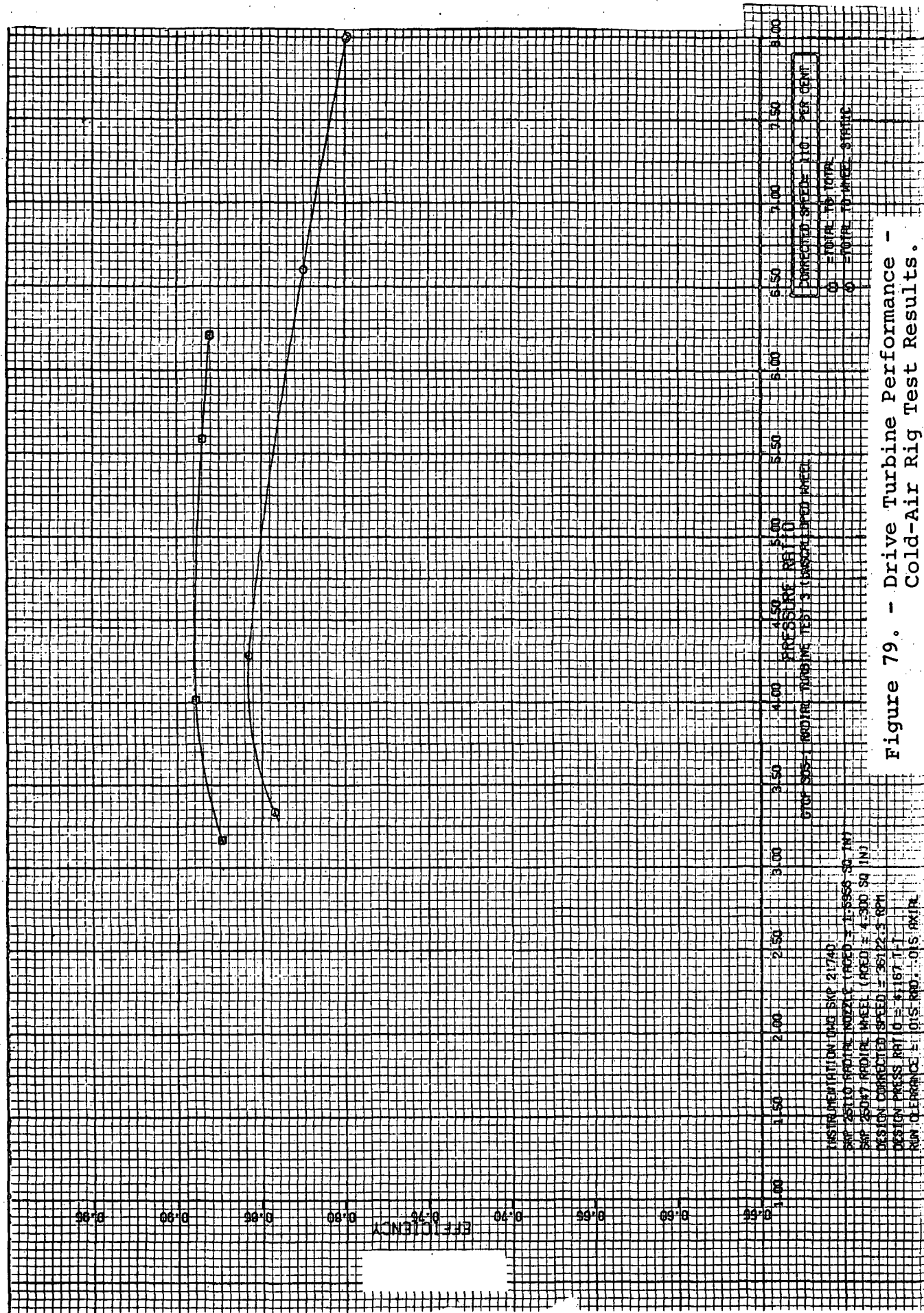


Figure 78. - Drive Turbine Performance - Cold-Air Rig Test Results.



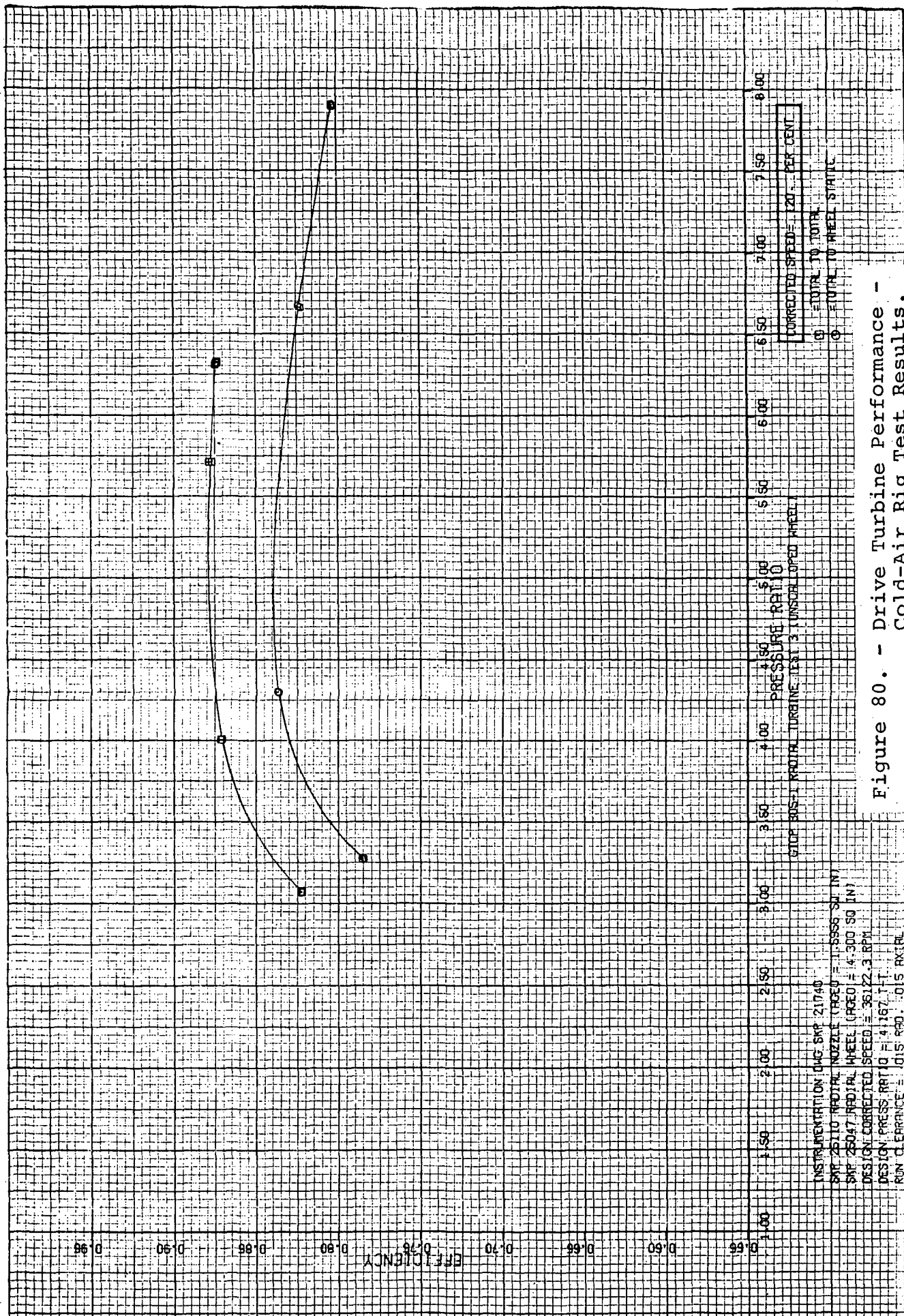
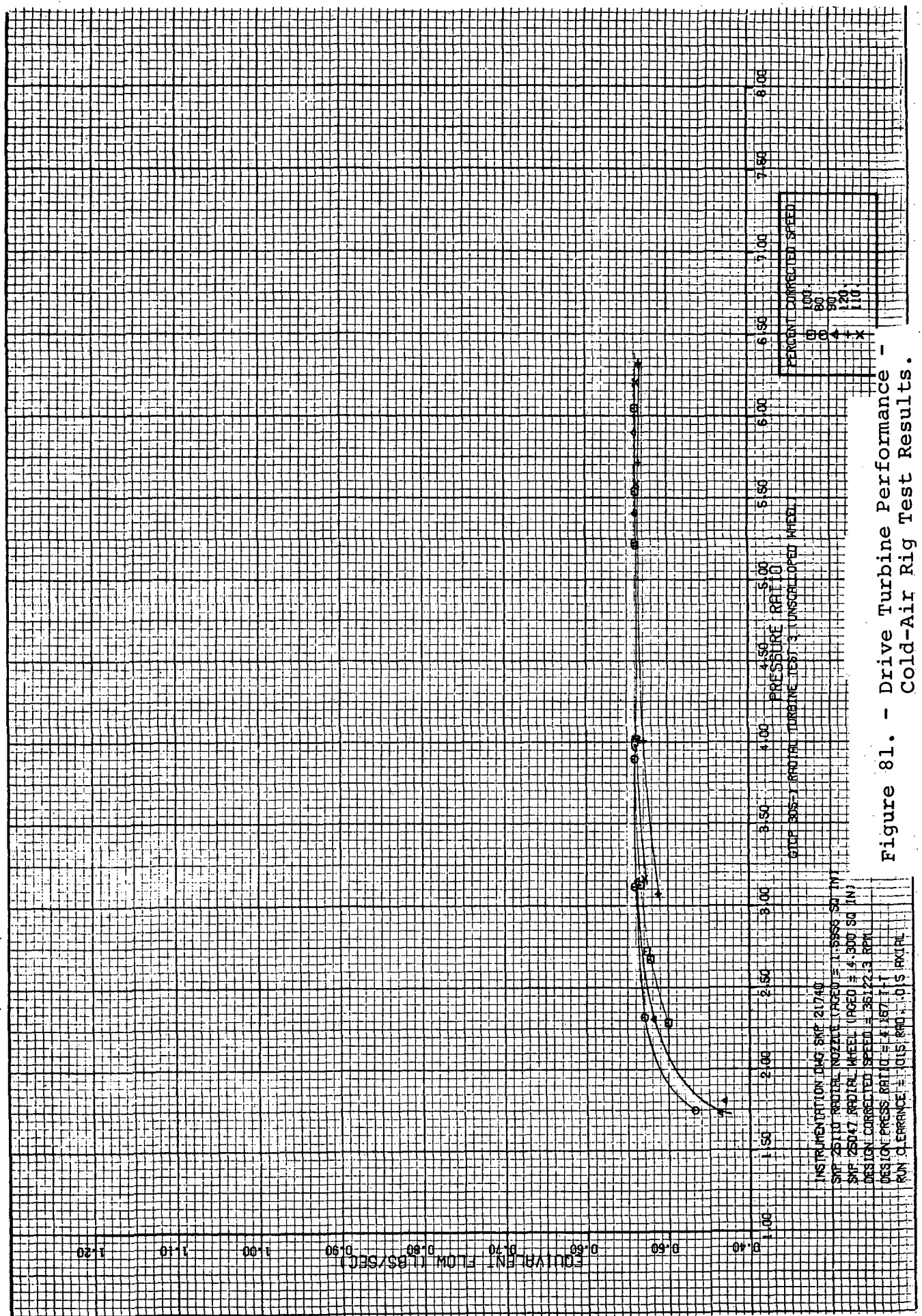


Figure 80. - Drive Turbine Performance -
Cold-Air Rig Test Results.



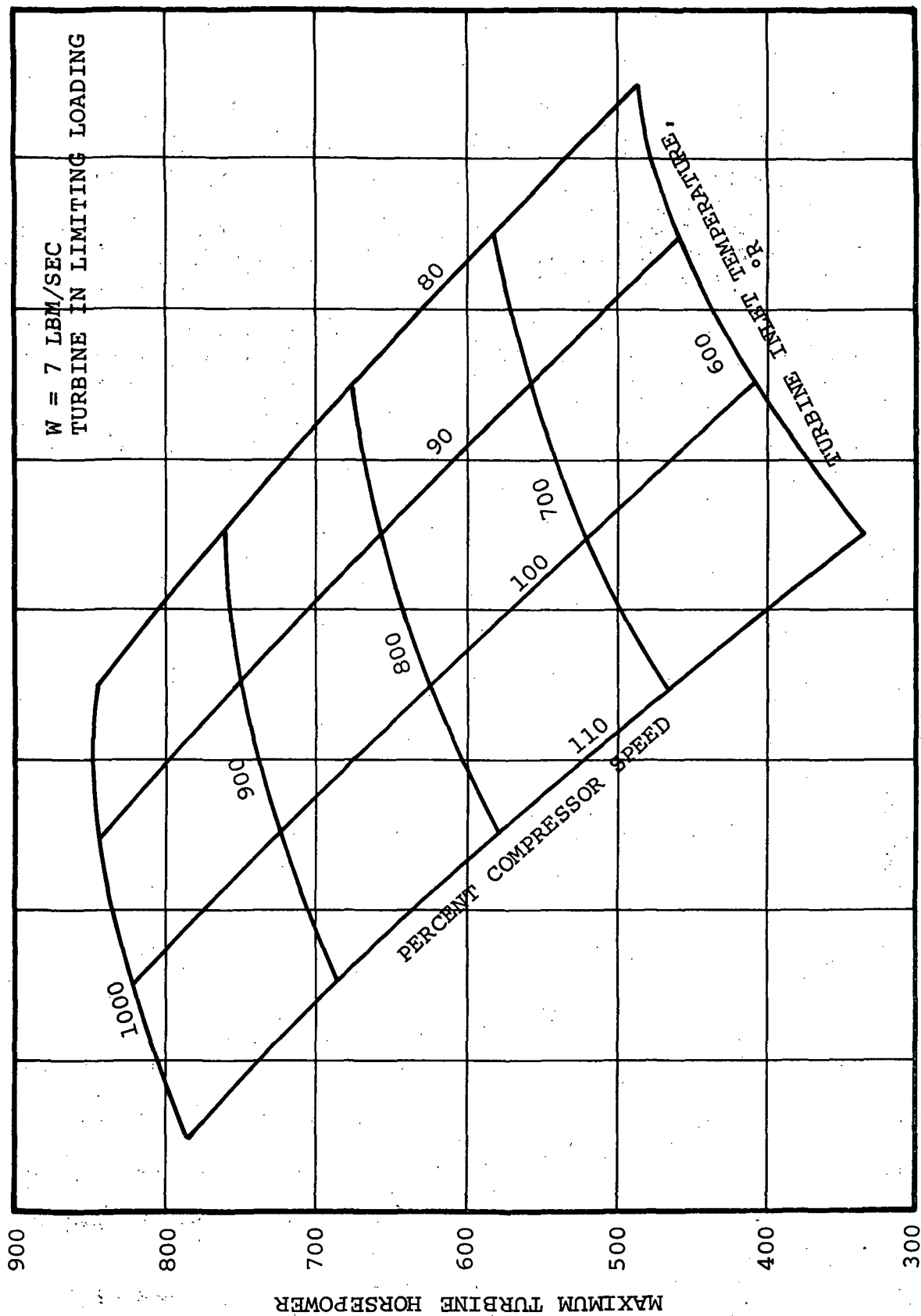


Figure 82. - Maximum Available Radial Turbine Horsepower.

Turbine Design Point

Despite the fact that the radial turbine will operate at higher than design pressure ratios, the initial selection of design point was critical to the proper prediction of the off-design performance. The following aerodynamic summary is based on the design point previously given in the preceding section of this report.

Figure 83 presents a vector diagram of design point, figures 84 through 87 are loading diagrams at the hub, mean, and shroud streamtube for the meridional shape shown in figure 88. The loading diagrams present the nondimensional velocity ratios for the pressure, average, and suction surfaces of the blade as a function of percent meridional distance. The symbols used in figures 83 and 84 through 91 are defined as follows:

- Z - axial distance
- R - radial distance
- m - meridonal distance
- t_n - thickness normal to blade
- t_t - thickness tangential to blade
- β_B - blade angle
- θ_B - blade tangential angle
- V - velocity
- $a'_{cr} = \frac{\sqrt{2\gamma}}{\gamma+1} \sqrt{gRT'}$ velocity of sound
based on stagnation temperature
- T' - stagnation temperature
- T'' - relative stagnation temperature

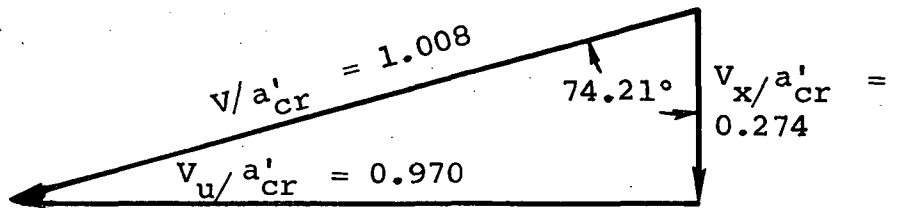
The objective of utilizing loading diagrams is to produce a geometry that will minimize blade surface diffusion while achieving the desired blade circulation. Since actual cold air test data indicates that measured efficiency is very close to design efficiency, the objective was achieved. The geometry required to produce these loadings and efficiency is illustrated in figures 89 through 91. In these figures, the streamtube axial distance (Z), radial distance (R), normal (t_n) and tangential (t_t) thickness, blade beta angle (β_B), and blade theta angle (θ_B) are presented as a function of percent meridional distance.

A complete geometrical description of the turbine wheel and nozzle is given in Appendix B.

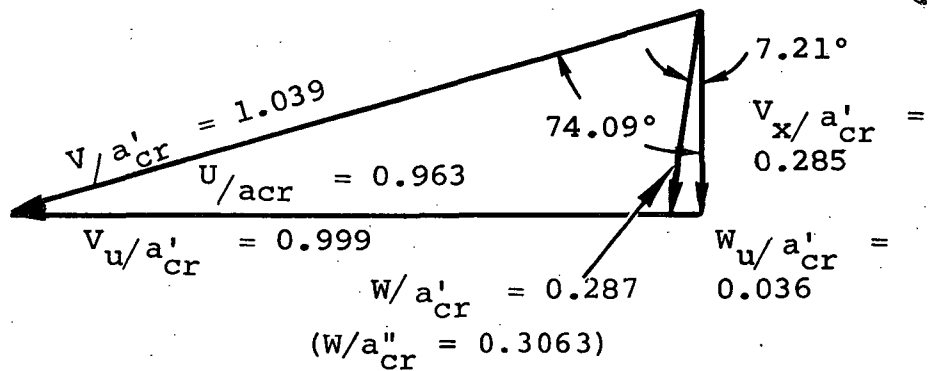


NOZZLE EXIT $R = 3.1599$ IN.

19 VANES



ROTOR TIP $R = 3.0679$ IN.



ROTOR EXIT HUB $R = 1.2500$ IN.

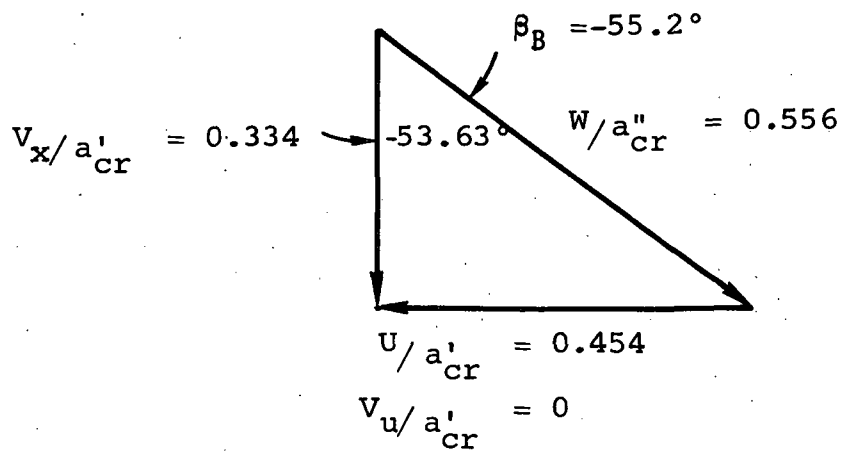
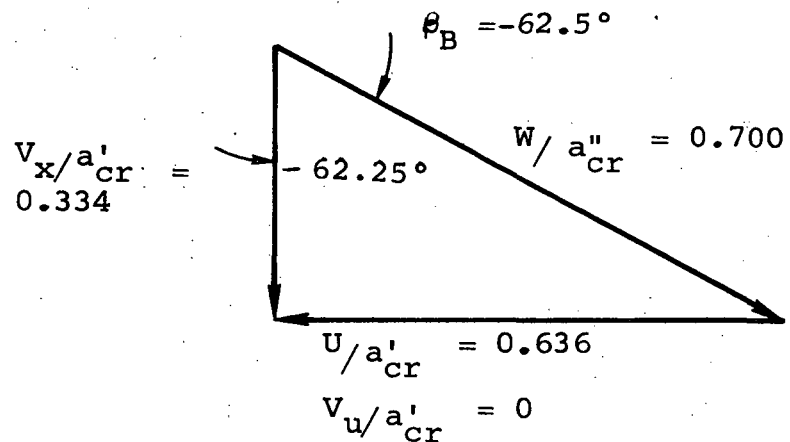


Figure 83. - Radial Turbine Vector Diagram (Sheet 1 of 2).



ROTOR EXIT MEAN LINE $R = 1.75$ IN.



ROTOR EXIT TIP , $R = 2.183$ IN.

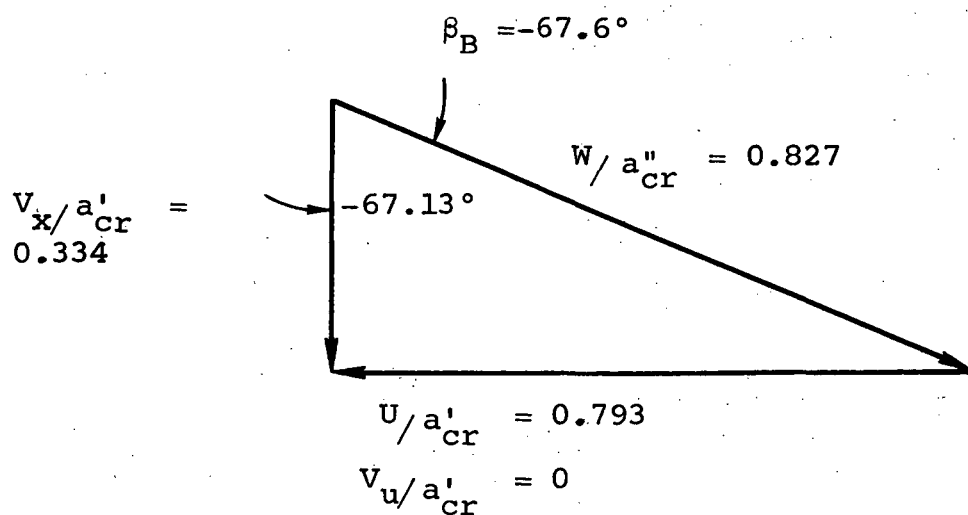


Figure 83. - Radial Turbine Vector Diagram (Sheet 2 of 2).

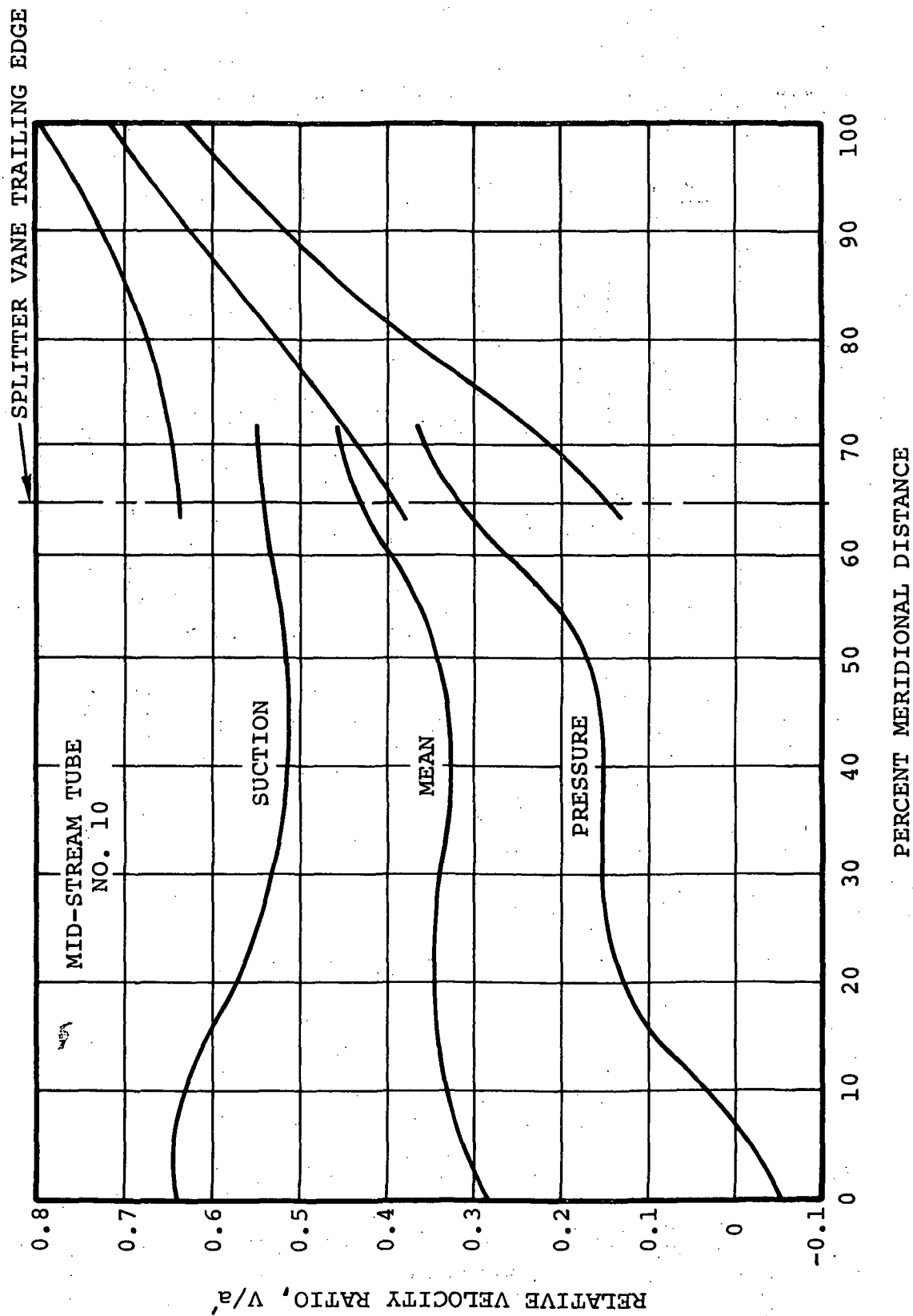


Figure 84. - Radial Turbine - Mean Streamtube Blade Loading.

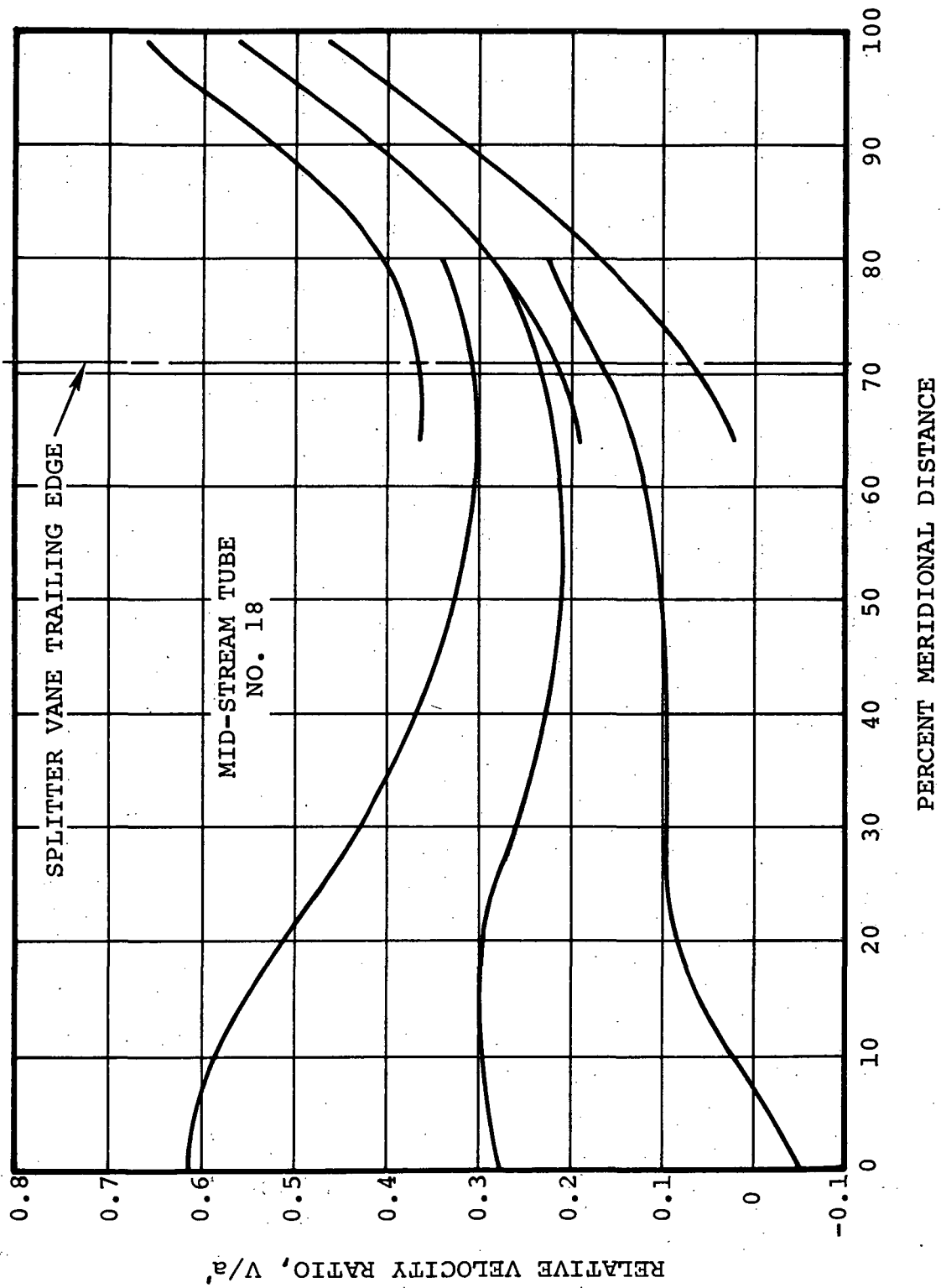


Figure 85. - Radial Turbine - Hub Streamtube Blade Loading.

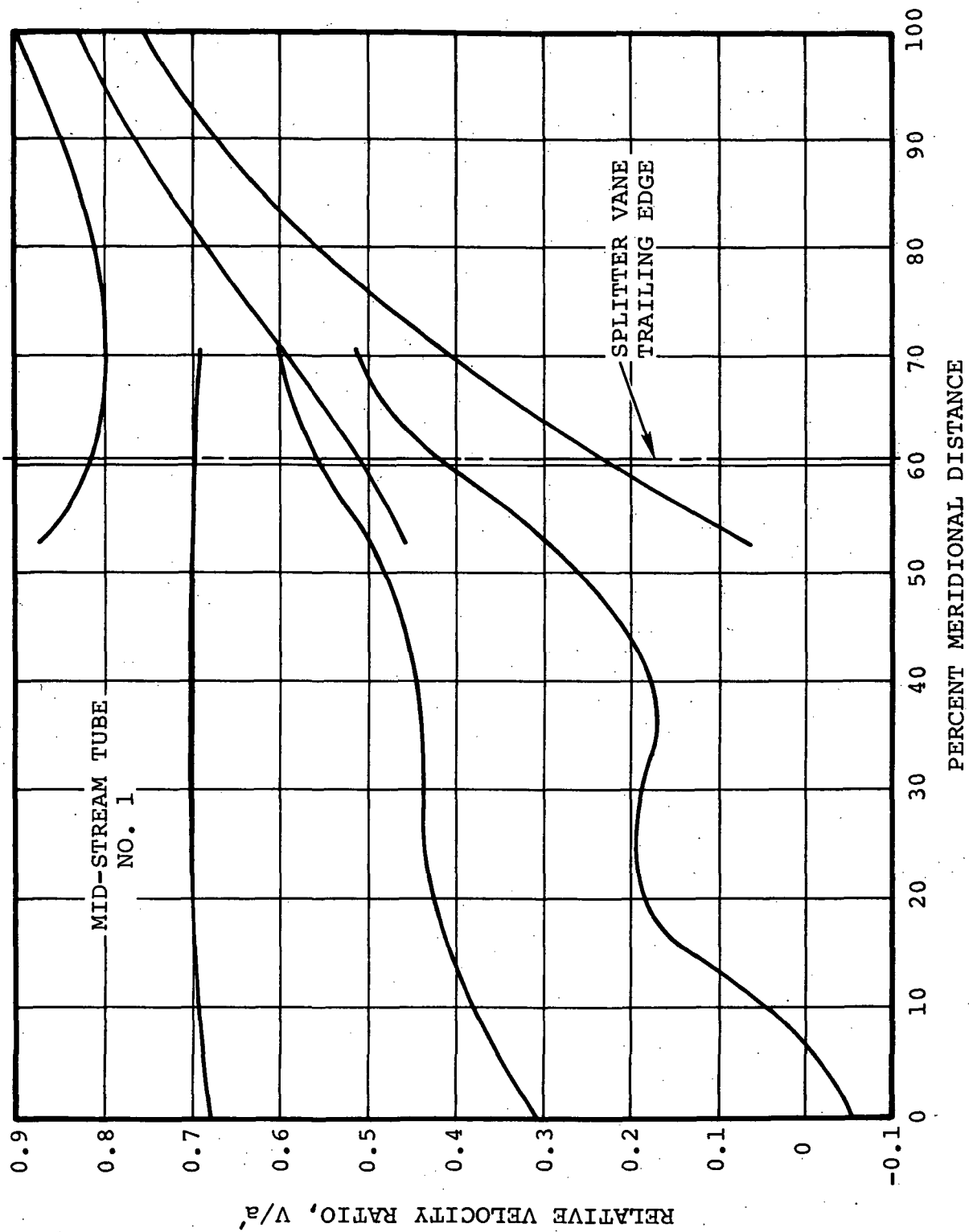


Figure 86. - Radial Turbine - Shroud Streamtube Blade Loading.

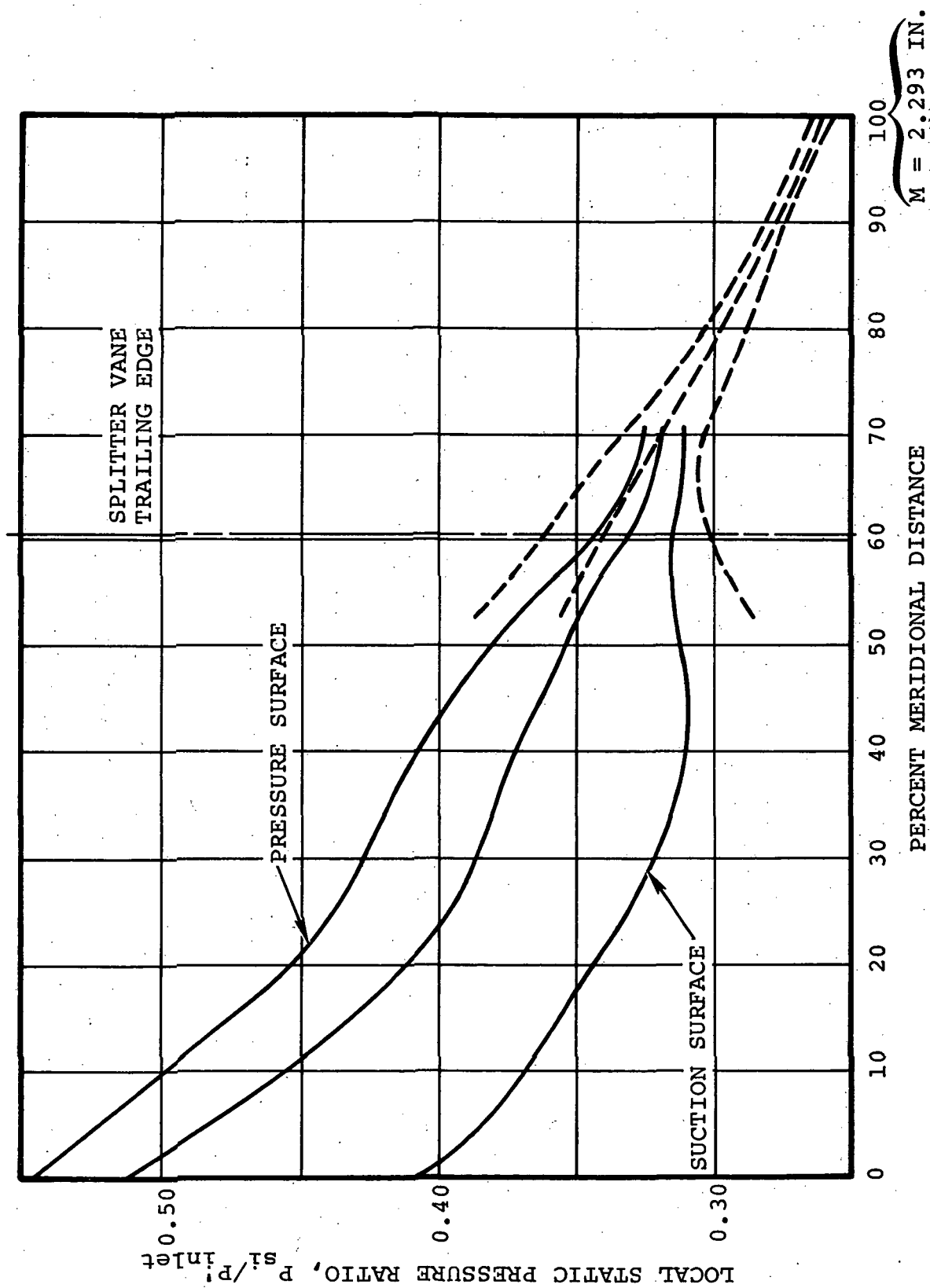


Figure 87. - Radial Turbine - Streamtube 1 - Shroud.

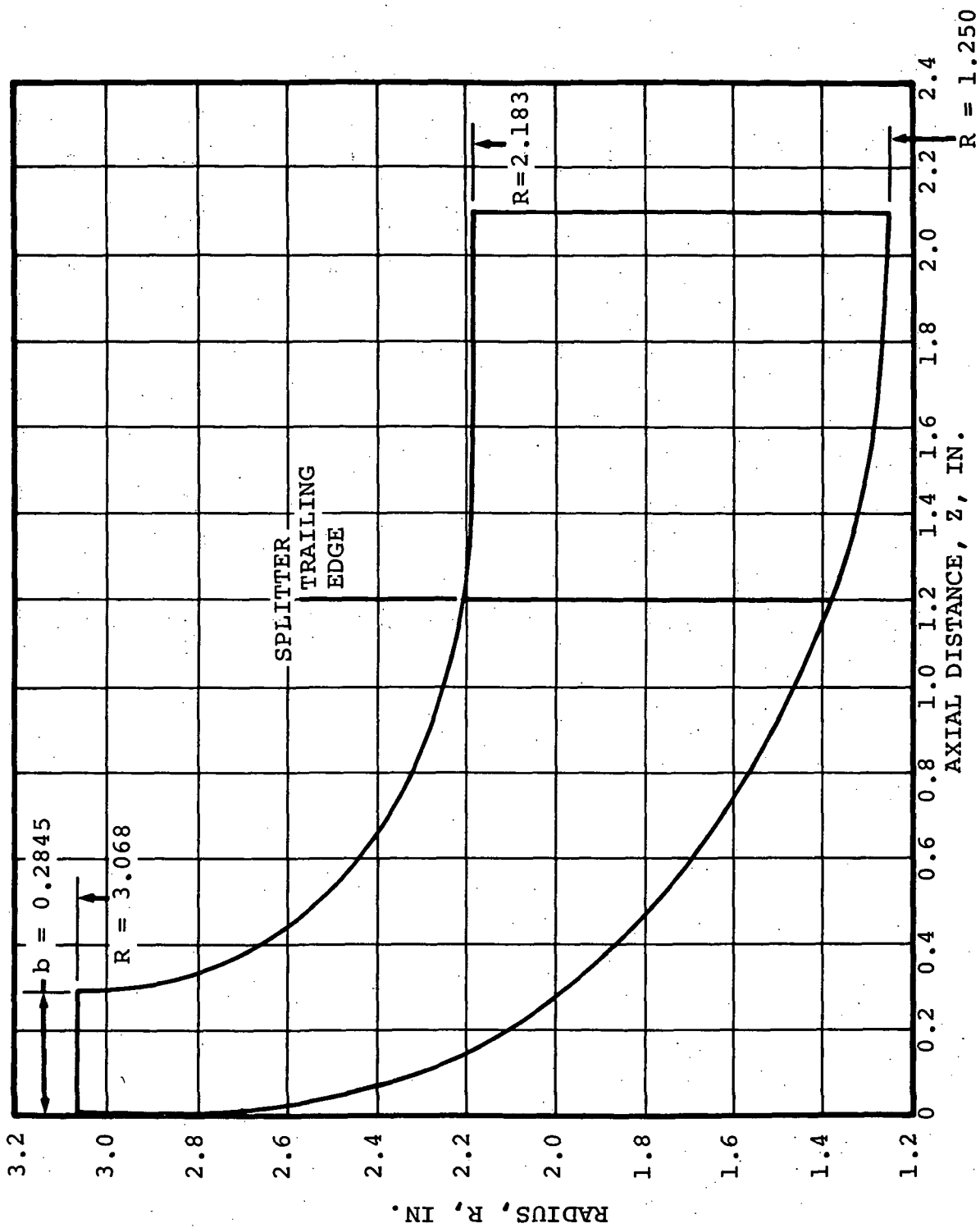


Figure 88. - Meridional Plane View of Radial Turbine.

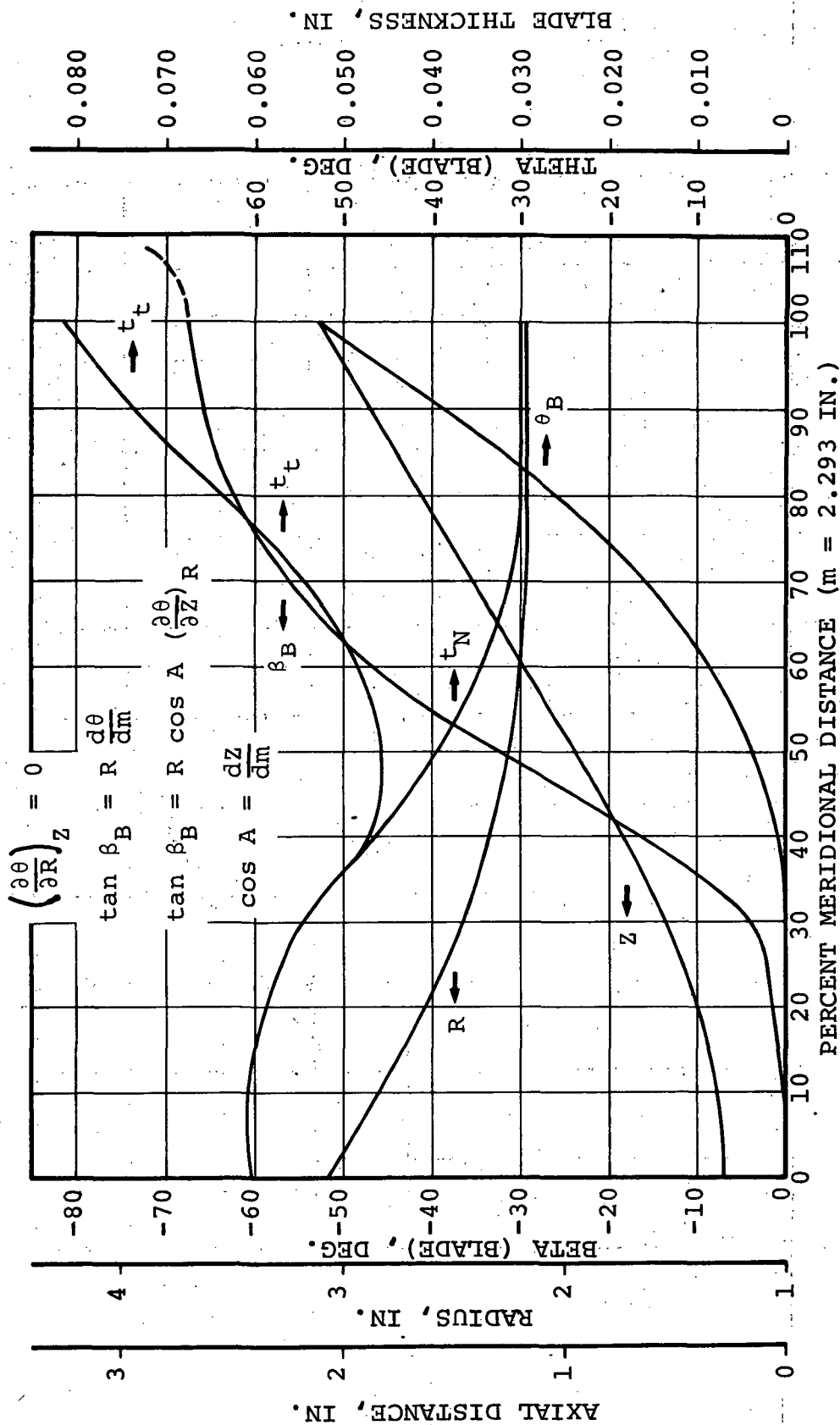


Figure 89.- Radial Turbine, Streamtube 1 - Shroud.

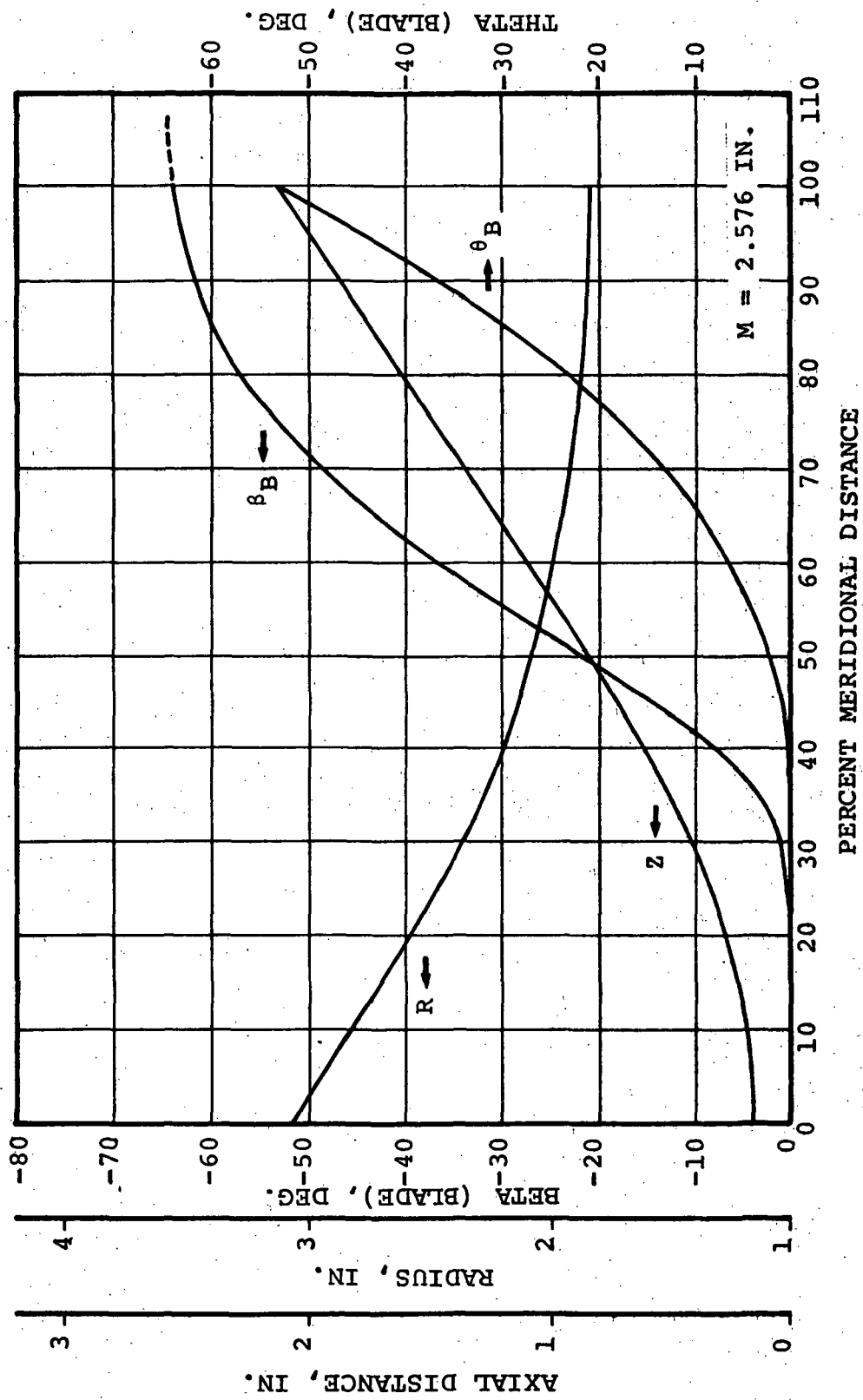


Figure 90. - Radial Turbine, Streamtube 9 - Mean.

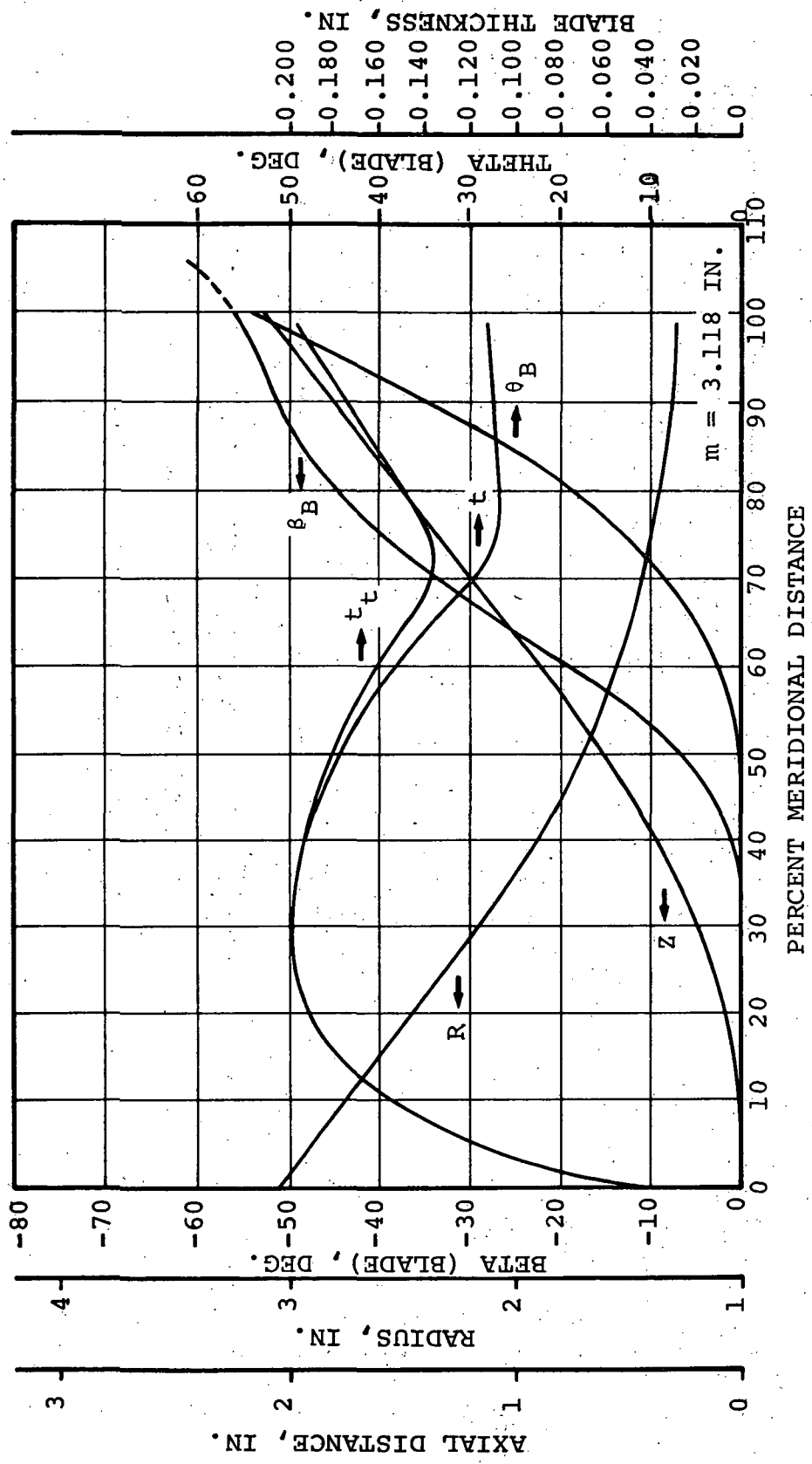


Figure 91. - Radial Turbine, Streamtube 18 - Hub.

APPENDIX A
DEVIATION ANGLE DETERMINATION
FOR
CASCADE/AIRFOILS

(32 pages)

DEVIATION ANGLE PREDICTION FOR THE CONICAL FLOW COMPRESSOR

The traditional approach to deviation or exit flow angle prediction consists of using an empirical rule derived from two-dimensional cascade data. This rule is applied to a rotor by considering flow in the relative plane and, in cases where there are significant variations from two-dimensional conditions, corrections of one form or another to account for differences in meridional velocity ratio, radius change, and other three-dimensional effects have been applied.

Measurements on transonic compressors have indicated deviation angles near the rotor hub are larger than predicted by conventional design rules which include correction factors. In cases where there are large radius and meridional velocity changes in the rotor hub regions, it has been found that these conventional design rules are even more deficient. This apparently is caused by the interacting effects of radial and circumferential equilibrium and other effects such as secondary flows, hub blade boundary layer interaction, sweep effects, and numerous other flow effects.

To account for the interacting effects of radial and circumferential equilibrium on the prediction of deviation angle at the conical flow compressor, the following analysis was used. A quasi orthogonal program was used to obtain stream sheet characteristics at several radial locations. For each stream sheet and exit flow angle, a finite difference program was used to compute blade loading. Iterations were carried out on exit flow angle until the Kutta condition was achieved (the loading diagram at the trailing edge closed). For flow in the rotor, a correction was still applied to account for other flow effects. A detailed description of this method is presented in the following section together with comparison experimental data.

BASIC CONCEPTS

Given a particular stream surface configuration (r as a function of Z), the prediction of deviation angle is equivalent to prediction of total turning and thereby the loading. Any technique to predict this total loading must first correctly predict the guided channel loading and second, correctly handle the isolated airfoil (uncovered) regions at the leading and trailing edge.

The following analysis is offered:

For the rotating blade row:

$$C_p (T' - T'_1) = \omega(r_2 V_{U_2} - r_1 V_{U_1})$$

Energy balance yields:

$$\dot{m} C_p (T' - T_1') = \int_{m_1}^{m_2} U (P_p - P_s) b dm$$

$$U = \omega r$$

$$\dot{m} (U_2 V_{U_2} - U_1 V_{U_1}) = \int_{m_1}^{m_2} U (P_p - P_s) b dm$$

$$V_{U_2} = \frac{U_1}{U_2} V_{U_1} + \int_{m_1}^{m_2} U/U_2 \frac{(P_p - P_s)}{\dot{m}} b dm$$

$$V_U = W_U + U$$

$$W_{U_2} = V_{U_2} - U_2 = V_{U_1} \frac{U_1}{U_2} - U_2 + \int_{m_1}^{m_2} U/U_2 \frac{(P_p - P_s)}{\dot{m}} b dm$$

The W_m can be determined from continuity, thereby yielding the exit flow angle.

$$\tan \beta_2 = \frac{W_{U_2}}{W_m} = \frac{V_{U_1} U_1 - U_2^2}{U_2 W_m} + \int_{m_1}^{m_2} U/U_2 \frac{(P_p - P_s)}{W_m \dot{m}} b dm$$

From this equation it can be seen that the problem of predicting β_2 rests with predicting the loading $(P_p - P_s)$ through the rotor. For stationary cascades, a similar relationship can be derived from the tangential momentum equation.

It should be noted that the upstream and downstream values of velocity represented in the above equation represent an averaged (circumferential) value of the upstream and downstream conditions. In reality the flow conditions may vary circumferentially. Secondly, the assumption is made that no flow crosses the axisymmetric stream

surfaces. This assumption is violated in the cases of warped stream sheets, in separated flow regions where flow migrates towards the tip, and in the blade boundary layers.

- FINITE-DIFFERENCE TECHNIQUE

The traditional approach to exit flow angle prediction consists of using an empirical rule derived from cascade data. This rule is applied to a rotor by considering flow in the relative plane and making corrections of one form or another to account for differences in meridional velocity ratio, radius change, and other three-dimensional effects. Since these corrections have not been verified experimentally, much rests on extrapolation from similar rotor designs to produce new designs. The recent advent of finite difference techniques for determining blade-to-blade solutions allows for the development of an approach more readily applicable to noncascade situations. Two such computer programs currently are in use at AiResearch for obtaining blade-to-blade solutions. Both programs are restricted to subsonic flows with reasonably successful transonic corrections. The first is an outgrowth of the program developed by Katsanis and McNally (Reference 1)* at NASA. The second is a program developed at AiResearch to handle interactions between blade rows and other objects in the flow path such as downstream struts. Because the periodic boundary conditions used in the Katsanis-derived program simplify the input requirements, this program was used for the deviation angle analysis.

*Refer to Page 30 of Appendix A for the noted reference.

The basic equation used by this program is the stream function equation:

$$\frac{1}{r^2} \frac{\partial^2 \psi}{\partial \theta^2} + \frac{\partial^2 \psi}{\partial m^2} - \frac{1}{r^2} \frac{1}{\rho} \frac{\partial \rho}{\partial \theta} \frac{\partial \psi}{\partial \theta_r} + \frac{\sin \alpha}{r} - \frac{1}{b\rho} \frac{\partial (b\rho)}{\partial m} \frac{\partial \psi}{\partial m} = \frac{2b\rho\omega}{m} \sin \alpha$$

The boundary conditions for its solution are shown in Figure 1. As can be seen, they are of three types. At the upstream and downstream boundaries, the flow angle is specified and assumed constant with α . The straight boundaries connecting the upstream and downstream boundaries with the blade, utilize the condition of periodicity. On these boundaries

$$\psi_{\text{upper}} = \psi_{\text{lower}} + 1.$$

The blade boundaries have specified values of stream function since the flow passing between them is known.

To use this technique, the angle on the downstream boundary is specified and velocity distributions throughout the region and on the boundaries are calculated by a finite-difference relaxation technique described in Reference 1. This blade velocity distribution may take on one of the three shapes indicated in figure 2. All three loadings represent valid inviscid solutions for the cascade. However, the requirement of satisfying the Kutta condition for an airfoil is based on viscous effects and compliance with this condition must be determined on separate grounds. Reference 2 describes the Kutta condition basically as the inability of an airfoil to maintain continuous flow around the sharp trailing edge. Because of the requirement for a static pressure balance across the wake, velocities on the suction and pressure surfaces must be equal at the trailing edge. This is equivalent to stating that the stagnation point, where the dividing streamline leaves the blade, occurs in the trailing edge region.

The basic technique is then one of iteration where a variety of exit flow angles in the vicinity of the expected exit flow angle are specified until the one giving equal exit suction and pressure surface velocities is determined. In practice this is done graphically with a final computer run to verify the results at the determined exit flow angle.

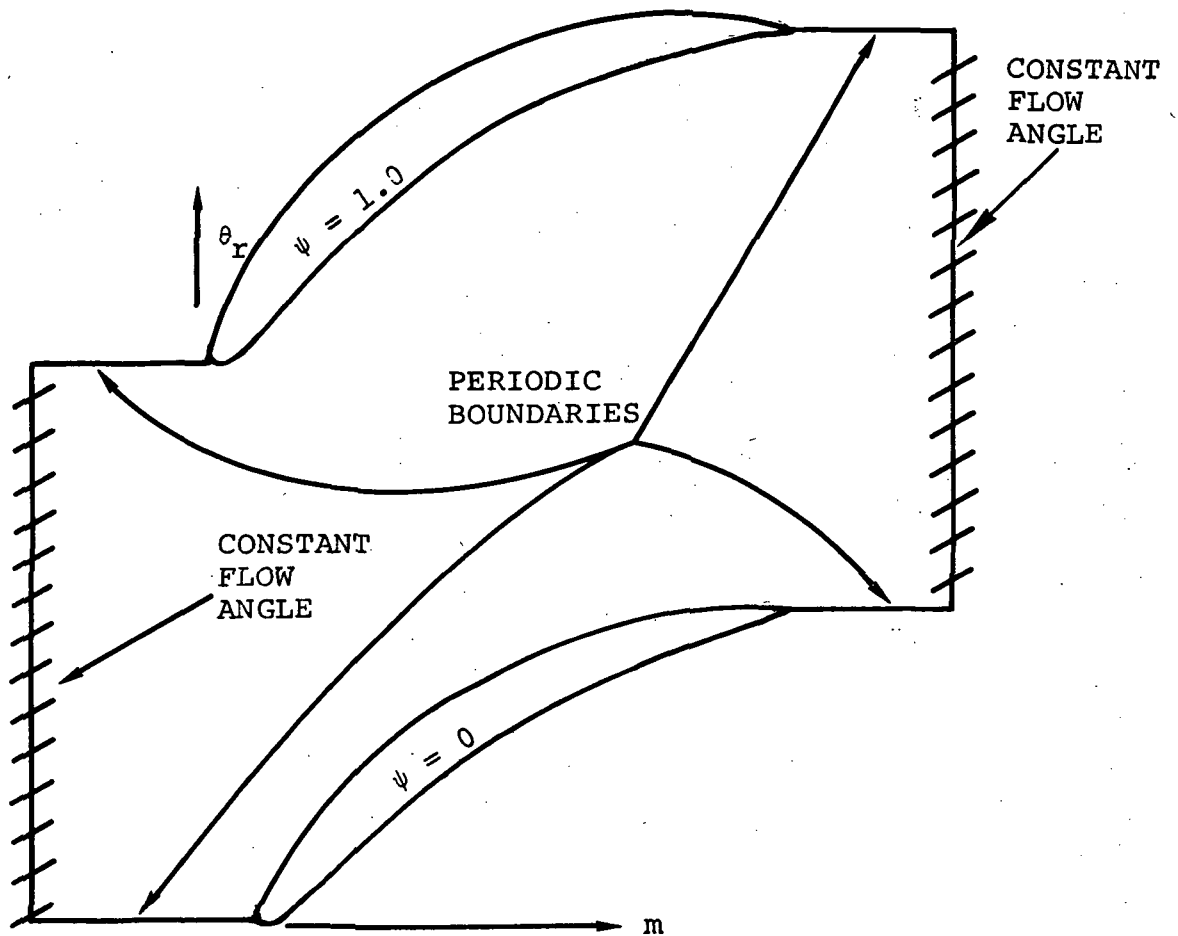


Figure 1. - Boundary conditions for solution of the stream function equation.

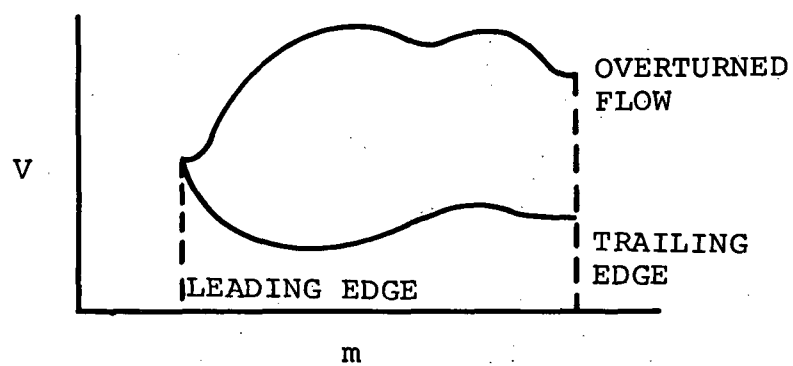
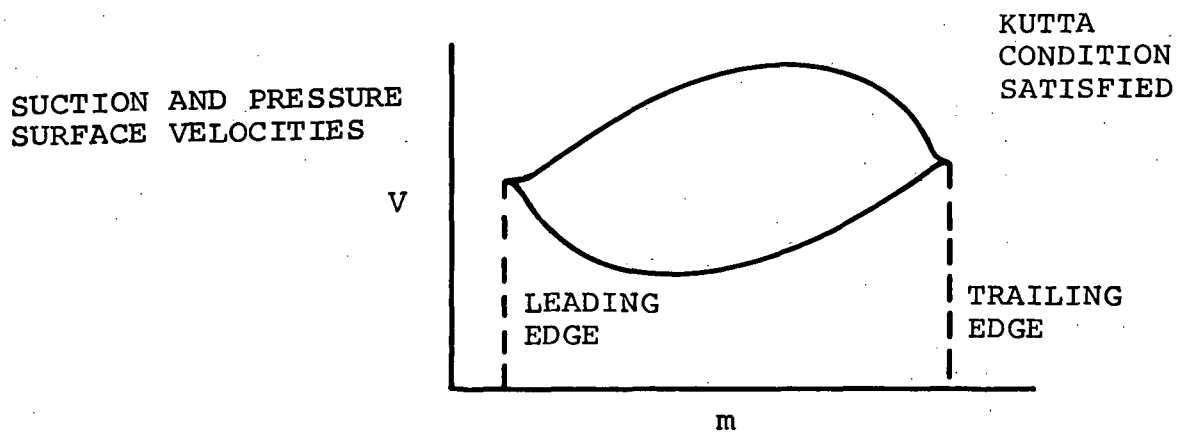
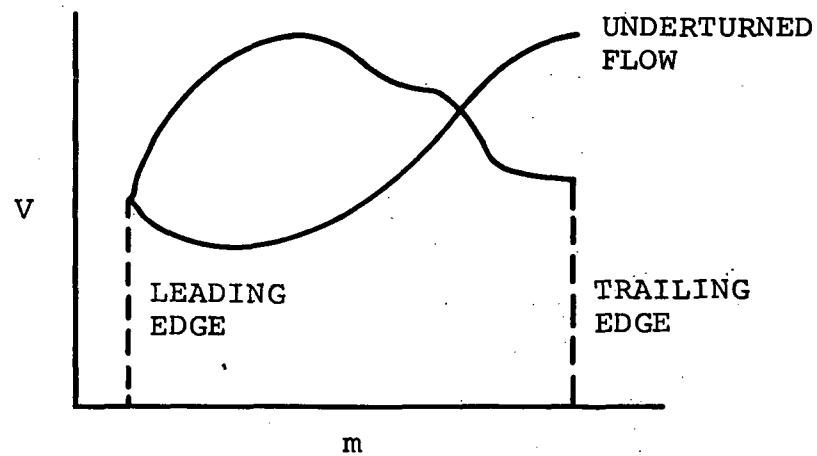


Figure 2. - Inviscid cascade solutions.

ACCURACY OF TECHNIQUE

The accuracy of the finite difference technique is expected to be influenced by the following factors:

- (a) Accuracy of the inviscid solution for a given input
- (b) Accuracy of the satisfaction of the trailing edge Kutta condition
- (c) Accuracy of input geometries, flows, etc.
- (d) The effects of viscous flows

Since integration of the solution is all that is required, the accuracy of the overall inviscid solution is expected to be excellent. To verify this point Carter's Rule can be analyzed for the effect of geometry on exit deviation angle (total turning). Since this technique represents a fit to experimental cascade data, the effect of errors in cascade parameter input and the accuracy of blade loading solutions for the finite-difference technique should be approximated. Carter's Rule is represented in Reference 3 as follows:

$$\delta = \frac{\beta_1 - i - \beta_2 e}{\frac{\sqrt{\sigma}}{m_c} - 1} \quad (1)$$

The m-factor describes the effect of setting angle and geometry. figure 3 gives the dependence of geometry (max. camber rise point) and setting angle utilized by Reference 3. For an axial low speed cascade, equation 1 can be expressed in terms of the total turning in a cascade as follows:

$$\theta = \frac{\left(\frac{\sqrt{\sigma}}{m_c} - 1\right) (\alpha + \xi_2) + \alpha - \xi_1}{\sqrt{\sigma}/m_c} \quad (2)$$

where the angles are described in figure 4. Differentiating equation 2 the result is

$$\frac{d\theta}{dm_c} = - \delta / m_c$$

For a typical value of δ of 10 degrees and m_c of 0.25

$$\Delta\theta = -40 \Delta m_c$$

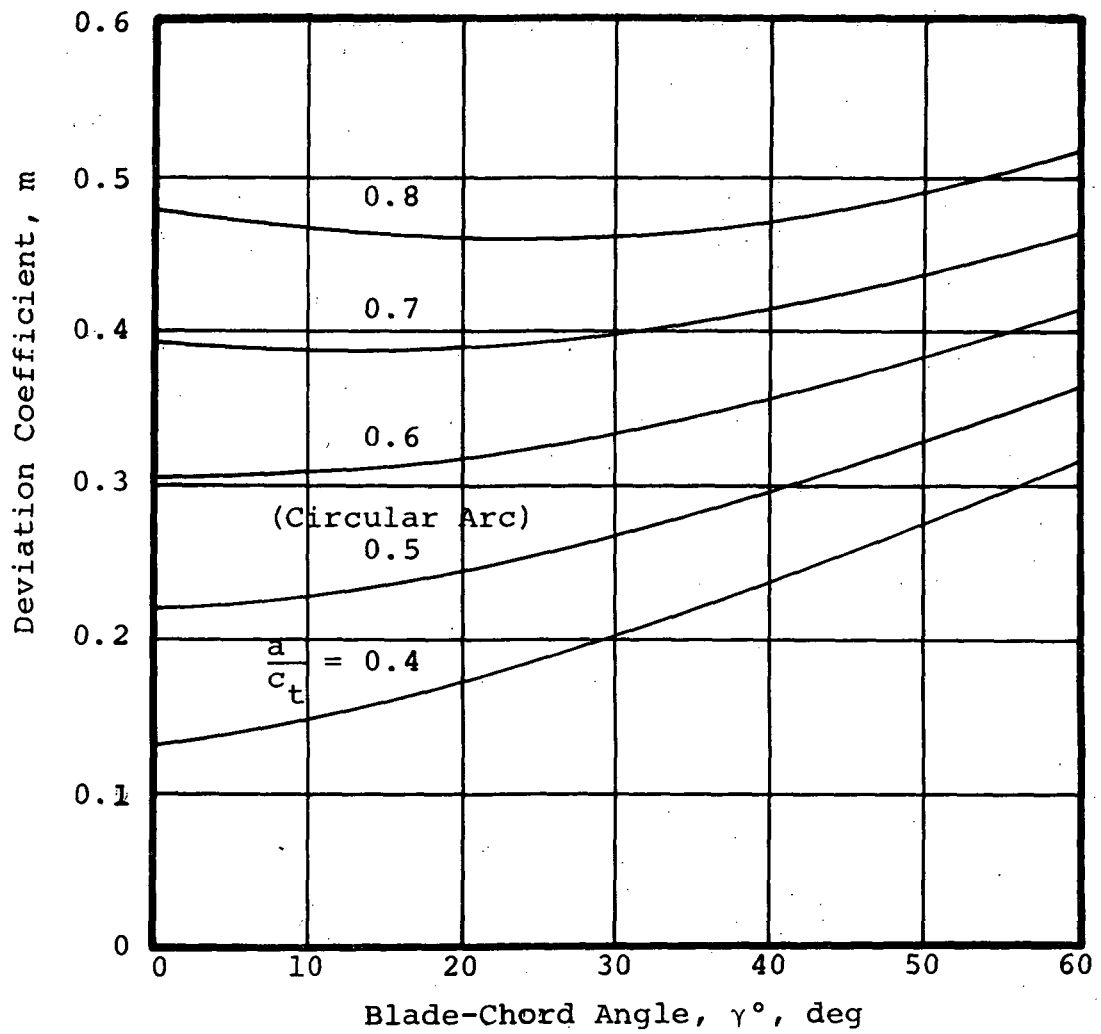


Figure 3. - Coefficients for design deviation angle rule.

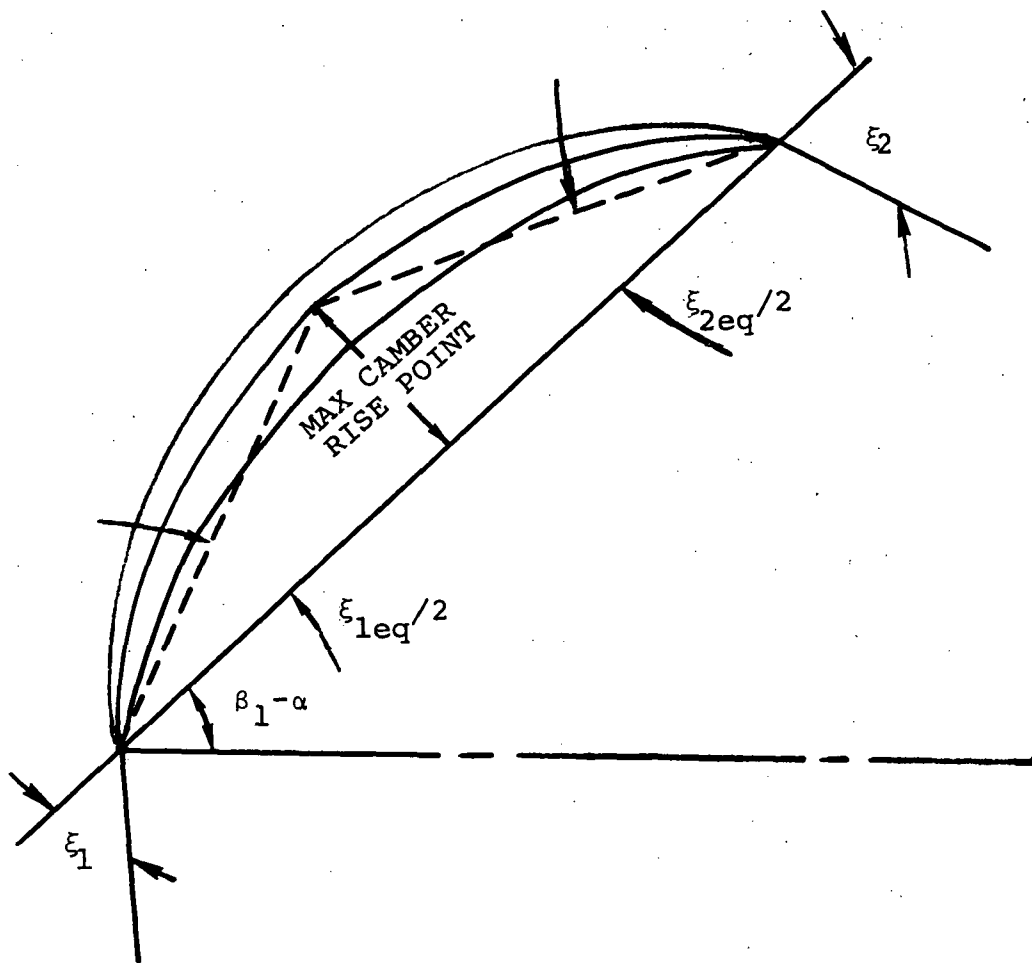


Figure 4. - Angle definitions.

To illustrate the use of this equation, if a 1-percent chord error is assumed in specifying input geometry (maximum camber rise point), the error in the turning would be 0.15 degree for the values of δ and m_c given above. This leads to the expectation that inaccuracies due to errors in input geometry specification should be slight.

Utilizing the finite-difference technique requires determination of the exit flow angle for which suction and pressure surface velocity are equal. Due to the finite-difference nature of this calculation, there is an uncertainty of the point of achievement of this equality in velocity of one-mesh spacing. The inaccuracy caused by this uncertainty in stagnation point can be evaluated as follows for the cascade situation. Assuming a triangular loading (pressure) distribution typical of compressor sections, as shown below, the uncertainty in turning can be evaluated from simple areas.

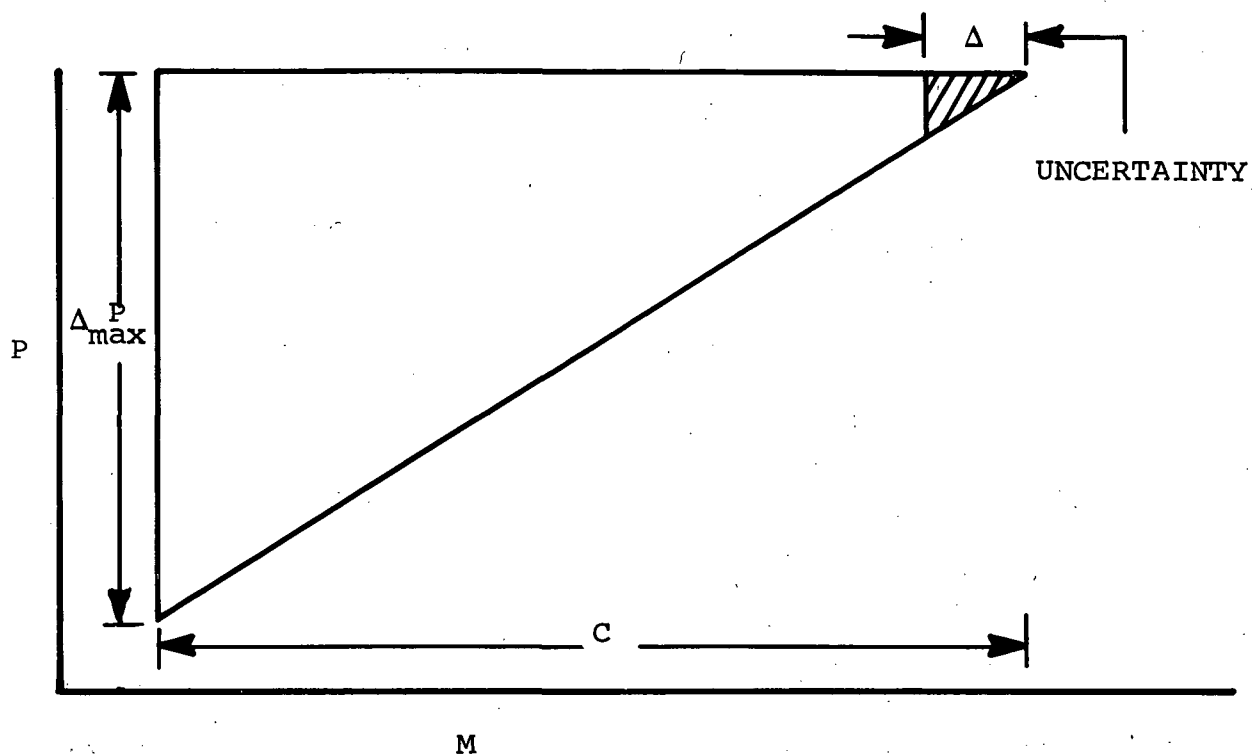
Normal values of N_m range from 20 to 40 making this error insignificant.

Real flow effects are expected to be the largest source of error. As stated earlier, this form of approximating the Kutta conditions consists of selecting θ that gives equal velocities at the trailing edge. Although the calculation differs slightly in detail, it is equivalent to the well-known technique used on isolated airfoils where the proper circulation is selected to give a dividing streamline at the trailing edge. Viscous effects including the effects of suction surface separation will modify the resultant lift. The magnitude of these effects is expected to be similar to those experienced with isolated airfoils, where useful results can be obtained for moderate cambers at nominal angles of attack.

COMPARISON WITH EXPERIMENTAL CASCADE DATA

To verify the expected accuracy of the finite-difference technique, the technique was applied to cases where experimental data was available. The obvious starting place for this comparison is with two-dimensional cascade data such as that contained in References 4, 5, and 6. This data provides the closest experimental agreement with the analysis technique since no three-dimensional flow effects were incurred. In addition, a variety of blade shapes are available for analysis. For comparison purposes data was taken from three different classes of blade shapes as follows:

- (a) Front loaded, A_4K_6
- (b) Mid-loaded A_{10} , circular arc
- (c) Rear loaded, A_2I_{8b}



$$\Delta = C/N_m$$

where N_m is the number of mesh points between blade inlet and outlet used in the finite difference calculation

$$\frac{\Delta \theta}{\theta} = \frac{\Delta \cdot (\Delta/C) \Delta P_{\max}}{\Delta P_{\max} C} = \Delta^2/C^2$$

$$\frac{\Delta \theta}{\theta} = 1/N_m^2$$

Eleven cases were examined in detail. These were selected to cover a range of setting angles, inlet Mach numbers, and blade shapes.

Comparison with Carter's Rule was made utilizing the form of the rule given in Reference 3 along with the M-factor curve shown in Reference 3 and figure 3. The equations are:

$$\beta_{2e} = \tan^{-1} \left[\frac{U_1}{V_{m1}} - r_2/r_1 \left(\frac{U_2}{V_{m1}} - \frac{V_{m2}}{V_{m1}} \tan \beta_2 \right) \right]$$

$$\delta^o = \frac{\beta_1 - i - \beta_{2e}}{\frac{\sqrt{\sigma}}{m} - 1}$$

Figures 5 through 10 show a comparison of turning angles and the ratio of change in momentum to that given by a reference turning angle, (θ Ref) for experimental data, Carter's Rule, and the finite-difference technique. Figure 11 shows the geometric angle used for the reference turning and the two approaches to Carter's Rule.

Equivalent leading and trailing edge angles were selected on the basis of the angles shown in Figure 11. For a circular-arc camber line, the true leading and trailing edge angles are equal to the equivalent leading and trailing edge angles.

An attempt was made to correlate the differences between experimental and calculated (finite-difference method) deviation angles. No correlation was found with D-factor or other conventional techniques. Stewart's calculations were also utilized and they likewise did not come close to predicting either magnitude or signs of the observed differences. What did seem consistent was that the front-loaded blades 63(A₄K₆)06 and the 65(12A₁₀)10 mid-loaded blade shapes provided consistently more experimental turning than calculated. The heavily rear-loaded blades 65(12A₂I_{8b})10 and the thickened circular-arc blade gave consistently less turning than calculated.

Figures 12 and 13 show the effect of Mach number on turning. As can be seen, Carter's Rule does not fit this data as well as other cases examined. Figure 14 summarizes the results on turning angle for all cases examined. The inviscid calculation has indicated a relative error of less than 5-percent error in tangential momentum change across the cascade. Although more comparisons to cascade data would be desirable, the basic characteristics and accuracy of the finite-difference method of predicting deviation angle have been demonstrated.

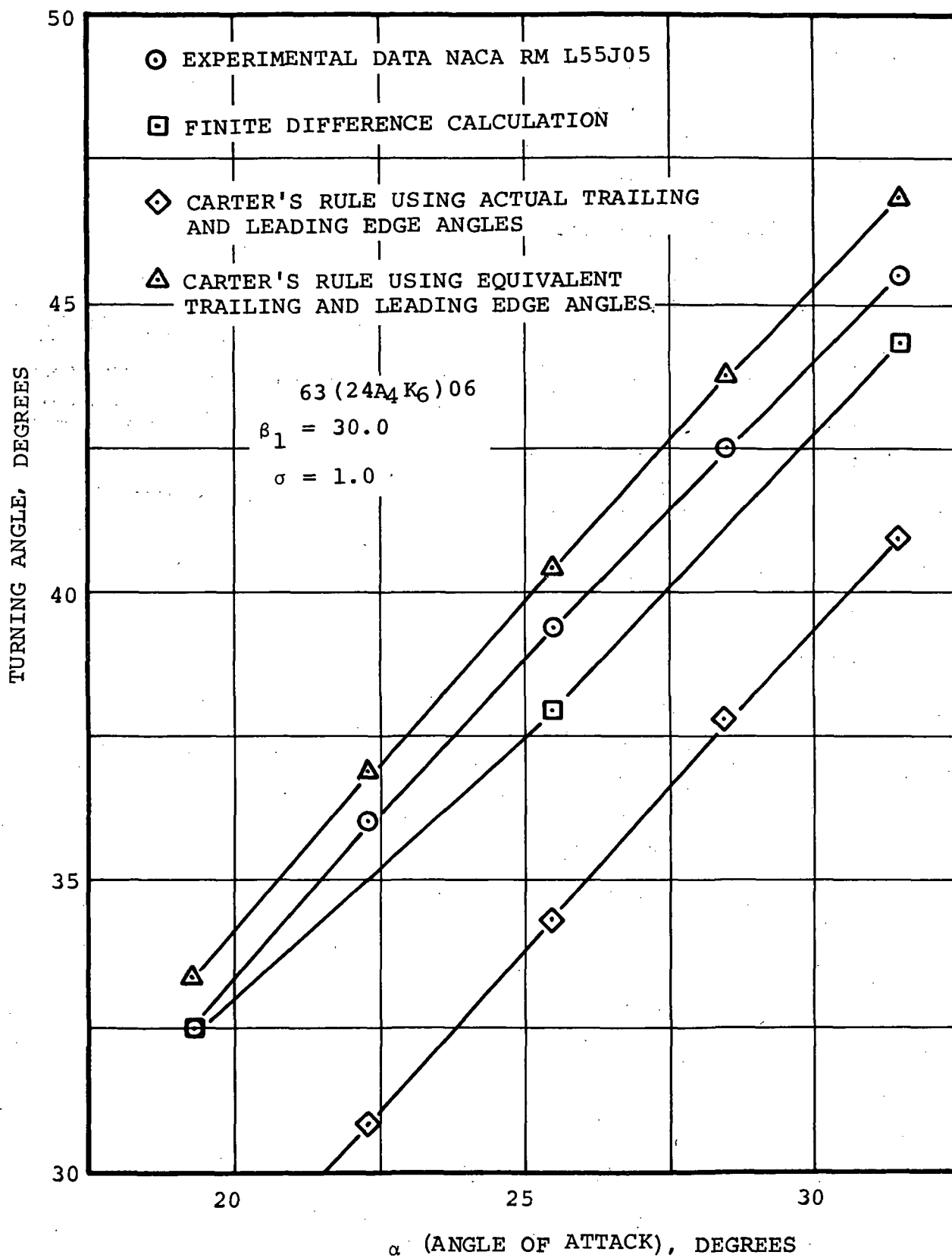


Figure 5. - Turning angle versus angle of attack.

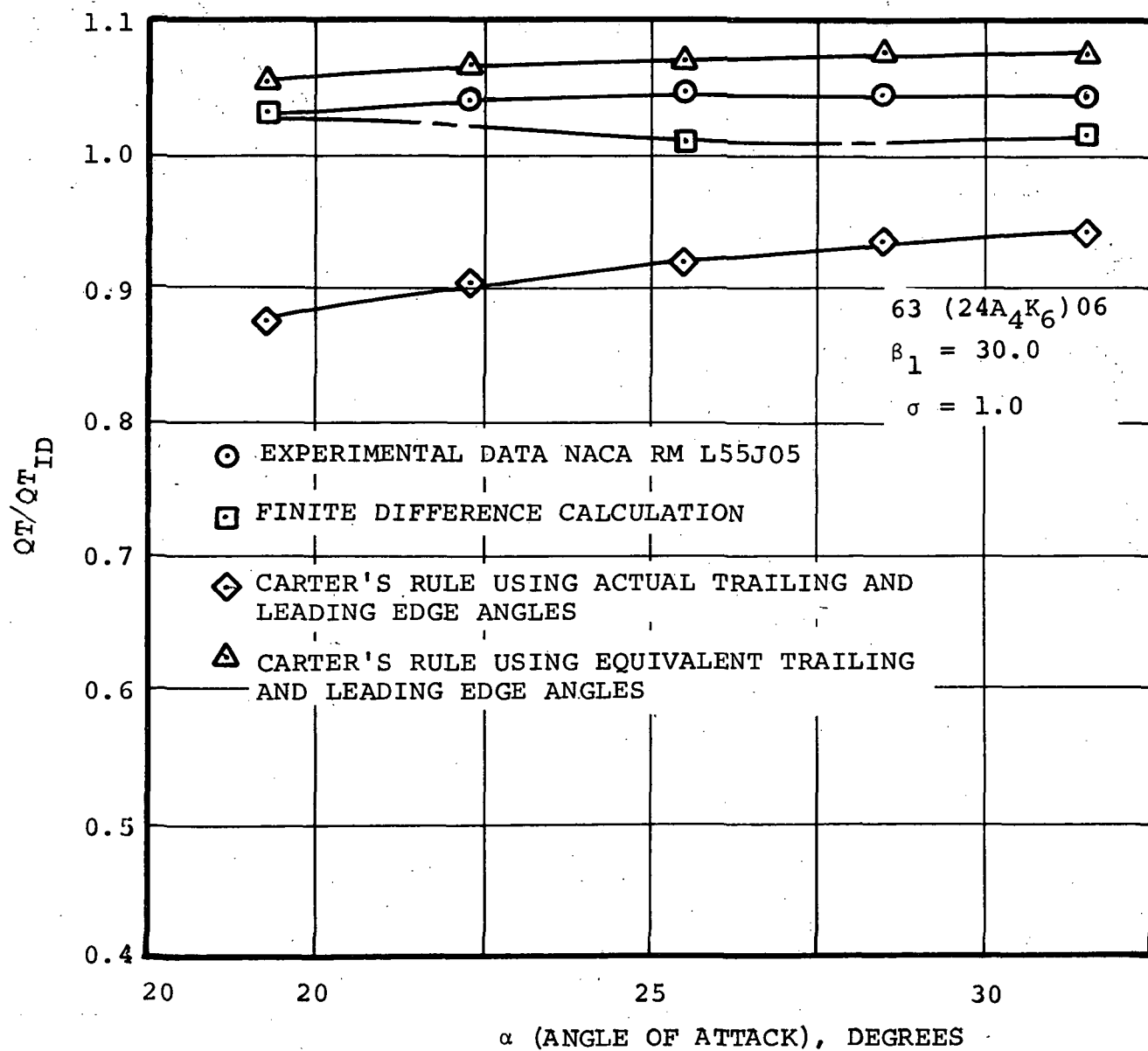


Figure 6. - Change in tangential momentum/ideal versus angle of attack.

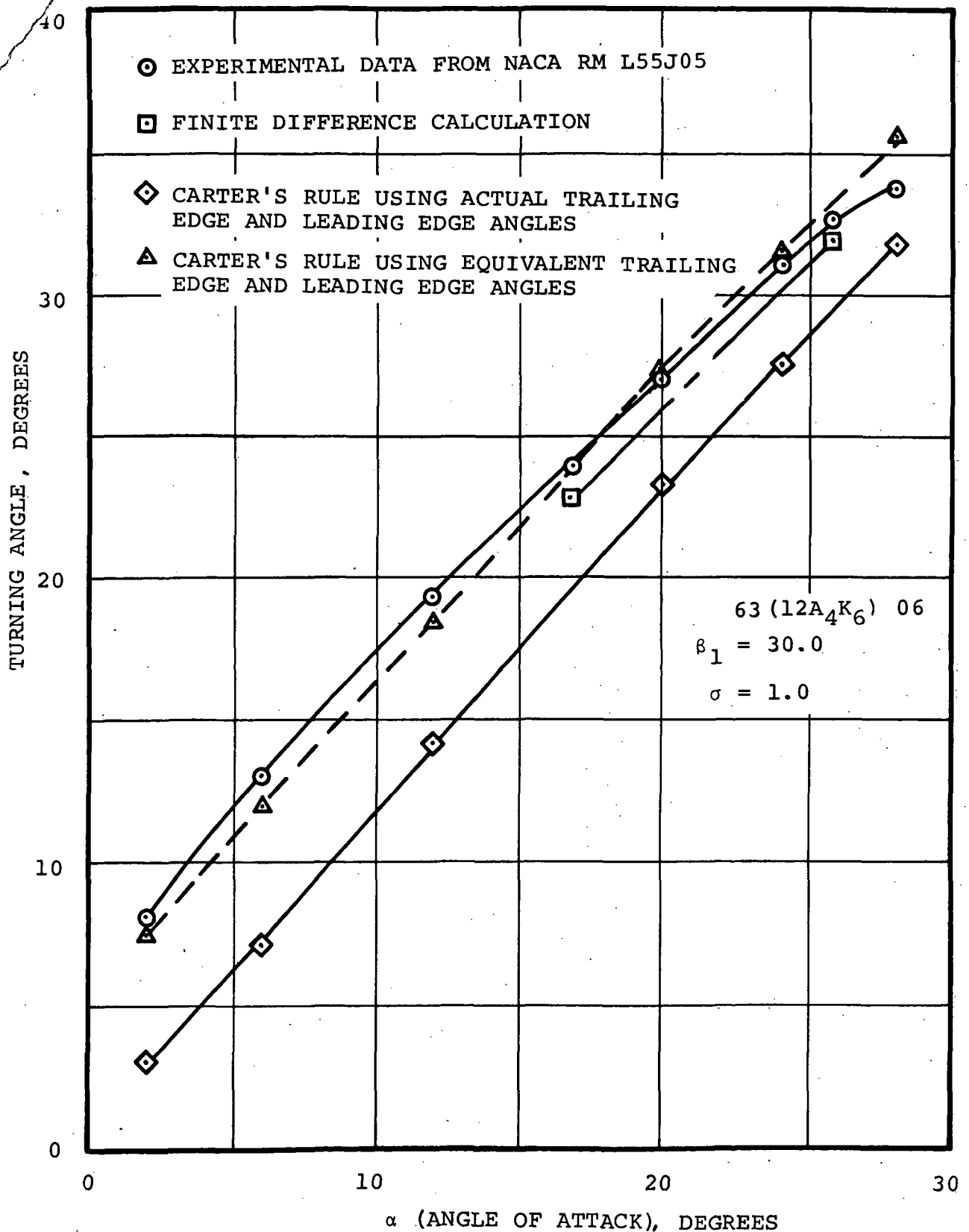


Figure 7. - Turning angle versus angle of attack.

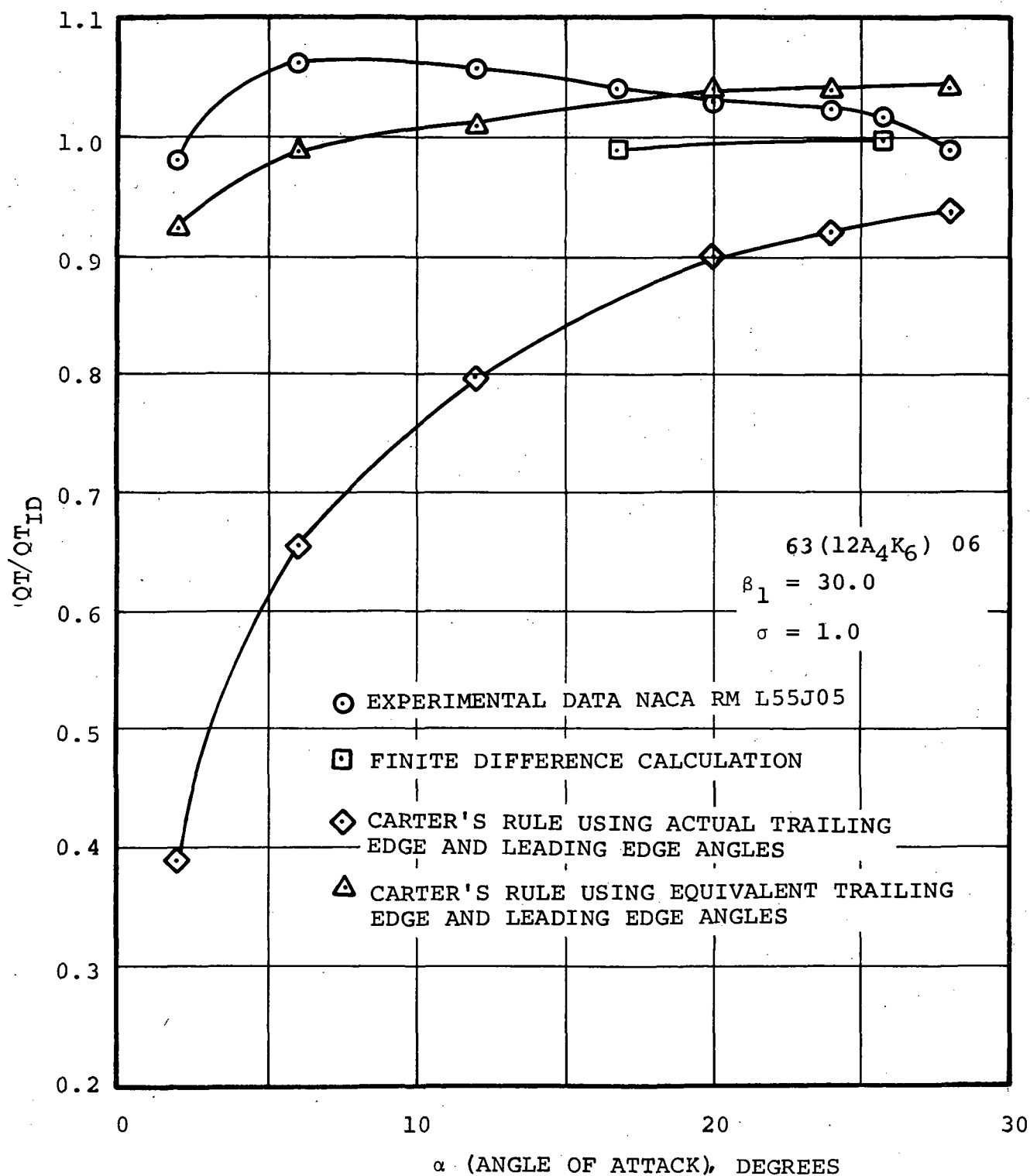


Figure 8. - Change in tangential momentum/ideal versus angle of attack.

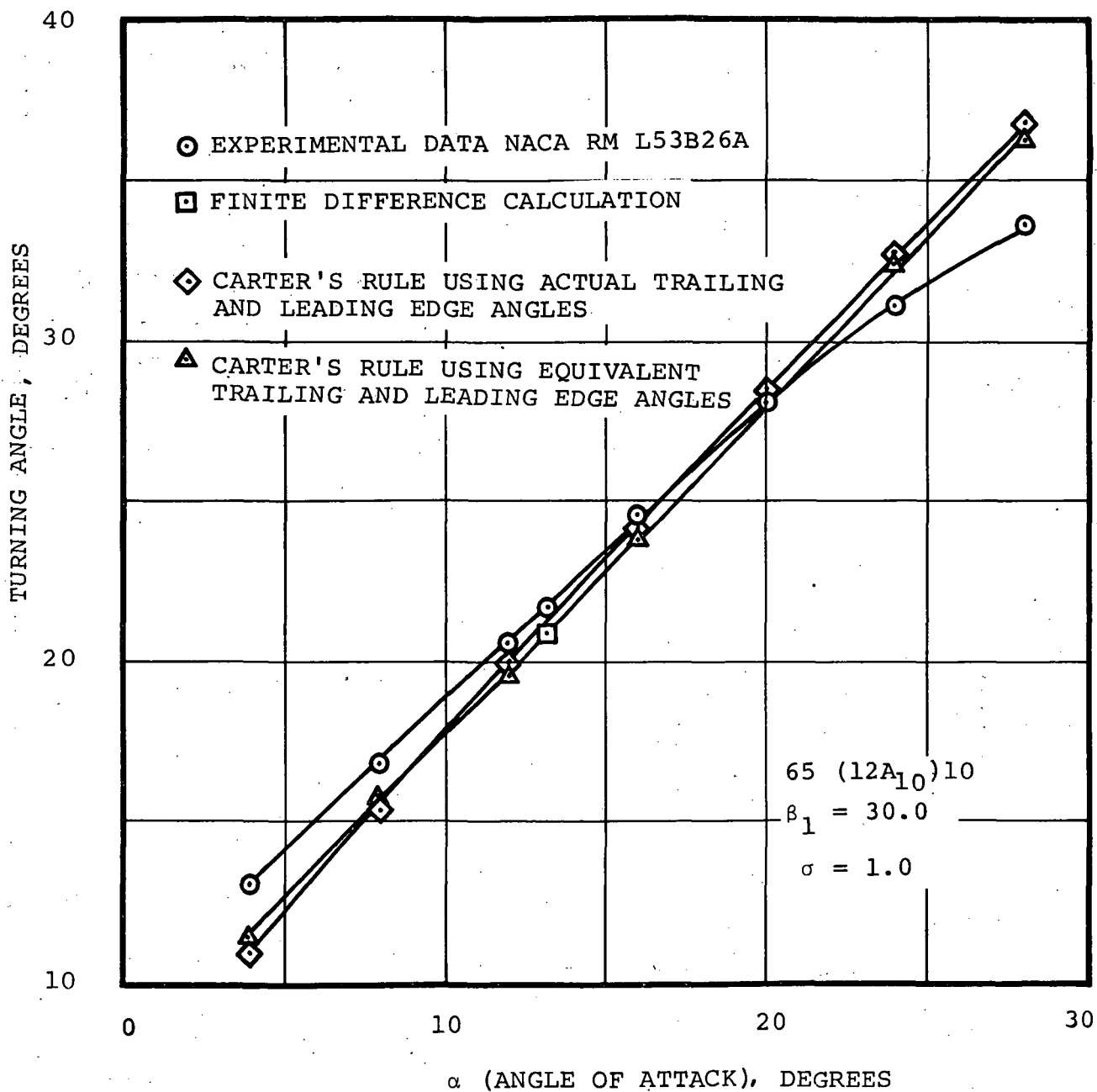


Figure 9. - Turning angle versus angle of attack.

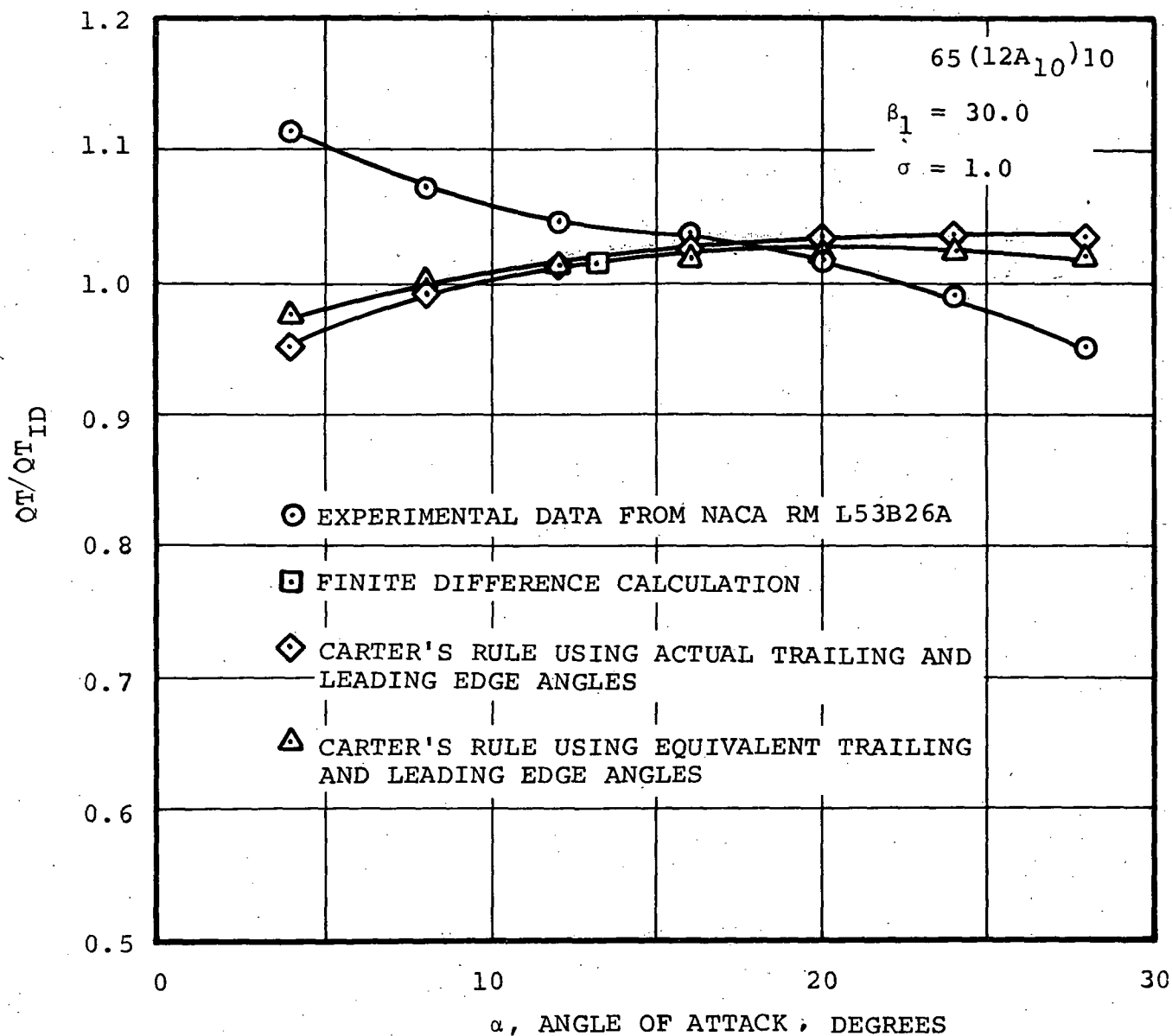
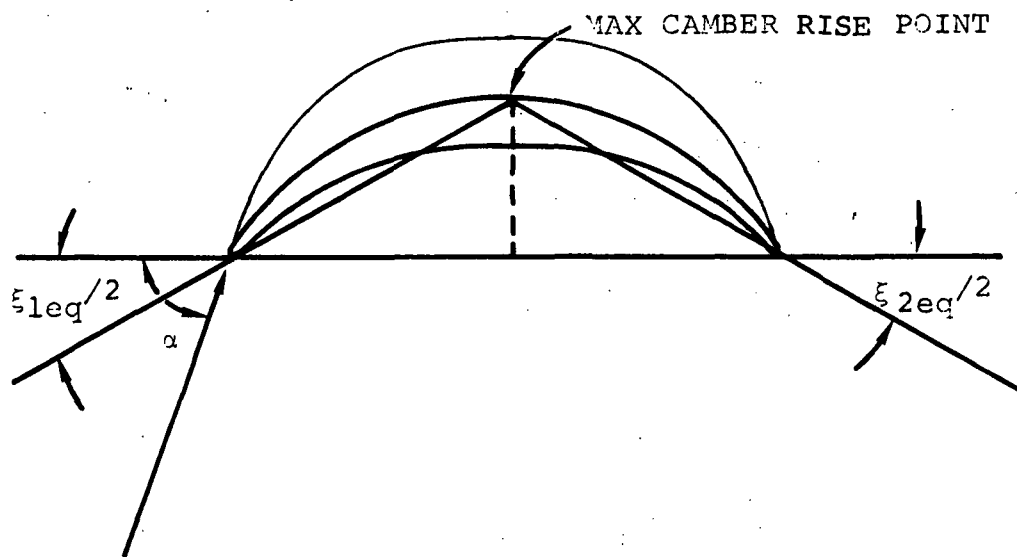


Figure 10. - Change in tangential momentum/ideal versus angle of attack.



$$\theta_{Ref} = \alpha + \xi_{2eq}/2$$

Figure 11.

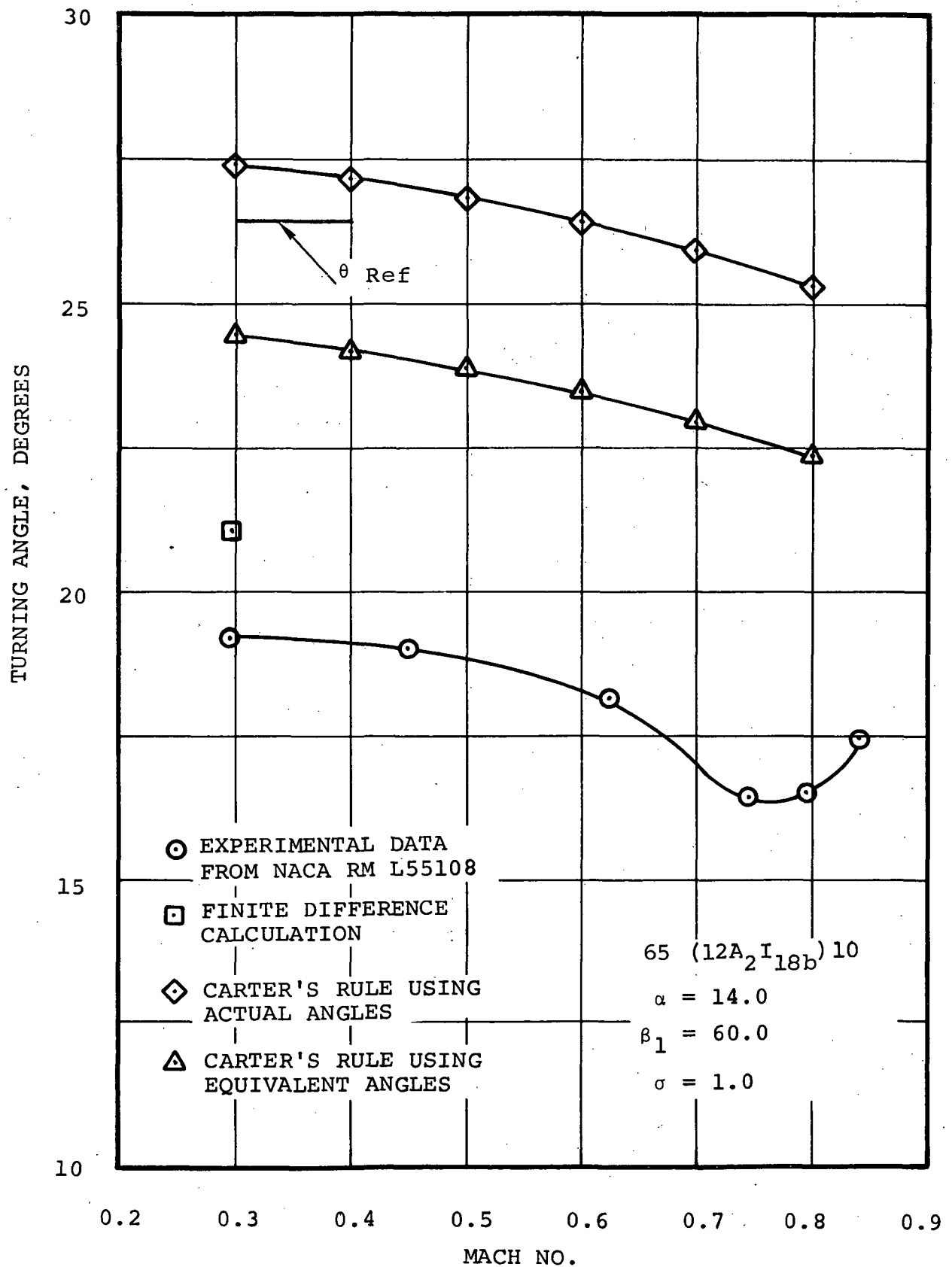


Figure 12. - Turning angle versus mach number.

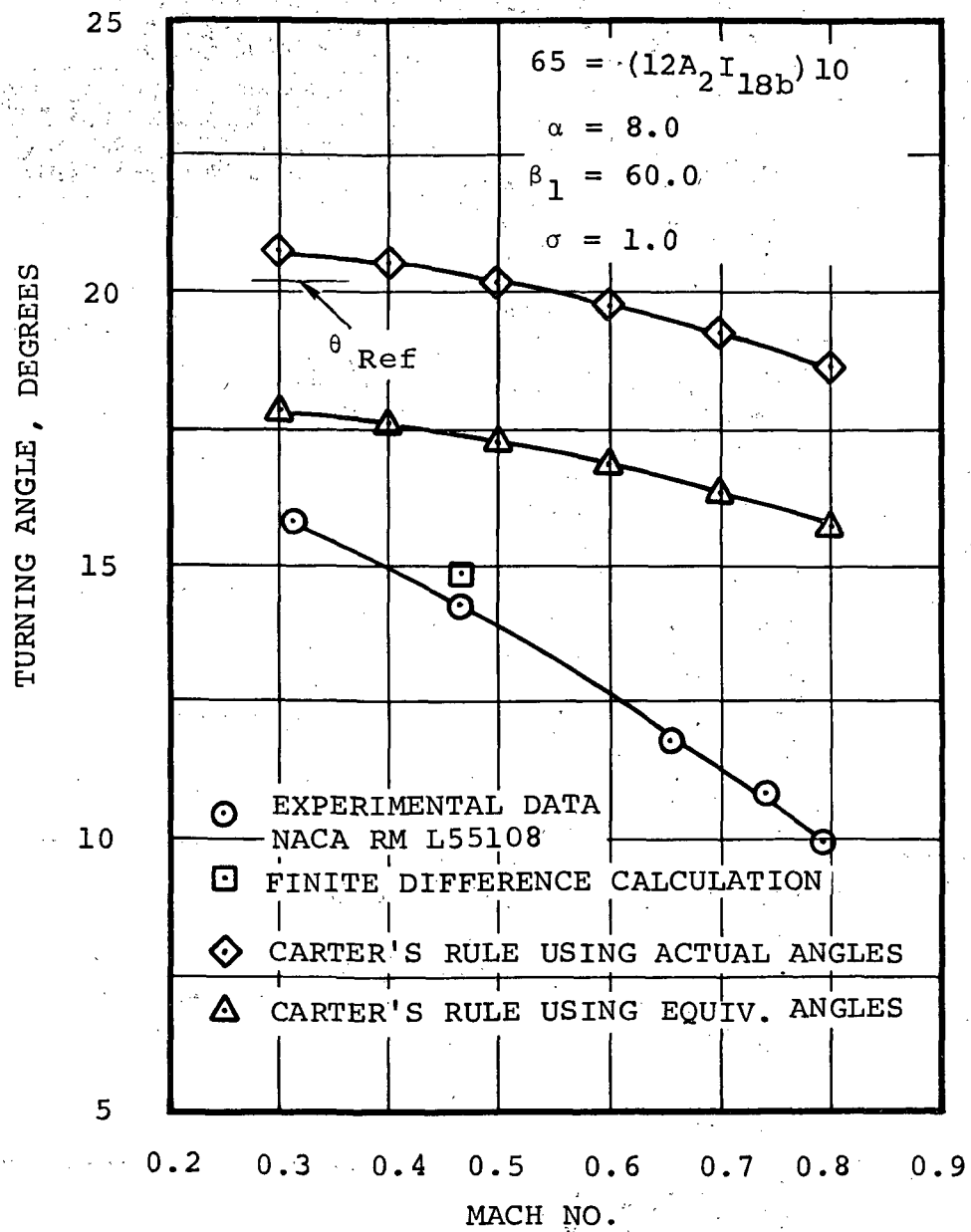


Figure 13. - Turning angle versus Mach No.

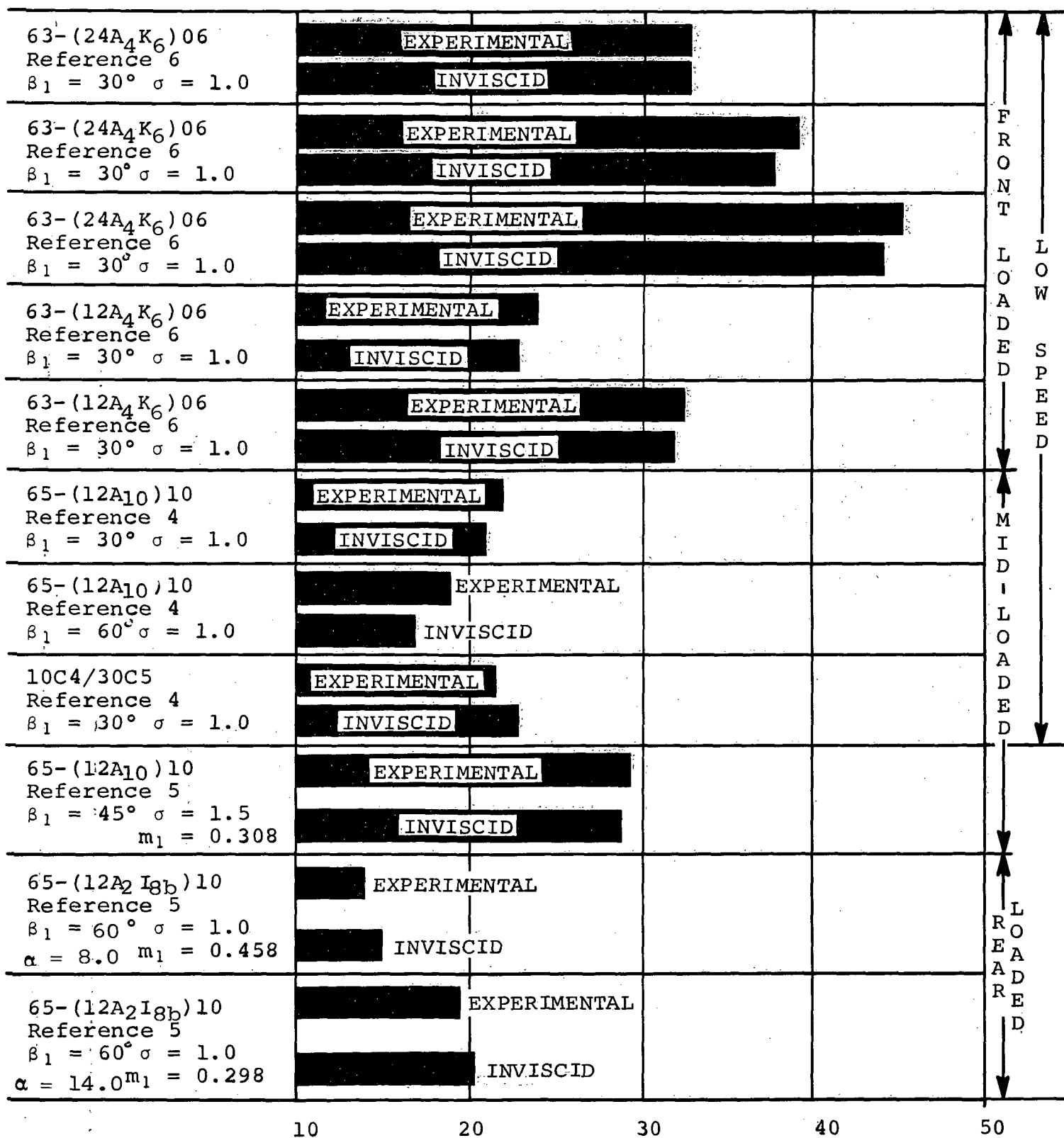


Figure 14. - Total turning θ .

APPLICATION TO THREE-DIMENSIONAL SITUATIONS

Because of the more fundamental nature of the finite-difference technique when compared to techniques used in the past, one would expect that much of the uncertainty in determining deviation angle in axial and mixed flow rotors could be eliminated. This expectation is clouded by two effects not considered by the present technique. The first is the effect of Mach number at conditions where the critical Mach number is exceeded. The finite-difference technique described herein does not provide rigorous inviscid solutions where local Mach numbers are supersonic. This restricts the direct application of this technique to the hub sections of many rotors. However, by application of this technique to lower Mach numbers for a given section and comparison with previous cascade data, the basic radius change and area change characteristics can be determined and extrapolated to high Mach numbers. There is considerable hope that the restriction in Mach number will soon be lifted resulting in a finite-difference technique of reasonable computer run times and a Mach number capability through the entire rotor design range.

The second and more serious deficiency from a long range standpoint is the effect of three-dimensional factors not taken into account by the application of successive radial equilibrium and blade-to-blade solutions. These are as follows:

- (a) Secondary flow
 - (1) Cross flow in boundary layer
 - (2) Vorticity generation in boundary layer
- (b) Blade sweep effects
- (c) Stream sheet warpage and twist
- (d) Effects of blade separation and the migration of low energy flow away from blade hub

Attempts to analytically evaluate these three-dimensional effects have met with limited success (Reference 7-10). Therefore, a decision was made to attempt to derive an empirical method for accounting for these effects.

Deviation angle data from a series of fan tests of an AiResearch experimental fan was employed in the empirical development. This data

is presented in figure 15 which includes a comparison of design and measured deviation angles as a function of exit radius for the rotor. The design conditions shown in figure 15 are really immaterial to the following argument. A postulation is made that the difference between the measured deviation angle and that calculated by the finite difference, blade-to-blade computer program represents the viscous component of the deviation. A comparison of the measured and blade-to-blade calculated deviations for the experimental fan is presented in figure 16. The difference between the measured and calculated deviation angle for each streamline is shown in figure 17. Figures 16 and 17 indicate that most of the postulated viscous effects are in the lower half of the blade with the largest influence at the rotor hub.

Assuming that this difference represents the viscous effects on deviation, consideration is given to how these effects may be applied for other rotor configurations. Several correlating parameters were investigated with the diffusion factor (D) across the blade seeming to offer the most promise. Since the diffusion factor is representative of the losses within the blade row, the deviation correction term for a particular streamline may indeed scale directly to the ratio of diffusion factors.

The proposed approach for calculating deviation angles for the conical flow compressor is then to: (1) use the finite difference, blade-to-blade program to compute the non-viscous deviation angle, (2) obtain a deviation correction term from figure 4 for the corresponding streamline, (3) adjust the deviation correction by the corresponding diffusion factor ratios, and (4) combine the non-viscous and viscous components to get total deviation angle. A sample calculation showing this procedure is presented as table I. This tabulation shows how data from the AiResearch experimental fan was employed to predict the deviation for a rotor designed for NASA by the General Electric Company. The comparison is made at the 10-percent streamline in the hub region where considerable deviation was measured. The results of the comparison indicate very good agreement between the predicted and measured deviation for G.E. Rotor 1B. Obviously this result could just be fortuitous, but time limitations and a lack of sufficiently precise experimental information in this area did not permit further investigation.

The negative portion of the deviation correction shown in figure 17 will be neglected in the design of the conical compressor. This means the deviation angle in the region between the 90- and 50-percent streamlines will come from the finite-difference calculations without correction. The reasons for omitting the correction in this region are: (1) the correction shown is small, being less than 1 degree and (2) a reasonable explanation could not be determined for applying a negative correction for viscous effects to the deviation angle prediction.

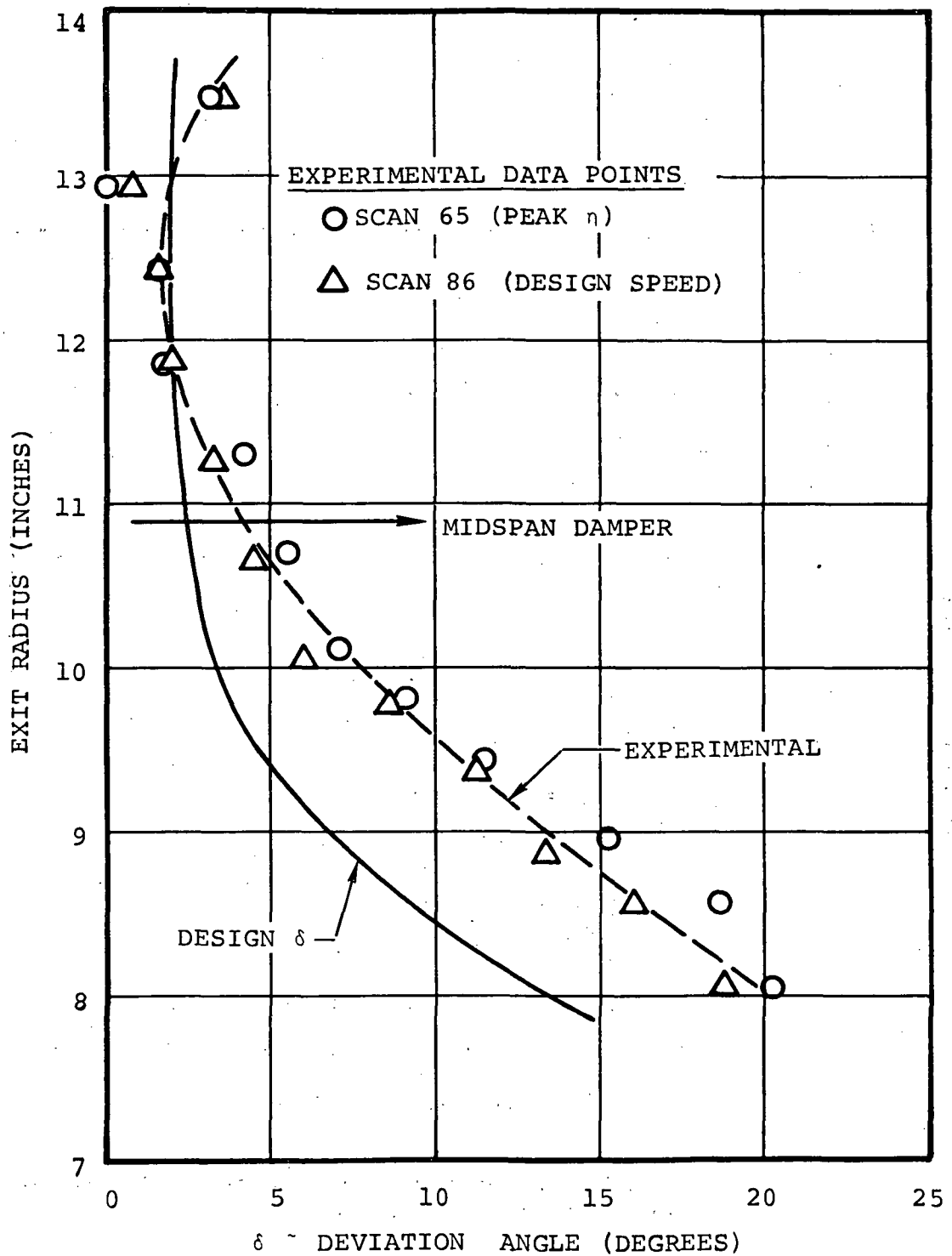


Figure 15. - AiResearch experimental fan, deviation versus blade radius.

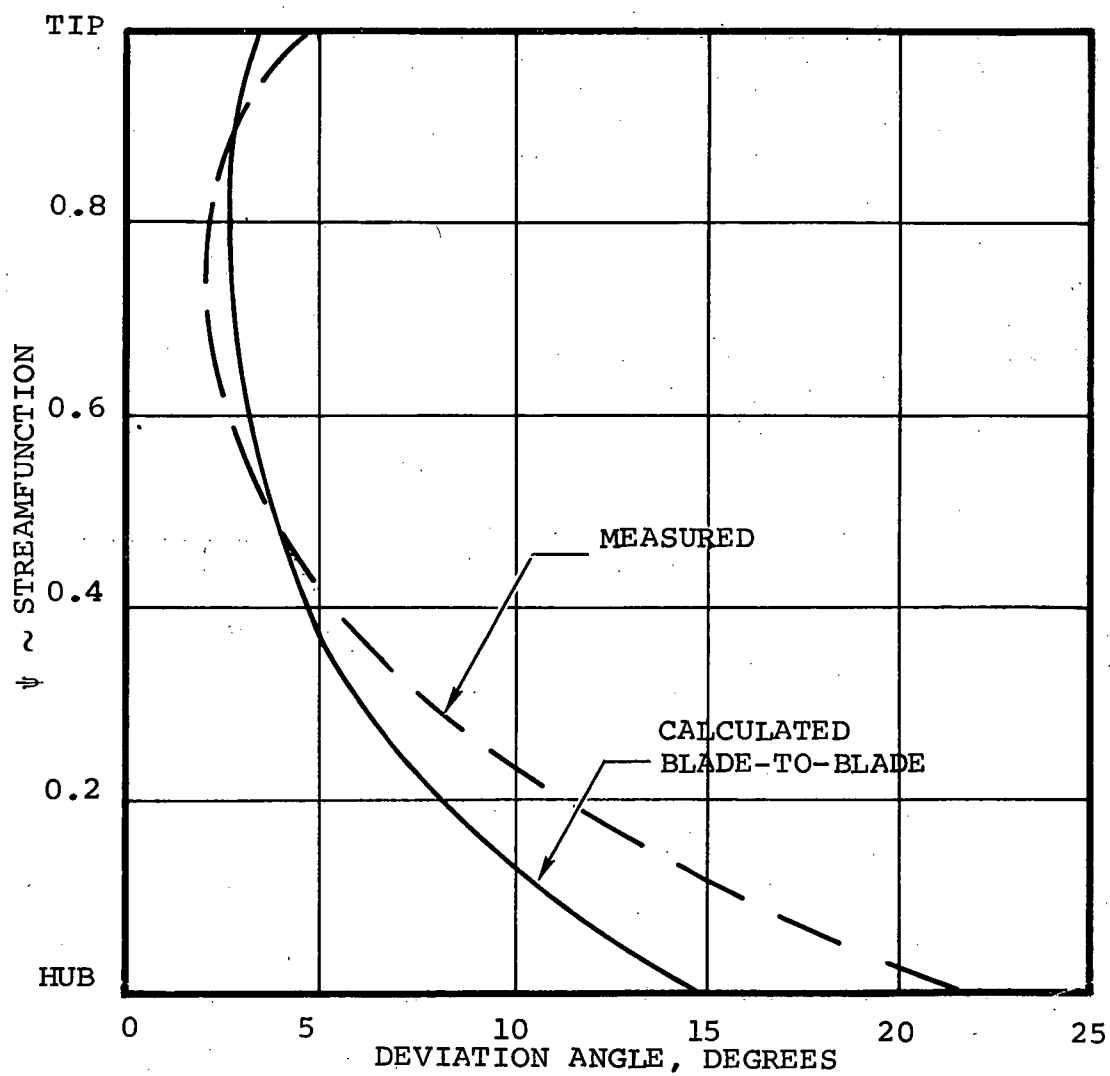


Figure 16. - AiResearch experimental fan, calculated and measured streamline deviation.

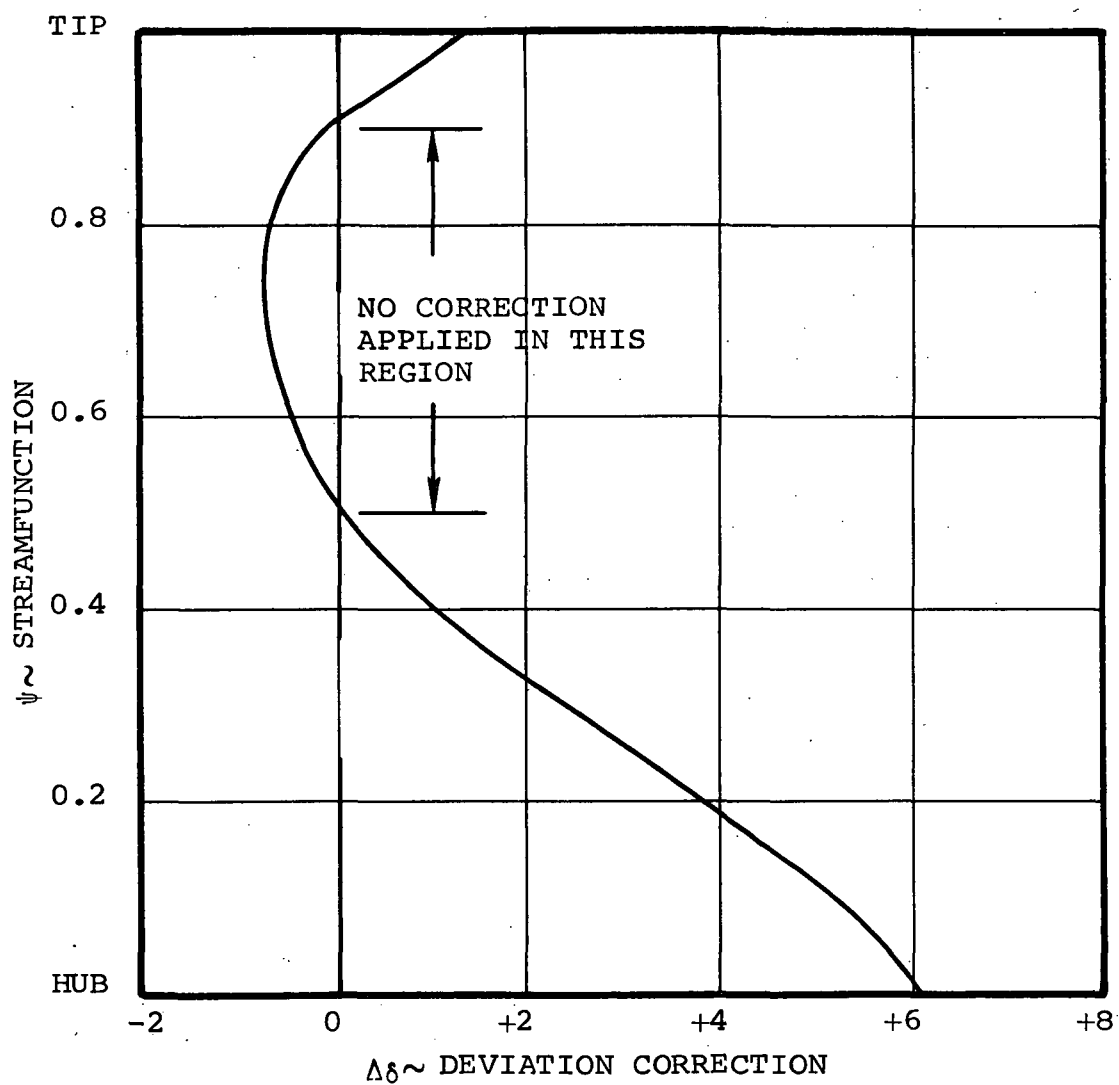


Figure 17. - AiResearch experimental fan results, deviation correction for each streamline.

TABLE I
SAMPLE CALCULATION
OF DEVIATION FOR G.E. ROTOR 1B*

10% STREAMLINE (HUB REGION)

BASIS - AIRESEARCH EXPERIMENTAL FAN RESULTS:

$$\begin{aligned}\delta \text{ (MEASURED)} &= 15.8 \\ \delta \text{ (CALCULATED)} &= 10.6 \text{ degrees (BLADE-TO-BLADE RESULTS)}\end{aligned}$$

$$\nabla\delta = 5.2 \text{ degrees}$$

$$\text{"D" FACTOR (AEF)} = 0.47$$

ROTOR 1B RESULTS:

$$\delta \text{ (CALCULATED)} = 8.2 \text{ degrees (BLADE-TO-BLADE RESULTS)}$$

$$\text{"D" FACTOR (R-1B)} = 0.49$$

DEVIATION CORRECTION FOR ROTOR 1B

$$\nabla\delta \text{ (R-1B)} = \nabla\delta \text{ (731)} \times \frac{D \text{ (R-1B)}}{D \text{ (AEF)}}$$

$$\nabla\delta = 5.2 \times \frac{0.49}{0.47} = 5.4 \text{ degrees}$$

$$\text{PREDICTED DEVIATION} = \delta \text{ (CALC)} + \nabla\delta = 13.6 \text{ degrees.}$$

$$\text{MEASURED DEVIATION} = 14.0 \text{ degrees.}$$

*Seyler, D.R. and L. H. Smith Jr. Single Stage Experimental Evaluation of High Mach Number Compressor Rotor Blading, NASA CR-54581, 1967.

In summary, the foregoing discussion indicates that the finite difference, blade-to-blade program predicts most of the effects of blade loading on the air turning in compressor cascades. In the regions where the analysis indicates that the finite-difference program was lacking, an empirical correction is recommended. The combination analytical and empirical approach should provide a reasonably precise prediction of deviation angles for the conical flow compressor.

CONCLUSION

The finite-difference inviscid technique discussed herein presents a step forward in numerical determination of deviation angles. Particularly, the effects of radius change and meridional velocity ratio on the blade geometry can be evaluated to an accuracy not previously obtainable. However, three-dimensional, secondary flow effects must be evaluated when applying the technique to three-dimensional cases. These serve to make the finite-difference technique of primary use in removing many of the uncertainties associated with Carter's Rule. This does not remove the need for added factors correlated to experimental results from existing axial compressors. However, the combined analytical-empirical approach for predicting deviation angle should instill a much higher degree of confidence in the blade angle settings than experienced through the use of sonic modification of Carter's Rule.

1. Katsanis, Theodore and William D. McNally, Fortran Program for Calculating Velocities and Streamlines on a Blade-to-Blade Stream Surface of a Tandem Blade Turbomachine, NASA, TND-5044, March 1969.
2. Milne-Thomson, L.M., Theoretical Hydrodynamics, The MacMillan Company, New York, 1960.
3. Seyler, D.R. and L.H. Smith Jr., Single Stage Experimental Evaluation of High Mach Number Compressor Rotor Blading, NASA CR-54581, 1967.
4. Felix, A. Richard and James C. Emery, A Comparison of Typical National Gas Turbine Establishment and NACA Axial-Flow Compressor Blade Sections in Cascade at Low Speed, NACA RM L53B26A, 1953.
5. Dunavant, James C., James C. Emery, Howard C. Walch, and Willard R. Westphal, High Speed Cascade Tests of the NACA 6-(RA10)10 and NACA 65-(12A2K80)10 Compressor Blade Sections, NACA RML55I08, 1955.
6. Emery, James C., Low-Speed Cascade Investigation of Loaded Leading Edge Compressor Blades, RM L55J05, 1956.
7. Lieblein, Seymour, and Richard H. Ackley, Secondary Flows in Annular Cascade and Effects on Flow in Inlet Guide Vanes, NACA RM L251627, 1951.
8. Hauser, Arthur G., and Howard Z. Herzig, Cross Flows in Laminar Incompressible Boundary Layers, NACA TN3651, 1956.
9. Lakshminarayana, B., Methods of Predicting the Tip Clearance Effects in Axial Flow Turbomachinery, ASME Paper 69-WA/FE-26, 1969.
10. Wheeler, A.J., and J.P. Johnston, Three-Dimensional Turbulent Boundary Layers - An Assessment of Prediction Methods, Stanford University, Thermoscience Division, Report MD-30, 1971.

APPENDIX A

NOTATION

b	Axisymmetric streamtube thickness
c	Chord
C_p	Specific heat at constant pressure
i	Incidence angle
m	Meridional distance
\dot{m}	Mass flow rate
m_c	Geometry constant in Carter's rule
N_m	Number of mesh points leading edge to trailing edge
P_p	Pressure surface static pressure
P_s	Suction surface static pressure
r	Radius
T'	Total temperature
U	Wheel speed, free stream velocity
u	Boundary layer velocity
V	Velocity in absolute frame
W	Relative velocity

APPENDIX A

NOTATION (Contd)

α	Streamline slope
β	Relative flow angle
δ	Deviation angle
δ_{bl}	Boundary layer thickness
ω	Rotor rotational frequency
ω_v	Vorticity
ω_s	Streamwise component of vorticity
ψ	Stream function
σ	Solidity
θ	Total turning angle
θ_r	Tangential coordinate in a cylindrical coordinate system
ρ	Density
Γ	Circulation

Subscripts

U	Tangential direction
1	Inlet
2	Outlet
m	Meridional

APPENDIX B

DESCRIPTION OF BLADE SECTIONS FOR ROTORS AND STATORS (Page i)

(Rotor 1A, 8 pages)
(Rotor 1B, 8 pages)
(Stator 1A, 8 pages)
(Stator 1B, 9 pages)

APPENDIX B

COMPRESSOR BLADE STACKING PROGRAM

The basic calculation performed by the Blade Stacking Program is to take the specification of airfoil shapes along a set of axisymmetric stream surfaces, interpolate the input data to cylindrical surfaces, and "stack" the blade using the cylindrical sections. The type of airfoil shape can be 65-series, multiple or double circular arc or arbitrary. Axisymmetric stream surfaces can be cylindrical, conical, or arbitrary.

Required input specification parameters for airfoil sections are mean camber line direction and tangential thickness. Each input axisymmetric stream surface must be specified by axial and radial location and slope.

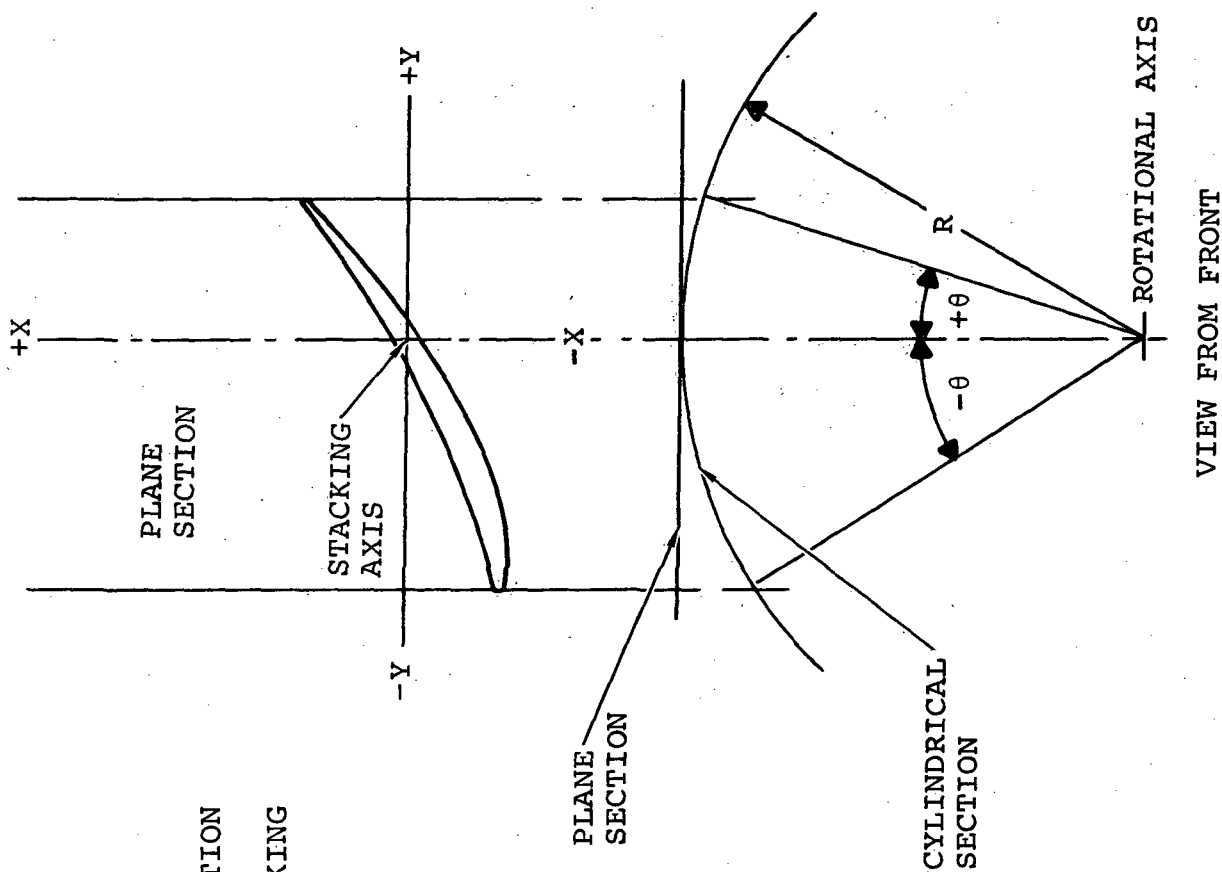
The blade stacking axis must be defined on two, mutually perpendicular surfaces, the r - z plane and the r - θ plane. Normal blade stacking procedure has been to calculate the center of gravity for each cylindrical stacking section and align each section center of gravity along a straight, radial line. However, this program can stack the blade on an arbitrarily specified axis in both planes.

For purposes of this design, the axial location of the program stacking axis for rotor 1A is taken at the leading edge center location. All other sections have the stack point axial location at about the blade section center of gravity (C.G.). Tangential location of the stack point for all sections is near the section C.G. location. (Refer to center of gravity coordinates, (X, S) , defined on each blade section printout).

The output from the stacking routine gives the parameters of cylindrical blade angle, tangential (or normal) thickness and the blade lean angle for input to the through-the-blade flow field calculation. It also provides the blade geometry along any axisymmetric stream surface for input to the blade-to-blade analysis program. Plane sections are also generated for blade manufacturing purposes.

COORDINATE TERMS

- X - AXIAL DISTANCE FROM STACKING
AXIS ON CYLINDRICAL OR PLANE SECTION
- S - $R\theta$ TANGENTIAL DISTANCE FROM STACKING
AXIS ON CYLINDRICAL SECTION
- Y - $R \sin \theta$, TANGENTIAL DISTANCE FROM
STACKING AXIS ON PLANE SECTION



DEFINITION OF BLADE SECTION COORDINATE PARAMETERS

..... R A D I U S
..... 1.00000
.....
..... NUMBER OF BLADES

PROPERTIES OF CYLINDRICAL PROFILE

LE THICKNESS=	.00966	SPACING =	.314159
TE THICKNESS=	.022859	AXIAL CHORD=	.563783
TRUE CHORD =	.604859	SOLIDITY =	1.794577

DIRECTION OF ROTOR ROTATION = CLOCKWISE (VIEWED FROM THE TRAILING EDGE)

CALCULATED COORDINATES

[illegible]

ADVANCED TWO-STAGE COMPRESSOR ** CONICAL FLOW ROTOR NO. 1

**** R A D I U S *****
 . 1.200000 .

 NUMBER OF BLADES
 20

CENTER OF GRAVITY
 CYLINDRICAL PROFILE
 X = .251015
 S = .000541
 LE THICKNESS = .008613
 TE THICKNESS = .017330
 TRUE CHORD = .631986
 SPACING = .376991
 AXIAL CHORD = .539732
 SOLIDITY = 1.431693

DIRECTION OF ROTOR ROTATION = CLOCKWISE (VIEWED FROM THE TRAILING EDGE)

*** C A L C U L A T E O C O O R D I N A T E S ***

CYLINDRICAL COORDINATES			PLANE COORDINATES		
NO.	X	Y	NO.	X	Y
1	.521341	.018025	26	.052516	.017916
2	.494166	.040830	27	.064235	.040659
3	.467948	.068940	28	.069880	.064046
4	.443300	.070770	29	.071705	.088125
5	.419868	.069826	30	.070475	.112969
6	.397179	.065956	31	.066660	.138317
7	.374923	.059978	32	.060504	.164193
8	.352621	.052028	33	.052371	.190518
9	.329952	.042102	34	.042287	.217208
10	.306332	.030666	35	.030741	.244449
11	.281745	.017400	36	.017416	.272295
12	.256451	.001149	37	.001149	.301183
13	.230548	-.018132	38	-.018132	.330965
14	.204285	-.040579	39	-.040617	.361135
15	.177519	-.066036	40	-.066214	.391418
16	.150108	-.096337	41	-.094825	.421366
17	.122362	-.125350	42	-.126361	.450668
18	.093770	-.158680	43	-.160422	.478805
19	.064523	-.194073	44	-.196690	.505433
20	.034703	-.231205	45	-.234699	.531045
21	.004343	-.268642	46	-.273807	.534653
22	-.001171	-.271884	47	-.276056	.533215
23	-.002667	-.271226	48	-.275394	.527706
24	-.004898	-.268054	49	-.272206	.521236
25	-.004241	-.264226	50	-.268358	.000046
L.E.R.C. 51			L.E.R.C. 51		
.526382			.526147		
.059008			T.E.R.C.		
			.059792		

ADVANCED TWO-STAGE COMPRESSOR ♦♦ CONICAL FLOW ROTOR NO. 1

```

..... R A D I U S .....
..... 1.60000 .....
.....
..... NUMBER OF BLADES

```

CENTER OF GRAVITY
CYLINDRICAL PROFILE

X =	.234473	LE THICKNESS =	.006578	AXIAL CHORD =	.494174
S =	.000337	TE THICKNESS =	.011296	SOLIDITY =	.983128
		TRUE CHORD =	.788951		

DIRECTION OF ROTOR ROTATION = CLOCKWISE (VIEWED FROM THE TRAILING EDGE)

*** CALCULATED COORDINATES ***

[illegible]

ADVANCED TWO-STAGE COMPRESSOR •• CONICAL FLOW ROTOR NO. 1

..... R A D I U S
..... 2.00000
.....
..... NUMBER OF BLADES

CENTER OF GRAVITY

CYLINDRICAL PROFILE

X = .235465
S = .000454

PROPERTIES OF CYLINDRICAL PROFILE

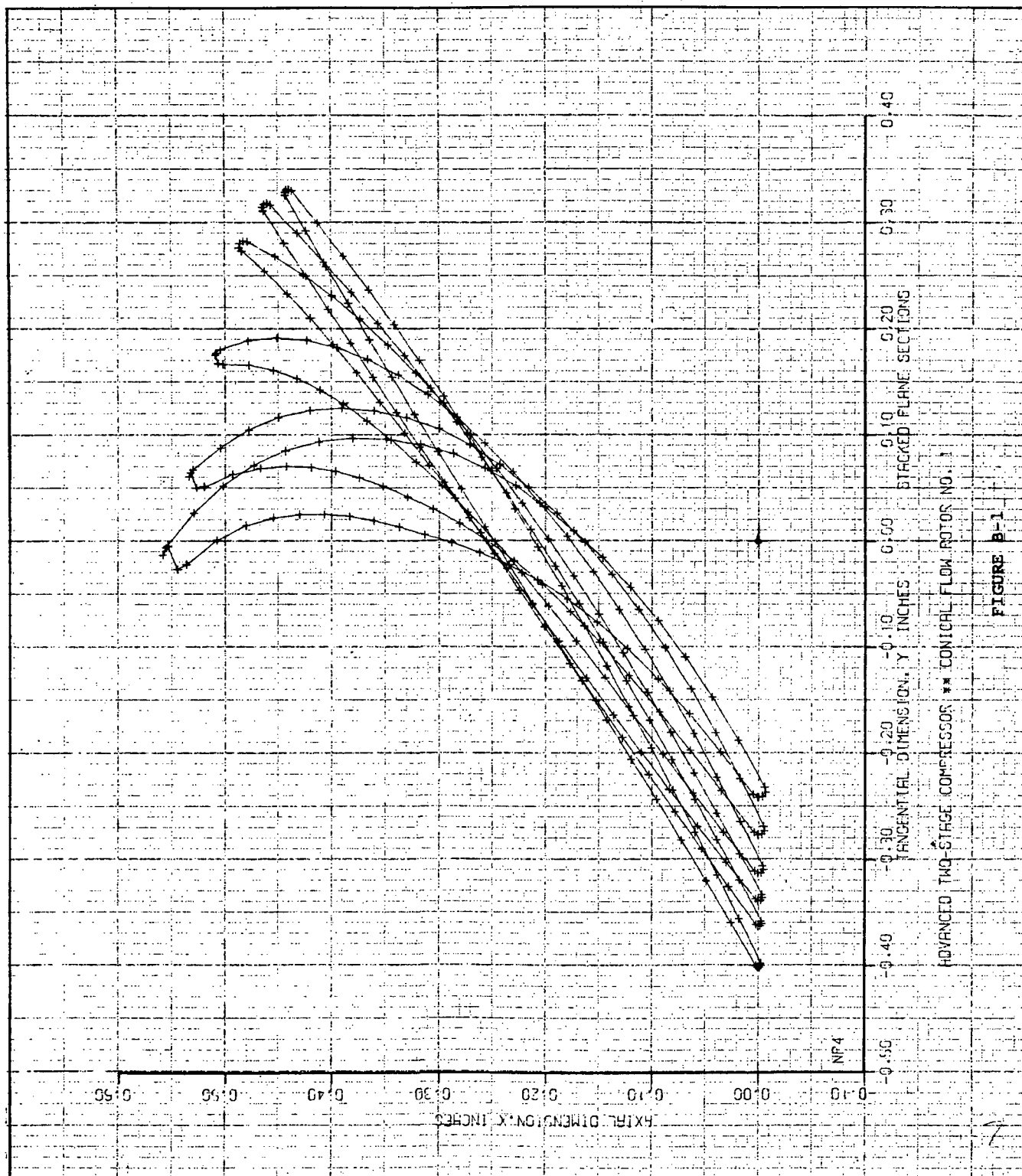
LE THICKNESS=	.004792	SPACING	=	.62A319
TE THICKNESS=	.010170	AXIAL CHORD=		.451148
		SOLIDITY	=	.718024

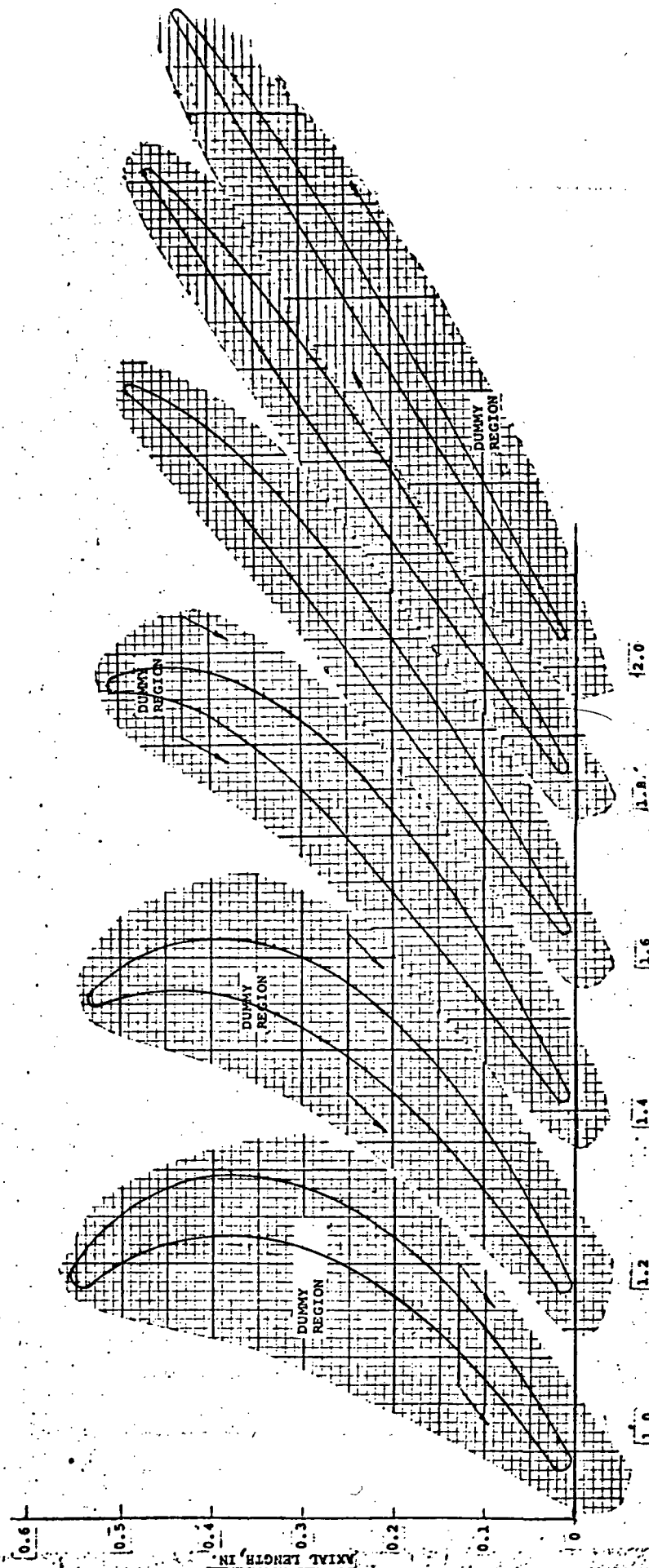
TRUE CHORD = .856056

DIRECTION OF ROTOR ROTATION = CLOCKWISE (VIEWED FROM THE TRAILING EDGE)

*****CALCULATED COORDINATES*****

[illegible]





SECTION RADIUS, IN.
 CYLINDRICAL SECTIONS FOR ROTOR 1A
 FIGURE B-2

NASA10/1 ROTOR1B

```

... R A D I U S ....
.      2.25900      .
.....
NUMBER OF BLADES

```

20

CENTER OF GRAVITY CYLINDRICAL PROFILE

X ■ .008795
S ■ .000750

PROPERTIES OF CYLINDRICAL PROFILE

LE THICKNESS=	.005647	SPACING =	.709686
TE THICKNESS=	.013401	AXIAL CHORD=	.319077
TRUE CHORD =	.506618	SOLIDITY =	.449603

TRUE CHORD = .506618
DIRECTION OF ROTOR ROTATION = CLOCKWISE (VIEWED FROM THE TRAILING EDGE)

DIRECTION OF ROTATION
 CYCLOTHICAL COORDINATES
 *** CALCULATED COORDINATES ***
 PLANE COORDINATES

[illegible]

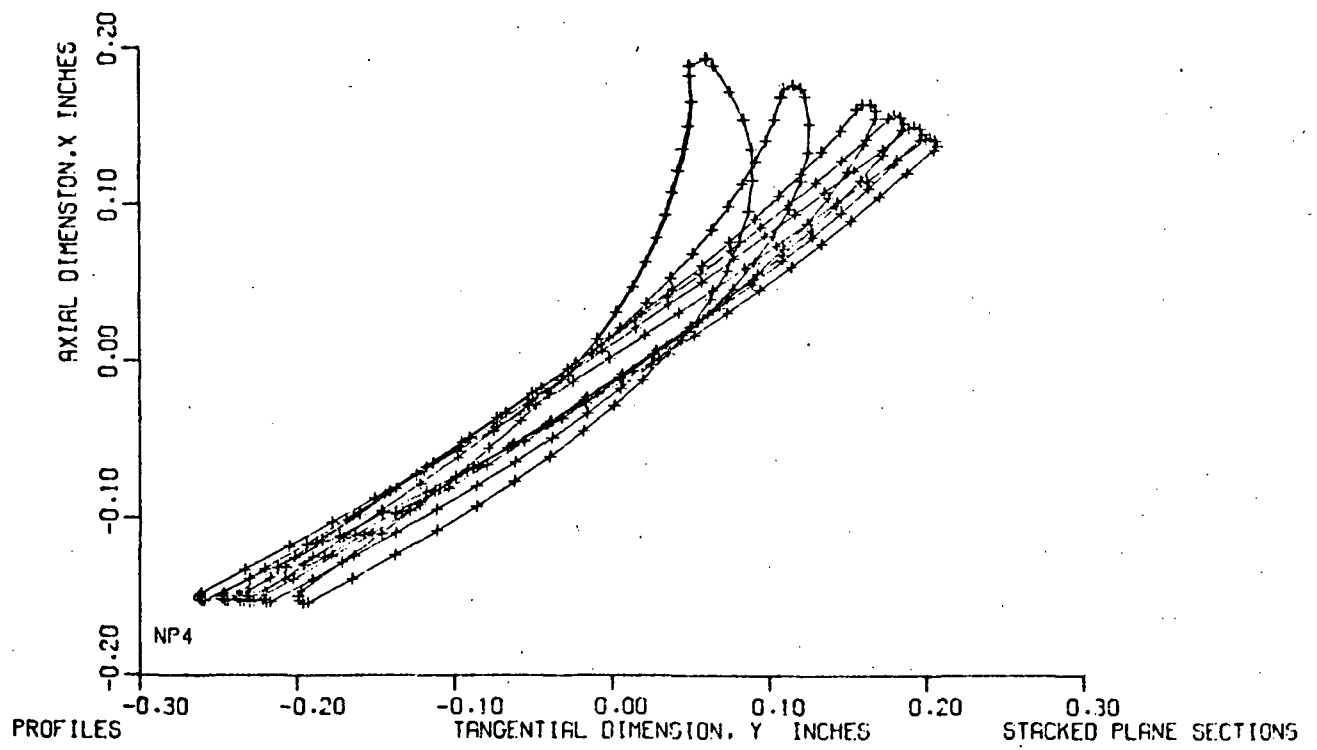
... R A D I U S ...
... 2.442800 ...
... NUMBER OF BLADES

PROPERTIES OF CYLINDRICAL PROFILE	
LE THICKNESS=	.004165
TE THICKNESS=	.008456
TRUE CHORD =	.549258
SPACING =	.767428
AXIAL CHORD=	.296716
SOLIDITY =	.386637

TRUE CHORD = .549258
DIRECTION OF ROTOR ROTATION = CLOCKWISE (VIEWED FROM THE TRAILING EDGE)
*** CALCULATED COORDINATES ***

PLANE COORDINATES

[illegible]



NASA10/1 ROTOR 1B

FIGURE B-3

0.5

0.4

0.3

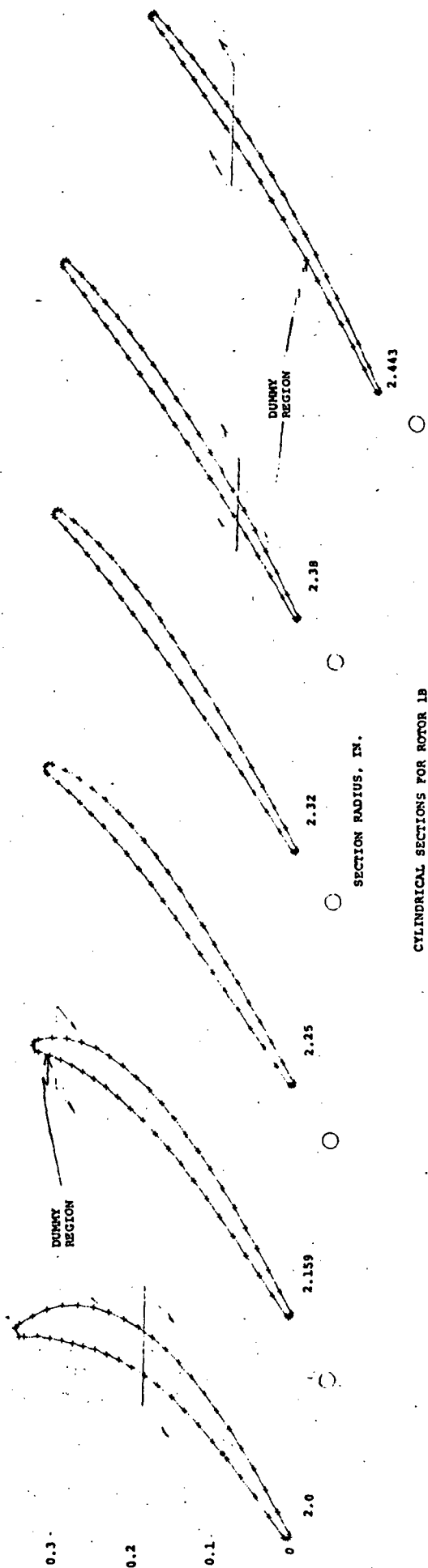
0.2

0.1

0

AXIAL LENGTH, IN.

91



CYLINDRICAL SECTIONS FOR ROTOR 1B

FIGURE B-4

..... R A D I U S
..... 2.60000
..... NUMBER OF VANES

5-017A07
5-000074

LE THICKNESS=	.007609	SPACING =	.30A232
TE THICKNESS=	.009232	AXIAL CHORD=	.3A6910
		SOLIDITY =	1.125A84

*** CALCULATED COORDINATES ***
ORIGINAL COORDINATES PLANE COORDINATES

SONIX

NO.

183

..... R A D I U S
..... 3.00000
.....
..... NUMBER OF VANES

NUMBER OF VANES

PROPERTIES OF CYLINDRICAL PROFILE	
LE THICKNESS=	.006729
TE THICKNESS=	.009942
TRUE CHORD =	.508957
SPACING =	.355652
AXIAL CHORD=	.306096
SOLIDITY =	.860661

DIRECTION OF ROTOR ROTATION = COUNTER CLOCKWISE (VIEWED FROM THE TRAILING EDGE)

DECLASSIFIED COORDINATES

CYLINDRICAL COORDINATES

NO.	X
1	.125428
2	.011539
3	.097666
4	.083777
5	.069871
6	.055927
7	.041919
8	.027822
9	.013622
10	-.000867
11	-.015436
12	-.030015
13	-.044606
14	-.059517
15	-.074755
16	-.090283
17	-.106018
18	-.122099
19	-.138439
20	-.154997
21	-.171767
22	-.173621
23	-.176358
24	-.179374
25	-.179490

X	-.165471	.191168	S
-.152421	.155430		
-.138794	.122797		
-.125087	.092823		
-.111074	.065134		
-.096773	.039406		
-.082223	.015A62		
-.057347	-.006148		
-.052149	-.026543		
-.036941	-.045655		
-.021722	-.063573		
-.006422	-.080313		
.009165	-.095721		
.024856	-.109977		
.040637	-.123129		
.056480	-.135239		
.072362	-.146371		
.098261	-.156594		
.104176	-.165953		
.120076	-.174541		
.123923	-.175206		
.126942	-.173027		
.127606	-.169280		
.125428	-.166162		
-.175128	.231478		
15E.			
15E.R.C.			
.122752	-.170352		

NO.
1
2
3
4
5
6
7
8
9
10
11
12
13
14
15
16
17
18
19
20
21
22
23
24
25

x

PLANE COORDINATES

NO.	X
26	-.165476
27	-.152265
28	-.138824
29	-.125113
30	-.111091
31	-.096781
32	-.082222
33	-.067347
34	-.052155
35	-.036959
36	-.021761
37	-.006492
38	.009054
39	.024703
40	.040432
41	.056217
42	.072037
43	.087871
44	.103719
45	.119550
46	.135295
47	.151044
48	.166798
49	.182556
50	-.175086
	T.E.
51	.122261

Y
 .192025
 .155883
 .123023
 .092925
 .065223
 .039616
 .015862
 -.006148
 -.026543
 -.045661
 -.063594
 -.080364
 -.095418
 -.110139
 -.123376
 -.135586
 -.146830
 -.157171
 -.166646
 -.175339
 -.179017
 -.173823
 -.170082
 -.166802
 .233443
 -.171115

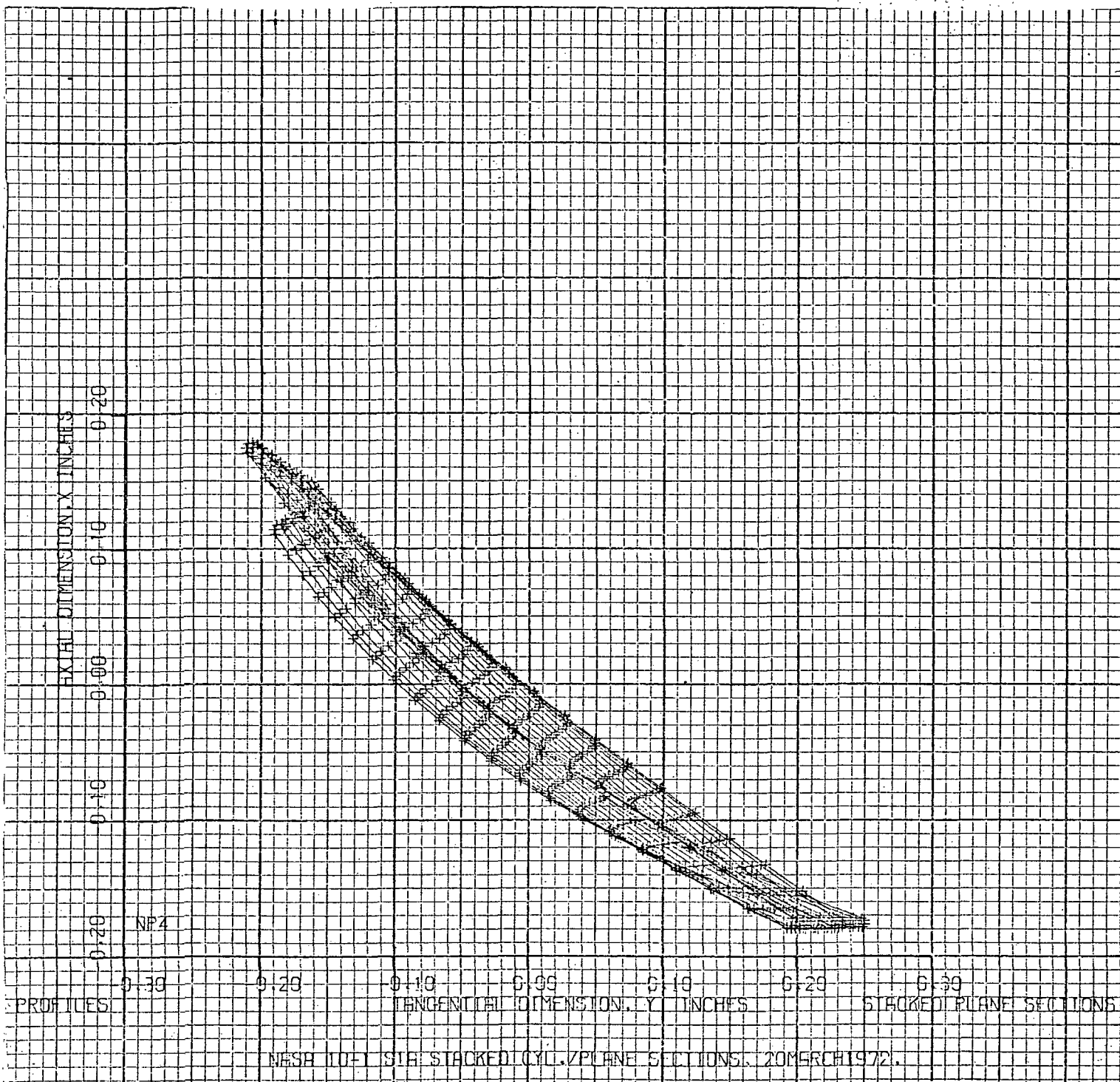


Figure B5.

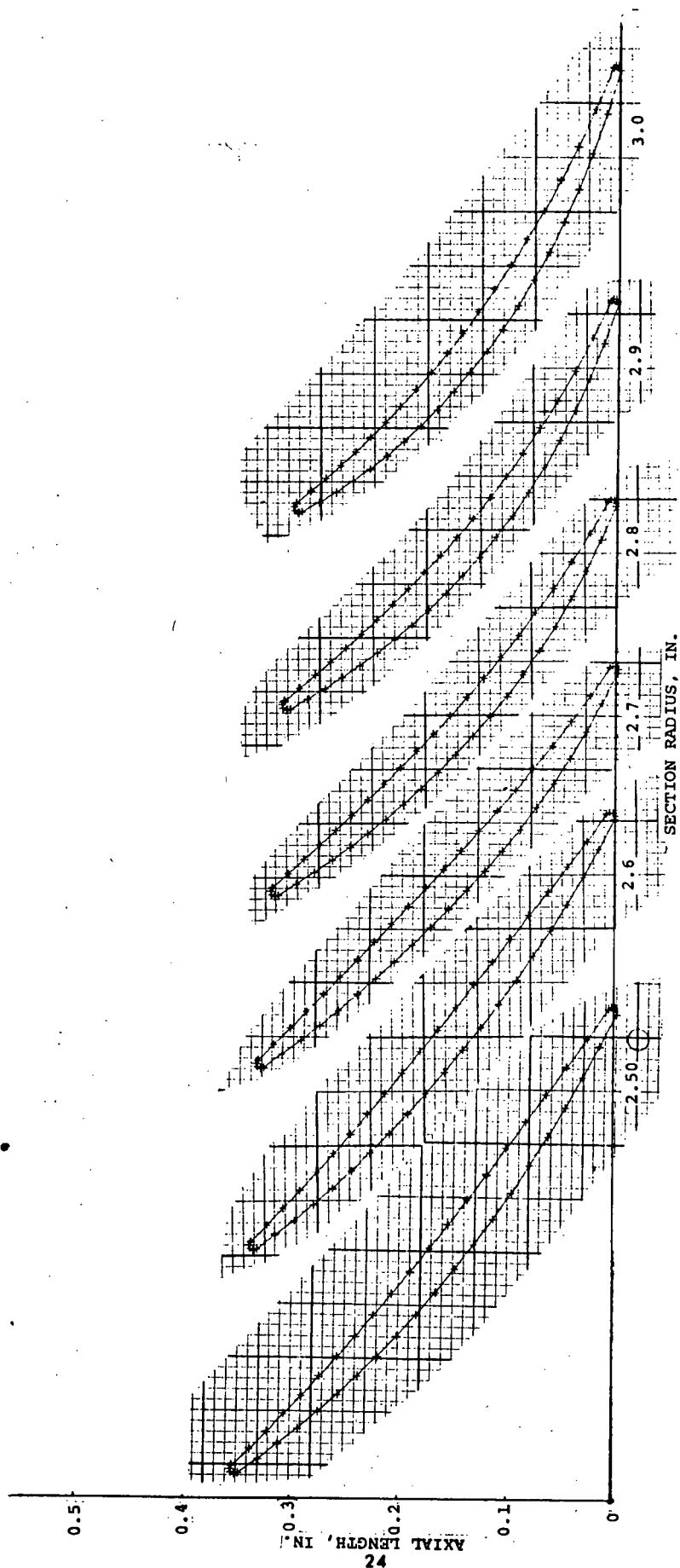


Figure B-6. Cylindrical Section for Stator 1A

NASA 10-1 S18 STACKED CYLINDRICAL/PLANE SECTIONS. 21 MARCH 1972.

..... R A D I U S
..... 2.95400
..... NUMBER OF VANES

CENTER OF GRAVITY
CYLINDRICAL PROFILE

2 x 5

PROPERTIES OF CYLINDRICAL PROFILE

LE THICKNESS=	.006343	SPACING =	.350199
TE THICKNESS=	.009988	AXIAL CHORD=	.699655
TRUE CHORD =	.530952	SOLIDITY =	1.426776

NASA 10-1 S18 STACKED CYLINDRICAL/PLANE SECTIONS. 21MARCH1972.

.... R A D I U S
 3.150000

 NUMBER OF VANES

53

CENTER OF GRAVITY CYLINDRICAL PROFILE

X = .00052
 S = -.000016

PROPERTIES OF CYLINDRICAL PROFILE

LE THICKNESS = .006406
 TE THICKNESS = .010007
 TRUE CHORD = .528030
 SPACING = .373435
 AXIAL CHORD = .499691
 SOLIDITY = 1.338095

DIRECTION OF ROTOR ROTATION = COUNTER CLOCKWISE (VIEWED FROM THE TRAILING EDGE)
 *** C A L C U L A T E D C O O R D I N A T E S ***

CYLINDRICAL COORDINATES

NO.	X
1	.254766
2	.230402
3	.206192
4	.182115
5	.158144
6	.134269
7	.110454
8	.086680
9	.062921
10	.039079
11	.015193
12	-.008690
13	-.032572
14	-.056581
15	-.080826
16	-.105271
17	-.129948
18	-.154905
19	-.180186
20	-.205814
21	-.231821
22	-.258699
23	-.284458
24	-.309693
25	-.334179

NO.	S
26	-.043567
27	-.041960
28	-.039775
29	-.037012
30	-.033664
31	-.029718
32	-.025164
33	-.019940
34	-.014140
35	-.007871
36	-.000930
37	.007221
38	.016331
39	.026271
40	.036949
41	.048771
42	.061737
43	.076011
44	.091743
45	.109140
46	.128434
47	.129669
48	.128154
49	.124778
50	.121517

L.E.R.C.

.255000

-.048565

PLANE COORDINATES

NO.	X	Y
26	-.043554	-.215186
27	-.041950	-.191814
28	-.039767	-.168095
29	-.037006	-.144052
30	-.033660	-.119729
31	-.029716	-.095174
32	-.025163	-.070419
33	-.019980	-.045428
34	-.014140	-.020310
35	-.007871	.004807
36	-.000830	.029922
37	.007221	.055040
38	.016331	.090321
39	.026269	.105547
40	.036985	.130733
41	.048764	.155854
42	.061724	.180886
43	.075990	.205809
44	.091711	.230599
45	.109092	.255234
46	.128362	.258699
47	.129595	.259998
48	.128082	.258369
49	.124710	.254766
50	.121453	-.235000

L.E.R.C.

.255000

-.048549

NASA 10-1 S18 STACKED CYLINDRICAL/PLANE SECTIONS. 21MARCH1972.

```
..... R A D I U S .....  
..... 3.25000 .....  
.....  
..... NUMBER OF VANES .....
```

35

CENTER OF GRAVITY CYLINDRICAL PROFILE

X = .000321
S = -.000010

PROPERTIES OF CYLINDRICAL PROFILE

LE THICKNESS=	.006414	SPACING =	.385290
TE THICKNESS=	.010010	AXIAL CHORD=	.499697
TRUE CHORD =	.526554	SOLIDITY =	1.296939

*** CALCULATED COORDINATES ***
DIRECTION OF ROTOR ROTATION = COUNTER CLOCKWISE (VIEWED FROM THE TRAILING EDGE)

***** CALIFORNIA COORDINATES *****

[illegible]

..... R A D I U S
..... 3.35000
..... NUMBER OF VANES

PROPERTIES OF CYLINDRICAL PROFILE

LE THICKNESS=	.00648	SPACING	= .397145
TE THICKNESS=	.010004	AXIAL CHORD=	.499698
TRUE CHORD =	.525631	SOLIDITY	= 1.258201

DIRECTION OF ROTATION = COUNTER CLOCKWISE (VIEWED FROM THE TRAILING EDGE)
 TRUE CHORD = .52833
 **** CALCULATED COORDINATES ***

[illegible]

NASA 10-1 S18 STACKED CYLINDRICAL/PLANE SECTIONS. 21MARCH1972.

..... R A D I U S
..... 3.45000
.....

CENTER OF GRAVITY CYLINDRICAL PROFILE

X	=	.000134
S	=	.000002

PROPERTIES OF CYLINDRICAL PROFILE

LE THICKNESS=	.006440	SPACING =	.409000
TE THICKNESS=	.009994	AXIAL CHORD=	.499690
TRUE CHORD =	.525331	SOLINITY =	1.221736

1. DIRECTION OF ROTOR ROTATION - COUNTER CLOCKWISE (VIEWED FROM THE TRAILING EDGE)

***** COALITION COORDINATES *****

[illegible]

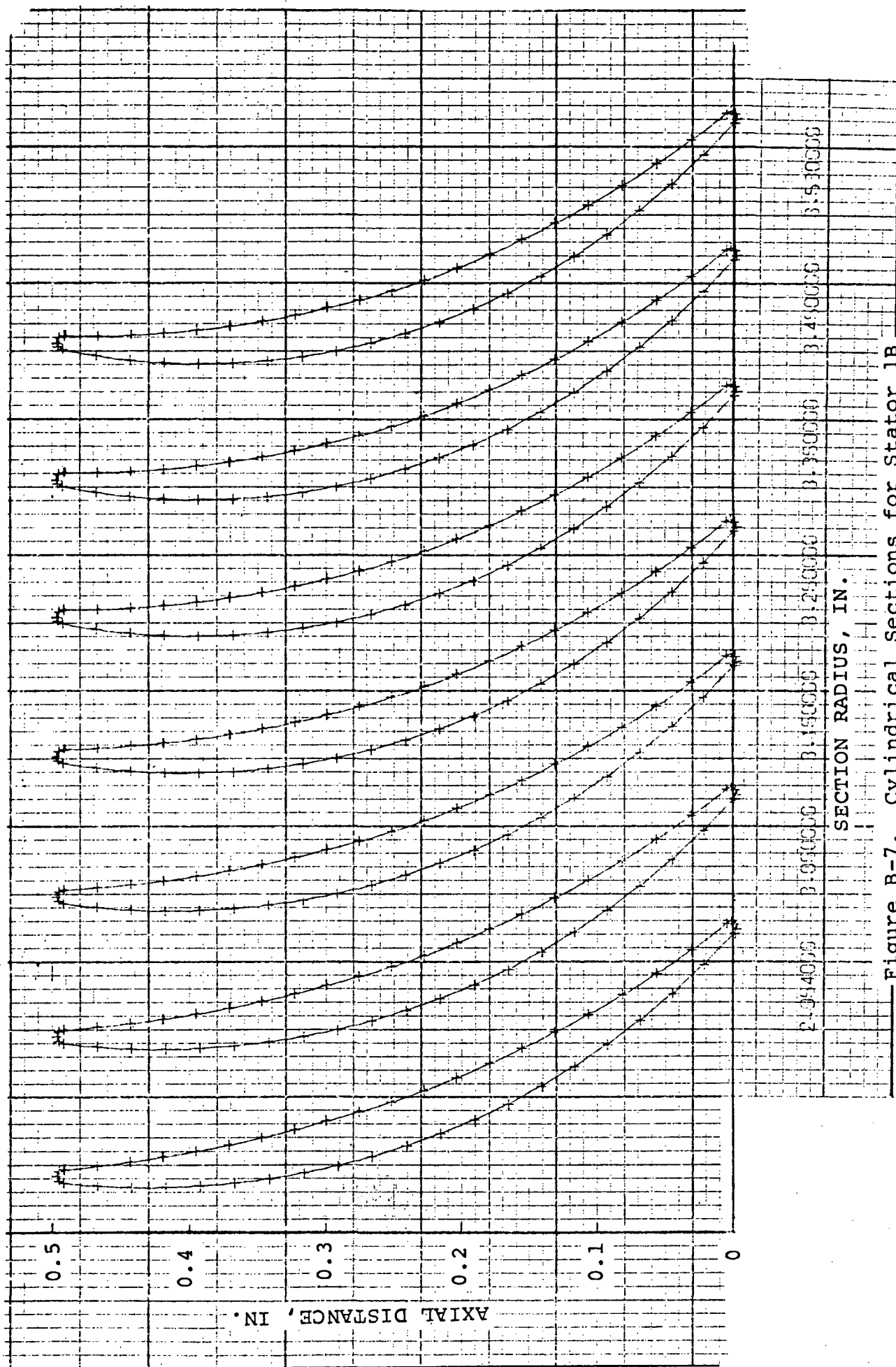
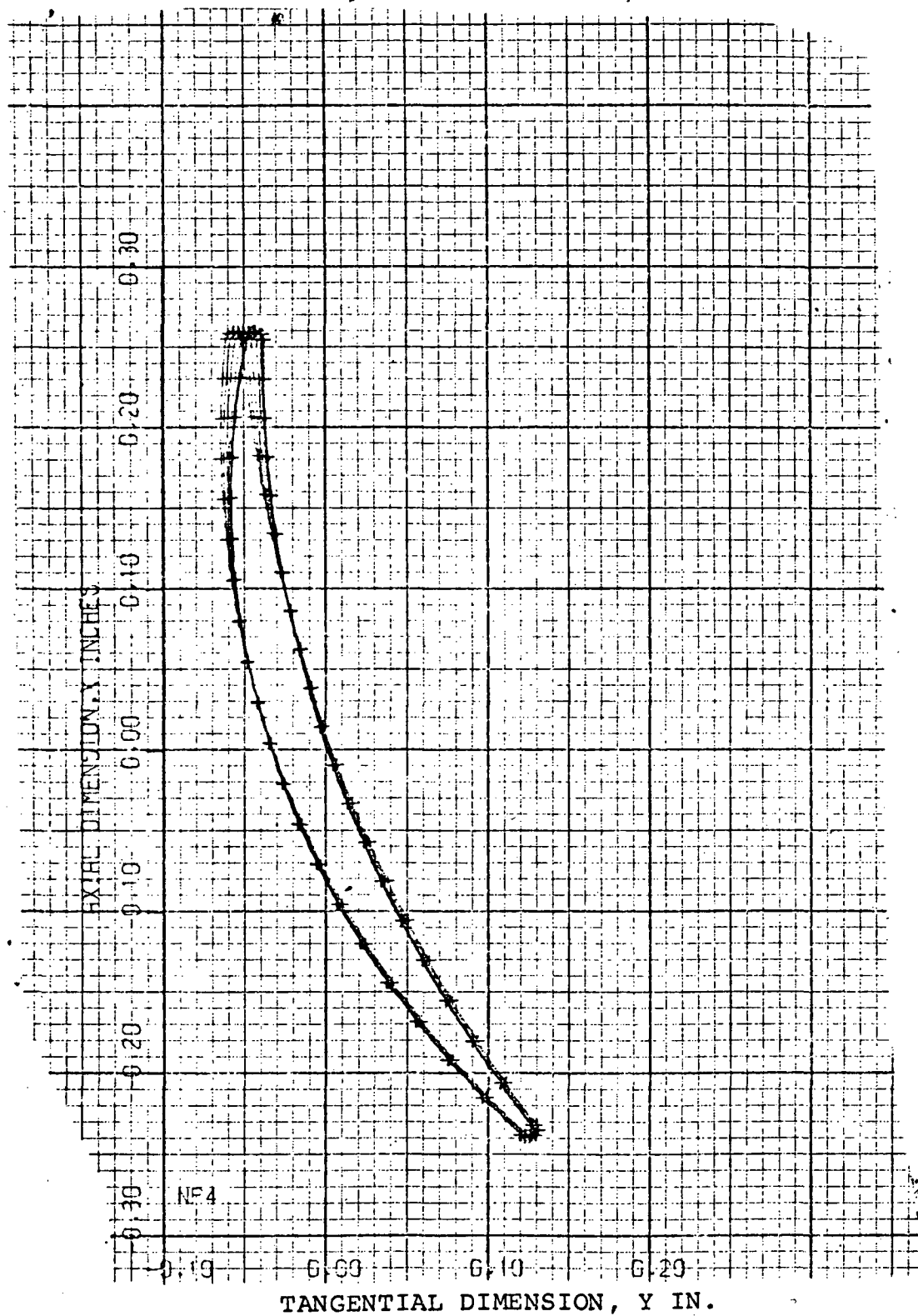


Figure B-7. Cylindrical Sections for Stator 1B



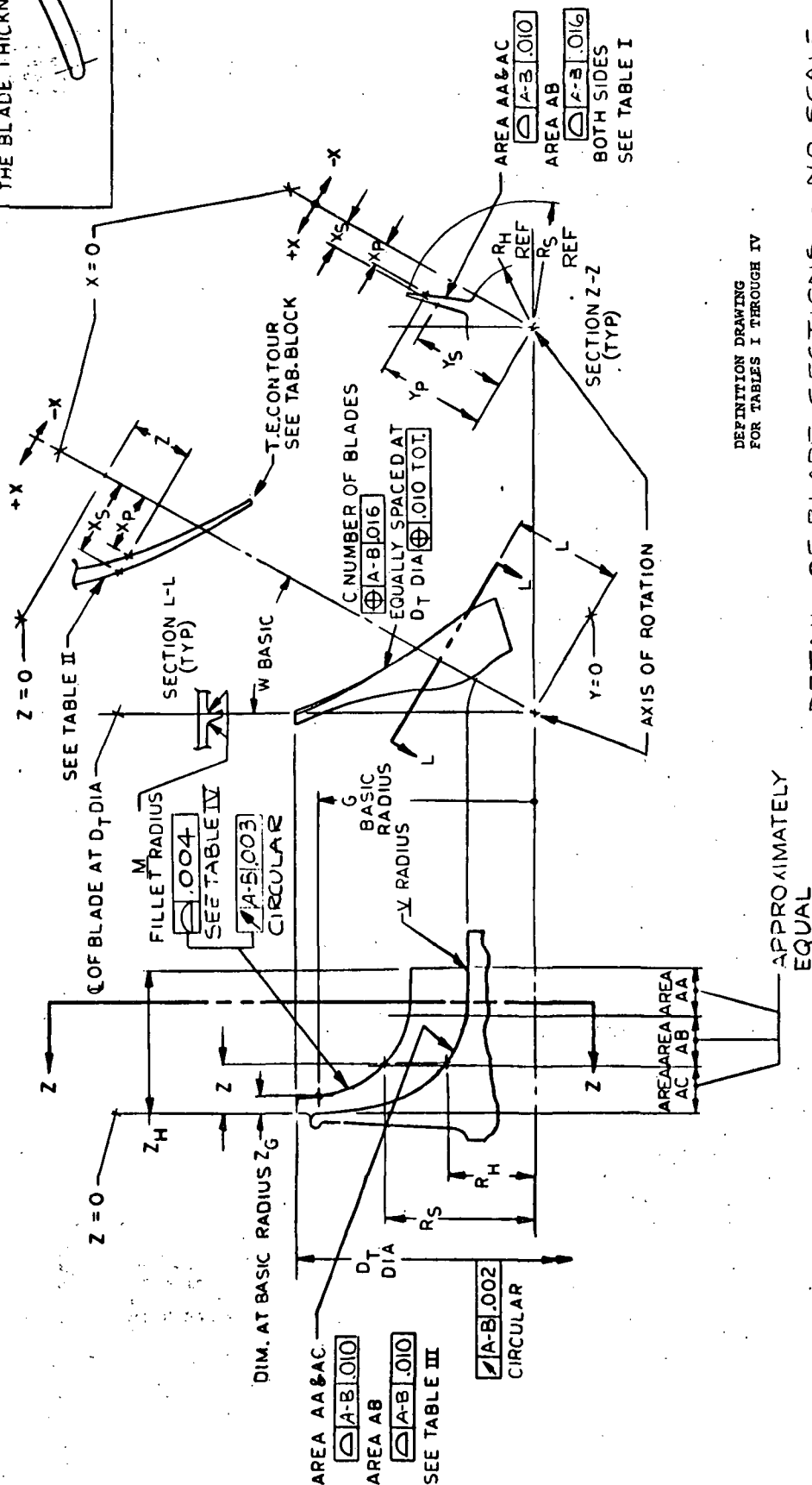
APPENDIX C

TURBINE BLADE SECTIONS

(9 pages)

D _T	G	Z _G		Z _H	M	W	C	V
6.138	2.851	0.297-0.300		2.095-2.105	0.020	5.7406	20	0.11
6.134					0.050			0.08

TRAILING EDGE CONTOUR TO
BE A 4/ ELLIPSE, TRUE WITHIN
3.5/1 TO 4.5/1, CENTERED ON
THE BLADE CONTOUR WITH
THE MINOR AXIS EQUAL TO
THE BLADE THICKNESS.



DEFINITION DRAWING
FOR TABLES I THROUGH IV

DETAIL OF BLADE SECTIONS - NO SCALE

BLADE CONTOUR MUST FAIR SMOOTHLY BETWEEN SECTIONS. THE ALLOWABLE WAVINESS RATE OF CHANGE OF BLADE CONTOUR OR BLEND BETWEEN SECTIONS SHALL NOT BE MORE THAN .005 IN./IN.

TABLE I

$Z = 0.0375$						$Z = 0.1175$						$Z = 0.2175$					
SUCTION SIDE			PRESSURE SIDE			SUCTION SIDE			PRESSURE SIDE			SUCTION SIDE			PRESSURE SIDE		
X _S	Y _S		X _P	Y _P		X _S	Y _S		X _P	Y _P		X _S	Y _S		X _P	Y _P	
0.0932	2.5100		-0.0932	2.5100		0.1000	2.2325		-0.1000	2.2325		0.1040	2.0250		-0.1040	2.0250	
0.0890	2.5604		-0.0890	2.5604		0.0941	2.3116		-0.0941	2.3116		0.0966	2.1237		-0.0966	2.1237	
0.0864	2.5886		-0.0864	2.5886		0.0909	2.3536		-0.0909	2.3536		0.0929	2.1762		-0.0929	2.1762	
0.0836	2.6167		-0.0836	2.6167		0.0878	2.3956		-0.0878	2.3956		0.0885	2.2286		-0.0885	2.2286	
0.0807	2.6449		-0.0807	2.6449		0.0845	2.4376		-0.0845	2.4376		0.0845	2.2811		-0.0845	2.2811	
0.0779	2.6731		-0.0779	2.6731		0.0813	2.4796		-0.0813	2.4796		0.0805	2.3335		-0.0805	2.3335	
0.0749	2.7013		-0.0749	2.7013		0.0780	2.5217		-0.0780	2.5217		0.0766	2.3860		-0.0766	2.3860	
0.0712	2.7295		-0.0712	2.7295		0.0746	2.5637		-0.0746	2.5637		0.0726	2.4384		-0.0726	2.4384	
0.0681	2.7577		-0.0681	2.7577		0.0712	2.6057		-0.0712	2.6057		0.0687	2.4909		-0.0687	2.4909	
0.0650	2.7859		-0.0650	2.7859		0.0675	2.6477		-0.0675	2.6477		0.0647	2.5433		-0.0647	2.5433	
0.0619	2.8141		-0.0619	2.8141		0.0637	2.6897		-0.0637	2.6897		0.0606	2.5958		-0.0606	2.5958	
0.0584	2.8423		-0.0584	2.8423		0.0598	2.7317		-0.0598	2.7317		0.0567	2.6483		-0.0567	2.6483	
0.0548	2.8705		-0.0548	2.8705		0.0557	2.7738		-0.0557	2.7738		0.0527	2.7007		-0.0527	2.7007	
0.0513	2.8987		-0.0513	2.8987		0.0516	2.8158		-0.0516	2.8158		0.0487	2.7532		-0.0487	2.7532	
0.0468	2.9269		-0.0468	2.9269		0.0473	2.8578		-0.0473	2.8578		0.0447	2.8056		-0.0447	2.8056	
0.0429	2.9551		-0.0429	2.9551		0.0431	2.8998		-0.0431	2.8998		0.0406	2.8581		-0.0406	2.8581	
0.0388	2.9833		-0.0388	2.9833		0.0385	2.9418		-0.0385	2.9418		0.0366	2.9105		-0.0366	2.9105	
0.0343	3.0115		-0.0343	3.0115		0.0340	2.9839		-0.0340	2.9839		0.0327	2.9630		-0.0327	2.9630	
0.0296	3.0397		-0.0296	3.0397		0.0294	3.0259		-0.0294	3.0259		0.0288	3.0154		-0.0288	3.0154	
0.0230	3.0800		-0.0230	3.0800		0.0220	3.0950		-0.0220	3.0950		0.0229	3.1000		-0.0229	3.1000	

TABLE I (Contd)

$Z = 0.3000$						$Z = 0.5000$						$Z = 0.7725$					
SUCTION SIDE			PRESSURE SIDE			SUCTION SIDE			PRESSURE SIDE			SUCTION SIDE			PRESSURE SIDE		
X_s	Y_s	X_p	Y_p	X_s	Y_s	X_s	Y_s	X_p	Y_p	X_s	Y_s	X_s	Y_s	X_p	Y_p	X_p	Y_p
0.1012	1.9250	-0.1012	1.9250	0.0980	1.7250	0.0980	1.7250	-0.0970	1.7250	0.1200	1.5209	0.1200	1.5209	-0.0600	1.5245	-0.0600	1.5245
0.0952	2.0193	-0.0952	2.0193	0.0913	1.8059	0.0913	1.8059	-0.0906	1.8059	0.1100	1.6170	0.1100	1.6170	-0.0462	1.6201	-0.0462	1.6201
0.0913	2.0711	-0.0913	2.0711	0.0882	1.8457	0.0882	1.8457	-0.0872	1.8457	0.1065	1.6568	0.1065	1.6568	-0.0411	1.6597	-0.0411	1.6597
0.0872	2.1228	-0.0872	2.1228	0.0849	1.8854	0.0849	1.8854	-0.0839	1.8855	0.1029	1.6965	0.1029	1.6965	-0.0359	1.6992	-0.0359	1.6992
0.0831	2.1746	-0.0831	2.1746	0.0815	1.9252	0.0815	1.9252	-0.0804	1.9252	0.0999	1.7362	0.0999	1.7362	-0.0314	1.7388	-0.0314	1.7388
0.0788	2.2263	-0.0788	2.2263	0.0783	1.9649	0.0783	1.9649	-0.0772	1.9650	0.0970	1.7759	0.0970	1.7759	-0.0269	1.7784	-0.0269	1.7784
0.0748	2.2781	-0.0748	2.2781	0.0748	2.0047	0.0748	2.0047	-0.0737	2.0047	0.0942	1.8156	0.0942	1.8156	-0.0226	1.8179	-0.0226	1.8179
0.0703	2.3299	-0.0703	2.3299	0.0712	2.0444	0.0712	2.0444	-0.0701	2.0445	0.0918	1.8553	0.0918	1.8553	-0.0186	1.8575	-0.0186	1.8575
0.0663	2.3816	-0.0663	2.3816	0.0679	2.0842	0.0679	2.0842	-0.0667	2.0842	0.0893	1.8950	0.0893	1.8950	-0.0145	1.8971	-0.0145	1.8971
0.0621	2.4334	-0.0621	2.4334	0.0641	2.1240	0.0641	2.1240	-0.0630	2.1240	0.0871	1.9347	0.0871	1.9347	-0.0108	1.9367	-0.0108	1.9367
0.0577	2.4852	-0.0577	2.4852	0.0606	2.1637	0.0606	2.1637	-0.0594	2.1638	0.0849	1.9744	0.0849	1.9744	-0.0070	1.9762	-0.0070	1.9762
0.0530	2.5369	-0.0530	2.5369	0.0568	2.2035	0.0568	2.2035	-0.0556	2.2035	0.0828	2.0141	0.0828	2.0141	-0.0034	2.0158	-0.0034	2.0158
0.0489	2.5887	-0.0489	2.5887	0.0529	2.2432	0.0529	2.2432	-0.0517	2.2433	0.0808	2.0538	0.0808	2.0538	0.0002	2.0554	0.0002	2.0554
0.0441	2.6405	-0.0441	2.6405	0.0492	2.2830	0.0492	2.2830	-0.0480	2.2830	0.0788	2.0935	0.0788	2.0935	0.0038	2.0950	0.0038	2.0950
0.0400	2.6922	-0.0400	2.6922	0.0453	2.3228	0.0453	2.3228	-0.0440	2.3228	0.0769	2.1332	0.0769	2.1332	0.0073	2.1346	0.0073	2.1346
0.0355	2.7440	-0.0355	2.7440	0.0416	2.3625	0.0416	2.3625	-0.0403	2.3625	0.0749	2.1729	0.0749	2.1729	0.0108	2.1742	0.0108	2.1742
0.0320	2.7958	-0.0320	2.7958	0.0377	2.4023	0.0377	2.4023	-0.0364	2.4023	0.0730	2.2126	0.0730	2.2126	0.0142	2.2138	0.0142	2.2138
0.0281	2.8475	-0.0281	2.8475	0.0338	2.4420	0.0338	2.4420	-0.0324	2.4420	0.0712	2.2523	0.0712	2.2523	0.0176	2.2534	0.0176	2.2534
0.0250	2.8993	-0.0250	2.8993	0.0308	2.4818	0.0308	2.4818	-0.0294	2.4818	0.0693	2.2920	0.0693	2.2920	0.0211	2.2929	0.0211	2.2929
0.0207	2.9950	-0.0207	2.9950	0.0257	2.5500	0.0257	2.5500	-0.0243	2.5500	0.0665	2.3561	0.0665	2.3561	0.0265	2.3569	0.0265	2.3569

TABLE I (Contd)

$Z=1.0350$				$Z=1.2000$				$Z=1.2100$			
SUCTION SIDE		PRESSURE SIDE		SUCTION SIDE		PRESSURE SIDE		SUCTION SIDE		PRESSURE SIDE	
X_s	Y_s	X_p	Y_p	X_s	Y_s	X_p	Y_p	X_s	Y_s	X_p	Y_p
0.1970	1.3964	0.0375	1.4098	0.2709	1.2989	0.1318	1.3203	0.2917	1.2953	0.1240	1.3219
0.1931	1.4793	0.0551	1.4909	0.2826	1.4009	0.1512	1.4211	0.3017	1.3941	0.1450	1.4190
0.1919	1.5216	0.0633	1.5323	0.2864	1.4446	0.1608	1.4639	0.3055	1.4379	0.1550	1.4618
0.1908	1.5638	0.0714	1.5738	0.2894	1.4884	0.1711	1.5065	0.3091	1.4817	0.1651	1.5046
0.1901	1.6060	0.0791	1.6153	0.2924	1.5322	0.1813	1.5492	0.3116	1.5258	0.1764	1.5472
0.1899	1.6482	0.0863	1.6568	0.2952	1.5760	0.1919	1.5919	0.3148	1.5697	0.1870	1.5900
0.1897	1.6903	0.0935	1.6984	0.2984	1.6198	0.2019	1.6346	0.3177	1.6136	0.1979	1.6327
0.1902	1.7324	0.1000	1.7399	0.3012	1.6636	0.2124	1.6773	0.3203	1.6576	0.2090	1.6753
0.1906	1.7745	0.1066	1.7815	0.3049	1.7073	0.2221	1.7201	0.3227	1.7017	0.2204	1.7179
0.1914	1.8166	0.1128	1.8232	0.3083	1.7511	0.2319	1.7628	0.3251	1.7457	0.2317	1.7605
0.1924	1.8586	0.1188	1.8648	0.3124	1.7947	0.2411	1.8057	0.3278	1.7897	0.2427	1.8032
0.1935	1.9007	0.1246	1.9064	0.3166	1.8384	0.2503	1.8486	0.3308	1.8336	0.2535	1.8459
0.1951	1.9427	0.1301	1.9481	0.3212	1.8819	0.2589	1.8915	0.3344	1.8775	0.2637	1.8887
0.1966	1.9847	0.1355	1.9898	0.3261	1.9254	0.2674	1.9345	0.3384	1.9213	0.2735	1.9316
0.1985	2.0267	0.1406	2.0315	0.3313	1.9689	0.2754	1.9775	0.3427	1.9650	0.2829	1.9745
0.2004	2.0687	0.1457	2.0732	0.3373	2.0123	0.2828	2.0206	0.3474	2.0087	0.2920	2.0175
0.2024	2.1106	0.1507	2.1150	0.3427	2.0557	0.2907	2.0637	0.3526	2.0523	0.3005	2.0605
0.2045	2.1526	0.1556	2.1567	0.3490	2.0990	0.2976	2.1069	0.3588	2.0957	0.3081	2.1037
0.2067	2.1946	0.1604	2.1984	0.3556	2.1423	0.3044	2.1501	0.3656	2.1390	0.3150	2.1471
0.2090	2.2365	0.1651	2.2402	0.3618	2.1856	0.3115	2.1933	0.3722	2.1824	0.3222	2.1903

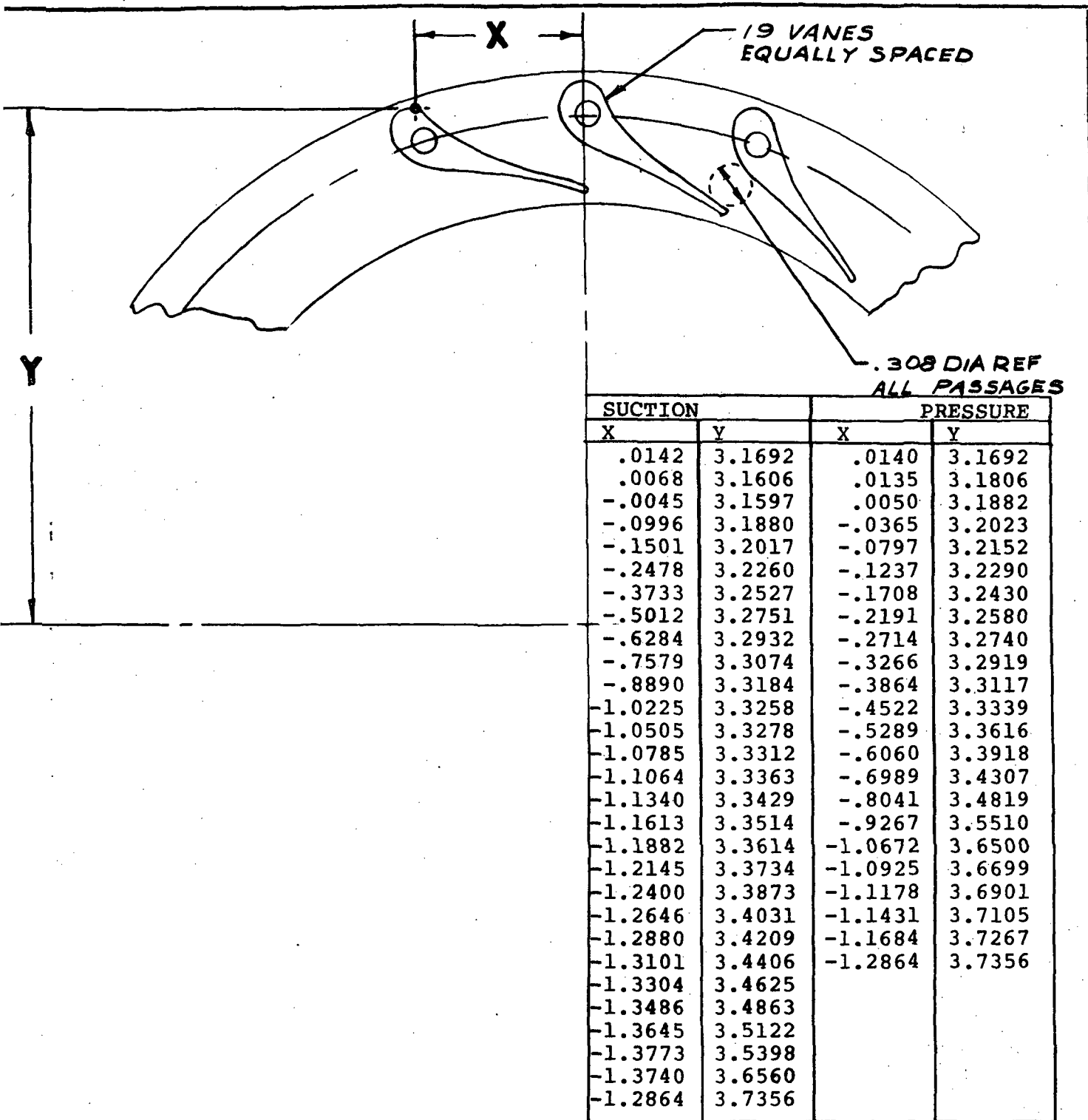
TABLE I (Contd)

Z = 1.4000						Z = 1.7100						Z = 1.9000					
SUCTION SIDE			PRESSURE SIDE			SUCTION SIDE			PRESSURE SIDE			SUCTION SIDE			PRESSURE SIDE		
X _g	Y _s	X _p	Y _p	X _s	Y _s	X _s	Y _s	X _p	Y _p	X _s	Y _s	X _s	Y _s	X _p	Y _p	X _p	Y _p
0.4657	1.1635	0.2943	1.2182	0.6679	1.0011	0.5094	1.0903	0.8488	0.8540	0.5972	0.9817	0.8488	0.8540	0.5972	0.9817	0.8488	0.8540
0.4891	1.2627	0.3326	1.3126	0.7140	1.1102	0.5787	1.1863	0.9073	0.9435	0.7754	1.0546	0.9073	0.9435	0.7754	1.0546	0.9073	0.9435
0.5000	1.3081	0.3501	1.3559	0.7333	1.1545	0.6066	1.2258	0.9348	0.9841	0.8107	1.0885	0.9348	0.9841	0.8107	1.0885	0.9348	0.9841
0.5106	1.3536	0.3678	1.3992	0.7527	1.1988	0.6344	1.2654	0.9620	1.0248	0.8462	1.1223	0.9620	1.0248	0.8462	1.1223	0.9620	1.0248
0.5210	1.3992	0.3857	1.4424	0.7727	1.2428	0.6616	1.3053	0.9900	1.0649	0.8810	1.1567	0.9900	1.0649	0.8810	1.1567	0.9900	1.0649
0.5315	1.4447	0.4035	1.4856	0.7927	1.2867	0.6889	1.3451	1.0178	1.1052	0.9160	1.1910	1.0178	1.1052	0.9160	1.1910	1.0178	1.1052
0.5420	1.4903	0.4213	1.5288	0.8131	1.3304	0.7156	1.3853	1.0462	1.1450	0.9503	1.2257	1.0462	1.1450	0.9503	1.2257	1.0462	1.1450
0.5527	1.5358	0.4390	1.5720	0.8335	1.3742	0.7425	1.4254	1.0744	1.1849	0.9849	1.2603	1.0744	1.1849	0.9849	1.2603	1.0744	1.1849
0.5633	1.5813	0.4567	1.6153	0.8543	1.4176	0.7688	1.4657	1.1031	1.2244	1.0189	1.2953	1.1031	1.2244	1.0189	1.2953	1.1031	1.2244
0.5737	1.6269	0.4746	1.6585	0.8750	1.4612	0.7953	1.5061	1.1317	1.2640	1.0531	1.3302	1.1317	1.2640	1.0531	1.3302	1.1317	1.2640
0.5841	1.6725	0.4926	1.7016	0.8964	1.5043	0.8211	1.5467	1.1609	1.3031	1.0866	1.3657	1.1609	1.3031	1.0866	1.3657	1.1609	1.3031
0.5944	1.7181	0.5106	1.7448	0.9177	1.5475	0.8470	1.5874	1.1901	1.3422	1.1202	1.4011	1.1901	1.3422	1.1202	1.4011	1.1901	1.3422
0.6049	1.7636	0.5284	1.7880	0.9396	1.5904	0.8722	1.6283	1.2198	1.3809	1.1533	1.4369	1.2198	1.3809	1.1533	1.4369	1.2198	1.3809
0.6158	1.8090	0.5458	1.8314	0.9615	1.6333	0.8976	1.6693	1.2495	1.4196	1.1864	1.4727	1.2495	1.4196	1.1864	1.4727	1.2495	1.4196
0.6275	1.8542	0.5625	1.8749	0.9837	1.6760	0.9225	1.7104	1.2795	1.4580	1.2191	1.5089	1.2795	1.4580	1.2191	1.5089	1.2795	1.4580
0.6396	1.8992	0.5787	1.9187	1.0060	1.7186	0.9474	1.7516	1.3096	1.4963	1.2517	1.5451	1.3096	1.4963	1.2517	1.5451	1.3096	1.4963
0.6520	1.9442	0.5946	1.9625	1.0291	1.7608	0.9716	1.7932	1.3405	1.5340	1.2837	1.5819	1.3405	1.5340	1.2837	1.5819	1.3405	1.5340
0.6649	1.9890	0.6100	2.0065	1.0523	1.8030	0.9955	1.8350	1.3715	1.5716	1.3154	1.6189	1.3715	1.5716	1.3154	1.6189	1.3715	1.5716
0.6783	2.0336	0.6249	2.0506	1.0762	1.8447	1.0188	1.8770	1.4032	1.6086	1.3465	1.6564	1.4032	1.6086	1.3465	1.6564	1.4032	1.6086
0.6923	2.0780	0.6393	2.0949	1.1003	1.8864	1.0419	1.9192	1.4351	1.6454	1.3773	1.6941	1.4351	1.6454	1.3773	1.6941	1.4351	1.6454

TABLE I (Contd)

$Z=2.1000$				
SIDE		PRECEDING SIDE		
X_S	Y_S	X_P	Y_P	
1.0215	0.6386	0.8937	0.8078	
1.0932	0.7093	0.9813	0.8575	
1.1292	0.7432	1.0237	0.8828	
1.1646	0.7773	1.0663	0.9078	
1.2011	0.8107	1.1083	0.9336	
1.2373	0.8442	1.1504	0.9592	
1.2739	0.8771	1.1921	0.9854	
1.3104	0.9102	1.2339	1.0115	
1.3473	0.9428	1.2753	1.0380	
1.3841	0.9754	1.3168	1.0645	
1.4214	1.0075	1.3579	1.0916	
1.4589	1.0392	1.3986	1.1190	
1.4964	1.0710	1.4395	1.1463	
1.5341	1.1025	1.4801	1.1740	
1.5721	1.1336	1.5204	1.2021	
1.6102	1.1646	1.5606	1.2302	
1.6486	1.1948	1.6002	1.2591	
1.6877	1.2247	1.6396	1.2884	
1.7271	1.2539	1.6785	1.3183	
1.7668	1.2829	1.7172	1.3485	

[illegible]



PROJECT AUTHORIZATION		For Development Only		m. D. Goomy APPD	11-15-71
Alternate	for Dwg No. <u>NASA 10/1 RIG</u>	Next Assy.			
Rework		Outline		APPD	
W. O. No.				CHK	
AIRESEARCH MANUFACTURING COMPANY OF ARIZONA PHOENIX, ARIZONA				DFT	
Title <u>NOZZLE, RADIAL TURBINE</u>				PAP	216124

APPENDIX D

COMPLETE RADIAL EQUILIBRIUM
FLOW SOLUTION
ALL BLADE ROWS

(61 pages)

10/1 NASA COMP.*3/30/72**THRU THE BLADE**ALL STAGES** FINAL

DATE 04/05/72 TIME 17:54:48

CODE	RADIUS	SPEED	FLOW	STRMLNS	MAX IT
70000.00000	.08333	610.00000	2.00000	6	19

GAMMA	SPEC HEAT	TEMP	PRESSURE	DENSITY	RPM
1.39470	6065.37000	518.68800	2116.22000	.076474	69900.88

MAJOR ITES	FLOW TOL	CUR TOL	SENSE SW	SHOK LOC	OD LOSS
20	.00100	.00100	89	-0.00000	-0.00000

FLOW					
.10000	.15000	.25000	.25000	.25000	

STATIONS	DM(M=1)	DM(N+1)	ANGL DAMP	ROT DELW	DEL LOSS
30	1.00000	.30000	.95000	.30000	-0.00000

SLOPE M-1					
-5.23000	-5.61700	-6.09160	-6.58860	-6.86600	-6.33000

SLOPE N+1					
22.00000	22.00000	22.00000	22.00000	22.00000	22.50000

CURVATURE M-1					
-.08240	-.10324	-.11402	-.12200	-.12515	-.09970

CURVATURE N+1					
-.25000	-.25000	-.26000	-.31200	-.31200	-.31200

	STATION	AVERAGE P/P	AVERAGE T/T	AVERAGE EFF
	.03000	1.00000	1.00000	1.00000
	.04000	1.00000	1.00000	1.00000
	.05000	1.00000	1.00000	1.00000
	.50000	1.00000	1.00000	1.00000
	.06000	1.00000	1.00000	1.00000
	.07000	1.00000	1.00000	1.00000
Rotor 1A Inlet	1.00000	1.00000	1.00000	1.00000
	1.20000	1.14542	1.04028	.96102
	1.40000	1.32628	1.08659	.95856
	1.60000	1.52199	1.13212	.95688
	1.80000	1.70059	1.17001	.95597
Rotor 1A Exit	2.00000	1.78018	1.18605	.95509
Rotor 1B Inlet	3.00000	1.77876	1.18605	.95364
	3.20000	2.12780	1.24888	.95890
	3.40000	2.43015	1.29793	.96042
	3.60000	2.78528	1.35027	.96144
	3.80000	3.10595	1.39515	.95811
Rotor 1B Exit	4.00000	3.24146	1.41210	.95963
Stator 1A Inlet	5.00000	3.24146	1.41210	.95963
	5.10000	3.21130	1.41210	.95073
	5.20000	3.18373	1.41210	.94254
	5.30000	3.15247	1.41210	.93319
	5.40000	3.12463	1.41210	.92480
Stator 1A Exit	5.50000	3.09619	1.41210	.91617
Stator 1B Inlet	6.00000	3.09619	1.41210	.91617
	6.10000	3.09036	1.41210	.91439
	6.20000	3.08335	1.41210	.91225
	6.30000	3.07634	1.41210	.91010
	6.40000	3.06934	1.41210	.90795
Stator 1B Exit	6.50000	3.06243	1.41210	.90583

STATION .03000 STATOR XI = 0.00000

P = -0. ZTIP = -4.12500 AR = 1.30000 XN = 0. BNXT = -0.
 = 0. ZHUB = -4.12500 LOSS = 1. EXP = .8000 BLADES = -0.

RADIUS
 3.54000 3.47000 3.32000 3.15000 2.75000 2.28000

SLOPE
 -14.32000 -16.00000 -17.00000 -19.00000 -20.00000 -18.14000

CURVATURE
 -.22220 -.19000 -.21000 -.23000 -.25000 -.28540

LOSS COEFF
 -0.00000 -0.00000 -0.00000 -0.00000 -0.00000 -0.00000

SOLIDITY
 1.00000 1.00000 1.00000 1.00000 1.00000 1.00000

AERO BLOCKAGE
 .99600 .99600 .99600 .99600 .99600 .99600

TOTAL BLOCKAGE
 .99600 .99600 .99600 .99600 .99600 .99600

BLADE ANGLE
 -0.00000 -0.00000 -0.00000 -0.00000 -0.00000 -0.00000

LEAN
 -0.00000 -0.00000 -0.00000 -0.00000 -0.00000 -0.00000

Y
 -0.00000 -0.00000 -0.00000 -0.00000 -0.00000 -0.00000

MINOR ITERS = 1 AREA RATIO = .99938 EXP = .80000 CHOKE = .26613

RADIUS
 3.54000 3.42314 3.24461 2.93771 2.61665 2.28000

Z
 -4.12500 -4.12500 -4.12500 -4.12500 -4.12500 -4.12500

CROSS PASSAGE DIST P
 1.26000 1.14314 .96461 .65771 .33665 0.00000

SLOPE
 -14.32000 -15.23712 -15.97222 -17.39095 -18.47023 -18.14000

CURVATURE
 -.22220 -.20663 -.20057 -.20908 -.22670 -.28540

DELTA CURVATURE
 0.00000 -.00001 -.00015 -.00006 .00010 0.00000

VM
 152.62197 156.30901 162.17091 173.40452 187.53331 207.89497

VU2
 0.00000 0.00000 0.00000 0.00000 0.00000 0.00000

U
 2159.40000 2088.11380 1979.21147 1792.00433 1596.15566 1390.80000

VR
 -37.74911 -41.08026 -44.62479 -51.82892 -59.41279 -64.72603

BETA2
 0.00000 0.00000 0.00000 0.00000 0.00000 0.00000

BETA2*
 0.00000 0.00000 0.00000 0.00000 0.00000 0.00000

INCIDENCE					
0.00000	0.00000	0.00000	0.00000	0.00000	0.00000
.13722	.14054	.14584	.15599	.16876	.18721
V2					
152.62197	156.30901	162.17091	173.40452	187.53331	207.89497
TOTAL TEMP					
1.00000	1.00000	1.00000	1.00000	1.00000	1.00000
TOTAL PRESS					
1.00000	1.00000	1.00000	1.00000	1.00000	1.00000
EFFICIENCY					
0.00000	0.00000	0.00000	0.00000	0.00000	0.00000
STATIC TEMP					
.99630	.99612	.99582	.99522	.99441	.99313
STATIC PRESS					
.98698	.98635	.98531	.98322	.98039	.97594
DENSITY					
.99065	.99019	.98944	.98794	.98590	.98269
DELTA T					
0.00000	0.00000	0.00000	0.00000	0.00000	0.00000
WORK COEF = $2*CP*DELTA T/U**2$					
0.00000	0.00000	0.00000	0.00000	0.00000	0.00000
FLOW COEF = VM/U					
.07068	.07486	.08194	.09677	.11749	.14948
R BAR					
3.54000	3.42314	3.24461	2.93771	2.61665	2.28000
D-FACTOR					
0.00000	0.00000	0.00000	0.00000	0.00000	0.00000
VM2/VM1					
1.00000	1.00000	1.00000	1.00000	1.00000	1.00000
DELP/Q					
0.00000	0.00000	0.00000	0.00000	0.00000	0.00000
TANG BLADE FORCE LB/IN					
0.00000	0.00000	0.00000	0.00000	0.00000	0.00000
AXIAL BLADE FORCE LB/IN					
0.00000	0.00000	0.00000	0.00000	0.00000	0.00000
VEL HEAD 2					
.01302	.01365	.01469	.01678	.01961	.02406
Q=E**(-S/CP)					
1.00000	1.00000	1.00000	1.00000	1.00000	1.00000
RVU/					
0.00000	0.00000	0.00000	0.00000	0.00000	0.00000
DRVU/UM					
-0.00000	-0.00000	-0.00000	-0.00000	-0.00000	-0.00000
STRMLN DIST M					
-4.12500	-4.12500	-4.12500	-4.12500	-4.12500	-4.12500

STATION .04000 STATOR XI = 0.00000
P = -0. ZTIP = -3.12500 AR = 1.40000 XN = -0. BNXT = -0.
= -0. ZHUB = -3.12500 LOSS = 1. EXP = .8000 BLADES = -0.

RADIUS	3.16000	3.09000	2.89000	2.68000	2.25000	1.77000
SLOPE	-26.90000	-26.00000	-28.00000	-30.00000	-32.00000	-35.30000
CURVATURE	-.18410	-.20000	-.18000	-.16000	-.13000	-.23290
LOSS COEFF	-0.00000	-0.00000	-0.00000	-0.00000	-0.00000	-0.00000
SOLIDITY	1.00000	1.00000	1.00000	1.00000	1.00000	1.00000
AERO BLOCKAGE	.99500	.99500	.99500	.99500	.99500	.99500
TOTAL BLOCKAGE	.99500	.99500	.99500	.99500	.99500	.99500
BLADE ANGLE	-0.00000	-0.00000	-0.00000	-0.00000	-0.00000	-0.00000
LEAN	-0.00000	-0.00000	-0.00000	-0.00000	-0.00000	-0.00000
Y	-0.00000	-0.00000	-0.00000	-0.00000	-0.00000	-0.00000

MINOR ITER = 1 AREA RATIO = .99955 EXP = .80000 CHOKE = .31431

RADIUS	3.16000	3.03550	2.84602	2.51674	2.16501	1.77000
Z	-3.12500	-3.12500	-3.12500	-3.12500	-3.12500	-3.12500
CROSS PASSAGE DIST P	1.39000	1.26550	1.07602	.74674	.39501	0.00000
SLOPE	-26.90000	-26.92155	-27.94293	-29.20354	-30.97242	-35.30000
CURVATURE	-.18410	-.19573	-.19355	-.17729	-.17489	-.23290
DELTA CURVATURE	0.00000	.00004	.00036	.00024	-.00003	0.00000
VM	174.29387	180.49529	189.66782	206.04046	225.55094	250.64984
VU2	0.00000	0.00000	0.00000	0.00000	0.00000	0.00000
U	1927.60000	1851.65420	1736.07441	1535.20893	1320.65751	1079.70000
VR	-78.85663	-81.72291	-88.87682	-100.52999	-116.07429	-144.83998
BETA2	0.00000	0.00000	0.00000	0.00000	0.00000	0.00000
BETA2*	0.00000	0.00000	0.00000	0.00000	0.00000	0.00000

INCIDENCE					
0.00000	0.00000	0.00000	0.00000	0.00000	0.00000
.15679	.16240	.17070	.18553	.20323	.22606
V2					
174.29387	180.49529	189.66782	206.04046	225.55094	250.64984
TOTAL TEMP					
1.00000	1.00000	1.00000	1.00000	1.00000	1.00000
TOTAL PRESS					
1.00000	1.00000	1.00000	1.00000	1.00000	1.00000
EFFICIENCY					
0.00000	0.00000	0.00000	0.00000	0.00000	0.00000
STATIC TEMP					
.99517	.99482	.99428	.99325	.99191	.99002
STATIC PRESS					
.98304	.98182	.97994	.97636	.97172	.96516
DENSITY					
.98781	.98693	.98558	.98299	.97964	.97490
DELTA T					
0.00000	0.00000	0.00000	0.00000	0.00000	0.00000
WORK COEF = $2*CP*DELT/U**2$					
0.00000	0.00000	0.00000	0.00000	0.00000	0.00000
FLOW COEF = VM/U					
.09042	.09748	.10925	.13421	.17079	.23215
R BAR					
3.35000	3.22932	3.04532	2.72722	2.39083	2.02500
D-FACTOR					
-.14200	-.15473	-.16956	-.18821	-.20272	-.20566
VM2/VM1					
1.14200	1.15473	1.16956	1.18821	1.20272	1.20566
DELP/Q					
-.30230	-.33122	-.36519	-.40832	-.44197	-.44787
TANG BLADE FORCE LB/IN					
0.00000	0.00000	0.00000	0.00000	0.00000	0.00000
AXIAL BLADE FORCE LB/IN					
-.84090	-.84793	-.94707	-1.06570	-1.24716	-1.74702
VEL HEAD 2					
.01696	.01818	.02006	.02364	.02828	.03484
$Q=E*(-S/CP)$					
1.00000	1.00000	1.00000	1.00000	1.00000	1.00000
RVU/					
0.00000	0.00000	0.00000	0.00000	0.00000	0.00000
DRVU/DM					
-0.00000	-0.00000	-0.00000	-0.00000	-0.00000	-0.00000
STRMLN DIST M					
-3.05308	-3.05064	-3.04653	-3.03808	-3.02556	-2.99825

STATION .05000 STATOR XI = 0.00000

P = -0. ZTIP = -2.12500 AR = 1.50000 XN = -0. BNXT = -0.
 Z = -0. ZHUB = -2.12500 LOSS = 1. EXP = .8000 BLADES = -0.

RADIUS

2.54000	2.46000	2.26000	2.03000	1.58000	1.00600
---------	---------	---------	---------	---------	---------

SLOPE

-35.08000	-34.50000	-32.90000	-30.85000	-29.78000	-34.40000
-----------	-----------	-----------	-----------	-----------	-----------

CURVATURE

-.06112	0.00000	.05000	.08000	.15000	.24700
---------	---------	--------	--------	--------	--------

LOSS COEFF

-0.00000	-0.00000	-0.00000	-0.00000	-0.00000	-0.00000
----------	----------	----------	----------	----------	----------

SOLIDITY

1.00000	1.00000	1.00000	1.00000	1.00000	1.00000
---------	---------	---------	---------	---------	---------

AERO BLOCKAGE

.99400	.99400	.99400	.99400	.99400	.99400
--------	--------	--------	--------	--------	--------

TOTAL BLOCKAGE

.99400	.99400	.99400	.99400	.99400	.99400
--------	--------	--------	--------	--------	--------

BLADE ANGLE

-0.00000	-0.00000	-0.00000	-0.00000	-0.00000	-0.00000
----------	----------	----------	----------	----------	----------

LEAN

-0.00000	-0.00000	-0.00000	-0.00000	-0.00000	-0.00000
----------	----------	----------	----------	----------	----------

Y

-0.00000	-0.00000	-0.00000	-0.00000	-0.00000	-0.00000
----------	----------	----------	----------	----------	----------

MINOR ITER = 1 AREA RATIO = .99909 EXP = .80000 CHOKE = .40515

RADIUS

2.54000	2.41891	2.23506	1.91191	1.53748	1.00600
---------	---------	---------	---------	---------	---------

Z

-2.12500	-2.12500	-2.12500	-2.12500	-2.12500	-2.12500
----------	----------	----------	----------	----------	----------

CROSS PASSAGE DIST P

1.53400	1.41291	1.22906	.90591	.53148	0.00000
---------	---------	---------	--------	--------	---------

SLOPE

-35.08000	-34.11692	-32.60263	-30.56561	-29.79860	-34.40000
-----------	-----------	-----------	-----------	-----------	-----------

CURVATURE

-.06112	-.01536	.03878	.11473	.19184	.24700
---------	---------	--------	--------	--------	--------

DELTA CURVATURE

0.00000	-.00007	-.00051	-.00067	-.00055	0.00000
---------	---------	---------	---------	---------	---------

VM

245.72929	254.46730	265.03657	275.91751	275.72465	255.08052
-----------	-----------	-----------	-----------	-----------	-----------

VU2

0.00000	0.00000	0.00000	0.00000	0.00000	0.00000
---------	---------	---------	---------	---------	---------

U

1549.40000	1475.53422	1363.38743	1166.26276	937.86308	613.66000
------------	------------	------------	------------	-----------	-----------

VR

-141.22550	-142.72655	-142.80425	-140.31093	-137.02219	-144.11213
------------	------------	------------	------------	------------	------------

BETA2

0.00000	0.00000	0.00000	0.00000	0.00000	0.00000
---------	---------	---------	---------	---------	---------

BETA2*

0.00000	0.00000	0.00000	0.00000	0.00000	0.00000
---------	---------	---------	---------	---------	---------

INCIDENCE

0.00000	0.00000	0.00000	0.00000	0.00000	0.00000
.22158	.22954	.23918	.24912	.24894	.23010
V2					
245.72929	254.46730	265.03657	275.91751	275.72465	255.08052
TOTAL TEMP					
1.00000	1.00000	1.00000	1.00000	1.00000	1.00000
TOTAL PRESS					
1.00000	1.00000	1.00000	1.00000	1.00000	1.00000
EFFICIENCY					
0.00000	0.00000	0.00000	0.00000	0.00000	0.00000
STATIC TEMP					
.99040	.98971	.98884	.98790	.98792	.98966
STATIC PRESS					
.96650	.96411	.96111	.95790	.95796	.96394
DENSITY					
.97586	.97413	.97196	.96963	.96967	.97401
DELTA T					
0.00000	0.00000	0.00000	0.00000	0.00000	0.00000
WORK COEF = $2*CP*DELTA T/U**2$					
0.00000	0.00000	0.00000	0.00000	0.00000	0.00000
FLOW COEF = VM/U					
.15860	.17246	.19440	.23658	.29399	.41567
R BAR					
2.85000	2.72720	2.54054	2.21432	1.85125	1.38800
D-FACTOR					
-.40986	-.40983	-.39737	-.33914	-.22245	-.01768
VM2/VM1					
1.40986	1.40983	1.39737	1.33914	1.22245	1.01768
DELTA P/Q					
-.97570	-.97476	-.93920	-.78116	-.48682	-.03520
TANG BLADE FORCE LB/IN					
0.00000	0.00000	0.00000	0.00000	0.00000	0.00000
AXIAL BLADE FORCE LB/IN					
-2.09020	-1.99288	-1.68336	-1.10594	-.49723	.01465
VEL HEAD 2					
.03350	.03589	.03889	.04210	.04204	.03606
Q=E**(-S/CP)					
1.00000	1.00000	1.00000	1.00000	1.00000	1.00000
RVU/					
0.00000	0.00000	0.00000	0.00000	0.00000	0.00000
DRVU/DM					
-0.00000	-0.00000	-0.00000	-0.00000	-0.00000	-0.00000
STRMLN DIST M					
-1.87648	-1.87582	-1.87466	-1.86940	-1.84497	-1.73980

STATION .50000 STATOR XI = 0.00000

P = -0. ZTIP = -1.42500 AR = 4.00000 XN = -0. BNXT = -0.
 . -0. ZHUB = -1.42500 LOSS = 1. EXP = .8000 BLADES = -0.

RADIUS

2.07530 1.97900 1.83000 1.55000 1.20000 .63660

SLOPE

-29.56000 -26.30000 -23.90000 -20.00000 -17.00000 -19.55000

CURVATURE

.28750 .31000 .36000 .41600 .45600 .49144

LOSS COEFF

-0.00000 -0.00000 -0.00000 -0.00000 -0.00000 -0.00000

SOLIDITY

1.00000 1.00000 1.00000 1.00000 1.00000 1.00000

AERO BLOCKAGE

.99000 .99000 .99000 .99000 .99000 .99000

TOTAL BLOCKAGE

.99000 .99000 .99000 .99000 .99000 .99000

BLADE ANGLE

-0.00000 -0.00000 -0.00000 -0.00000 -0.00000 -0.00000

LEAN

-0.00000 -0.00000 -0.00000 -0.00000 -0.00000 -0.00000

Y

-0.00000 -0.00000 -0.00000 -0.00000 -0.00000 -0.00000

MINOR ITES = 1 AREA RATIO = .99960 EXP = .80000 CHOKE = .51896

DIUS

2.07530 1.98155 1.83549 1.56235 1.21659 .63660

Z

-1.42500 -1.42500 -1.42500 -1.42500 -1.42500 -1.42500

CROSS PASSAGE DIST P

1.43870 1.34495 1.19889 .92575 .57999 0.00000

SLOPE

-29.56000 -27.07022 -24.44119 -20.49675 -17.50555 -19.55000

CURVATURE

.28750 .31778 .33380 .35811 .39100 .49144

DELTA CURVATURE

0.00000 .00033 -.00006 -.00035 -.00061 0.00000

VM

382.37042 384.52282 380.44635 362.41394 331.20066 260.09312

VU2

0.00000 0.00000 0.00000 0.00000 0.00000 0.00000

U

1265.93300 1208.74730 1119.65136 953.03341 742.11704 388.32600

VR

-188.63668 -174.98953 -157.41317 -126.90085 -99.62459 -87.03483

BETA2

0.00000 0.00000 0.00000 0.00000 0.00000 0.00000

BETA2*

0.00000 0.00000 0.00000 0.00000 0.00000 0.00000

INCIDENCE					
0.00000	0.00000	0.00000	0.00000	0.00000	0.00000
.34720	.34920	.34541	.32868	.29984	.23467
V2					
382.37042	384.52282	380.44635	362.41394	331.20066	260.09312
TOTAL TEMP					
1.00000	1.00000	1.00000	1.00000	1.00000	1.00000
TOTAL PRESS					
1.00000	1.00000	1.00000	1.00000	1.00000	1.00000
EFFICIENCY					
0.00000	0.00000	0.00000	0.00000	0.00000	0.00000
STATIC TEMP					
.97676	.97650	.97700	.97913	.98257	.98925
STATIC PRESS					
.92028	.91941	.92106	.92817	.93975	.96252
DENSITY					
.94217	.94153	.94274	.94796	.95642	.97298
DELTA T					
0.00000	0.00000	0.00000	0.00000	0.00000	0.00000
WORK COEF = $2*CP*DELT/U**2$					
0.00000	0.00000	0.00000	0.00000	0.00000	0.00000
FLOW COEF = VM/U					
.30205	.31812	.33979	.38027	.44629	.66978
R BAR					
2.30765	2.20023	2.03528	1.73713	1.37703	.82130
D-FACTOR					
-.55606	-.51109	-.43545	-.31349	-.20120	-.01965
VM2/VM1					
1.55606	1.51109	1.43545	1.31349	1.20120	1.01965
DELP/Q					
-1.37969	-1.24535	-1.02971	-.70610	-.43310	-.03915
TANG BLADE FORCE LB/IN					
0.00000	0.00000	0.00000	0.00000	0.00000	0.00000
AXIAL BLADE FORCE LB/IN					
-1.68566	-.97244	-.29188	.44067	.70291	.58296
VEL HEAD 2					
.07972	.08059	.07894	.07183	.06025	.03748
Q=E*(-S/CP)					
1.00000	1.00000	1.00000	1.00000	1.00000	1.00000
RVU/					
0.00000	0.00000	0.00000	0.00000	0.00000	0.00000
DRVU/DM					
-0.00000	-0.00000	-0.00000	-0.00000	-0.00000	-0.00000
STRMLN DIST M					
-1.03627	-1.05043	-1.06865	-1.08596	-1.07344	-.94609

STATION .06000 STATOR XI = 0.00000
P = -0. ZTIP = -.92500 AR = 4.00000 YN = -0. BNXT = -0.
= -0. ZHUB = -.92500 LOSS = 1. EXP = .8000 BLADES = -0.

	1.86100	1.79800	1.66500	1.41200	1.11200	.52900
RADIUS						
SLOPE	-15.26000	-13.30000	-10.80000	-7.10000	-3.50000	-4.23000
CURVATURE	.64400	.55000	.55000	.50000	.55000	.67400
LOSS COEFF	-0.00000	-0.00000	-0.00000	-0.00000	-0.00000	-0.00000
SOLIDITY	1.00000	1.00000	1.00000	1.00000	1.00000	1.00000
AERO BLOCKAGE	.99200	.99200	.99200	.99200	.99200	.99200
TOTAL BLOCKAGE	.99200	.99200	.99200	.99200	.99200	.99200
BLADE ANGLE	-0.00000	-0.00000	-0.00000	-0.00000	-0.00000	-0.00000
LEAN	-0.00000	-0.00000	-0.00000	-0.00000	-0.00000	-0.00000
Y	-0.00000	-0.00000	-0.00000	-0.00000	-0.00000	-0.00000

MINOR ITES = 1 AREA RATIO = 1.00050 EXP = .80000 CHOKE = .59568

	1.86100	1.78713	1.66710	1.43122	1.11439	.52900
DIUS						
Z	-.92500	-.92500	-.92500	-.92500	-.92500	-.92500
CROSS PASSAGE DIST P	1.33200	1.25813	1.13810	.90222	.58539	0.00000
SLOPE	-15.26000	-13.52046	-11.27682	-7.75818	-4.38250	-4.23000
CURVATURE	.64400	.58437	.55928	.51867	.52899	.67400
DELTA CURVATURE	0.00000	.00092	.00015	.00019	-.00080	0.00000
VM	525.71339	507.87795	480.81325	429.94544	368.21261	253.36926
VU2	0.00000	0.00000	0.00000	0.00000	0.00000	0.00000
U	1135.21000	1090.14947	1016.93365	873.04370	679.77695	322.69000
VR	-138.36761	-118.73817	-94.02279	-58.03937	-28.13678	-18.68862
BETA2	0.00000	0.00000	0.00000	0.00000	0.00000	0.00000
BETA2*	0.00000	0.00000	0.00000	0.00000	0.00000	0.00000

INCIDENCE					
0.00000	0.00000	0.00000	0.00000	0.00000	0.00000
.48249	.46541	.43963	.39163	.33405	.22854
V2					
525.71339	507.87795	480.81325	429.94544	368.21261	253.36926
TOTAL TEMP					
1.00000	1.00000	1.00000	1.00000	1.00000	1.00000
TOTAL PRESS					
1.00000	1.00000	1.00000	1.00000	1.00000	1.00000
EFFICIENCY					
0.00000	0.00000	0.00000	0.00000	0.00000	0.00000
STATIC TEMP					
.95608	.95901	.96326	.97062	.97845	.98980
STATIC PRESS					
.85323	.86251	.87610	.89999	.92591	.96441
DENSITY					
.89243	.89938	.90952	.92723	.94631	.97435
DELTA T					
0.00000	0.00000	0.00000	0.00000	0.00000	0.00000
WORK COEF = $2*CP*DELT/U**2$					
0.00000	0.00000	0.00000	0.00000	0.00000	0.00000
FLOW COEF = VM/U					
.46310	.46588	.47281	.49247	.54167	.78518
R BAR					
1.96815	1.88434	1.75130	1.49678	1.16549	.58280
D-FACTOR					
-.37488	-.32080	-.26381	-.18634	-.11175	.02585
VM2/VM1					
1.37488	1.32080	1.26381	1.18634	1.11175	.97415
DELP/Q					
-.84101	-.70598	-.56947	-.39223	-.22953	.05037
TANG BLADE FORCE LB/IN					
0.00000	0.00000	0.00000	0.00000	0.00000	0.00000
AXIAL BLADE FORCE LB/IN					
2.01929	1.82111	1.55149	1.01093	.55108	.21490
VEL HEAD 2					
.14677	.13749	.12390	.10001	.07409	.03559
Q=E**(-S/CP)					
1.00000	1.00000	1.00000	1.00000	1.00000	1.00000
RVU/					
0.00000	0.00000	0.00000	0.00000	0.00000	0.00000
DRVU/DM					
-0.00000	-0.00000	-0.00000	-0.00000	-0.00000	-0.00000
STRMLN DIST M					
-.49087	-.51270	-.53990	-.56799	-.56199	-.43312

STATION .07000 STATOR XI = 0.00000

P = -0. ZTIP = -.42500 AR = 4.00000 XN = -0. BNXT = -0.
 ZHUB = -.42500 LOSS = 1. EXP = 1.5000 BLADES = -0.

RADIUS	1.81450	1.74500	1.64060	1.43400	1.14900	.60000
SLOPE	4.49000	2.87000	4.37000	7.31000	10.15000	20.18000
CURVATURE	.70287	.60400	.56000	.60000	.75000	.80000
LOSS COEFF	-0.00000	-0.00000	-0.00000	-0.00000	-0.00000	-0.00000
SOLIDITY	1.00000	1.00000	1.00000	1.00000	1.00000	1.00000
AERO BLOCKAGE	.99100	.99100	.99100	.99100	.99100	.99100
TOTAL BLOCKAGE	.99100	.99100	.99100	.99100	.99100	.99100
BLADE ANGLE	-0.00000	-0.00000	-0.00000	-0.00000	-0.00000	-0.00000
LEAN	-0.00000	-0.00000	-0.00000	-0.00000	-0.00000	-0.00000
Y	-0.00000	-0.00000	-0.00000	-0.00000	-0.00000	-0.00000

MINOR ITES = 1 AREA RATIO = 1.00028 EXP = 1.50000 CHOKE = .65051

DIUS	1.81450	1.75004	1.64433	1.43403	1.14673	.60000
Z	-.42500	-.42500	-.42500	-.42500	-.42500	-.42500
CROSS PASSAGE DIST P	1.21450	1.15004	1.04433	.83403	.54673	0.00000
SLOPE	4.49000	4.64561	5.93979	8.54635	11.81866	20.18000
CURVATURE	.70287	.67334	.64514	.63737	.69777	.80000
DELTA CURVATURE	0.00000	.00144	.00096	-.00062	-.00154	0.00000
VM	633.45865	605.67597	563.88868	490.16335	401.62704	264.40266
VU2	0.00000	0.00000	0.00000	0.00000	0.00000	0.00000
U	1106.84500	1067.52709	1003.04067	874.75960	699.50432	366.00000
VR	49.59039	49.05518	58.35309	72.84291	82.25918	91.21118
BETA2	0.00000	0.00000	0.00000	0.00000	0.00000	0.00000
BETA2*	0.00000	0.00000	0.00000	0.00000	0.00000	0.00000

INCIDENCE

0.00000	0.00000	0.00000	0.00000	0.00000	0.00000
.58751	.56010	.51932	.44852	.36513	.23860
V2					
633.45865	605.67597	563.88868	490.16335	401.62704	264.40266
TOTAL TEMP					
1.00000	1.00000	1.00000	1.00000	1.00000	1.00000
TOTAL PRESS					
1.00000	1.00000	1.00000	1.00000	1.00000	1.00000
EFFICIENCY					
0.00000	0.00000	0.00000	0.00000	0.00000	0.00000
STATIC TEMP					
.93623	.94170	.94946	.96182	.97436	.98889
STATIC PRESS					
.79227	.80875	.83257	.87147	.91232	.96129
DENSITY					
.84624	.85882	.87688	.90607	.93632	.97209
DELTA T					
0.00000	0.00000	0.00000	0.00000	0.00000	0.00000
WORK COEF = $2*CP*DELT/U**2$					
0.00000	0.00000	0.00000	0.00000	0.00000	0.00000
FLOW COEF = VM/U					
.57231	.56736	.56218	.56034	.57416	.72241
R BAR					
1.83775	1.76859	1.65572	1.43263	1.13056	.56450
D-FACTOR					
-.20495	-.19256	-.17278	-.14006	-.09075	-.04355
VM2/VM1					
1.20495	1.19256	1.17278	1.14006	1.09075	1.04355
DELP/Q					
-.41540	-.39100	-.35135	-.28520	-.18355	-.08773
TANG BLADE FORCE LB/IN					
0.00000	0.00000	0.00000	0.00000	0.00000	0.00000
AXIAL BLADE FORCE LB/IN					
1.45106	.96504	.39911	-.16793	-.34909	-.22459
VEL HEAD 2					
.20773	.19125	.16743	.12853	.08768	.03871
$Q=E**(-S/CP)$					
1.00000	1.00000	1.00000	1.00000	1.00000	1.00000
RVU/					
0.00000	0.00000	0.00000	0.00000	0.00000	0.00000
DRVU/DM					
-0.00000	-0.00000	-0.00000	-0.00000	-0.00000	-0.00000
STRMLN DIST M					
.01379	-.00922	-.03749	-.06629	-.05927	.07574

Rotor 1A Inlet

STATION 1.00000 ROTOR XI = 0.00000

P = 1. ZTIP = 0.00000 AR = 3.40000 XN = 0. BNXT = 1.
 = 0. ZHUB = 0.00000 LOSS = 3. EXP = -0.0000 BLADES = 1.

RADIUS

1.91300	1.84000	1.74000	1.56000	1.33000	.86450
SLOPE					
20.33000	21.10000	22.23000	28.53000	35.00000	42.53000
CURVATURE					
.49296	.28700	.28600	.52900	.59900	.56700
LOSS COEFF					
1.00000	1.00000	1.00000	1.00000	1.00000	1.00000
SOLIDITY					
1.00000	1.00000	1.00000	1.00000	1.00000	1.00000
BLADE THICKNESS					
.01174	.01201	.01255	.01432	.01835	.02630
AERO BLOCKAGE					
.98000	.98000	.98000	.98000	.98000	.98000
TOTAL BLOCKAGE					
.97904	.97898	.97887	.97857	.97785	.97525
BLADE ANGLE					
59.26314	58.35051	57.17567	56.57143	57.55473	56.48617
LEAN					
.94632	2.23809	3.55011	4.35245	2.60429	5.91810
Y					
0.00000	0.00000	0.00000	0.00000	0.00000	0.00000

VOR ITES = 1 AREA RATIO = 1.00082 EXP = 1.50000 CHOKE = .74162

RADIUS

1.91300	1.85028	1.75006	1.56071	1.31442	.86450
Z					
0.00000	0.00000	0.00000	0.00000	0.00000	0.00000
CROSS PASSAGE DIST P					
1.04850	.98578	.88556	.69621	.44992	0.00000
SLOPE					
20.33000	20.24422	20.64932	24.97660	31.49755	42.53000
CURVATURE					
.49296	.40247	.34868	.44057	.55846	.56700
DELTA CURVATURE					
0.00000	.00351	.00671	.00603	.00303	0.00000
VM					
675.36652	656.86940	636.21722	592.00793	498.98170	371.73075
VU2					
1166.93000	1128.66885	1067.53566	952.03020	801.79782	527.34500
U					
1166.93000	1128.66885	1067.53566	952.03020	801.79782	527.34500
VR					
234.64044	227.29167	224.36034	249.97430	260.69912	251.28121
BETA2					
59.93965	59.80117	59.20638	58.12508	58.10479	54.81959
BETA2*					
61.51117	61.36391	60.85240	60.59075	62.04793	62.54969

INCIDENCE					
2.22555	2.76422	3.29834	3.55899	4.27953	5.03112
1.25633	1.21428	1.15293	1.03531	.86477	.58546
V2					
1348.27503	1305.89846	1242.74081	1121.08648	944.38471	645.19493
TOTAL TEMP					
1.00000	1.00000	1.00000	1.00000	1.00000	1.00000
TOTAL PRESS					
1.00000	1.00000	1.00000	1.00000	1.00000	1.00000
EFFICIENCY					
0.00000	0.00000	0.00000	0.00000	0.00000	0.00000
STATIC TEMP					
.92751	.93143	.93567	.94430	.96043	.97804
STATIC PRESS					
.76651	.77800	.79060	.81667	.86704	.92453
DENSITY					
.82641	.83528	.84496	.86485	.90276	.94529
SUCT SURF VEL					
0.00000	0.00000	0.00000	0.00000	0.00000	0.00000
PRESS SURF VEL					
0.00000	0.00000	0.00000	0.00000	0.00000	0.00000
DELTA T					
0.00000	0.00000	0.00000	0.00000	0.00000	0.00000
WORK COEF = $2*CP*DELT/U**2$					
0.00000	0.00000	0.00000	0.00000	0.00000	0.00000
FLOW COEF = VM/U					
.57875	.58199	.59597	.62184	.62233	.70491
R BAR					
1.86375	1.80016	1.69719	1.49737	1.23058	.73225
D-FACTOR					
-1.12843	-1.15610	-1.20388	-1.28717	-1.35140	-1.44020
VM2/VM1					
1.06616	1.08452	1.12827	1.20778	1.24240	1.40593
DELP/Q					
-.12401	-.16076	-.25064	-.42636	-.51634	-.94954
TANG BLADE FORCE LB/IN					
0.00000	0.00000	0.00000	0.00000	0.00000	0.00000
AXIAL BLADE FORCE LB/IN					
-4.26027	-3.95459	-3.70427	-4.14983	-3.71917	-2.05651
VEL HEAD 2					
.61641	.59445	.56096	.49239	.38518	.20649
Q=E**(-S/CP)					
1.00000	1.00000	1.00000	1.00000	1.00000	1.00000
RVU/					
0.00000	0.00000	0.00000	0.00000	0.00000	0.00000
DRVU/DM					
1.53101	1.98077	2.38156	2.92120	3.00299	2.46391
STRMLN DIST M					
.45144	.42879	.40167	.37871	.39987	.57951

STATION 1.20000 ROTOR XI = .81762

P = 1. ZTIP = .08600 AR = 10.00000 XN = 0. BNXT = 1.
 = 0. ZHUB = .10000 LOSS = 3. EXP = -0.0000 BLADES = 20.

RADIUS	1.94700	1.87700	1.77800	1.59700	1.35500	.96600
SLOPE	23.00000	26.00000	27.00000	32.00000	36.00000	46.40000
CURVATURE	.48400	.41000	.39000	.37000	.35000	.39900
LOSS COEFF	.99760	.99715	.99848	.99915	.99949	.99937
SOLIDITY	1.00000	1.00000	1.00000	1.00000	1.00000	1.00000
BLADE THICKNESS	.03884	.04130	.04638	.05614	.07071	.05472
AERO BLOCKAGE	.97800	.97800	.97800	.97800	.97800	.97800
TOTAL BLOCKAGE	.91590	.90950	.89679	.86857	.81556	.80167
BLADE ANGLE	59.17886	58.35729	57.22589	56.37186	55.95303	48.13260
LEAN	.46646	1.15476	1.77076	.16200	-2.88071	.34465
Y	-.17150	-.22400	-.27580	-.36000	-.41000	-.45000

NOR ITES = 2 AREA RATIO = 1.00053 EXP = 1.50000 CHOKE = .79880

RADIUS	1.94700	1.88408	1.78557	1.60363	1.37143	.96600
Z	.08600	.08690	.08830	.09090	.09421	.10000
CROSS PASSAGE DIST P	.98110	.91817	.81966	.63770	.40547	0.00000
SLOPE	23.00000	24.30210	25.51653	28.96800	33.38571	46.40000
CURVATURE	.48400	.50565	.58653	.49929	.31142	.39900
DELTA CURVATURE	0.00000	.00190	.00361	.00206	-.00194	0.00000
VM	679.10299	682.26624	682.41207	657.34676	574.68693	329.97218
VU2	1133.93862	1076.76211	994.97995	841.27789	654.20934	304.86549
U	1187.67000	1149.28576	1089.20059	978.21685	836.57348	589.26000
VR	265.34678	280.78528	293.96380	318.36697	316.23456	238.95664
BETA2	59.08306	57.64050	55.55550	51.99708	48.70245	42.73522
BETA2*	61.13291	59.99437	58.24423	55.64306	53.74036	53.26189

INCIDENCE					
1.97828	1.48051	.73095	-.81329	-1.72876	5.00144
1.21917	1.17261	1.10666	.97234	.78509	.39858
V2					
1321.74039	1274.71717	1206.51205	1067.63910	870.77834	449.24894
TOTAL TEMP					
1.02028	1.02649	1.03262	1.04258	1.04849	1.05327
TOTAL PRESS					
1.06446	1.08580	1.11411	1.15527	1.18001	1.19860
EFFICIENCY					
.87928	.88958	.95188	.97919	.98897	.98754
STATIC TEMP					
.94653	.95168	.95720	.97092	.99072	1.02307
STATIC PRESS					
.81655	.83102	.85219	.89828	.96584	1.08150
DENSITY					
.86267	.87322	.89029	.92518	.97489	1.05712
SUCT SURF VEL					
1474.02201	1447.33108	1390.36306	1258.98112	1050.77412	597.63334
PRESS SURF VEL					
1169.45877	1102.10325	1022.66104	876.29708	690.78256	300.86454
DELTA T					
10.52123	13.74201	16.91985	22.08538	25.15279	27.62936
WORK COEF = $2*CP*DELTA T/U**2$					
.09048	.12621	.17301	.27998	.43598	.96526
FLOW COEF = VM/U					
.57179	.59364	.62653	.67198	.68695	.55998
R BAR					
1.93000	1.86718	1.76782	1.58217	1.34293	.91525
D-FACTOR					
.03978	.05190	.06744	.10958	.17654	.53632
VM2/VM1					
1.00553	1.03866	1.07261	1.11037	1.15172	.88766
DELP/Q					
.04063	.04649	.06096	.10302	.18189	.65245
TANG BLADE FORCE LB/IN					
5.27018	6.77611	8.15294	9.77808	9.03406	5.62317
AXIAL BLADE FORCE LB/IN					
8.12354	9.65081	11.80633	14.62866	14.88641	12.39769
VEL HEAD 2					
.59704	.57188	.53464	.45366	.33344	.10335
Q=E**(-S/CP)					
.99760	.99715	.99848	.99915	.99949	.99937
RVU/					
.17150	.22400	.27580	.36000	.41000	.45037
DRVU/DM					
3.30292	3.61985	3.70066	3.65233	3.41331	2.57688
STRMLN DIST M					
.54392	.52203	.49685	.47924	.50999	.72200

STATION 1.40000 ROTOR XI = 1.76046

P = 1. ZTIP = .17200 AR = 9.00000 XN = 0. BNXT = 1.
 = 0. ZHUB = .20000 LOSS = 3. EXP = -0.0000 BLADES = 20.

RADIUS	1.98500	1.91700	1.82500	1.65300	1.42500	1.07400
SLOPE	25.56000	29.00000	33.00000	36.00000	42.00000	49.25000
CURVATURE	.47100	.41000	.45000	.39000	.32000	.27400
LOSS COEFF	.99155	.99147	.99612	.99793	.99900	.99877
SOLIDITY	1.00000	1.00000	1.00000	1.00000	1.00000	1.00000
BLADE THICKNESS	.05372	.06013	.06590	.07658	.08744	.07592
AERO BLOCKAGE	.97600	.97600	.97600	.97600	.97600	.97600
TOTAL BLOCKAGE	.89193	.87855	.86381	.83207	.78537	.75640
BLADE ANGLE	59.07060	58.30032	57.19764	55.91262	53.52590	38.79420
LEAN	.34847	.25606	.10707	-1.86332	-3.57562	-.34511
Y	-.62050	-.69020	-.72360	-.75000	-.76000	-.74000

NOR ITES = 2 AREA RATIO = 1.00097 EXP = 1.50000 CHOKE = .80065

RADIUS	1.98500	1.92408	1.82947	1.65489	1.43316	1.07400
Z	.17200	.17387	.17678	.18215	.18896	.20000
CROSS PASSAGE DIST P	.91143	.85048	.75583	.58116	.35933	0.00000
SLOPE	25.56000	27.50226	30.56697	33.64937	37.53989	49.25000
CURVATURE	.47100	.38531	.40496	.47264	.45323	.27400
DELTA CURVATURE	0.00000	.00219	.00224	.00283	.00243	0.00000
VM	622.95147	643.54557	665.15009	652.40416	599.14774	450.69835
VU2	1020.16738	954.86873	874.70747	733.02958	550.75036	234.34766
U	1210.85000	1173.68647	1115.97723	1009.48298	874.23033	655.14000
VR	268.77629	297.17890	338.25900	361.50323	365.06904	341.43339
BETA2	58.59021	56.02149	52.74968	48.33055	42.58992	27.47287
BETA2*	61.15066	59.12901	56.78507	53.46582	49.21866	38.53960

INCIDENCE					
2.13580	.74484	-.50880	-2.16403	-3.50747	-.00879
1.06951	1.02913	.98318	.87672	.72447	.44981
V2					
1195.32841	1151.48825	1098.88025	981.30706	813.82060	507.98408
TOTAL TEMP					
1.07339	1.08163	1.08558	1.08871	1.08989	1.08763
TOTAL PRESS					
1.24641	1.28020	1.31842	1.34044	1.35070	1.33973
EFFICIENCY					
.87641	.88698	.95078	.97459	.98788	.98473
STATIC TEMP					
1.00594	1.00820	1.00602	1.00891	1.01621	1.02710
STATIC PRESS					
.99097	.99860	1.00749	1.02433	1.05472	1.09432
DENSITY					
.98512	.99047	1.00147	1.01528	1.03790	1.06545
SUCT SURF VEL					
1435.74494	1395.25521	1326.97959	1173.23247	974.75540	633.81377
PRESS SURF VEL					
954.91189	907.72129	870.78090	789.38166	652.88581	382.15439
DELTA T					
27.54538	28.60057	27.47176	23.92583	21.47190	17.82176
WORK COEF = $2*CP*DELTA T/U**2$					
.22791	.25186	.26759	.28481	.34081	.50370
FLOW COEF = VM/U					
.51447	.54831	.59602	.64628	.68534	.68794
R BAR					
1.96600	1.90408	1.80752	1.62926	1.40230	1.02000
D-FACTOR					
.14834	.15525	.15184	.14925	.15283	.06262
VM2/VM1					
.91732	.94325	.97470	.99248	1.04256	1.36587
DELP/Q					
.14417	.15096	.15863	.16899	.18395	.10285
TANG BLADE FORCE LB/IN					
13.96201	14.45875	13.69554	11.09546	8.36079	3.89658
AXIAL BLADE FORCE LB/IN					
25.33687	24.52577	22.01105	16.52824	11.24311	2.69990
VEL HEAD 2					
.51288	.48865	.46041	.39289	.29409	.12921
$Q=E**(-S/CP)$					
.99155	.99147	.99612	.99793	.99900	.99877
RVU/					
.62050	.69020	.72360	.75000	.76000	.74087
DRVU/DM					
5.26826	5.05612	4.44283	3.53191	2.83097	1.90756
STRMLN DIST M					
.63794	.61776	.59562	.58390	.62307	.86918

STATION 1.60000 ROTOR XI = 2.88642

AR = 1. ZTIP = .25800 AR = 8.50000 XN = 0. BNXT = 1.
 = 0. ZHUB = .30000 LOSS = 3. EXP = -0.0000 BLADES = 20.

RADIUS	2.02800	1.96200	1.87500	1.71300	1.50000	1.19500
SLOPE	28.05000	30.00000	33.00000	37.00000	44.00000	51.17000
CURVATURE	.43850	.38000	.40000	.37000	.30000	.16800
LOSS COEFF	.98453	.98554	.99389	.99681	.99852	.99818
SOLIDITY	1.00000	1.00000	1.00000	1.00000	1.00000	1.00000
BLADE THICKNESS	.05866	.06151	.06646	.07406	.07946	.07774
AERO BLOCKAGE	.97400	.97400	.97400	.97400	.97400	.97400
TOTAL BLOCKAGE	.88431	.87680	.86411	.83997	.80977	.77230
BLADE ANGLE	58.76147	58.10414	56.97868	54.73916	50.63974	28.24758
LEAN	.17521	.22499	-.35545	-1.59983	-2.23997	3.66601
Y	-1.17550	-1.20720	-1.16840	-1.11500	-1.06500	-1.03000

NOR ITES = 1 AREA RATIO = .99921 EXP = 1.50000 CHOKE = .76550

RADIUS	2.02800	1.97022	1.88049	1.71516	1.50516	1.19500
Z	.25800	.26091	.26544	.27377	.28436	.30000
CROSS PASSAGE DIST P	.83406	.77621	.68636	.52083	.31056	0.00000
SLOPE	28.05000	29.32366	31.36749	35.38910	40.82717	51.17000
CURVATURE	.43850	.39979	.32942	.25764	.30264	.16800
DELTA CURVATURE	0.00000	.00107	-.00013	.00136	.00419	0.00000
VM	582.55347	592.07595	610.76159	594.97936	576.57891	553.41793
VU2	883.50258	828.07518	768.08661	649.69959	486.53656	203.56435
U	1237.08000	1201.83595	1147.09697	1046.25044	918.15046	728.95000
VR	273.94116	289.96491	317.91694	344.56821	376.95563	431.11810
BETA2	56.60039	54.43511	51.50921	47.51727	40.15877	20.19509
BETA2*	59.80412	58.06109	55.82523	53.25587	48.11667	30.39765

INCIDENCE

1.07353	-.17743	-1.23243	-1.18776	-1.85675	-.95057
.92016	.88526	.85693	.77130	.66275	.52159
V2					
1058.27471	1017.96976	981.31889	880.97105	754.42763	589.66927
TOTAL TEMP					
1.13903	1.14278	1.13819	1.13188	1.12596	1.12173
TOTAL PRESS					
1.49916	1.52218	1.54610	1.53180	1.51284	1.49106
EFFICIENCY					
.87326	.88427	.94968	.97262	.98677	.98323
STATIC TEMP					
1.06523	1.06487	1.05608	1.05062	1.04352	1.02928
STATIC PRESS					
1.18316	1.18604	1.18666	1.17729	1.15639	1.10025
DENSITY					
1.11071	1.11379	1.12365	1.12056	1.10816	1.06895
SUCT SURF VEL					
1305.99580	1247.92872	1177.64426	1047.41850	903.33513	719.57768
PRESS SURF VEL					
810.55363	788.01081	784.99352	714.52361	605.52013	459.76085
DELTA T					
34.04829	31.71706	27.28771	22.39212	18.71122	17.69092
WORK COEF = $2*CP*DELTA T/U**2$					
.26989	.26637	.25157	.24815	.26925	.40387
FLOW COEF = VM/U					
.47091	.49264	.53244	.56868	.62798	.75920
R BAR					
2.00650	1.94715	1.85498	1.68503	1.46916	1.13450
D-FACTOR					
.18524	.18628	.17354	.16957	.15078	-.00819
VM2/VM1					
.93515	.92002	.91823	.91198	.96233	1.22791
DELP/Q					
.18421	.19642	.20841	.23074	.23137	.03650
TANG BLADE FORCE LB/IN					
17.77488	16.73405	14.52202	10.91417	7.79031	5.03029
AXIAL BLADE FORCE LB/IN					
30.54475	28.03795	25.58445	18.99156	11.39760	2.33108
VEL HEAD 2					
.42074	.39839	.38011	.32447	.25454	.16873
Q=E*(-S/CP)					
.98453	.98554	.99389	.99681	.99852	.99818
RVU/					
1.17550	1.20720	1.16840	1.11500	1.06500	1.02924
DRVU/DM					
5.17283	4.58244	3.70900	2.98142	2.44438	1.81881
STRMLN DIST M					
.73409	.71627	.69790	.69357	.74259	1.02616

STATION 1.80000 ROTOR XI = 4.24198
P = 1. ZTIP = .34400 AR = 8.00000 XN = 0. BNXT = 1.
= 0. ZHUB = .40000 LOSS = 3. EXP = -0.0000 BLADES = 20.

RADIUS	2.07600	2.01400	1.93500	1.78400	1.58700	1.32100
SLOPE	30.36000	33.00000	35.00000	39.00000	46.00000	52.22000
CURVATURE	.39500	.36000	.39000	.37000	.28000	.10420
LOSS COEFF	.97917	.98124	.99235	.99604	.99806	.99761
SOLIDITY	1.00000	1.00000	1.00000	1.00000	1.00000	1.00000
BLADE THICKNESS	.04829	.04956	.05155	.05429	.05278	.04982
AERO BLOCKAGE	.97200	.97200	.97200	.97200	.97200	.97200
TOTAL BLOCKAGE	.90004	.89586	.88958	.87784	.86911	.85531
BLADE ANGLE	57.80893	57.40181	56.47022	53.50556	46.75384	15.13302
LEAN	-1.03805	-.52280	-.31771	-.54264	1.58310	9.81008
Y	-1.62450	-1.60210	-1.48920	-1.41300	-1.36000	-1.31900

VOR ITES = 1 AREA RATIO = .99980 EXP = 1.50000 CHOKE = .72113

RADIUS	2.07600	2.02196	1.93658	1.78181	1.58784	1.32100
Z	.34400	.34801	.35434	.36582	.38021	.40000
CROSS PASSAGE DIST P	.75707	.70288	.61727	.46208	.26758	0.00000
SLOPE	30.36000	32.20885	33.65790	37.22678	43.60244	52.22000
CURVATURE	.39500	.39718	.46160	.41899	.34295	.10420
DELTA CURVATURE	0.00000	.00151	.00160	.00074	.00242	0.00000
VM	569.05498	560.62979	573.51394	552.09384	534.22265	556.09083
VU2	789.02618	750.06049	712.23189	603.16532	446.11491	196.82175
U	1266.36000	1233.39444	1181.31282	1086.90387	968.58454	805.81000
VR	287.61842	298.81973	317.86045	334.00108	368.42700	439.51704
BETA2	54.20039	53.22384	51.15775	47.53125	39.86433	19.49080
BETA2*	58.10558	57.68981	56.16815	53.91441	49.06945	30.01650

INCIDENCE

.49658	.34722	-.27445	.63285	1.56243	2.66848
.83070	.80036	.78640	.70561	.60321	.51713
V2					
972.82367	936.42752	914.43562	817.68944	695.99738	589.89475
TOTAL TEMP					
1.19214	1.18949	1.17614	1.16712	1.16086	1.15598
TOTAL PRESS					
1.72744	1.72675	1.72656	1.70245	1.68236	1.65490
EFFICIENCY					
.87076	.88224	.94892	.97234	.98600	.98229
STATIC TEMP					
1.10446	1.10241	1.08889	1.08149	1.07211	1.04792
STATIC PRESS					
1.31878	1.31995	1.31493	1.30057	1.27022	1.16991
DENSITY					
1.19405	1.19734	1.20758	1.20257	1.18478	1.11642
SUCT SURF VEL					
1136.09084	1077.71637	1028.70432	926.84144	807.70420	696.69691
PRESS SURF VEL					
809.55650	795.13868	800.16692	708.53743	584.29056	483.09260
DELTA T					
27.54538	24.22643	19.68053	18.28179	18.09774	17.76461
WORK COEF = $2*CP*DEL T/U**2$					
.20836	.19318	.17108	.18773	.23401	.33188
FLOW COEF = VM/U					
.44936	.45454	.48549	.50795	.55155	.69010
R BAR					
2.05200	1.99609	1.90853	1.74849	1.54650	1.25800
D-FACTOR					
.14381	.13938	.12040	.13084	.15457	.11868
VM2/VM1					
.97683	.94689	.93901	.92792	.92654	1.00483
DELP/Q					
.15781	.17051	.17628	.21801	.28829	.31195
TANG BLADE FORCE LB/IN					
15.25267	13.19168	10.87085	9.25958	7.99653	6.36669
AXIAL BLADE FORCE LB/IN					
23.00964	20.06602	17.88906	15.82280	12.83092	7.79054
VEL HEAD 2					
.36310	.34338	.33429	.28192	.21733	.16617
$Q=E**(-S/CP)$					
.97917	.98124	.99235	.99604	.99806	.99761
RVU/					
1.62450	1.60210	1.48920	1.41300	1.36000	1.31881
DRVU/DM					
3.14583	2.67227	2.07773	1.86961	1.70276	1.34754
STRMLN DIST M					
.83258	.81758	.80302	.80721	.86917	1.18702

Rotor 1A Exit

STATION 2.00000 ROTOR XI = 5.91192

P = 1. ZTIP = .43000 AR = 7.50000 XN = 0. BNXT = 1.

 0. ZHUB = .50000 LOSS = 3. EXP = -0.0000 BLADES = 1.

RADIUS	2.13000	2.08300	2.00700	1.86700	1.69200	1.45400
SLOPE	32.54000	34.10000	36.20000	40.10000	45.50000	53.40000
CURVATURE	.35550	.27500	.28400	.23900	.19200	.10670
LOSS COEFF	.97719	.97969	.99180	.99577	.99761	.99706
SOLIDITY	1.00000	1.00000	1.00000	1.00000	1.00000	1.00000
BLADE THICKNESS	.01230	.01242	.01269	.01315	.01254	.01237
AERO BLOCKAGE	.96900	.96900	.96900	.96900	.96900	.96900
TOTAL BLOCKAGE	.96811	.96808	.96803	.96791	.96786	.96769
BLADE ANGLE	56.26243	56.19262	55.43665	51.94140	40.38929	-4.48826
LEAN	-5.07140	-3.45422	-1.09982	2.06675	9.18285	21.12723
Y	-1.79600	-1.74920	-1.60560	-1.54170	-1.49950	-1.46470

NOR ITES = 1 AREA RATIO = 1.00052 EXP = 1.50000 CHOKE = .67449

RADIUS	2.13000	2.07962	1.99985	1.85675	1.68272	1.45400
Z	.43000	.43522	.44348	.45829	.47632	.50000
CROSS PASSAGE DIST P	.67961	.62896	.54877	.40491	.22994	0.00000
SLOPE	32.54000	34.37235	36.54114	40.38325	46.03186	53.40000
CURVATURE	.35550	.32311	.37959	.39267	.30595	.10670
DELTA CURVATURE	0.00000	.00081	.00157	.00232	.00173	0.00000
VM	533.75767	520.44278	531.17269	513.16549	494.64680	492.21442
VU2	784.95258	755.48596	730.16081	626.12523	482.87482	272.26824
U	1299.30000	1268.56680	1219.90639	1132.62029	1026.45714	886.94000
VR	287.10210	293.82584	316.26026	332.47861	356.01024	395.15846
BETA2	55.78478	55.43761	53.96508	50.66230	44.31002	28.94915
BETA2*	60.17691	60.37760	59.69481	58.02329	54.58017	42.85372

INCIDENCE

5.25179	5.27168	4.90401	5.94908	9.70528	14.19160
.80309	.77722	.77015	.69277	.59376	.48693
V2					
949.23538	917.39834	902.92814	809.55026	691.26229	562.49892
TOTAL TEMP					
1.21242	1.20689	1.18990	1.18235	1.17735	1.17329
TOTAL PRESS					
1.82049	1.80754	1.79552	1.78050	1.76557	1.74073
EFFICIENCY					
.86981	.88152	.94862	.97257	.98413	.98009
STATIC TEMP					
1.12510	1.12200	1.10694	1.09972	1.09151	1.07469
STATIC PRESS					
1.39790	1.39690	1.39086	1.37839	1.35113	1.27649
DENSITY					
1.24247	1.24501	1.25649	1.25339	1.23786	1.18778
SUCT SURF VEL					
0.00000	0.00000	1804.31950	0.00000	0.00000	0.00000
PRESS SURF VEL					
0.00000	0.00000	1.53678	0.00000	0.00000	0.00000
DELTA T					
10.52123	9.02433	7.14094	7.89552	8.55808	8.97689
WORK COEF = $2*CP*DELTA/U**2$					
.07560	.06803	.05821	.07466	.09853	.13843
FLOW COEF = VM/U					
.41080	.41026	.43542	.45308	.48190	.55496
R BAR					
2.10300	2.05079	1.96821	1.81928	1.63528	1.38750
D-FACTOR					
.04981	.04368	.03231	.03634	.04419	.10097
VM2/VM1					
.93797	.92832	.92617	.92949	.92592	.88513
DELP/Q					
.10523	.11148	.11500	.15240	.22941	.45712
TANG BLADE FORCE LB/IN					
6.31613	5.23518	4.17981	4.25519	4.07574	3.66045
AXIAL BLADE FORCE LB/IN					
10.09841	9.16290	7.89000	8.22464	8.77219	10.91845
VEL HEAD 2					
.34515	.32832	.32372	.27368	.21154	.14921
$Q=E*(-S/CP)$					
.97719	.97969	.99180	.99577	.99761	.99706
RVU/					
1.79600	1.74920	1.60560	1.54170	1.49950	1.46514
DRVU/DM					
1.29161	1.06866	.80059	.79600	.73766	.59052
STRMLN DIST M					
.93413	.92212	.91233	.92624	1.00422	1.35342

Rotor 1B Inlet

STATION 3.00000 ROTOR XI = 0.00000

P = 1. ZTIP = .70000 AR = 6.00000 XN = 0. BNXT = 1.
 = -0. ZHUB = .70000 LOSS = 3. EXP = -0.0000 BLADES = 1.

RADIUS

2.32000	2.27700	2.21070	2.08780	1.93780	1.73000
---------	---------	---------	---------	---------	---------

SLOPE

36.59429	37.15283	38.57043	42.26202	47.34751	54.44440
----------	----------	----------	----------	----------	----------

CURVATURE

.10760	.08914	.08409	.09035	.00719	-0.00000
--------	--------	--------	--------	--------	----------

LOSS COEFF

.97791	.98049	.99034	.99548	.99711	.99811
--------	--------	--------	--------	--------	--------

SOLIDITY

1.00000	1.00000	1.00000	1.00000	1.00000	1.00000
---------	---------	---------	---------	---------	---------

BLADE THICKNESS

.01168	.01225	.01327	.01510	.01698	.01955
--------	--------	--------	--------	--------	--------

AERO BLOCKAGE

.96100	.96100	.96100	.96100	.96100	.96100
--------	--------	--------	--------	--------	--------

TOTAL BLOCKAGE

.96023	.96018	.96008	.95989	.95966	.95927
--------	--------	--------	--------	--------	--------

BLADE ANGLE

59.33508	58.61771	58.23417	58.29549	58.27538	58.69649
----------	----------	----------	----------	----------	----------

LEAN

-2.46299	-1.98986	-1.78518	-1.98243	-1.58136	-0.02982
----------	----------	----------	----------	----------	----------

Y

-1.79603	-1.74922	-1.60563	-1.54172	-1.49950	-1.46465
----------	----------	----------	----------	----------	----------

VOR ITES = 1 AREA RATIO = 1.00017 EXP = 1.50000 CHOKE = .76461

RADIUS

2.32000	2.27686	2.20915	2.08457	1.93523	1.73000
---------	---------	---------	---------	---------	---------

Z

.70000	.70000	.70000	.70000	.70000	.70000
--------	--------	--------	--------	--------	--------

CROSS PASSAGE DIST P

.59000	.54686	.47915	.35457	.20523	0.00000
--------	--------	--------	--------	--------	---------

SLOPE

36.59429	37.31240	39.18222	43.04870	48.18286	54.44440
----------	----------	----------	----------	----------	----------

CURVATURE

.10760	.00969	-.06598	-.11688	-.12324	-0.00000
--------	--------	---------	---------	---------	----------

DELTA CURVATURE

0.00000	-.00224	-.00272	-.00178	.00006	0.00000
---------	---------	---------	---------	--------	---------

VM

659.79561	655.37553	648.12690	625.72504	575.42108	487.70786
-----------	-----------	-----------	-----------	-----------	-----------

VU2

942.96797	920.24467	904.22478	820.44093	707.83470	538.82859
-----------	-----------	-----------	-----------	-----------	-----------

U

1415.20000	1388.88351	1347.57905	1271.58847	1180.48946	1055.30000
------------	------------	------------	------------	------------	------------

VR

393.33391	397.26293	409.47944	427.13243	428.84802	396.77563
-----------	-----------	-----------	-----------	-----------	-----------

BETA2

55.01946	54.54245	54.36792	52.66833	50.89123	47.85091
----------	----------	----------	----------	----------	----------

BETA2*

60.67385	60.47176	60.94332	60.86737	61.54112	62.24107
----------	----------	----------	----------	----------	----------

INCIDENCE

1.99044	2.48105	3.42964	3.44488	4.26901	4.14459
.98126	.96503	.95543	.88781	.78437	.62383
V2					
1150.87742	1129.76428	1112.51559	1031.82127	912.21675	726.77039
TOTAL TEMP					
1.21243	1.20689	1.18991	1.18235	1.17735	1.17324
TOTAL PRESS					
1.82525	1.81277	1.78622	1.77868	1.76244	1.74697
EFFICIENCY					
.87392	.88619	.93947	.97069	.98081	.98720
STATIC TEMP					
1.10780	1.10372	1.09191	1.08777	1.08923	1.09304
STATIC PRESS					
1.32686	1.32194	1.31836	1.32483	1.33881	1.36024
DENSITY					
1.19775	1.19771	1.20739	1.21793	1.22913	1.24446
SUCT SURF VEL					
0.00000	0.00000	0.00000	0.00000	0.00000	0.00000
PRESS SURF VEL					
0.00000	0.00000	0.00000	0.00000	0.00000	0.00000
DELTA T					
.00184	.00123	.00184	.00123	0.00000	-.02386
WORK COEF = $2*CP*DELT/U**2$					
.00001	.00001	.00001	.00001	0.00000	-.00026
FLOW COEF = VM/U					
.46622	.47187	.48096	.49208	.48744	.46215
R BAR					
2.22500	2.17824	2.10450	1.97066	1.80897	1.59200
D-FACTOR					
-.21242	-.23148	-.23211	-.27456	-.31964	-.29191
VM2/VM1					
1.23613	1.25927	1.22018	1.21934	1.16330	.99084
DELP/Q					
-.09642	-.10978	-.10890	-.10311	-.03400	.37408
TANG BLADE FORCE LB/IN					
.00107	.00069	.00103	.00063	0.00000	-.00819
AXIAL BLADE FORCE LB/IN					
-4.24324	-3.69989	-5.14662	-3.03693	1.13279	11.75259
VEL HEAD 2					
.45922	.44909	.44306	.40003	.33297	.23008
Q=E**(-S/CP)					
.97791	.98049	.99034	.99548	.99711	.99811
RVU/					
1.79603	1.74922	1.60563	1.54172	1.49950	1.46475
DRVU/DM					
6.67514	6.57895	5.44380	5.44477	3.96447	3.91197
STRMLN DIST M					
1.26428	1.25230	1.24340	1.25839	1.34156	1.69426

STATION 3.20000 ROTOR XI = .84563

P = 1. ZTIP = .75700 AR = 6.00000 XN = 0. BNXT = 1.
 = -0. ZHUB = .76500 LOSS = 3. EXP = -0.0000 BLADES = 40.

RADIUS	2.36200	2.31930	2.25660	2.14210	2.00680	1.82000
SLOPE	38.00376	38.12298	38.29803	41.82005	46.92217	53.25115
CURVATURE	.15000	.34853	.09474	-.20976	-.15283	-.04800
LOSS COEFF	.97496	.97768	.98929	.99506	.99688	.99782
SOLIDITY	1.00000	1.00000	1.00000	1.00000	1.00000	1.00000
BLADE THICKNESS	.02596	.02771	.03034	.03492	.03812	.04425
AERO BLOCKAGE	.96100	.96100	.96100	.96100	.96100	.96100
TOTAL BLOCKAGE	.89376	.88791	.87874	.86127	.84479	.81225
BLADE ANGLE	59.21263	58.36701	57.40559	56.60486	54.75606	51.76280
LEAN	-.96817	-1.37002	-2.15564	-3.59881	-3.25803	-2.45331
Y	-2.37000	-2.32900	-2.10850	-2.10000	-1.97130	-2.04000

NOR ITES = 2 AREA RATIO = 1.00078 EXP = 1.50000 CHOKE = .79636

RADIUS	2.36200	2.32053	2.25643	2.14046	2.00462	1.82000
Z	.75700	.75761	.75856	.76027	.76228	.76500
CROSS PASSAGE DIST P	.54206	.50059	.43648	.32049	.18464	0.00000
SLOPE	38.00376	37.61596	38.44405	41.92147	47.09760	53.25115
CURVATURE	.15000	.22837	-.04398	-.27358	-.22420	-.04800
DELTA CURVATURE	0.00000	-.00586	-.00910	-.00528	-.00463	0.00000
VM	658.11611	669.15864	659.76570	677.55026	620.42896	568.25061
VU2	828.75395	803.30054	806.41302	707.21106	622.95619	426.28117
U	1440.82000	1415.52593	1376.42197	1305.68056	1222.81740	1110.20000
VR	405.21092	408.43172	410.20956	452.67926	454.47331	455.31993
BETA2	51.54678	50.20529	50.71171	46.22704	45.11644	36.87590
BETA2*	57.96454	56.58136	57.34877	54.51663	55.86312	51.42517

INCIDENCE					
-1.14065	-1.63380	.48323	-1.13020	2.47947	.93493
.88485	.87691	.88015	.83105	.74727	.60355
V2					
1058.27687	1045.49751	1041.91781	979.39871	879.20789	710.36920
TOTAL TEMP					
1.28031	1.27546	1.24938	1.24838	1.23316	1.24135
TOTAL PRESS					
2.18924	2.18145	2.11426	2.15203	2.07408	2.13024
EFFICIENCY					
.88563	.89665	.94634	.97517	.98350	.98879
STATIC TEMP					
1.15194	1.14473	1.12857	1.11850	1.11479	1.11562
STATIC PRESS					
1.50713	1.48864	1.47599	1.45966	1.45200	1.46069
DENSITY					
1.30834	1.30043	1.30784	1.30502	1.30249	1.30930
SUCT SURF VEL					
1256.56349	1257.72594	1210.69616	1150.19510	1024.98909	862.48547
PRESS SURF VEL					
859.99025	833.26909	873.13947	808.60232	733.42668	558.25293
DELTA T					
35.21207	35.56850	30.85021	34.24952	28.94412	35.32421
WORK COEF = $2*CP*DELT/U**2$					
.20576	.21534	.19753	.24371	.23481	.34766
FLOW COEF = VM/U					
.45676	.47273	.47933	.51892	.50738	.51185
R BAR					
2.34100	2.29870	2.23279	2.11252	1.96992	1.77500
D-FACTOR					
.14544	.14268	.12520	.12892	.11626	.15870
VM2/VM1					
.99745	1.02103	1.01796	1.08282	1.07822	1.16515
DELP/Q					
.15999	.15469	.15029	.15264	.16937	.24713
TANG BLADE FORCE LB/IN					
21.38554	21.61404	18.24042	18.87127	13.20959	12.18578
AXIAL BLADE FORCE LB/IN					
37.37248	36.61744	34.40019	31.78009	24.08295	19.93177
VEL HEAD 2					
.39813	.39302	.39510	.36333	.30886	.21754
Q=E**(-S/CP)					
.97496	.97768	.98929	.99506	.99688	.99782
RVU/					
2.37000	2.32900	2.10850	2.10000	1.97130	2.04054
DRVU/DM					
7.15604	7.49107	6.08454	5.75185	4.90195	4.69454
STRMLN DIST M					
1.33508	1.32459	1.31867	1.34058	1.43480	1.80528

STATION 3.40000 ROTOR XI = 1.96300

R = 1. ZTIP = .81100 AR = 6.00000 XN = 0. BNXT = 1.
 = -0. ZHUB = .82800 LOSS = 3. EXP = -0.0000 BLADES = 40.

RADIUS	2.40500	2.36030	2.29970	2.19290	2.07060	1.90900
SLOPE	38.72212	38.83091	39.07845	41.09818	46.27763	53.84123
CURVATURE	.17500	.01196	-.02285	.07902	-.09458	-.08000
LOSS COEFF	.97200	.97487	.98825	.99464	.99666	.99753
SOLIDITY	1.00000	1.00000	1.00000	1.00000	1.00000	1.00000
BLADE THICKNESS	.03180	.03461	.03828	.04339	.04729	.05488
AERO BLOCKAGE	.96100	.96100	.96100	.96100	.96100	.96100
TOTAL BLOCKAGE	.88011	.87129	.85916	.83995	.82127	.78512
BLADE ANGLE	58.46244	57.50910	56.31321	54.03466	50.00377	43.70551
LEAN	2.53867	1.24787	-.42408	-2.51336	-2.20933	-1.72651
Y	-2.80000	-2.81140	-2.50030	-2.47000	-2.39000	-2.50000

NOR ITES = 1 AREA RATIO = .99966 EXP = 1.50000 CHOKE = .78809

RADIUS	2.40500	2.36248	2.29995	2.19192	2.06891	1.90900
Z	.81100	.81246	.81460	.81830	.82252	.82800
CROSS PASSAGE DIST P	.49629	.45375	.39118	.28309	.16000	0.00000
SLOPE	38.72212	38.05880	37.82425	40.96159	46.14184	53.84123
CURVATURE	.17500	.04437	-.19296	.02532	-.08146	-.08000
DELTA CURVATURE	0.00000	.00484	-.00094	-.00308	-.00366	0.00000
VM	566.27296	607.81630	622.80998	678.95802	641.73171	627.34216
VU2	756.86289	715.20340	739.82818	649.68724	557.35986	365.72191
U	1467.05000	1441.11493	1402.96688	1337.07402	1262.03211	1164.49000
VR	354.22873	374.70059	381.93302	445.09305	462.72544	506.50686
BETA2	53.19672	49.64040	49.90828	43.73793	40.97511	30.24091
BETA2*	59.72680	56.21135	56.37774	51.72049	51.41847	44.65542

INCIDENCE

.78628	-1.75854	.17045	-1.57220	2.44375	1.88908
.77434	.77211	.80433	.78852	.71493	.61255
V2					
945.25473	938.59286	967.07704	939.72204	849.98211	726.16162
TOTAL TEMP					
1.33117	1.33252	1.29573	1.29214	1.28268	1.29566
TOTAL PRESS					
2.48547	2.52050	2.39571	2.42702	2.38182	2.47571
EFFICIENCY					
.88745	.89930	.94852	.97629	.98484	.98918
STATIC TEMP					
1.20005	1.19006	1.16419	1.14378	1.13831	1.13174
STATIC PRESS					
1.72296	1.69031	1.64119	1.57730	1.56195	1.53505
DENSITY					
1.43574	1.42036	1.40973	1.37902	1.37216	1.35636
SUCT SURF VEL					
1121.98774	1112.18154	1138.26550	1091.68953	1002.55302	869.87035
PRESS SURF VEL					
768.52172	765.00417	795.88858	787.75455	697.41121	582.45289
DELTA T					
26.37976	29.59441	24.03626	22.69886	25.68652	28.17153
WORK COEF = $2*CP*DELTA T/U**2$					
.14869	.17286	.14814	.15402	.19564	.25201
FLOW COEF = VM/U					
.38599	.42177	.44392	.50779	.50849	.53873
K BAR					
2.38350	2.34151	2.27819	2.16619	2.03676	1.86450
D-FACTOR					
.15879	.16235	.12217	.09370	.10455	.08351
VM2/VM1					
.86045	.90833	.94399	1.00208	1.03434	1.10399
DELP/Q					
.21649	.20923	.17136	.14122	.16944	.18310
TANG BLADE FORCE LB/IN					
16.13329	18.69729	15.06031	13.92480	13.17996	11.23414
AXIAL BLADE FORCE LB/IN					
36.24671	35.94245	31.18779	24.66660	23.01029	15.04917
VEL HEAD 2					
.32645	.32499	.34596	.33567	.28793	.22309
$Q=E*(-S/CP)$					
.97200	.97487	.98825	.99464	.99666	.99753
RVU/					
2.80000	2.81140	2.50030	2.47000	2.39000	2.49975
ORVU/DM					
6.72371	6.16753	6.19900	5.01324	4.92320	4.24534
STRMLN DIST M					
1.40411	1.39364	1.38962	1.41815	1.52290	1.91432

STATION 3.60000 ROTOR XI = 2.88747

P = 1. ZTIP = .86700 AR = 6.00000 XN = 0. BNXT = 1.
 = -0. ZHUB = .89000 LOSS = 3. EXP = -0.0000 BLADES = 40.

RADIUS	2.45000	2.40520	2.34510	2.24370	2.13240	1.99400
SLOPE	39.50742	38.59819	38.84416	40.86195	45.25754	53.14836
CURVATURE	.20000	.07639	.09166	.01780	.28169	-.11920
LOSS COEFF	.96906	.97207	.98720	.99423	.99643	.99725
SOLIDITY	1.00000	1.00000	1.00000	1.00000	1.00000	1.00000
BLADE THICKNESS	.03097	.03396	.03838	.04447	.04788	.05525
AERO BLOCKAGE	.96100	.96100	.96100	.96100	.96100	.96100
TOTAL BLOCKAGE	.88366	.87462	.86087	.83974	.82363	.79148
BLADE ANGLE	57.25140	55.83620	54.34767	50.91125	43.81139	32.82765
LEAN	7.36479	5.71752	3.55145	1.27933	1.59436	1.71574
Y	-3.32000	-3.19400	-3.00000	-2.88000	-2.83000	-2.95000

NOR ITES = 2 AREA RATIO = .99981 EXP = 1.50000 CHOKE = .75771

RADIUS	2.45000	2.40684	2.34379	2.24274	2.13054	1.99400
Z	.86700	.86918	.87236	.87745	.88311	.89000
CROSS PASSAGE DIST P	.45658	.41336	.35024	.24906	.13671	0.00000
SLOPE	39.50742	38.20198	37.67940	40.11559	44.83716	53.14836
CURVATURE	.20000	.07274	.20614	-.19219	-.06571	-.11920
DELTA CURVATURE	0.00000	-.00050	.00643	-.00040	-.00267	0.00000
VM	517.27854	524.57425	595.94359	627.72697	650.80176	647.60327
VU2	667.88776	658.66926	648.92864	584.74504	489.36428	313.92687
U	1494.50000	1468.17118	1429.71411	1368.07215	1299.62875	1216.34000
VR	329.08142	324.41549	364.26616	404.46456	458.87674	518.20656
BETA2	52.24222	51.46563	47.43717	42.96971	36.94098	25.86186
BETA2*	59.13918	57.95953	53.98950	50.61539	46.67899	38.94733

INCIDENCE					
.20215	.74811	-1.29818	-.68550	2.07200	3.52469
.68037	.68137	.72132	.70857	.67756	.60151
V2					
844.77876	842.03524	881.05456	857.88572	814.26060	719.68054
TOTAL TEMP					
1.39268	1.37777	1.35483	1.34063	1.33472	1.34890
TOTAL PRESS					
2.88452	2.80752	2.79416	2.76045	2.73897	2.85143
EFFICIENCY					
.89027	.89814	.95113	.97729	.98576	.98937
STATIC TEMP					
1.24155	1.22989	1.20150	1.18049	1.16306	1.15284
STATIC PRESS					
1.92222	1.87967	1.82782	1.76099	1.68394	1.63694
DENSITY					
1.54824	1.52832	1.52129	1.49174	1.44785	1.41993
SUCT SURF VEL					
1012.06728	979.44960	1052.17825	1002.46777	978.18002	855.21794
PRESS SURF VEL					
677.49023	704.62087	709.93088	713.30368	650.34118	584.14314
DELTA T					
31.90110	23.47185	30.65573	25.15279	26.99324	27.61311
WORK COEF = $2*CP*DELTA T/U**2$					
.17326	.13209	.18193	.16303	.19387	.22641
FLOW COEF = VM/U					
.34612	.35730	.41683	.45884	.50076	.53242
R BAR					
2.42750	2.38466	2.32187	2.21733	2.09972	1.95150
D-FACTOR					
.17541	.15501	.15683	.14710	.11722	.10580
VM2/VM1					
.91348	.86305	.95686	.92454	1.01413	1.03230
DELP/Q					
.23863	.23267	.21499	.23049	.19316	.23117
TANG BLADE FORCE LB/IN					
18.88538	14.44547	19.97937	16.28372	15.55246	12.76721
AXIAL BLADE FORCE LB/IN					
38.46296	31.87692	36.89320	32.86703	25.67952	19.99862
VEL HEAD 2					
.26575	.26638	.29205	.28383	.26395	.21628
$Q=E*(-S/CP)$					
.96906	.97207	.98720	.99423	.99643	.99725
RVU/					
3.32000	3.19400	3.00000	2.88000	2.83000	2.94986
DRVU/DM					
6.20156	5.05842	5.89303	4.71978	4.99793	3.82061
STRMLN DIST M					
1.47595	1.46564	1.46214	1.49613	1.60933	2.01953

STATION	3.80000	ROTOR	XI =	4.25158		
P = 1.	ZTIP = .92500	AR = 6.00000	XN = 0.	BNXT = 1.		
= -0.	ZHUB = .95600	LOSS = 3.	EXP = -0.0000	BLADES = 40.		
RADIUS						
2.49600	2.45260	2.39450	2.29810	2.19620	2.07900	
SLOPE						
40.39805	39.58730	39.39818	41.37679	45.24561	51.93587	
CURVATURE						
.22000	-.01659	-.00959	.23315	-.19928	-.18000	
LOSS COEFF						
.96611	.96925	.98150	.99381	.99621	.99696	
SOLIDITY						
1.00000	1.00000	1.00000	1.00000	1.00000	1.00000	
BLADE THICKNESS						
.02357	.02623	.02945	.03385	.03769	.04408	
AERO BLOCKAGE						
.95300	.95300	.95300	.95300	.95300	.95300	
TOTAL BLOCKAGE						
.89571	.88811	.87838	.86364	.84888	.82436	
BLADE ANGLE						
55.65959	54.43986	52.19366	46.98038	36.48599	18.45993	
LEAN						
11.93187	10.32751	8.86219	8.23414	9.05259	9.51482	
Y						
-3.70000	-3.55400	-3.37240	-3.22000	-3.27350	-3.31000	
NOR ITES = 1	AREA RATIO = 1.00088	EXP = 1.50000	CHOKE = .73301			
RADIUS						
2.49600	2.45335	2.39165	2.29561	2.19420	2.07900	
Z						
.92500	.92817	.93276	.93990	.94744	.95600	
CROSS PASSAGE DIST P						
.41815	.37538	.31351	.21721	.11551	0.00000	
SLOPE						
40.39805	38.67128	39.12227	41.03700	44.88034	51.93587	
CURVATURE						
.22000	.00146	.22293	.54400	.13125	-.18000	
DELTA CURVATURE						
0.00000	-.00069	.00206	.00090	.00109	0.00000	
VM						
475.93052	485.77793	558.24571	616.12253	645.74998	685.08553	
VU2						
618.31321	612.87712	598.76248	544.69213	428.40587	296.81333	
U						
1522.56000	1496.54275	1458.90664	1400.32407	1338.45924	1268.19000	
VR						
308.44782	303.53914	352.24058	404.51311	455.65977	539.38250	
BETA2						
52.41363	51.59897	47.00558	41.47874	33.56123	23.42466	
BETA2*						
59.62152	58.24943	54.12159	49.52911	43.11484	35.09604	

INCIDENCE

1.03619	1.23387	-.57047	-.44542	1.27974	4.76099
.62093	.62553	.66193	.67253	.63769	.62024
V2					
780.26988	782.04767	818.62982	822.37248	774.93524	746.61927
TOTAL TEMP					
1.43762	1.42035	1.39887	1.38085	1.38718	1.39157
TOTAL PRESS					
3.19255	3.09437	3.06522	3.05976	3.13621	3.17989
EFFICIENCY					
.88867	.89610	.93512	.97756	.98642	.98920
STATIC TEMP					
1.27167	1.25875	1.23176	1.20416	1.18928	1.16694
STATIC PRESS					
2.06969	2.01933	1.95535	1.88616	1.82050	1.70705
DENSITY					
1.62754	1.60424	1.58744	1.56637	1.53076	1.46284
SUCT SURF VEL					
872.34953	892.25923	914.09841	919.58301	883.86019	838.56459
PRESS SURF VEL					
688.19023	671.83612	723.16123	725.16195	666.01029	654.67396
DELTA T					
23.31235	22.08538	22.84610	20.85841	27.20796	22.13368
WORK COEF = $2*CP*DELT/U**2$					
.12199	.11962	.13021	.12904	.18424	.16694
FLOW COEF = VM/U					
.31259	.32460	.38265	.43999	.48246	.54021
K BAR					
2.47300	2.43009	2.36772	2.26918	2.16237	2.03650
D-FACTOR					
.13184	.12490	.12530	.09467	.12512	.03765
VM2/VM1					
.92007	.92604	.93674	.98151	.99224	1.05788
DELP/Q					
.21196	.20462	.16913	.17935	.22614	.15519
TANG BLADE FORCE LB/IN					
13.73014	13.22218	15.24277	14.16186	17.46869	12.18285
AXIAL BLADE FORCE LB/IN					
28.24647	26.46145	21.70808	23.80633	26.66630	16.98435
VEL HEAD 2					
.22828	.23114	.25401	.26075	.23873	.22785
$Q=E**(-S/CP)$					
.96611	.96925	.98150	.99381	.99621	.99696
RVU/					
3.70000	3.55400	3.37240	3.22000	3.27350	3.31064
DRVU/DM					
3.35252	3.97501	3.17291	2.99272	3.07067	2.42315
STRMLN DIST M					
1.54998	1.54077	1.53920	1.57795	1.69983	2.12715

Rotor 1B Exit

STATION 4.00000 ROTOR XI = 5.98088

P = 1. ZTIP = .98000 AR = 6.00000 XN = 0. BNXT = -0.
 = -0. ZHUB = 1.02000 LOSS = 3. EXP = -0.0000 BLADES = 1.

RADIUS

2.54080 2.50020 2.44280 2.35350 2.25910 2.15900

SLOPE

40.34944 40.20571 40.53980 42.37657 45.85692 50.86984

CURVATURE

.24280 .31647 .30135 .06521 .00277 -.25180

LOSS COEFF

.96317 .96646 .98517 .99339 .99598 .99668

SOLIDITY

1.00000 1.00000 1.00000 1.00000 1.00000 1.00000

BLADE THICKNESS

.01078 .01188 .01298 .01408 .01408 .01365

AERO BLOCKAGE

.95300 .95300 .95300 .95300 .95300 .95300

TOTAL BLOCKAGE

.95236 .95228 .95219 .95209 .95205 .95204

BLADE ANGLE

53.46013 52.87353 50.15388 42.06407 26.71148 -1.28609

LEAN

14.67896 13.99358 13.72569 15.32252 18.48976 20.99815

Y

-3.81677 -3.78400 -3.48920 -3.36928 -3.38680 -3.46765

NOR ITERS = 1 AREA RATIO = 1.00089 EXP = 1.50000 CHOKE = .67667

RADIUS

2.54080 2.49839 2.44013 2.35017 2.25727 2.15900

Z

.98000 .98444 .99055 .99997 1.00970 1.02000

CROSS PASSAGE DIST P

.38389 .34124 .28267 .19222 .09880 0.00000

SLOPE

40.34944 39.71951 40.92017 43.15562 46.06735 50.86984

CURVATURE

.24280 .43332 .38684 .17027 .03806 -.25180

DELTA CURVATURE

0.00000 .00437 .00344 .00497 .00302 0.00000

VM

407.76993 439.03627 514.82116 551.20328 596.47451 644.54236

VU2

633.55074 600.12438 616.22463 559.09199 461.68960 337.07818

VU1

916.33726 923.89194 872.25395 874.51425 915.24316 979.91182

U

1549.88800 1524.01632 1488.47858 1433.60624 1376.93275 1316.99000

VR

264.00977 280.55734 337.21150 377.01336 429.55475 499.98089

BETA2

57.23358 53.81169 50.12311 45.40706 37.74096 27.60834

TA1

66.01092 64.58276 59.45005 57.77689 56.90722 56.66484

BETA2*

63.87138 60.63288 57.73656 54.27609 48.12812 39.64818

BETA1*						
71.26618	69.92173	65.96390	65.30698	65.66914	67.45669	
CIDENCE						
-63.84075	-65.85982	-73.85987	-82.25337	87.21228	72.49670	
M2						
.59494	.58951	.64461	.63563	.61512	.59798	
M1						
.79198	.81096	.81309	.83690	.89091	.96426	
V2						
753.43404	743.57388	802.97797	785.11713	754.28054	727.36273	
V1						
1002.97073	1022.90233	1012.85131	1033.73122	1092.45223	1172.88620	
TOTAL TEMP						
1.45143	1.44756	1.41269	1.39850	1.40058	1.41021	
TOTAL PRESS						
3.26688	3.27539	3.21566	3.19548	3.24193	3.32967	
EFFICIENCY						
.88159	.89152	.94923	.97680	.98594	.98859	
STATIC TEMP						
1.29156	1.28126	1.24965	1.22867	1.21090	1.19151	
STATIC PRESS						
2.16292	2.12811	2.08486	2.02232	1.93860	1.83564	
DENSITY						
1.67466	1.66094	1.66836	1.64594	1.60096	1.54060	
SUCT SURF VEL						
690.93919	0.00000	711.70516	0.00000	0.00000	0.00000	
PRESS SURF VEL						
915.92890	0.00000	894.25078	0.00000	0.00000	0.00000	
DELTA T						
7.16364	14.11010	7.16548	9.15807	6.95076	9.66864	
WORK COEF = $2*CP*DELTA T/U**2$						
.03618	.07370	.03923	.05405	.04447	.06762	
FLOW COEF = VM/U						
.26310	.28808	.34587	.38449	.43319	.48941	
R1 BAR						
2.51840	2.47587	2.41589	2.32289	2.22573	2.11900	
D-FACTOR						
.05252	.08543	.03713	.06914	.04669	.05617	
VM2/VM1						
.85678	.90378	.92221	.89463	.92369	.94082	
DELP/Q						
.15228	.17919	.19451	.20467	.20686	.25528	
TANG BLADE FORCE LB/IN						
4.24229	8.71048	5.04456	6.72546	5.08468	6.72325	
AXIAL BLADE FORCE LB/IN						
13.85118	18.38775	21.24493	18.35825	17.02458	22.74738	
VEL HEAD 2						
.21226	.20895	.24308	.23744	.22468	.21412	
VEL HEAD 1						
.33793	.35027	.35166	.36713	.40202	.44861	
Q=E**(-S/CP)						
.96317	.96646	.98517	.99339	.99598	.99668	
U/						
3.81677	3.78400	3.48920	3.36928	3.38680	3.46825	
DRVU/DM						
-.06030	2.40705	-.07603	.68625	-.51399	.65352	
STRMLN DIST M						
1.62092	1.61284	1.61463	1.65910	1.78846	2.22960	

Stator 1A Inlet

STATION 5.00000 STATOR XI = 0.00000

P = 0. ZTIP = 1.30000 AR = 3.00000 XN = -0. BNXT = -0.
 = -0. ZHUB = 1.30000 LOSS = 2. EXP = -0.0000 BLADES = 1.

RADIUS

2.82900	2.80000	2.73000	2.64000	2.56000	2.47300
SLOPE					
42.17000	41.00000	42.00000	44.00000	45.00000	46.00000
CURVATURE					
-.08767	-.13000	-.15000	-.16000	-.18000	-.13050
LOSS COEFF					
1.00000	1.00000	1.00000	1.00000	1.00000	1.00000
SOLIDITY					
1.00000	1.00000	1.00000	1.00000	1.00000	1.00000
BLADE THICKNESS					
.01821	.01772	.01722	.01665	.01649	.01708
AERO BLOCKAGE					
.94500	.94500	.94500	.94500	.94500	.94500
TOTAL BLOCKAGE					
.94403	.94405	.94405	.94405	.94403	.94396
BLADE ANGLE					
-64.05654	-62.67773	-61.24885	-59.10606	-58.72378	-60.71567
LEAN					
2.17206	.02951	-3.30363	-10.28877	-15.69511	-17.14941
Y					
-0.00000	-0.00000	-0.00000	-0.00000	-0.00000	-0.00000

VOR ITES = 1 AREA RATIO = 1.00029 EXP = 1.50000 CHOKE = .67317

RADIUS

2.82900	2.79243	2.73898	2.65199	2.56267	2.47300
Z					
1.30000	1.30000	1.30000	1.30000	1.30000	1.30000
CROSS PASSAGE DIST P					
.35600	.31943	.26598	.17899	.08967	0.00000
SLOPE					
42.17000	42.60118	43.52334	44.63871	45.63315	46.00000
CURVATURE					
-.08767	-.18711	-.18604	-.18796	-.12816	-.13050
DELTA CURVATURE					
0.00000	-.00175	.00042	.00037	-.00047	0.00000
VM					
479.06562	490.77282	528.43361	543.45949	575.73768	609.02632
VU2					
822.98682	826.60621	777.08113	774.98706	806.17146	855.52931
U					
1725.69000	1703.38231	1670.77963	1617.71615	1563.22611	1508.53000
VR					
321.61249	332.19989	363.90594	381.85318	411.58200	438.09702
BETA2					
59.79603	59.30151	55.78334	54.95993	54.46696	54.55402
BETA2*					
66.66309	66.39333	63.75295	63.48191	63.46344	63.68726

INCIDENCE					
3.52232	4.53728	2.06065	2.17932	.99235	-1.04916
.74740	.75643	.74763	.75790	.79687	.84805
V2					
952.26633	961.31982	939.73249	946.54802	990.64944	1050.16354
TOTAL TEMP					
1.45143	1.44756	1.41269	1.39850	1.40058	1.41021
TOTAL PRESS					
3.26688	3.27539	3.21566	3.19548	3.24193	3.32967
EFFICIENCY					
.88159	.89152	.94923	.97680	.98594	.98859
STATIC TEMP					
1.30731	1.30068	1.27234	1.25611	1.24460	1.23493
STATIC PRESS					
2.25760	2.24429	2.22173	2.18647	2.13609	2.08318
DENSITY					
1.72690	1.72547	1.74618	1.74067	1.71628	1.68688
SUCT SURF VEL					
0.00000	0.00000	0.00000	0.00000	0.00000	0.00000
PRESS SURF VEL					
0.00000	0.00000	0.00000	0.00000	0.00000	0.00000
DELTA T					
0.00000	0.00000	0.00000	0.00000	0.00000	0.00000
WORK COEF = $2*CP*DELTA T/U**2$					
0.00000	0.00000	0.00000	0.00000	0.00000	0.00000
FLOW COEF = VM/U					
.27761	.28812	.31628	.33594	.36830	.40372
K BAR					
2.68490	2.64541	2.58956	2.50108	2.40997	2.31600
D-FACTOR					
.05055	.06020	.07219	.08434	.09319	.10465
VM2/VM1					
1.17484	1.11784	1.02644	.98595	.96523	.94490
DELP/Q					
.08577	.10127	.12104	.13992	.15152	.16575
TANG BLADE FORCE LB/IN					
-.00000	-.00000	-.00000	-.00000	-.00000	.00650
AXIAL BLADE FORCE LB/IN					
29.95129	31.87609	31.72610	35.37090	42.08068	55.46356
VEL HEAD 2					
.30894	.31480	.30909	.31576	.34111	.37436
$Q=E**(-S/CP)$					
.96317	.96646	.98517	.99339	.99598	.99668
RVU/					
3.81677	3.78400	3.48920	3.36928	3.38680	3.46840
DRVU/DM					
-7.54163	-7.12164	-5.92516	-4.83079	-3.75732	-2.92013
STRMLN DIST M					
2.05157	2.04416	2.04483	2.08468	2.20981	2.65031

STATION 5.10000 STATOR XI = .83443

P = 0. ZTIP = 1.36000 AR = 4.00000 XN = 1. BNXT = 0.
 = -0. ZHUB = 1.36500 LOSS = 2. EXP = -0.0000 BLADES = 53.

RADIUS	2.88260	2.84000	2.79000	2.70000	2.62000	2.53930
SLOPE	41.68900	42.00000	43.00000	44.00000	45.00000	45.33150
CURVATURE	-.12135	-.14000	-.14000	-.14000	-.14000	-.15075
LOSS COEFF	.99691	.99695	.99744	.99830	.99733	.99603
SOLIDITY	1.00000	1.00000	1.00000	1.00000	1.00000	1.00000
BLADE THICKNESS	.04100	.03978	.03918	.03867	.03979	.04285
AERO BLOCKAGE	.94331	.94335	.94335	.94337	.94338	.94336
TOTAL BLOCKAGE	.83013	.83189	.83160	.82940	.82252	.80908
BLADE ANGLE	-58.01493	-56.74558	-55.49516	-53.62422	-53.45886	-55.59224
LEAN	-2.55017	-3.72303	-4.55138	-7.80551	-10.13416	-9.26323
Y	-50.70000	-50.20000	-48.08000	-47.62000	-47.80000	-48.64000

NOR ITERS = 1 AREA RATIO = .99944 EXP = 1.50000 CHOKE = .91667

RADIUS	2.88260	2.84845	2.79748	2.71297	2.62730	2.53930
Z	1.36000	1.36050	1.36124	1.36247	1.36372	1.36500
CROSS PASSAGE DIST P	.34334	.30919	.25821	.17369	.08801	0.00000
SLOPE	41.68900	42.10591	42.74873	43.30337	44.51415	45.33150
CURVATURE	-.12135	-.30510	-.42811	-.50772	-.44498	-.15075
DELTA CURVATURE	0.00000	-.00115	-.00385	-.00412	-.00383	0.00000
VM	536.35408	546.67429	558.86425	586.51717	626.11142	663.59530
VU2	655.29714	660.56095	629.86729	643.29447	690.10885	753.68468
U	1758.38600	1737.55593	1706.46566	1654.91356	1602.65195	1548.97300
VR	356.72225	366.54695	379.34848	402.26946	438.95773	471.93990
BETA2	50.70000	50.38913	48.41820	47.64330	47.78363	48.63709
BETA2*	58.56586	58.45025	56.91341	56.43560	57.09914	58.24362

INCIDENCE

-.08326	.60754	-.01940	.34850	.43898	-.16576
.65710	.66703	.66276	.69103	.74419	.80604
V2					
846.81169	857.43429	842.05823	870.53441	931.80778	1004.19088
TOTAL TEMP					
1.45143	1.44756	1.41269	1.39850	1.40058	1.41021
TOTAL PRESS					
3.23135	3.24018	3.18669	3.17635	3.21151	3.28325
EFFICIENCY					
.87202	.88197	.94061	.97088	.97666	.97500
STATIC TEMP					
1.33746	1.33071	1.30000	1.27806	1.26258	1.24994
STATIC PRESS					
2.42042	2.40664	2.37555	2.31059	2.22604	2.14373
DENSITY					
1.80971	1.80854	1.82735	1.80789	1.76308	1.71506
SUCT SURF VEL					
1022.28594	1026.61076	995.85888	1013.53923	1063.74831	1123.01222
PRESS SURF VEL					
671.33745	688.25781	688.25757	727.52960	799.86724	885.36953
DELTA T					
0.00000	0.00000	0.00000	0.00000	0.00000	0.00000
WORK COEF = $2*CP*DELT/U**2$					
0.00000	0.00000	0.00000	0.00000	0.00000	0.00000
FLOW COEF = VM/U					
.30503	.31462	.32750	.35441	.39067	.42841
R BAR					
2.85580	2.82044	2.76823	2.68248	2.59498	2.50615
O-FACTOR					
.19150	.18675	.17436	.14136	.10857	.08213
VM2/VM1					
1.11958	1.11391	1.05759	1.07923	1.08749	1.08960
DELP/Q					
.16132	.15746	.15476	.12301	.08134	.04858
TANG BLADE FORCE LB/IN					
-25.71603	-25.38746	-22.87246	-19.75665	-16.34520	-13.09659
AXIAL BLADE FORCE LB/IN					
50.52536	49.71053	44.01699	37.59349	28.90475	21.06481
VEL HEAD 2					
.25096	.25725	.25454	.27256	.30686	.34707
$Q=E**(-S/CP)$					
.96019	.96351	.98265	.99170	.99333	.99273
RVU/					
3.09665	3.08455	2.88860	2.86105	2.97233	3.13743
DRVU/DM					
-8.70669	-8.31977	-7.26621	-6.67322	-6.22702	-5.80077
STRMLN DIST M					
2.13202	2.12662	2.12953	2.17198	2.30057	2.74315

STATION 5.20000 STATOR XI = 1.72583

P = -0. ZTIP = 1.41500 AR = 4.00000 XN = 1. BNXT = -0.
 = -0. ZHUB = 1.42500 LOSS = 2. EXP = -0.0000 BLADES = 53.

RADIUS	2.93108	2.89000	2.84000	2.76000	2.67000	2.59919
SLOPE	41.11230	42.00000	43.00000	43.00000	44.00000	44.52400
CURVATURE	-.15349	-.16000	-.17000	-.17000	-.18000	-.18223
LOSS COEFF	.99717	.99723	.99763	.99843	.99752	.99636
SOLIDITY	1.00000	1.00000	1.00000	1.00000	1.00000	1.00000
BLADE THICKNESS	.04564	.04430	.04332	.04309	.04417	.04715
AERO BLOCKAGE	.94178	.94186	.94183	.94186	.94187	.94187
TOTAL BLOCKAGE	.81808	.82009	.82065	.81783	.81044	.79774
BLADE ANGLE	-52.62893	-51.41668	-50.23110	-49.03793	-49.04520	-51.36890
LEAN	-4.98158	-5.82798	-5.92520	-6.22135	-6.72153	-4.14150
Y	-45.50000	-44.83000	-43.38000	-42.30000	-42.40000	-42.60000

NOR ITES = 1 AREA RATIO = .99966 EXP = 1.50000 CHOKE = .83773

RADIUS	2.93108	2.89769	2.84802	2.76517	2.68295	2.59919
Z	1.41500	1.41601	1.41750	1.42000	1.42248	1.42500
CROSS PASSAGE DIST P	.33204	.29864	.24895	.16605	.08379	0.00000
SLOPE	41.11230	41.40934	41.86401	41.96615	43.13245	44.52400
CURVATURE	-.15349	-.13664	-.10039	-.05288	-.12327	-.18223
DELTA CURVATURE	0.00000	.00072	-.00048	-.00283	-.00232	0.00000
VM	506.08948	521.86408	523.08847	553.13392	585.29689	631.06646
VU2	515.00075	521.67700	498.46310	503.82078	533.98048	580.28705
U	1787.95880	1767.59113	1737.29456	1686.75112	1636.59655	1585.50590
VR	332.77268	345.17884	349.09103	369.87601	400.16010	442.50898
BETA2	45.50000	44.98971	43.61909	42.32873	42.37493	42.59957
BETA2*	53.48427	53.12011	51.99156	50.77466	51.34340	52.21193

INCIDENCE					
-.72718	-.37631	-.48717	-.61181	-.25534	-.71660
.55388	.56761	.56231	.58673	.62338	.67648
V2					
722.04733	737.89498	722.55588	748.19283	792.28000	857.30854
TOTAL TEMP					
1.45143	1.44756	1.41269	1.39850	1.40058	1.41021
TOTAL PRESS					
3.19921	3.20853	3.16008	3.15872	3.18343	3.24123
EFFICIENCY					
.86329	.87333	.93264	.96541	.96804	.96258
STATIC TEMP					
1.36857	1.36102	1.32971	1.30954	1.30082	1.29340
STATIC PRESS					
2.59917	2.58053	2.55156	2.50404	2.45187	2.38792
DENSITY					
1.89918	1.89603	1.91888	1.91215	1.88488	1.84624
SUCT SURF VEL					
875.69116	891.14155	864.82969	890.21071	937.37929	1005.39156
PRESS SURF VEL					
568.40349	584.64842	580.28207	606.17495	647.18072	709.22552
DELTA T					
0.00000	0.00000	0.00000	0.00000	0.00000	0.00000
WORK COEF = 2*CP*DELT/U**2					
0.00000	0.00000	0.00000	0.00000	0.00000	0.00000
FLOW COEF = VM/U					
.28305	.29524	.30109	.32793	.35763	.39802
K BAR					
2.90684	2.87307	2.82275	2.73907	2.65512	2.56924
D-FACTOR					
.22441	.21450	.21394	.21437	.22663	.22486
VM2/VM1					
.94357	.95462	.93598	.94308	.93481	.95098
DELP/Q					
.22043	.20862	.21700	.22344	.22917	.21429
TANG BLADE FORCE LB/IN					
-24.08355	-23.98616	-22.60406	-24.20329	-26.58490	-28.41719
AXIAL BLADE FORCE LB/IN					
44.42298	43.48173	41.98918	45.98877	51.77275	54.93544
VEL HEAD 2					
.18756	.19573	.19256	.20726	.22980	.26327
Q=E**(-S/CP)					
.95748	.96084	.98032	.99014	.99086	.98912
RVU/					
2.47460	2.47813	2.32727	2.28385	2.34859	2.47258
DRVU/UM					
-6.97910	-6.88229	-6.23984	-6.12844	-6.33107	-6.58885
STRMLN DIST M					
2.20534	2.20082	2.20515	2.24965	2.38150	2.82793

STATION 5.30000 STATOR XI = 3.62137

P = -0. ZTIP = 1.47500 AR = 4.00000 XN = 1. BNXT = -0.
 = -0. ZHUB = 1.49500 LOSS = 2. EXP = -0.0000 BLADES = 53.

RADIUS

2.98275 2.95000 2.89000 2.82000 2.74000 2.66674

SLOPE

40.33100 41.00000 41.00000 42.00000 42.00000 43.39600

CURVATURE

-.19161 -.20000 -.20000 -.20000 -.20000 -.22377

LOSS COEFF

.99694 .99683 .99737 .99819 .99712 .99572

SOLIDITY

1.00000 1.00000 1.00000 1.00000 1.00000 1.00000

BLADE THICKNESS

.04002 .03915 .03862 .03854 .03935 .04104

AERO BLOCKAGE

.94012 .94016 .94014 .94013 .94013 .94012

TOTAL BLOCKAGE

.83371 .83492 .83417 .83175 .82624 .81808

BLADE ANGLE

-46.84601 -45.48986 -44.19821 -43.80426 -43.99808 -46.56846

LEAN

-6.71432 -7.46853 -7.18996 -5.15956 -3.88857 .19175

Y

-41.70000 -40.70000 -39.50000 -37.80000 -37.55000 -37.15000

NOR ITES = 1 AREA RATIO = 1.00055 EXP = 1.50000 CHOKE = .76556

RADIUS

2.98275 2.95044 2.90256 2.82243 2.74462 2.66674

Z

1.47500 1.47704 1.48007 1.48515 1.49007 1.49500

CROSS PASSAGE DIST P

.31664 .28427 .23630 .15601 .07804 0.00000

SLOPE

40.33100 40.63542 40.77724 41.37999 42.04346 43.39600

CURVATURE

-.19161 -.16847 -.18299 -.16119 -.14714 -.22377

DELTA CURVATURE

0.00000 -.00023 -.00008 .00188 .00307 0.00000

VM

470.71372 489.20562 484.84543 522.42112 552.31914 595.25271

VU2

419.39089 420.96115 402.88279 405.97415 424.87807 450.98375

U

1819.47750 1799.76974 1770.56380 1721.68531 1674.21813 1626.71140

VR

304.64712 318.59205 316.66228 345.34654 369.88498 408.96065

BETA2

41.70000 40.71196 39.72490 37.85081 37.56970 37.14879

BETA2*

49.44947 48.59112 47.65674 46.00365 46.00887 46.19693

INCIDENCE

.05374	.09476	.24297	-.11385	.21843	-.27571
.48017	.49278	.48697	.51504	.54359	.58297
V2					
630.44438	645.39169	630.38848	661.61835	696.83414	746.80127
TOTAL TEMP					
1.45143	1.44756	1.41269	1.39850	1.40058	1.41021
TOTAL PRESS					
3.16476	3.17269	3.13079	3.13852	3.15118	3.19252
EFFICIENCY					
.85388	.86346	.92380	.95910	.95808	.94804
STATIC TEMP					
1.38826	1.38136	1.34953	1.32893	1.32340	1.32157
STATIC PRESS					
2.70430	2.68900	2.66358	2.62071	2.57927	2.53812
DENSITY					
1.94798	1.94664	1.97371	1.97204	1.94897	1.92053
SUCT SURF VEL					
735.14932	753.29718	730.49010	759.63035	796.16420	851.91157
PRESS SURF VEL					
525.73944	537.48619	530.28687	563.60634	597.50407	641.69097
DELTA T					
0.00000	0.00000	0.00000	0.00000	0.00000	0.00000
WORK COEF = $2*CP*DELTA T/U^{**2}$					
0.00000	0.00000	0.00000	0.00000	0.00000	0.00000
FLOW COEF = VM/U					
.25871	.27182	.27384	.30344	.32990	.36592
K BAR					
2.95691	2.92407	2.87529	2.79380	2.71378	2.63296
D-FACTOR					
.18742	.18784	.18778	.17487	.18245	.19660
VM2/VM1					
.93010	.93742	.92689	.94447	.94366	.94325
DELP/Q					
.17521	.17273	.18407	.17822	.17414	.17602
TANG BLADE FORCE LB/IN					
-16.86146	-18.13250	-16.95246	-17.64193	-19.54492	-23.04548
AXIAL BLADE FORCE LB/IN					
24.34687	25.29719	25.34783	26.22906	28.51699	33.02691
VEL HEAD 2					
.14550	.15245	.14923	.16498	.18149	.20498
Q=E**(-S/CP)					
.95455	.95779	.97774	.98835	.98801	.98489
RVU/					
2.05072	2.03610	1.91704	1.87842	1.91169	1.97157
DRVU/DM					
-4.37341	-4.43345	-4.05731	-3.88111	-3.94372	-4.18526
STRMLN DIST M					
2.28452	2.28149	2.28816	2.33639	2.47300	2.92521

STATION 5.40000 STATOR XI = 3.68557

P = -0. ZTIP = 1.53500 AR = 4.00000 XN = 1. BNXT = -0.
 = -0. ZHUB = 1.55500 LOSS = 2. EXP = -0.0000 BLADES = 53.

RADIUS	3.03287	3.00000	2.95000	2.87000	2.79000	2.72238
SLOPE	39.38000	40.00000	40.00000	41.00000	41.00000	42.25380
CURVATURE	-.23374	-.23000	-.23000	-.23000	-.23000	-.26448
LOSS COEFF	.99697	.99704	.99748	.99839	.99752	.99633
SOLIDITY	1.00000	1.00000	1.00000	1.00000	1.00000	1.00000
BLADE THICKNESS	.02769	.02721	.02707	.02733	.02799	.02923
AERO BLOCKAGE	.93848	.93858	.93854	.93860	.93863	.93862
TOTAL BLOCKAGE	.86620	.86677	.86590	.86321	.85918	.85361
BLADE ANGLE	-40.96506	-39.57368	-38.31786	-38.66671	-39.55225	-42.38635
LEAN	-8.37788	-8.91084	-8.39222	-4.77394	-1.92047	2.81818
Y	-39.34000	-38.15000	-37.35000	-35.03000	-34.84000	-34.20000

NOR ITES = 1 AREA RATIO = 1.00047 EXP = 1.50000 CHOKE = .70798

RADIUS	3.03287	3.00088	2.95349	2.87406	2.79825	2.72238
Z	1.53500	1.53706	1.54011	1.54523	1.55011	1.55500
CROSS PASSAGE DIST P	.31113	.27907	.23159	.15199	.07603	0.00000
SLOPE	39.38000	39.72089	39.95845	40.50369	41.22299	42.25380
CURVATURE	-.23374	-.23201	-.16813	-.21618	-.20055	-.26448
DELTA CURVATURE	0.00000	-.00031	.00030	-.00123	-.00280	0.00000
VM	437.87178	457.16175	449.53830	491.02652	517.33267	559.06760
VU2	358.90489	359.42973	343.61025	345.60601	360.35491	379.91410
U	1850.05070	1830.53398	1801.63031	1753.17380	1706.93287	1660.65180
VR	277.81255	292.14854	288.70797	318.92038	340.91783	375.92607
BETA2	39.34000	38.17512	37.39293	35.13955	34.85964	34.19803
BETA2*	46.67967	45.62816	44.91960	42.78940	42.80262	42.55487

INCIDENCE

1.94096	1.80515	2.32239	1.55092	2.07392	1.47942
.42933	.44204	.43512	.46529	.48923	.52448
V2					
566.16641	581.53813	565.82037	600.45863	630.46709	675.93735
TOTAL TEMP					
1.45143	1.44756	1.41269	1.39850	1.40058	1.41021
TOTAL PRESS					
3.13102	3.13967	3.10303	3.12075	3.12362	3.15133
EFFICIENCY					
.84458	.85431	.91538	.95354	.94950	.93562
STATIC TEMP					
1.40049	1.39381	1.36181	1.34120	1.33740	1.33760
STATIC PRESS					
2.75965	2.74675	2.72580	2.69188	2.65357	2.61437
DENSITY					
1.97049	1.97068	2.00160	2.00706	1.98412	1.95453
SUCT SURF VEL					
604.41277	629.95351	606.00545	641.94606	681.46075	735.45028
PRESS SURF VEL					
527.92006	533.12275	525.63529	558.97119	579.47343	616.42443
DELTA T					
0.00000	0.00000	0.00000	0.00000	0.00000	0.00000
WORK COEF = $2*CP*DELTA/U^{**2}$					
0.00000	0.00000	0.00000	0.00000	0.00000	0.00000
FLOW COEF = VM/U					
.23668	.24974	.24952	.28008	.30308	.33666
K BAR					
3.00781	2.97566	2.92803	2.84825	2.77144	2.69456
D-FACTOR					
.14478	.14148	.14429	.13291	.13609	.13673
VM2/VM1					
.93023	.93450	.92718	.93991	.93666	.93921
DELP/Q					
.12020	.11939	.13317	.13744	.12992	.11652
TANG BLADE FORCE LB/IN					
-10.56195	-11.02472	-10.40531	-11.03889	-11.74725	-13.05149
AXIAL BLADE FORCE LB/IN					
11.35957	11.90294	12.34327	14.84290	14.63525	15.02985
VEL HEAD 2					
.11861	.12515	.12157	.13743	.15048	.17039
Q=E**(-S/CP)					
.95166	.95495	.97528	.98676	.98556	.98127
RVU/					
1.78445	1.76820	1.66369	1.62835	1.65305	1.69553
DRVU/DM					
-1.48180	-1.84514	-1.51614	-1.52427	-1.87340	-2.18208
STRMLN DIST M					
2.36270	2.35988	2.36689	2.41561	2.55351	3.00703

Stator 1A Exit

STATION 5.50000 STATOR XI = 5.74866

C = 0. ZTIP = 1.59000 AR = 3.00000 XN = 1. BNXT = -0.
 = -0. ZHUB = 1.62000 LOSS = 2. EXP = -0.0000 BLADES = 53.

RADIUS	3.07700	3.04000	3.00000	2.90000	2.82000	2.77900
SLOPE	38.35000	38.50000	39.00000	39.00000	40.00000	40.35000
CURVATURE	-.27690	-.15000	-.20000	-.25000	-.25000	-.29450
LOSS COEFF	.99725	.99704	.99759	.99832	.99730	.99600
SOLIDITY	1.00000	1.00000	1.00000	1.00000	1.00000	1.00000
BLADE THICKNESS	.01200	.01183	.01160	.01150	.01150	.01136
AERO BLOCKAGE	.93700	.93700	.93700	.93700	.93700	.93700
TOTAL BLOCKAGE	.90618	.90624	.90644	.90567	.90476	.90470
BLADE ANGLE	-35.37778	-33.94082	-32.57263	-33.30880	-34.90349	-37.35585
LEAN	-10.05552	-10.35747	-9.82442	-5.06253	-.38821	4.51900
Y	-41.00000	-38.50000	-39.02000	-35.50000	-36.00000	-34.50000

NOR ITES = 1 AREA RATIO = 1.00078 EXP = 1.50000 CHOKE = .67707

RADIUS	3.07700	3.04636	3.00098	2.92407	2.85208	2.77900
Z	1.59000	1.59309	1.59765	1.60540	1.61264	1.62000
CROSS PASSAGE DIST P	.29951	.26871	.22310	.14580	.07345	0.00000
SLOPE	38.35000	38.56134	39.11304	39.26516	40.21386	40.35000
CURVATURE	-.27690	-.22466	-.21224	-.16328	-.24100	-.29450
DELTA CURVATURE	0.00000	-.00085	.00017	.00179	.00198	0.00000
VM	411.03116	434.23695	419.30620	461.20854	477.95310	516.24041
VU2	357.30416	348.31419	339.63694	341.13623	344.71382	354.63262
U	1876.97000	1858.27681	1830.59704	1783.68058	1739.77074	1695.19000
VR	255.02998	270.68262	264.52040	291.90370	308.58690	334.24260
BETA2	41.00000	38.73410	39.00737	36.48873	35.80023	34.48720
BETA2*	47.94451	45.73015	46.23157	43.69192	43.36396	42.03117

INCIDENCE					
7.30093	5.94156	7.80873	6.73144	7.27017	6.53811
.41243	.42246	.41426	.44370	.45592	.48412
V2					
544.62177	556.67271	539.60258	573.66126	589.29346	626.31338
TOTAL TEMP					
1.45143	1.44756	1.41269	1.39850	1.40058	1.41021
TOTAL PRESS					
3.10075	3.10693	3.07670	3.10229	3.09396	3.10706
EFFICIENCY					
.83618	.84516	.90734	.94772	.94021	.92214
STATIC TEMP					
1.40429	1.39831	1.36641	1.34620	1.34539	1.34787
STATIC PRESS					
2.75929	2.74923	2.73510	2.71137	2.68422	2.64827
DENSITY					
1.96490	1.96611	2.00167	2.01409	1.99513	1.96478
SUCT SURF VEL					
539.17143	565.41498	537.46396	571.66057	600.22227	646.55703
PRESS SURF VEL					
550.07211	547.93044	541.74119	575.66196	578.36466	606.06974
DELTA T					
0.00000	0.00000	0.00000	0.00000	0.00000	0.00000
WORK COEF = $2*CP*DELTA T/U**2$					
0.00000	0.00000	0.00000	0.00000	0.00000	0.00000
FLOW COEF = VM/U					
.21899	.23368	.22905	.25857	.27472	.30453
K BAR					
3.05494	3.02362	2.97724	2.89906	2.82517	2.75069
D-FACTOR					
.04121	.04774	.04764	.04584	.07238	.08652
VM2/VM1					
.93870	.94985	.93275	.93927	.92388	.92340
DELP/Q					
-.00096	.00632	.02467	.04545	.06520	.06312
TANG BLADE FORCE LB/IN					
.72260	-1.21542	.30033	.31642	-1.93443	-3.97202
AXIAL BLADE FORCE LB/IN					
-3.35485	-1.84184	-1.35962	1.66176	2.74449	4.01748
VEL HEAD 2					
.11012	.11513	.11103	.12601	.13243	.14766
$Q=E**(-S/CP)$					
.94905	.95213	.97293	.98510	.98290	.97735
RVU/					
1.80234	1.73949	1.67089	1.63525	1.61173	1.61561
DRVU/DM					
.20652	-.32210	.07747	.06986	-.38966	-.70945
STRMLN DIST M					
2.43321	2.43205	2.44149	2.49384	2.63602	3.09324

Stator 1B Inlet

STATION 6.00000 STATOR XI = 0.00000

P = 0. ZTIP = 1.84000 AR = 3.00000 XN = -0. BNXT = -0.
 = -0. ZHUB = 1.84000 LOSS = 2. EXP = -0.0000 BLADES = 1.

RADIUS

3.25800 3.23000 3.18000 3.10000 3.00000 2.95400

SLOPE

33.38000 33.00000 34.00000 34.50000 35.00000 36.08000

CURVATURE

-.28210 -.28000 -.28000 -.28000 -.28000 -.29350

LOSS COEFF

1.00000 1.00000 1.00000 1.00000 1.00000 1.00000

SOLIDITY

1.00000 1.00000 1.00000 1.00000 1.00000 1.00000

BLADE THICKNESS

.01277 .01276 .01275 .01273 .01270 .01263

AERO BLOCKAGE

.93100 .93100 .93100 .93100 .93100 .93100

TOTAL BLOCKAGE

.93042 .93041 .93041 .93039 .93037 .93037

BLADE ANGLE

-42.56001 -42.56017 -42.57532 -42.61664 -42.63979 -42.43921

LEAN

-2.51652 -2.66727 -2.87708 -3.04335 -3.06200 -2.86163

Y

-0.00000 -0.00000 -0.00000 -0.00000 -0.00000 -0.00000

NOR ITES = 1 AREA RATIO = 1.00015 EXP = 1.50000 CHOKE = .51304

RADIUS

3.25800 3.22812 3.18326 3.10517 3.03053 2.95400

Z

1.84000 1.84000 1.84000 1.84000 1.84000 1.84000

CROSS PASSAGE DIST P

.30400 .27412 .22926 .15117 .07653 0.00000

SLOPE

33.38000 33.60852 34.24905 35.12798 35.48099 36.08000

CURVATURE

-.28210 -.29582 -.33810 -.31722 -.30995 -.29350

DELTA CURVATURE

0.00000 -.00067 -.00044 .00045 .00018 0.00000

VM

393.26146 410.33761 384.81860 417.30214 419.55221 438.70681

VU2

337.45393 328.70200 320.18873 321.24025 324.41611 333.62886

U

1987.38000 1969.15193 1941.78717 1894.15267 1848.62277 1801.94000

VR

216.36833 227.12826 216.57259 240.11774 243.52194 258.36080

BETA2

40.63256 38.69655 39.76217 37.58915 37.71275 37.25234

BETA2*

45.77997 43.88547 45.18832 43.26590 43.51827 43.25781

INCIDENCE					
2.28982	.36530	1.53990	-.46897	-.26758	-.28765
.39180	.39824	.38341	.40608	.40873	.42382
V2					
518.19854	525.75846	500.60582	526.62736	530.34882	551.15504
TOTAL TEMP					
1.45143	1.44756	1.41269	1.39850	1.40058	1.41021
TOTAL PRESS					
3.10075	3.10693	3.07670	3.10229	3.09396	3.10706
EFFICIENCY					
.83618	.84516	.90734	.94772	.94021	.92214
STATIC TEMP					
1.40875	1.40362	1.37286	1.35443	1.35587	1.36193
STATIC PRESS					
2.79040	2.78636	2.78098	2.77036	2.75890	2.74721
DENSITY					
1.98076	1.98512	2.02568	2.04541	2.03477	2.01714
SUCT SURF VEL					
0.00000	0.00000	0.00000	0.00000	0.00000	0.00000
PRESS SURF VEL					
0.00000	0.00000	0.00000	0.00000	0.00000	0.00000
DELTA T					
0.00000	0.00000	0.00000	0.00000	0.00000	0.00000
WORK COEF = $2*CP*DELT/U**2$					
0.00000	0.00000	0.00000	0.00000	0.00000	0.00000
FLOW COEF = VM/U					
.19788	.20838	.19818	.22031	.22695	.24346
R BAR					
3.16750	3.13724	3.09212	3.01462	2.94131	2.86650
D-FACTOR					
.04852	.05553	.07227	.08199	.10003	.12001
VM2/VM1					
.95677	.94496	.91775	.90480	.87781	.84981
DELP/Q					
.09112	.10379	.13429	.15090	.18226	.21566
TANG BLADE FORCE LB/IN					
0.00000	-.00000	-.00000	-.00000	-.00000	.00116
AXIAL BLADE FORCE LB/IN					
10.31254	11.20353	11.63334	13.05247	15.37957	17.89691
VEL HEAD 2					
.10009	.10318	.09612	.10699	.10830	.11582
Q=E**(-S/CP)					
.94905	.95213	.97293	.98510	.98290	.97735
RVU/					
1.80234	1.73949	1.67089	1.63525	1.61173	1.61564
DRVU/DM					
-3.46478	-2.93009	-3.13213	-2.52160	-2.49886	-2.57883
STRMLN DIST M					
2.74186	2.73865	2.74474	2.79022	2.92504	3.37435

STATION 6.10000 STATOR XI = 0.00000

P = 0. ZTIP = 1.92500 AR = 4.00000 XN = 1. BNXT = 0.
 z = -0. ZHUB = 1.92500 LOSS = 2. EXP = -0.0000 BLADES = 53.

RADIUS	3.31230	3.27000	3.23000	3.15000	3.08000	3.01380
SLOPE	31.75800	32.00000	33.00000	33.00000	33.00000	34.28300
CURVATURE	-.27834	-.27000	-.27000	-.27000	-.27000	-.28133
LOSS COEFF	.99943	.99945	.99952	.99957	.99949	.99916
SOLIDITY	1.00000	1.00000	1.00000	1.00000	1.00000	1.00000
BLADE THICKNESS	.02960	.02965	.02973	.02984	.02995	.03007
AERO BLOCKAGE	.92902	.92915	.92910	.92909	.92912	.92910
TOTAL BLOCKAGE	.85899	.85808	.85698	.85485	.85291	.85092
BLADE ANGLE	-33.29322	-33.27384	-33.24764	-33.23007	-33.28473	-33.32775
LEAN	-1.21188	-1.31286	-1.47931	-1.73056	-1.86968	-1.91519
Y	-29.90000	-29.78000	-29.40000	-29.50000	-29.30000	-28.90000

VOR ITES = 1 AREA RATIO = .99954 EXP = 1.50000 CHOKE = .60600

RADIUS	3.31230	3.28334	3.23933	3.16352	3.08982	3.01380
Z	1.92500	1.92500	1.92500	1.92500	1.92500	1.92500
CROSS PASSAGE DIST P	.29850	.26954	.22553	.14972	.07602	0.00000
SLOPE	31.75800	32.01613	32.57193	33.07773	33.50506	34.28300
CURVATURE	-.27834	-.33836	-.33176	-.41787	-.32499	-.28133
DELTA CURVATURE	0.00000	-.00063	-.00082	-.00432	-.00363	0.00000
VM	428.72926	435.23229	414.53995	438.18863	442.45862	457.75676
VU2	246.53038	249.75379	234.41757	247.74486	248.73348	252.70689
U	2020.50300	2002.83572	1975.99211	1929.74777	1884.78778	1838.41800
VR	225.65429	230.74193	223.17100	239.15309	244.24193	257.84574
BETA2	29.90000	29.84892	29.48765	29.48311	29.34303	28.90110
BETA2*	34.06966	34.08931	33.86282	34.00904	33.98733	33.74817

INCIDENCE					
.23767	.23434	-.02750	.01225	-.12547	-.44200
.37342	.37957	.36424	.38761	.39064	.40137
V2					
494.55637	501.80085	476.22996	503.37540	507.58051	522.87859
TOTAL TEMP					
1.45143	1.44756	1.41269	1.39850	1.40058	1.41021
TOTAL PRESS					
3.09447	3.10087	3.07153	3.09762	3.08835	3.09784
EFFICIENCY					
.83443	.84346	.90575	.94625	.93844	.91932
STATIC TEMP					
1.41256	1.40754	1.37664	1.35823	1.35963	1.36676
STATIC PRESS					
2.81142	2.80840	2.80344	2.79376	2.78095	2.77351
DENSITY					
1.99030	1.99526	2.03643	2.05691	2.04537	2.02926
SUCT SURF VEL					
619.12829	620.97376	591.56011	604.89570	607.15459	622.36372
PRESS SURF VEL					
369.98445	382.62794	360.89980	401.85509	408.00642	423.39346
DELTA T					
0.00000	0.00000	0.00000	0.00000	0.00000	0.00000
WORK COEF = $2*CP*DELT/U**2$					
0.00000	0.00000	0.00000	0.00000	0.00000	0.00000
FLOW COEF = VM/U					
.21219	.21731	.20979	.22707	.23475	.24899
K BAR					
3.28515	3.25573	3.21129	3.13434	3.06017	2.98390
O-FACTOR					
.12870	.11598	.12952	.10890	.10905	.11939
VM2/VM1					
1.09019	1.06067	1.07723	1.05005	1.05460	1.04342
DELP/Q					
.06772	.06877	.07596	.07050	.06582	.07309
TANG BLADE FORCE LB/IN					
-17.50736	-15.33166	-15.82773	-13.95749	-13.94192	-14.82801
AXIAL BLADE FORCE LB/IN					
13.71605	12.27059	12.76375	12.06016	11.64992	11.91641
VEL HEAD 2					
.09147	.09432	.08728	.09809	.09954	.10469
Q=E**(-S/CP)					
.94850	.95160	.97247	.98468	.98239	.97653
RVU/					
1.33866	1.34430	1.24485	1.28483	1.25990	1.24854
DRVU/DM					
-4.29822	-4.11463	-3.97232	-3.50433	-3.43930	-3.42878
STRMLN DIST M					
2.84272	2.84001	2.84657	2.89332	3.02867	3.47828

STATION 6.20000 STATOR XI = 0.00000
P = 0. ZTIP = 2.02500 AR = 4.00000 XN = 1. BNXT = 0.
= -0. ZHUB = 2.02500 LOSS = 2. EXP = -0.0000 BLADES = 53.

RADIUS	3.37200	3.33000	3.29000	3.21000	3.14000	3.07950
SLOPE	29.92500	30.00000	30.00000	30.00000	30.00000	32.36080
CURVATURE	-.27042	-.27000	-.27000	-.27000	-.27000	-.27868
LOSS COEFF	.99937	.99924	.99943	.99950	.99939	.99900
SOLIDITY	1.00000	1.00000	1.00000	1.00000	1.00000	1.00000
BLADE THICKNESS	.03624	.03632	.03645	.03666	.03688	.03716
AERO BLOCKAGE	.92686	.92660	.92684	.92686	.92690	.92685
TOTAL BLOCKAGE	.84284	.84136	.84023	.83757	.83507	.83250
BLADE ANGLE	-22.98716	-22.96542	-22.95318	-22.97066	-23.14303	-23.43325
LEAN	-.22307	-.27711	-.37393	-.51419	-.58997	-.60406
Y	-20.80000	-19.37000	-20.45000	-20.50000	-20.60000	-20.60000

VOR ITES = 1 AREA RATIO = 1.00082 EXP = 1.50000 CHOKE = .56170

RADIUS	3.37200	3.34336	3.30013	3.22554	3.15376	3.07950
Z	2.02500	2.02500	2.02500	2.02500	2.02500	2.02500
CROSS PASSAGE DIST P	.29250	.26386	.22063	.14604	.07426	0.00000
SLOPE	29.92500	30.00666	30.17291	30.49287	31.01146	32.36080
CURVATURE	-.27042	-.24247	-.25919	-.22648	-.29044	-.27868
DELTA CURVATURE	0.00000	-.00083	-.00180	-.00014	.00154	0.00000
VM	418.24868	429.44417	405.17255	434.48819	435.55481	449.28407
VU2	158.87785	152.42625	149.42925	162.31818	163.56271	168.87337
U	2056.92000	2039.45124	2013.07830	1967.57963	1923.79184	1878.49500
VR	208.65011	214.76541	203.64436	220.47293	224.40209	240.47895
BETA2	20.80000	19.54172	20.24417	20.48491	20.58252	20.59983
BETA2*	23.66778	22.28750	23.10325	23.43903	23.66088	23.98810

INCIDENCE					
.51587	-.72943	-.02159	.20572	.24392	.20685
.33698	.34383	.32953	.35635	.35721	.36751
V2					
447.40824	455.69294	431.84939	463.81805	465.25342	479.97333
TOTAL TEMP					
1.45143	1.44756	1.41269	1.39850	1.40058	1.41021
TOTAL PRESS					
3.08762	3.09256	3.06539	3.09218	3.08169	3.08686
EFFICIENCY					
.83252	.84112	.90387	.94453	.93634	.91595
STATIC TEMP					
1.41962	1.41455	1.38305	1.36431	1.36617	1.37360
STATIC PRESS					
2.85504	2.85053	2.84411	2.83323	2.82243	2.81285
DENSITY					
2.01113	2.01514	2.05640	2.07667	2.06594	2.04780
SUCT SURF VEL					
552.29279	566.78215	534.70406	566.23879	563.59389	575.00833
PRESS SURF VEL					
342.52368	344.60374	328.99472	361.39731	366.91296	384.93832
DELTA T					
0.00000	0.00000	0.00000	0.00000	0.00000	0.00000
WORK COEF = $2*CP*DELT/U**2$					
0.00000	0.00000	0.00000	0.00000	0.00000	0.00000
FLOW COEF = VM/U					
.20334	.21057	.20127	.22082	.22640	.23917
R BAR					
3.34215	3.31335	3.26973	3.19453	3.12179	3.04665
D-FACTOR					
.18029	.18523	.17868	.15948	.16313	.15787
VM2/VM1					
.97555	.98670	.97740	.99156	.98440	.98149
DELP/Q					
.15411	.14403	.15169	.12988	.13496	.12131
TANG BLADE FORCE LB/IN					
-18.05150	-20.37243	-16.84984	-17.59822	-16.96104	-16.30954
AXIAL BLADE FORCE LB/IN					
13.02157	13.50688	12.47174	13.19989	12.87090	11.33118
VEL HEAD 2					
.07533	.07826	.07219	.08375	.08413	.08877
Q=E*(-S/CP)					
.94791	.95088	.97192	.98420	.98179	.97555
RVU/					
.87826	.83544	.80842	.85830	.84563	.85253
DRVU/DM					
-3.41230	-3.59005	-3.34453	-3.34736	-3.22739	-3.13175
STRMLN DIST M					
2.95919	2.95664	2.96360	3.01099	3.14737	3.59793

STATION	6.30000	STATOR	XI =	0.00000		
R =	0.	ZTIP =	2.12500	AR =	4.00000	XN = 1. BNXT = 0.
	-0.	ZHUB =	2.12500	LOSS =	2.	EXP = -0.0000 BLADES = 53.
RADIUS						
	3.42750	3.39000	3.34000	3.27000	3.20000	3.14064
SLOPE						
	28.18870	29.00000	29.00000	30.00000	30.00000	30.50800
CURVATURE						
	-.25880	-.25000	-.25000	-.25000	-.25000	-.27248
LOSS COEFF						
	.99935	.99941	.99944	.99950	.99930	.99901
SOLIDITY						
	1.00000	1.00000	1.00000	1.00000	1.00000	1.00000
BLADE THICKNESS						
	.03441	.03450	.03463	.03482	.03505	.03535
AERO BLOCKAGE						
	.92461	.92462	.92460	.92462	.92433	.92461
TOTAL BLOCKAGE						
	.84630	.84525	.84375	.84158	.83892	.83682
BLADE ANGLE						
	-13.15601	-13.16994	-13.19334	-13.36500	-13.69501	-14.13522
LEAN						
	.37921	.36250	.34761	.37343	.43254	-.52372
Y						
	-13.50000	-12.20000	-12.20000	-12.35000	-12.50000	-12.50000
NOR ITES = 1 AREA RATIO = 1.00020 EXP = 1.50000 CHOKE = .53144						
RADIUS						
	3.42750	3.39918	3.35637	3.28308	3.21319	3.14064
Z						
	2.12500	2.12500	2.12500	2.12500	2.12500	2.12500
CROSS PASSAGE DIST P						
	.28686	.25854	.21573	.14244	.07255	0.00000
SLOPE						
	28.18870	28.57299	28.66508	29.36327	29.88712	30.50800
CURVATURE						
	-.25880	-.27205	-.27921	-.30472	-.23322	-.27248
DELTA CURVATURE						
	0.00000	.00076	.00125	.00038	-.00097	0.00000
VM						
	406.78347	416.70086	393.36177	428.49523	429.08505	443.21211
VU2						
	97.66011	91.74046	85.04786	93.54715	94.95269	98.25733
U						
	2090.77500	2073.49855	2047.38828	2002.68134	1960.04382	1915.79040
VR						
	192.15521	199.29889	188.69133	210.11061	213.81008	225.00055
BETA2						
	13.50000	12.41610	12.20000	12.31532	12.47795	12.49994
BETA2*						
	15.23684	14.07350	13.84237	14.06305	14.31819	14.43013

INCIDENCE

2.03097	.97533	.74640	.82926	.81640	.00445
.31464	.32148	.30667	.33652	.33695	.34712
V2					
418.34231	426.68011	402.45076	438.58777	439.46557	453.97299
TOTAL TEMP					
1.45143	1.44756	1.41269	1.39850	1.40058	1.41021
TOTAL PRESS					
3.08050	3.08608	3.05931	3.08672	3.07402	3.07605
EFFICIENCY					
.83053	.83930	.90200	.94281	.93392	.91262
STATIC TEMP					
1.42362	1.41862	1.38695	1.36793	1.36988	1.37746
STATIC PRESS					
2.87692	2.87357	2.86683	2.85482	2.84250	2.83093
DENSITY					
2.02085	2.02561	2.06701	2.08696	2.07500	2.05519
SUCT SURF VEL					
509.11301	515.56572	488.43764	529.16008	528.12211	539.43613
PRESS SURF VEL					
327.57161	337.79451	316.46389	348.01546	350.80904	368.50985
DELTA T					
0.00000	0.00000	0.00000	0.00000	0.00000	0.00000
WORK COEF = $2*CP*DELT/U**2$					
0.00000	0.00000	0.00000	0.00000	0.00000	0.00000
FLOW COEF = VM/U					
.19456	.20097	.19213	.21396	.21892	.23135
K BAR					
3.39975	3.37127	3.32825	3.25431	3.18347	3.11007
D-FACTOR					
.13104	.12804	.14032	.12609	.12657	.12500
VM2/VM1					
.97259	.97033	.97085	.98621	.98515	.98649
DELP/Q					
.09405	.09523	.10270	.08338	.07741	.06598
TANG BLADE FORCE LB/IN					
-12.94938	-13.03610	-13.15202	-14.81712	-14.25732	-14.49429
AXIAL BLADE FORCE LB/IN					
6.00297	5.85769	5.90540	6.27725	5.62460	5.69144
VEL HEAD 2					
.06609	.06886	.06291	.07513	.07531	.07969
$Q=E**(-S/CP)$					
.94729	.95031	.97137	.98370	.98110	.97458
RVU/					
.54874	.51122	.46795	.50348	.50017	.50589
DRVU/DM					
-2.82062	-2.75349	-2.66624	-2.81695	-2.76638	-2.67704
STRMLN DIST M					
3.07356	3.07116	3.07833	3.12636	3.26370	3.71514

STATION 6.40000 STATOR XI = 0.00000

P = 0. ZTIP = 2.22500 AR = 4.00000 XN = 1. BNXT = 0.
 : -0. ZHUB = 2.22500 LOSS = 2. EXP = -0.0000 BLADES = 53.

RADIUS

3.47930	3.45000	3.40000	3.33000	3.26000	3.19750
SLOPE					
26.56550	27.00000	27.00000	27.00000	27.00000	28.74200
CURVATURE					
-.24372	-.25000	-.25000	-.25000	-.25000	-.26270
LOSS COEFF					
.99931	.99924	.99944	.99949	.99939	.99901
SOLIDITY					
1.00000	1.00000	1.00000	1.00000	1.00000	1.00000
BLADE THICKNESS					
.02607	.02612	.02621	.02635	.02649	.02668
AERO BLOCKAGE					
.92222	.92209	.92237	.92234	.92211	.92238
TOTAL BLOCKAGE					
.86393	.86319	.86239	.86078	.85892	.85747
BLADE ANGLE					
-3.58613	-3.61283	-3.69188	-3.94111	-4.46423	-5.16844
LEAN					
.69020	.72157	.79733	.99723	1.27698	-1.51457
Y					
-6.13000	-5.30000	-5.50000	-5.40000	-5.35000	-5.90000

JOR ITES = 1 AREA RATIO = .99917 EXP = 1.50000 CHOKE = .50186

RADIUS

3.47930	3.45121	3.40876	3.33633	3.26830	3.19750
Z					
2.22500	2.22500	2.22500	2.22500	2.22500	2.22500
CROSS PASSAGE DIST P					
.28180	.25371	.21126	.13883	.07080	0.00000
SLOPE					
26.56550	26.76860	26.88784	27.02864	27.44866	28.74200
CURVATURE					
-.24372	-.24397	-.22638	-.26674	-.37492	-.26270
DELTA CURVATURE					
0.00000	-.00027	-.00041	-.00109	-.00196	0.00000
VM					
388.19074	397.48668	373.75262	411.63113	412.49350	424.08728
VU2					
41.69123	37.01687	35.86525	38.96125	38.65305	43.80101
U					
2122.37300	2105.23827	2079.34369	2035.16049	1993.66219	1950.47500
VR					
173.60696	179.02344	169.02796	187.06000	190.14047	203.92938
BETA2					
6.13000	5.32046	5.48131	5.40699	5.35331	5.89677
BETA2*					
6.84706	5.95473	6.14089	6.06527	6.02770	6.71826

INCIDENCE					
3.22945	2.41868	2.55757	2.36682	2.02908	.63911
.29328	.30040	.28576	.31685	.31726	.32553
V2					
390.42311	399.20660	375.46949	413.47088	414.30055	426.34323
TOTAL TEMP					
1.45143	1.44756	1.41269	1.39850	1.40058	1.41021
TOTAL PRESS					
3.07296	3.07785	3.05324	3.08118	3.06743	3.06527
EFFICIENCY					
.82842	.83697	.90013	.94105	.93184	.90929
STATIC TEMP					
1.42721	1.42223	1.39028	1.37133	1.37330	1.38132
STATIC PRESS					
2.89552	2.89173	2.88553	2.87480	2.86147	2.84909
DENSITY					
2.02880	2.03324	2.07550	2.09636	2.08365	2.06258
SUCT SURF VEL					
454.10807	473.14639	439.46148	480.24168	472.77691	491.08079
PRESS SURF VEL					
326.73816	325.26680	311.47750	346.70008	355.82418	361.60566
DELTA T					
0.00000	0.00000	0.00000	0.00000	0.00000	0.00000
WORK COEF = $2*CP*DELT/U**2$					
0.00000	0.00000	0.00000	0.00000	0.00000	0.00000
FLOW COEF = VM/U					
.18290	.18881	.17975	.20226	.20690	.21743
R BAR					
3.45340	3.42519	3.38257	3.30971	3.24074	3.16907
D-FACTOR					
.13238	.12737	.12698	.11828	.12002	.11944
VM2/VM1					
.95429	.95389	.95015	.96064	.96133	.95685
DELP/Q					
.09139	.08544	.09716	.08618	.08194	.07406
TANG BLADE FORCE LB/IN					
-12.25050	-12.17310	-10.35787	-12.39567	-12.38497	-11.74902
AXIAL BLADE FORCE LB/IN					
3.40931	3.24050	3.31056	4.54100	4.33940	3.10238
VEL HEAD 2					
.05774	.06047	.05493	.06698	.06714	.07053
$Q=E**(-S/CP)$					
.94663	.94960	.97082	.98320	.98051	.97361
RVU/					
.23780	.20943	.20042	.21309	.20710	.22960
DRVU/DM					
-1.89095	-2.19422	-1.90196	-1.98762	-1.74397	-1.93782
STRMLN DIST M					
3.18618	3.18389	3.19122	3.23966	3.37788	3.83017

Stator 1B Exit

STATION 6.50000 STATOR XI = 0.00000

P = 0. ZTIP = 2.33000 AR = 3.00000 XN = 1. BNXT = 1.
 : -0. ZHUB = 2.33000 LOSS = 2. EXP = -0.0000 BLADES = 53.

RADIUS

3.53000 3.51000 3.48000 3.40000 3.33000 3.25000

SLOPE

25.00000 25.00000 25.50000 26.00000 26.50000 27.00000

CURVATURE

-.28200 -.26900 -.27000 -.27200 -.27400 -.29350

LOSS COEFF

.99936 .99938 .99941 .99948 .99942 .99894

SOLIDITY

1.00000 1.00000 1.00000 1.00000 1.00000 1.00000

BLADE THICKNESS

.01005 .01005 .01005 .01005 .01004 .01002

AERO BLOCKAGE

.92000 .92000 .92000 .92000 .92000 .92000

TOTAL BLOCKAGE

.89790 .89777 .89758 .89707 .89661 .89607

BLADE ANGLE

6.33938 6.29478 6.14885 5.71909 4.96198 3.92472

LEAN

.59872 .71747 .93884 1.42878 2.00686 -2.54859

Y

-3.30000 0.00000 -1.00000 -1.00000 -2.75000 -1.60000

FOR ITES = 1 AREA RATIO = 1.00006 EXP = 1.50000 CHOKE = .47065

RADIUS

3.53000 3.50233 3.46035 3.38825 3.32094 3.25000

Z

2.33000 2.33000 2.33000 2.33000 2.33000 2.33000

CROSS PASSAGE DIST P

.28000 .25233 .21035 .13825 .07094 0.00000

SLOPE

25.00000 25.23034 25.55112 25.81480 26.04749 27.00000

CURVATURE

-.28200 -.15563 -.16866 -.14005 -.14975 -.29350

DELTA CURVATURE

0.00000 .00168 .00168 .00192 .00126 0.00000

VM

366.65550 376.60561 349.80675 388.48895 383.39979 387.81359

VU2

21.14123 2.02184 6.10590 8.99769 18.67358 10.82864

VU1

2132.15877 2134.39949 2104.71006 2057.83532 2007.10201 1971.67136

U

2153.30000 2136.42133 2110.81596 2066.83300 2025.77559 1982.50000

VR

154.95537 160.53134 150.87740 169.17288 168.35704 176.06376

BETA2

3.30000 .30759 1.00000 1.32677 2.78840 1.59941

L-FA1

80.24256 79.99337 80.56356 79.30919 79.18552 78.87235

BETA2*

3.64027 .34003 1.10838 1.47379 3.10305 1.79494

BETA1*						
81.14153	80.93131	81.47214	80.35495	80.26176	80.05957	
DENSITY						
74.24256	73.99776	74.63323	73.59784	74.17218	76.52902	
M2						
.27561	.28312	.26599	.29744	.29353	.29570	
M1						
1.62355	1.62933	1.62212	1.60297	1.56259	1.53156	
V2						
367.26449	376.61103	349.86004	388.59313	383.85428	387.96474	
V1						
2163.45494	2167.37006	2133.58131	2094.18477	2043.39274	2009.44951	
TOTAL TEMP						
1.45143	1.44756	1.41269	1.39850	1.40058	1.41021	
TOTAL PRESS						
3.06596	3.07105	3.04683	3.07549	3.06115	3.05379	
EFFICIENCY						
.82646	.83505	.89816	.93925	.92985	.90574	
STATIC TEMP						
1.42999	1.42501	1.39323	1.37451	1.37716	1.38629	
STATIC PRESS						
2.90892	2.90537	2.90114	2.89301	2.88409	2.87464	
DENSITY						
2.03422	2.03884	2.08231	2.10477	2.09423	2.07362	
SUCT SURF VEL						
370.41478	418.73161	382.73456	416.69578	385.62224	422.73746	
PRESS SURF VEL						
364.11421	334.49046	316.98552	360.49048	382.08631	353.19203	
DELTA T						
0.00000	0.00000	0.00000	0.00000	0.00000	0.00000	
WORK COEF = $2*CP*DELT/U**2$						
0.00000	0.00000	0.00000	0.00000	0.00000	0.00000	
FLOW COEF = VM/U						
.17028	.17628	.16572	.18796	.18926	.19562	
R BAR						
3.50465	3.47677	3.43456	3.36229	3.29462	3.22375	
D-FACTOR						
.08505	.10007	.10742	.09595	.09705	.12816	
VM2/VM1						
.94452	.94747	.93593	.94378	.92947	.91447	
DELP/Q						
.07553	.07329	.09309	.08823	.10982	.11819	
TANG BLADE FORCE LB/IN						
-4.56362	-8.01992	-6.39560	-7.01188	-4.47242	-7.29953	
AXIAL BLADE FORCE LB/IN						
.95699	1.09990	1.10046	1.64145	1.93936	1.71364	
VEL HEAD 2						
.05122	.05395	.04782	.05933	.05784	.05866	
VEL HEAD 1						
.77236	.77431	.77188	.76529	.75086	.73928	
Q=E*(-S/CP)						
.94602	.94900	.97025	.98269	.97994	.97258	
PMU/						
.12234	.01161	.03464	.04998	.10166	.05769	
DRVU/DM						
-.08942	-1.19365	-.93215	-.79745	-.05131	-.99084	
STRMLN DIST M						
3.30278	3.30067	3.30821	3.35679	3.49533	3.94757	

APPENDIX E

MECHANICAL DESIGN ANALYSIS
OF NASA 10/1 ADVANCED
COMPRESSOR RIG

(11 pages)

MECHANICAL DESIGN ANALYSIS
OF NASA 10/1 ADVANCED
COMPRESSOR RIG

This report summarizes the mechanical design analyses completed on the NASA 10/1 Advanced Compressor Test Rig. The analyses include (1) the first stage compressor blade stress and vibration and (2) the first-stage compressor disk stress.

First-Stage Compressor Blade Stress and Vibration Analysis

The first-stage compressor consists of two blade rows, rotor 1A and rotor 1B. The compressor is made of titanium (90Ti-6Al-4V). The material properties at room temperatures are as follows:

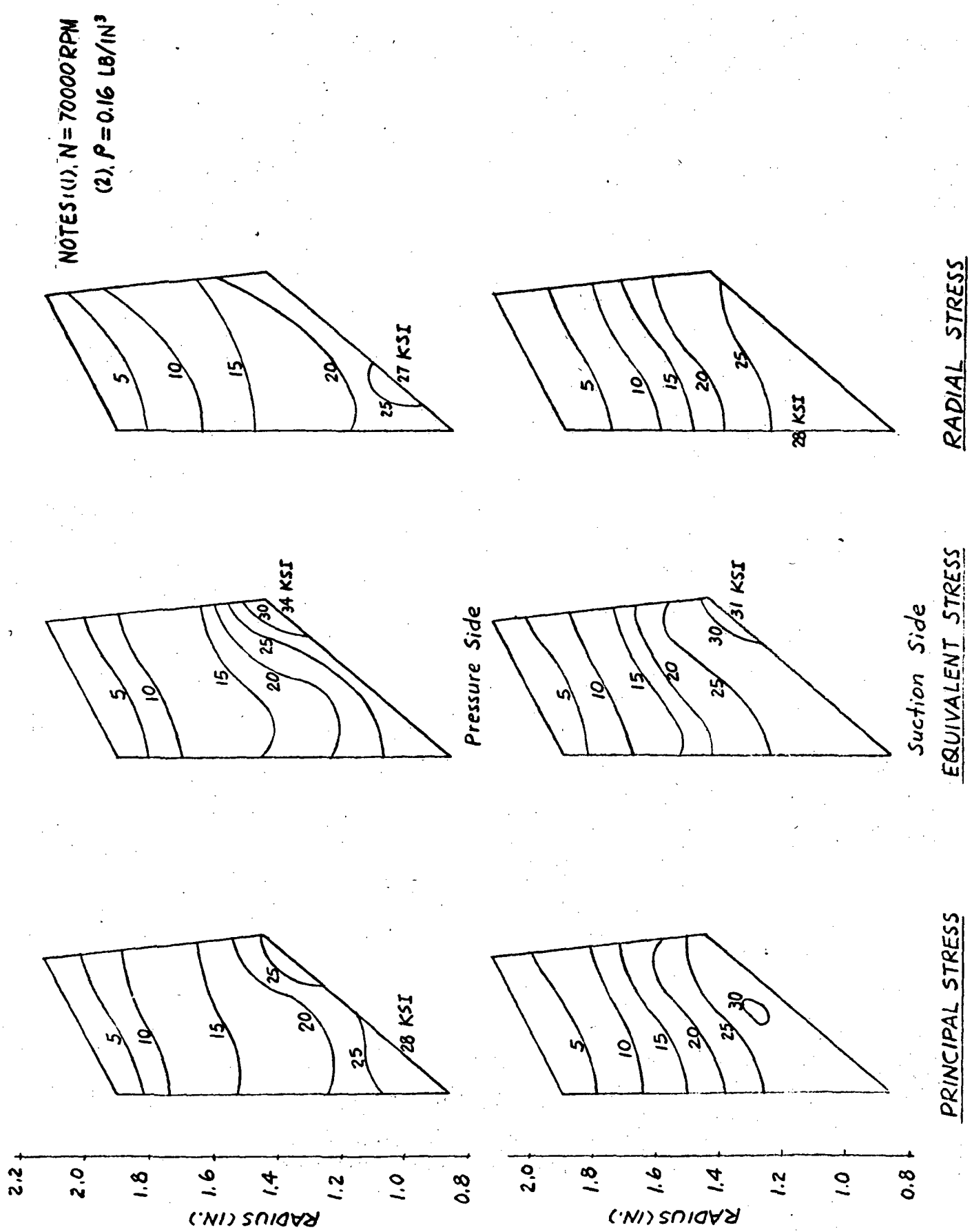
Tensile Strength = 130,000 psi

Yield Strength = 120,000 psi

Rotor 1A has 20 blades and rotor 1B has 40 blades. A finite element program has been employed to analyze the aerodynamically designed blade for the centrifugal, thermal, and gas pressure stresses. The same program also computes the natural frequencies and mode shapes of the compressor blade.

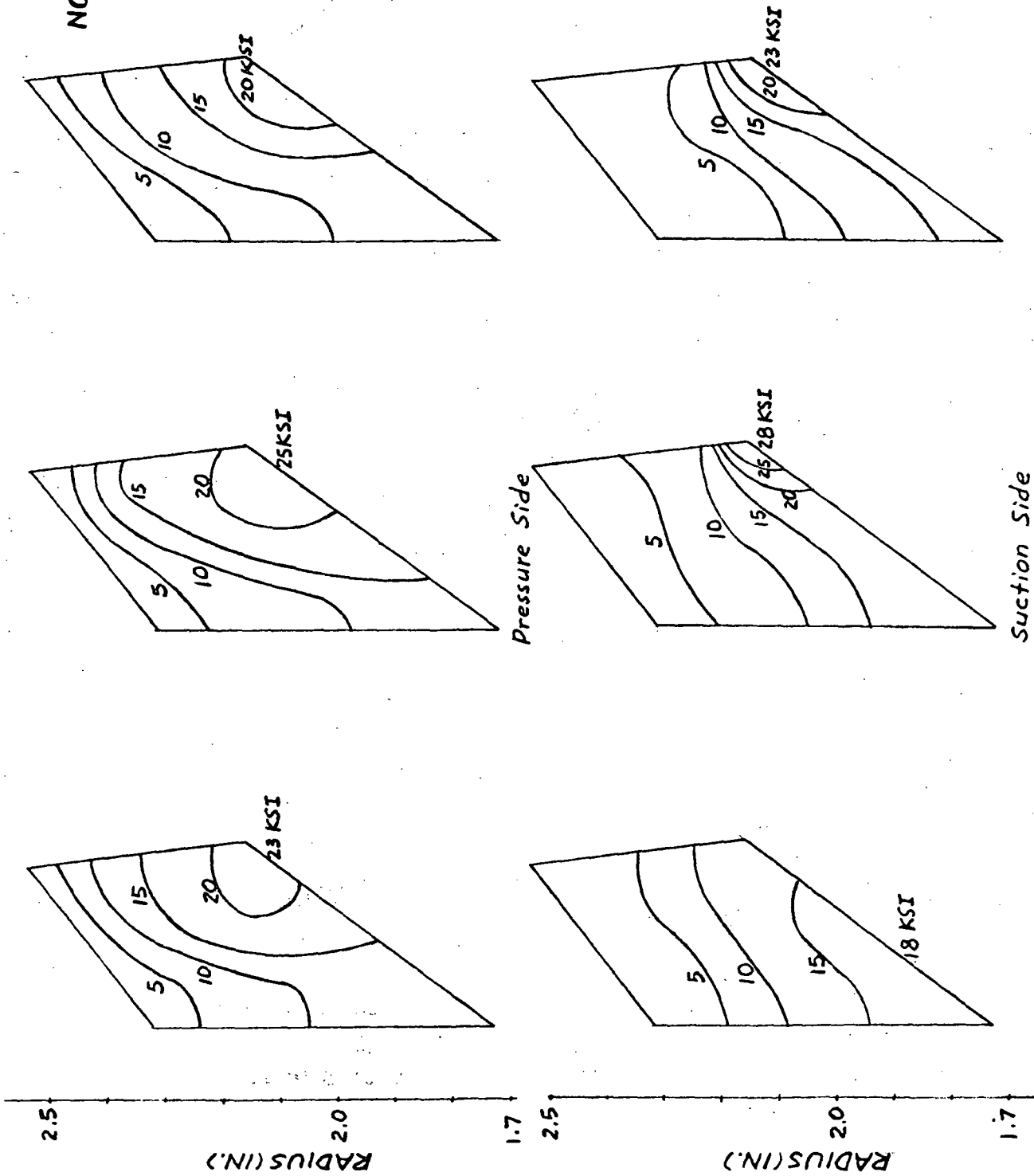
The distributions of centrifugal stresses in the blades of rotors 1A and 1B are shown in Figures 1 and 2. The stresses are based on the 100-percent operating speed (70,000 rpm). The distributions of the combined stresses due to centrifugal force, thermal gradient and gas pressure in the blades of rotors 1A and 1B are shown in Figure 3 and Figure 4. The tangential and axial forces acting on the blades resulting from gas pressure difference are listed in Table I. The temperature distribution of the blade is assumed to equal the total relative gas temperature. The calculated blade stresses are not excessive and they are within the acceptable level.

The interference diagrams drawn for the natural frequencies of the blades are shown in Figures 5 and 6. In Figure 5, a 10-percent to 20-percent increase of the first bending resonant frequency due to blade variations, as observed in the salt pattern test of NASA 6/1 Advanced Compressor rotor blade, would interfere with four-per-revolution excitation very close to the 100-percent operating speed. Four struts are currently used upstream of this rotor in the inlet duct. The interference possibility of seven and eleven struts is also indicated.



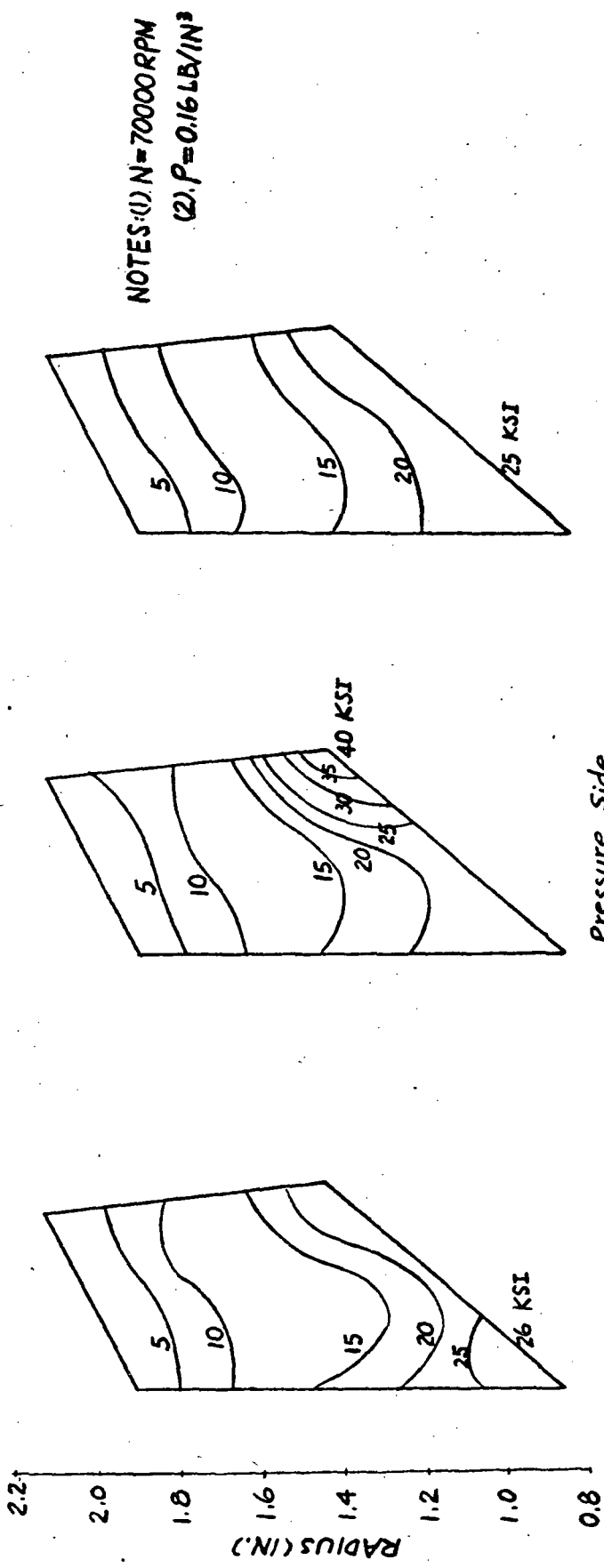
BLADE STRESSES DUE TO CENTRIFUGAL FORCE - ROTOR 1A FIGURE 1

NOTES: (1) $N = 70000 \text{ RPM}$
 (2) $P = 0.16 \text{ LB/IN}^3$

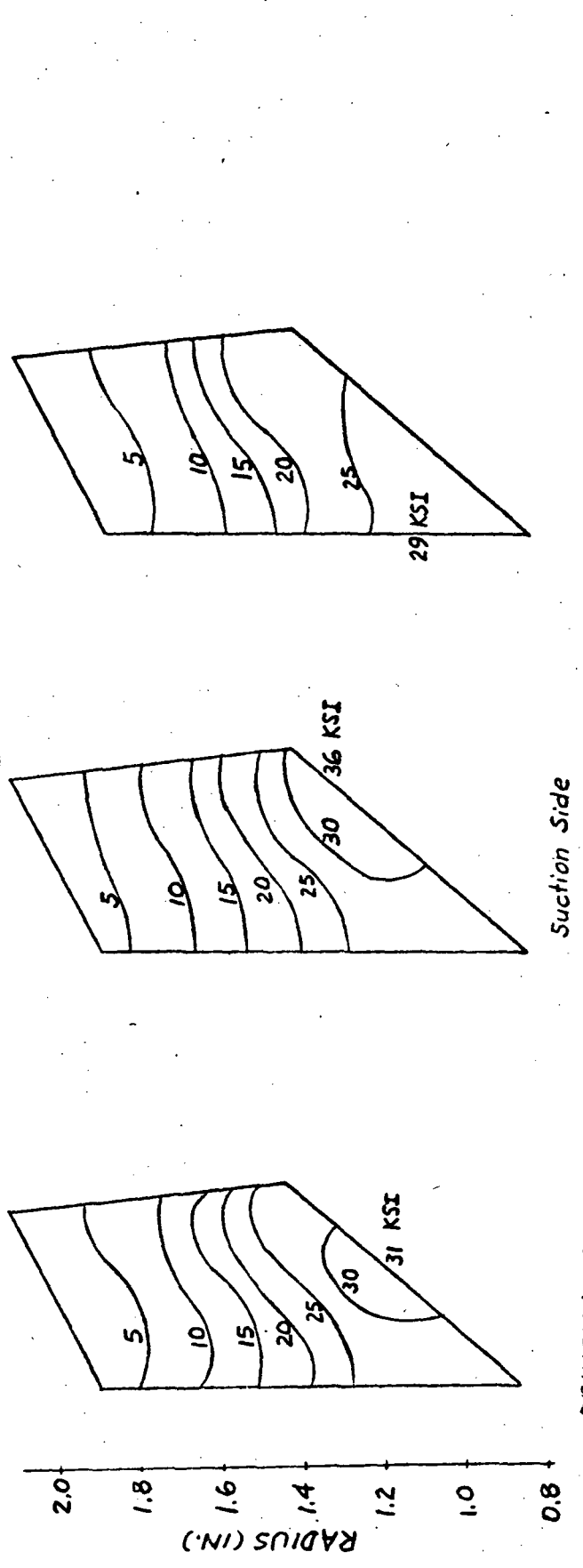


PRINCIPAL STRESS EQUIVALENT STRESS RADIAL STRESS
BLADE STRESSES DUE TO CENTRIFUGAL FORCE - ROTOR 1B

FIGURE 2



Pressure Side

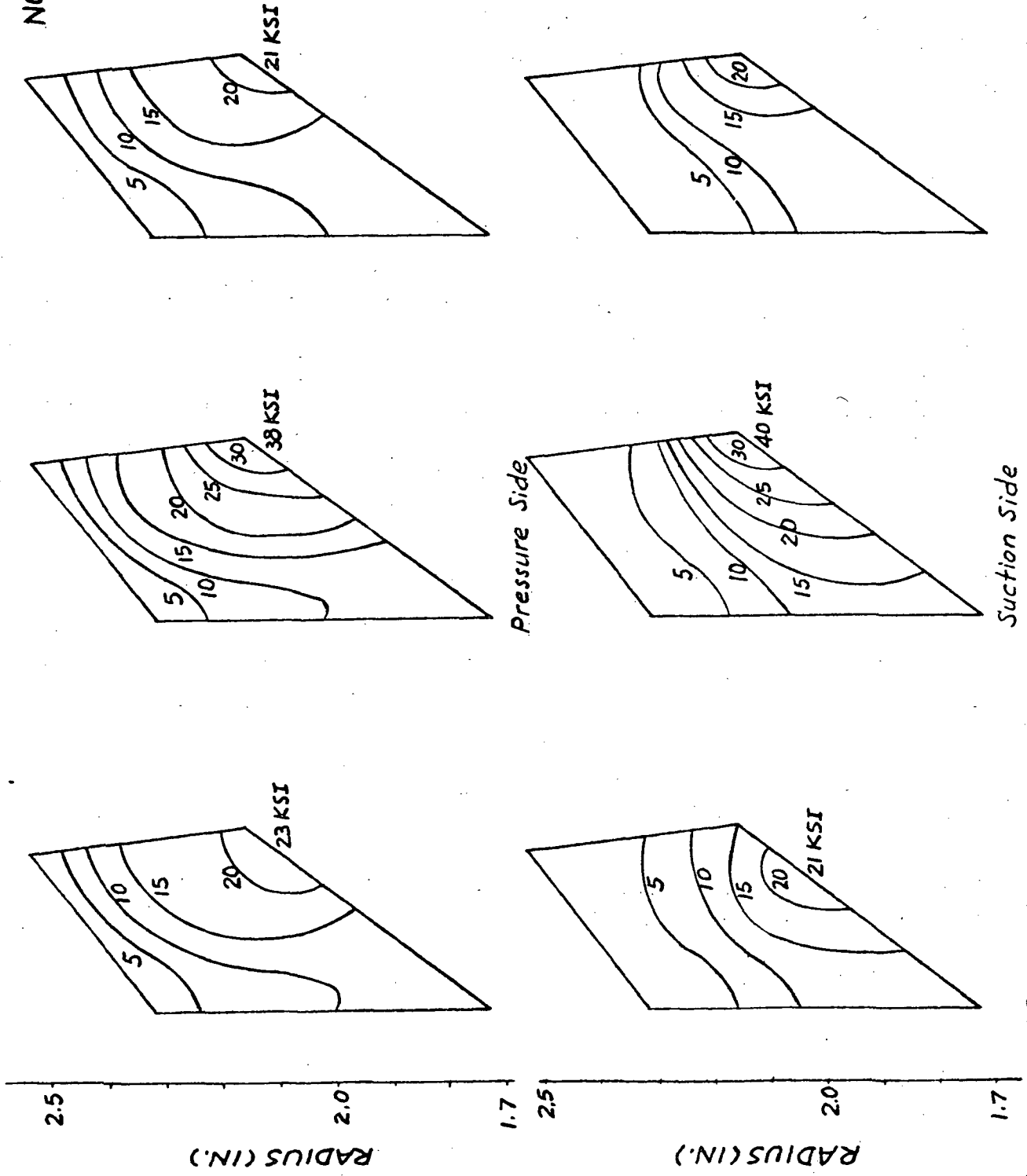


Suction Side

NOTES: (1) $N = 70000 \text{ RPM}$
 (2) $P = 0.16 \text{ LB/IN}^2$

PRINCIPAL STRESS
 EQUIVALENT STRESS
 RADIAL STRESS
 BLADE STRESSES DUE TO CENTRIFUGAL AND THERMAL FORCES AND GAS PRESSURE - ROTOR 1A
 FIGURE 3

NOTES: (1) $N = 7000 \text{ RPM}$
 (2) $P = 0.16 \text{ LB/IN}^3$



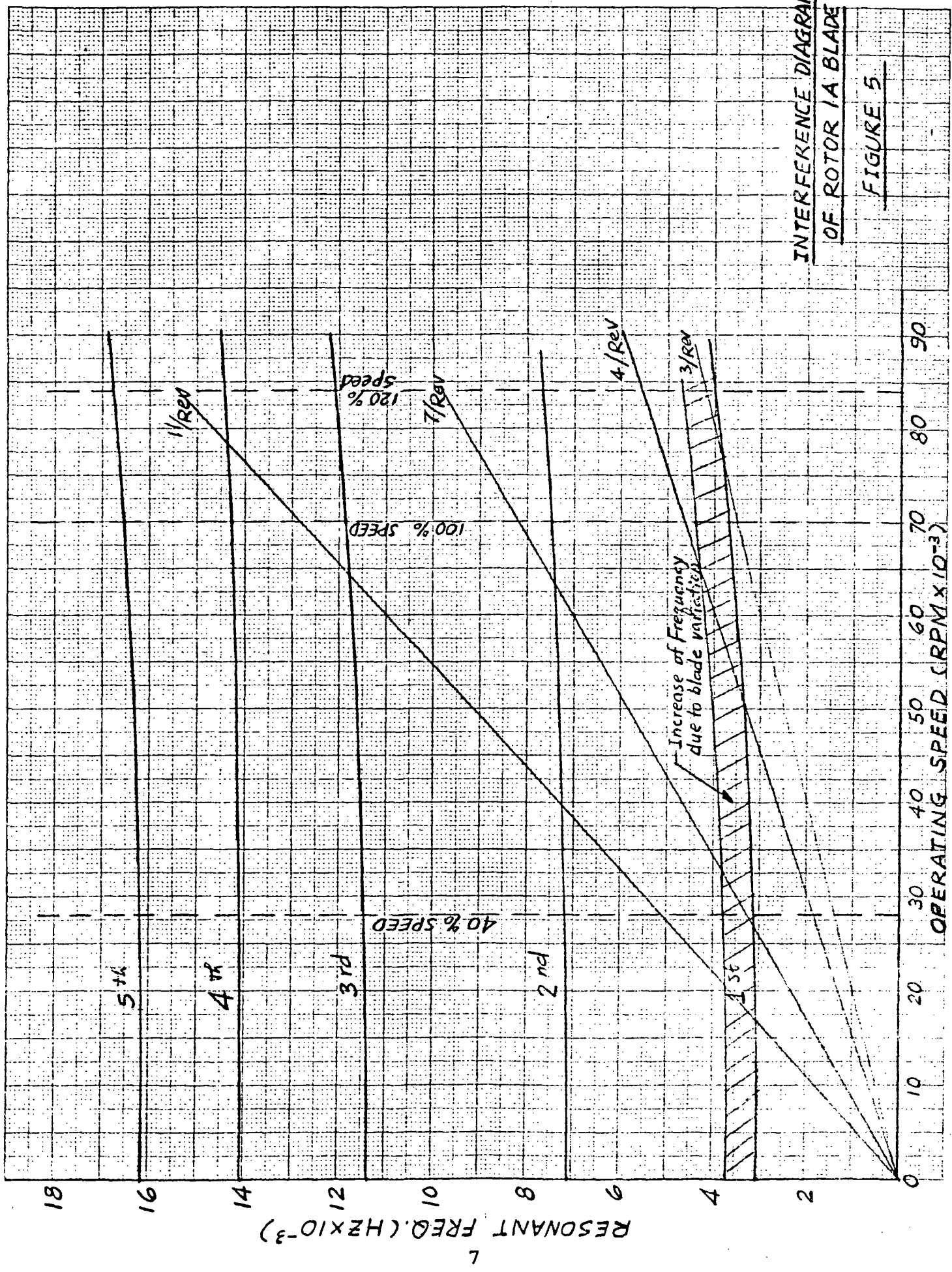
PRINCIPAL STRESS EQUIVALENT STRESS RADIAL STRESS
BLADE STRESSES DUE TO CENTRIFUGAL AND THERMAL FORCES AND GAS PRESSURE - ROTOR 1B FIGURE 4

A seven-strut inlet indicates the rotor 1A blade to be free of resonance (Figure 5), whereas the rotor 1B has a possible resonance condition near 100-percent speed (Figure 6). Eleven inlet struts appear to be a better configuration in that the interference (resonance) occurs at a low speed during a start transient.

TABLE I
PRESSURE LOADS vs. RADIUS

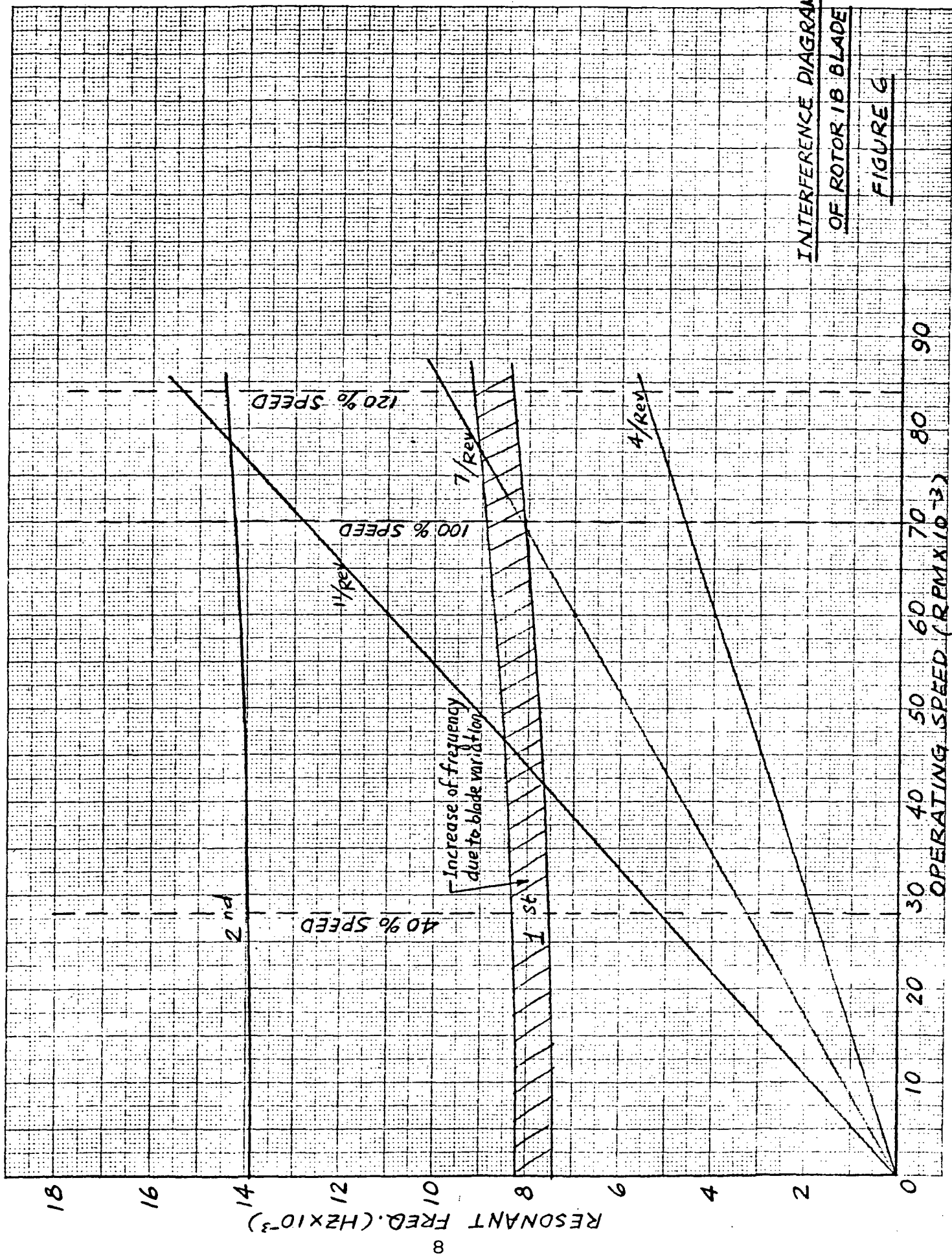
Rotor 1A 20 Blades						
Radius, in.	2.13	2.083	2.008	1.871	1.7	1.454
Tang., lb/in.	66.0*	61.8	54.7	46.36	36.87	25.14
Axial, lb/in.	93.84	90.57	86.86	77.91	64.25	41.72
Rotor 1B 40 Blades						
Radius, in.	2.541	2.503	2.447	2.360	2.264	2.159
Tang., lb/in.	81.34	80.28	76.7	72.75	70.3	64.84
Axial, lb/in.	147.9	144.3	143.3	134.1	123.3	108.4

* Loads indicated are pounds per radial inch and are totals for indicated blade numbers.



INTERFERENCE DIAGRAM
OF ROTOR 1A BLADE

FIGURE 5



First-Stage Compressor Disk Stress Analysis

A finite element program has been employed to analyze the centrifugal and thermal stresses of the disks. The calculated tangential, radial, and equivalent stresses of rotor 1A and rotor 1B are shown in Figures 7 and 8. A summary of pertinent information is listed in Table II. The stresses based on 100-percent operating speed (70,000 RPM) are satisfactory.

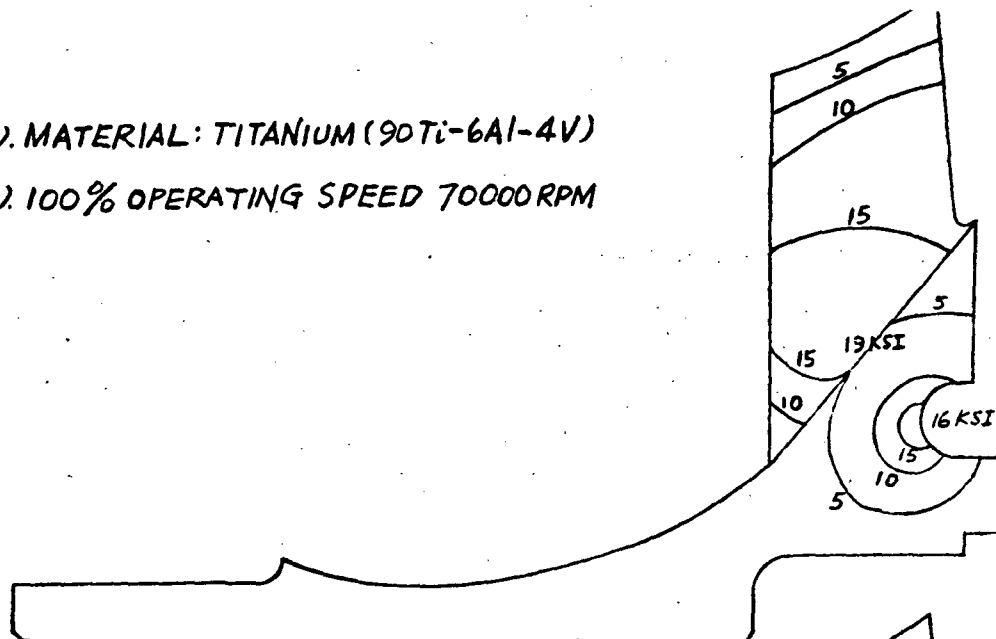
TABLE II

	ROTOR 1A	ROTOR 1B
Weight, pounds	0.56	0.55
Polar Moment of Inertia, in-lb-sec ²	0.00123	0.00293
Diametric Moment of Inertia, in-lb-sec ²	0.00129	0.0015
Maximum Tangential Stress at Bore, psi	38,000	66,000
Average Tangential Stress, psi	14,077	36,697
Average Burst Speed, rpm	190,100	117,800
Average Burst Margin, percent	271	168
Blade Tip Radial Growth, in.	0.003	0.005
Blade Tip Axial Growth, in.	0.005	0.008

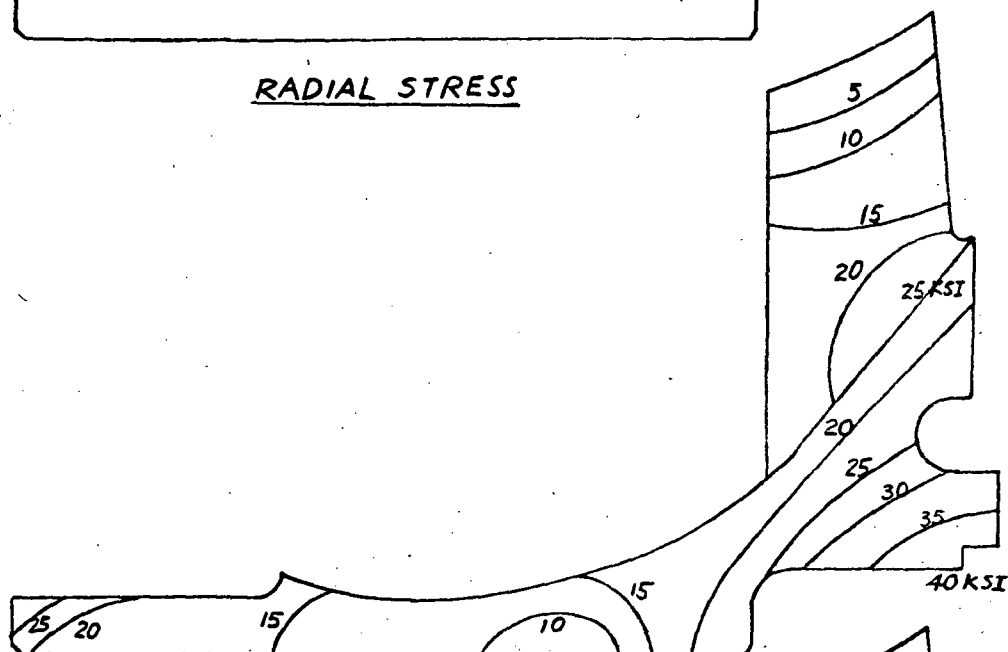
NOTES: (1) N = 70,000 rpm
(2) $\delta = 0.16 \text{ lb/in}^2$
(3) Burst Factor Assumed = 0.8

NOTE: (1). MATERIAL: TITANIUM (90Ti-6Al-4V)

(2). 100% OPERATING SPEED 70000RPM



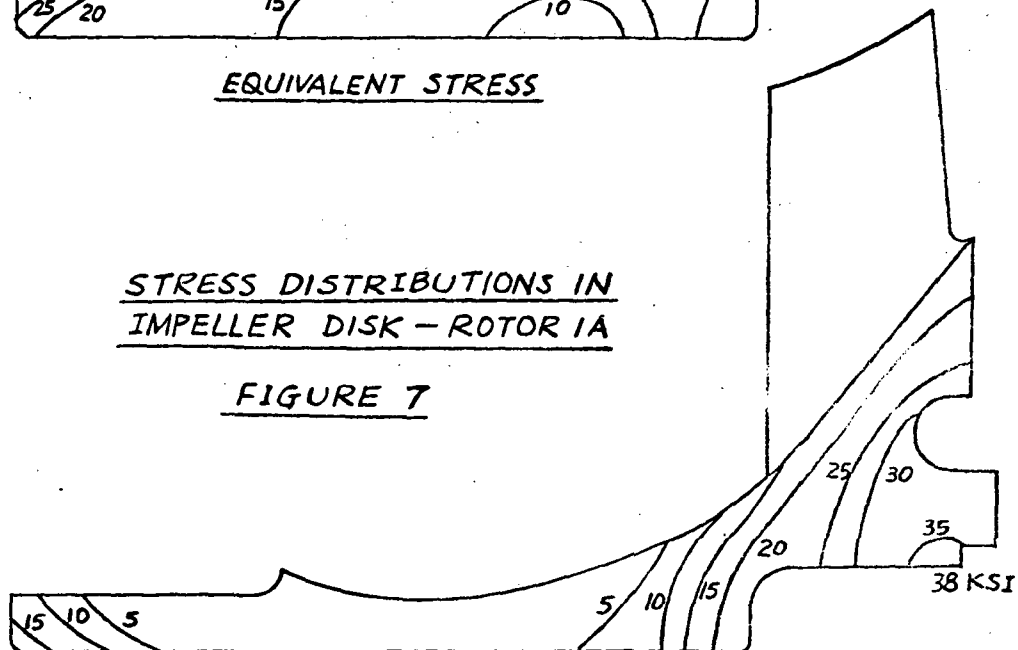
RADIAL STRESS



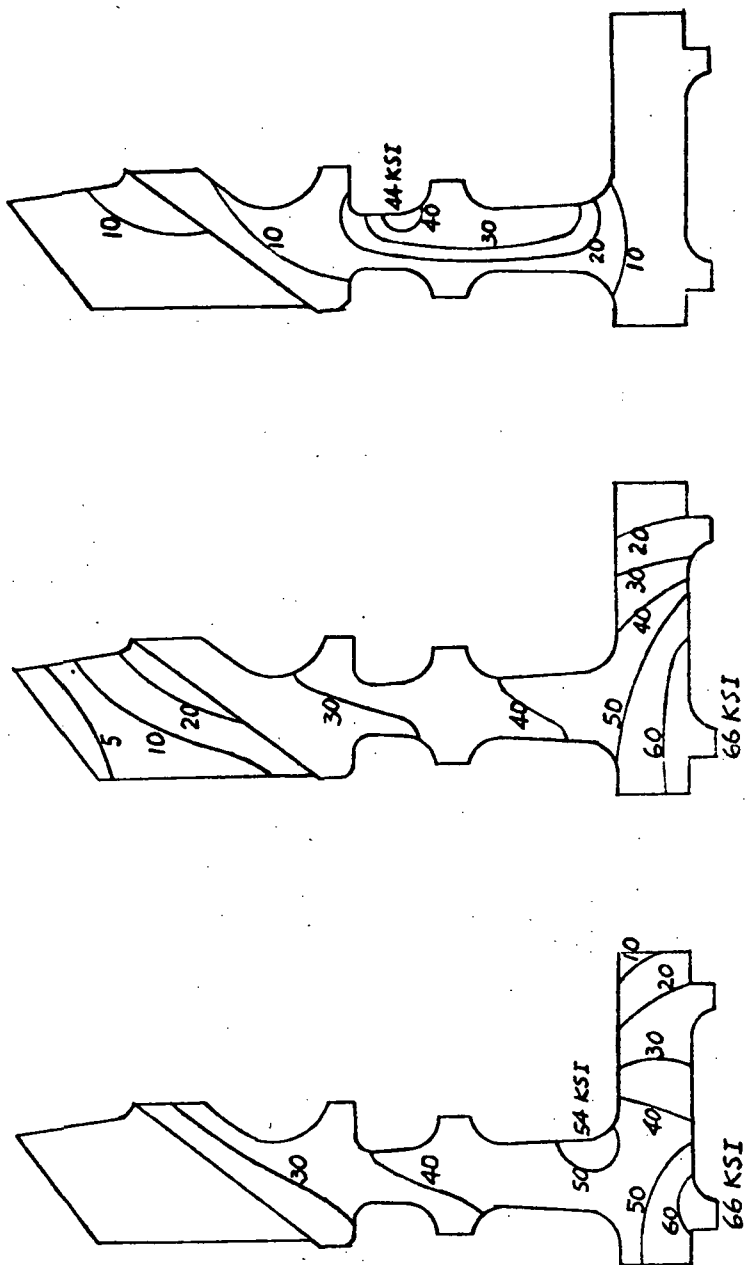
EQUIVALENT STRESS

STRESS DISTRIBUTIONS IN
IMPELLER DISK - ROTOR 1A

FIGURE 7



TANGENTIAL STRESS



TANGENTIAL STRESS EQUIVALENT STRESS RADIAL STRESS

NOTE: (1) MATERIAL: TITANIUM (90Ti-6Al-4V)

(2) 100 % OPERATING SPEED 70000 RPM

STRESS DISTRIBUTION OF IMPELLER DISK - ROTOR 1 B

FIGURE 8

APPENDIX F

REFERENCES

(1 page)

REFERENCES

1. Love, G., "Pressure Rise Associated with Shock-Induced Boundary-Layer Separation," NACA TN 3601, 1955.
2. Johnsen, I. A. and Bullock, R. O., "Aerodynamic Design of Axial-Flow Compressors," NASA SP-36, 1965.
3. Stark, U., "Flow Investigations Around Swept Cascades at Compressible Subsonic Flow," Institute for Aerodynamics of the German Research Laboratory for Aeronautics and Space, DFL Report No. 0331, June 1966.
4. Smith, L. H. Jr. and Yeh, H., "Sweep and Dihedral Effects in Axial Flow Turbomachinery," Trans-of ASME, Journal of Basic Engineering, Series D, Volume 85, No. 3, September 1963.
5. Beatty, L. A., Savage M., and Emery, J. C., "Low-Speed Cascade Tests of Two 45° Swept Compressor Blades with Constant Spanwise Loading," NACA RM L53L07, March 1954.
6. Godwin, W. R., "Effect of Sweep on Performance of Compressor Blade Sections as Indicated by Swept-Blade Rotor, Unswept - Blade Rotor, and Cascade Tests," NACA TN 4062, July 1957.
7. Gothert, B., "High-Speed Measurements on a Swept-Back Wing (Sweepback Angle $\phi = 35^\circ$)," NACA TM 1102, 1947.
8. Katsanis, T. and McNally, W. D., "Fortran Program for Calculating Velocities and Streamlines on a Blade-to-Blade Stream Surface of a Tandem Blade Turbomachine," NASA TN D-5044, March 1969.
9. Pampreen, R. C., "Design and Test of a Cascade Radial Diffuser," AiResearch Internal Report AD-5100-R, June 1966.
10. Keenan, M. J. and Bartok, J. A., "Experimental Evaluation of Transonic Stators," NASA CR-72298, 1969.
11. Von Doenhoff, A. E. and Tetervin, N., "Determination of General Relations for the Behavior of Turbulent Boundary Layers," NACA Rep. 772, 1943.
12. Garner, H. C., "The Development of Turbulent Boundary Layers," ARC Rep. 2133, 1944.
13. K. G. Harley, J. Harris, and E. A. Burdsall, P&W Report, "High Loading Low-Speed Fan Study," NASA CR-72895, 1972.
14. Seyler, D. R. and Smith, L. H., Jr. "Single Stage Experimental Evaluation of High Mach Number Compressor Rotor Blading," NASA CR-54581, 1967.

APPENDIX G
PERFORMANCE PARAMETER DEFINITIONS
SYMBOL DEFINITIONS

(4 pages)

PERFORMANCE PARAMETERS

Diffusion Factor

For the rotor,

$$D = 1.0 - \frac{V_2'}{V_1'} + \frac{r_2 V_{u2} - r_1 V_{u1}}{2\bar{r}\sigma V_1'}$$

and for the stator

$$D = 1.0 - \frac{V_2}{V_1} + \frac{r_2 V_{u2} - r_1 V_{u1}}{2\bar{r}\sigma V_1}$$

Loss Coefficient

For the rotor,

$$\bar{\omega} = \frac{P_{T1}' \left[T_2'/T_1' \right]^{\alpha/\alpha-1} - P_{T2}'}{P_{T1}' - P_{S1}}$$

and for the stator

$$\bar{\omega} = \frac{P_{T1} - P_{T2}}{P_{T1} - P_{S1}}$$

SYMBOL DEFINITIONS

a	Distance along chord line to point of maximum camber line rise (inches)
A	Flow area (square inches)
A*	Critical flow area (square inches)
AR	Blade aspect ratio (mean blade height/mean chord)
C	Blade chord (inches)
H _{act}	Actual stage enthalpy rise (feet)
i	Incidence angle (degrees), $\beta'_{air} - \beta_{blade}$
L	Distance along chord line from leading edge (inches)
m	Meridional length (inches)
M	Mach number
N	Shaft speed (rpm)
N _b	Number of blades
N _s	Specific speed defined on Figure 1
P	Pressure (psia)
PR	Pressure ratio
Q _{av}	Volumetric flow rate (cubic feet/second)
R, r	Radius (inches)
Re	Reynold's number, $\frac{2 \rho U_T R_T}{\mu_1}$
s	Blade circumferential spacing (inches)
t	Blade thickness (inches)
U _t REF	Reference tip speed = 610 feet/second
U _t	Rotor tip speed (feet/second)
V	Velocity (feet/second)

SYMBOL DEFINITIONS (Contd)

μ	Viscosity, lb/ft-sec
ρ	Density, slugs/ft ³
\dot{W}	Weight flow rate (pounds mass/second)
Z	Axial length
β	Relative air angle or blade angle (degrees)
α	Specific heat ratio
δ	Reduced pressure or deviation angle (degrees)
ψ	Stream function
η_{ad}	Adiabatic efficiency, $\frac{(P_2/P_1)^{\alpha-1/\alpha} - 1}{T_2/T_1 - 1}$
η_p	Polytropic efficiency, $\frac{\alpha-1/\alpha \ln(P_2/P_1)}{\ln(T_2/T_1)}$
θ	Reduced temperature, $T/518.68$
θ^*	Boundary layer momentum thickness
σ	Solidity, $\frac{CN_b}{2\pi r}$
ϕ	Blade camber, $\beta_2 - \beta_1$
$\bar{\omega}$	Total pressure loss parameter

Subscript

1	Upstream
2	Downstream
eff	Effective
geo	Geometric
LE	Leading edge
SS	Supersonic

SYMBOL DEFINITIONS (Contd)

Subscript (Contd)

S	Static condition
t	Tip
T	Stagnation condition
TE	Trailing edge
u, θ	Tangential component

Superscript

'	Relative condition
—	Averaged value